UNIVERSIDADE ESTADUAL DE CAMPINAS

Faculdade de Engenharia de Alimentos

ELEM TAMIRYS DOS SANTOS CARAMÊS

AVALIAÇÃO DE TÉCNICAS ANALÍTICAS VIBRACIONAIS E DE IMAGEM ASSOCIADAS A QUIMIOMETRIA PARA O CONTROLE DE QUALIDADE DE ALIMENTOS DE ALTO VALOR AGREGADO

EVALUATION OF VIBRATIONAL AND IMAGE ANALYTICAL TECHNIQUES ASSOCIATED WITH CHEMOMETRICS FOR THE QUALITY CONTROL OF HIGH VALUE FOODS

Campinas, 2020

ELEM TAMIRYS DOS SANTOS CARAMÊS

AVALIAÇÃO DE TÉCNICAS ANALÍTICAS VIBRACIONAIS E DE IMAGEM ASSOCIADAS A QUIMIOMETRIA PARA O CONTROLE DE QUALIDADE DE ALIMENTOS DE ALTO VALOR AGREGADO

EVALUATION OF VIBRATIONAL AND IMAGE ANALYTICAL TECHNIQUES ASSOCIATED WITH CHEMOMETRICS FOR THE QUALITY CONTROL OF HIGH VALUE FOODS

Tese apresentada a Faculdade de Engenharia de Alimentos da Universidade Estadual de Campinas como parte dos requisitos exigidos para a obtenção do título de Doutora em Ciência de Alimentos.

Thesis presented to the Faculty of food engineering of the University of Campinas in partial fulfillment of the requirements for the degree of Doctor in food science.

Orientadora: Juliana Azevedo Lima Pallone.

ESTE TRABALHO CORRESPONDE À VERSÃO FINAL DA TESE DEFENDIDA PELA ALUNA ELEM TAMIRYS DOS SANTOS CARAMÊS E ORIENTADA PELA PROFª DRª. JULIANA AZEVEDO LIMA PALLONE.

Campinas, 2020

Ficha catalográfica
Universidade Estadual de Campinas
Biblioteca da Faculdade de Engenharia de Alimentos
Claudia Aparecida Romano - CRB 8/5816

C176a

Caramês, Elem Tamirys dos Santos, 1992-
Avaliação de técnicas analíticas vibracionais e de imagem associadas a quimiometria para o controle de qualidade de alimentos de alto valor agregado / Elem Tamirys dos Santos Caramês. – Campinas, SP : [s.n.], 2020.

Orientador: Juliana Azevedo Lima Pallone.
Tese (doutorado) – Universidade Estadual de Campinas, Faculdade de Engenharia de Alimentos.

1. NIR. 2. Espectroscopia no infravermelho médio. 3. Infravermelho. 4. Aprendizado de máquina. 5. Alimentos. I. Pallone, Juliana Azevedo Lima. II. Universidade Estadual de Campinas. Faculdade de Engenharia de Alimentos. III. Título.

Informações para Biblioteca Digital

Título em outro idioma: Evaluation of vibrational and image analytical techniques associated with chemometrics for the quality control of high value foods
Palavras-chave em inglês:
NIR
Mid-infrared spectroscopy
Infrared
Machine learning
Foods
Área de concentração: Ciência de Alimentos
Titulação: Doutora em Ciência de Alimentos
Banca examinadora:
Juliana Azevedo Lima Pallone [Orientador]
Edenir Rodrigues Pereira Filho
Bruno Gonçalves Botelho
Douglas Fernandes Barbin
Flavio Luis Schmidt
Data de defesa: 15-12-2020
Programa de Pós-Graduação: Ciência de Alimentos

Identificação e informações acadêmicas do(a) aluno(a)
- ORCID do autor: https://orcid.org/0000-0002-9387-4641
- Currículo Lattes do autor: http://lattes.cnpq.br/6935952086284579

COMISSÃO EXAMINADORA

_____

Profª. Drª. Juliana Azevedo Lima Pallone (Orientadora/Presidente da Banca)
FACULDADE DE ENGENHARIA DE ALIMENTOS – UNICAMP

_____

Prof. Dr Douglas Fernandes Barbin (Membro – titular)
FACULDADE DE ENGENHARIA DE ALIMENTOS – UNICAMP

_____

Prof. Dr. Flavio Luis Schmidt (Membro – titular)
FACULDADE DE ENGENHARIA DE ALIMENTOS – UNICAMP

_____

Profª. Dr Edenir Rodrigues Pereira Filho (Membro – titular)
DEPARTAMENTO DE QUÍMICA - UFSCar

_____

Profª. Dr. Bruno Gonçalves Botelho (Membro – titular)
INSTITUTO DE QUÍMICA - UFMG

A Ata da Defesa, assinada pelos membros da Comissão Examinadora, consta no SIGA/Sistema de Fluxo de Dissertação/Tese e na Secretaria do Programa da Unidade.

DEDICO

A Deus por até aqui ter me ajudado e conduzido. Aos meus pais, Silvana e Cardoso, ao meu irmão João e ao meu avô Alberto *(in memorian).*

AGRADECIMENTOS

A Deus e ao meu anjo da guarda, por terem estado sempre comigo em todos os momentos desse projeto.

A minha família, Silvana e Cardoso, por terem sido meu suporte e inspiração, eu jamais teria conseguido sem vocês. E ao meu irmão, João por ser sempre garantia de boa risada em qualquer situação dessa vida.

A minha orientadora Juliana Pallone, pela oportunidade de trabalho, ensinamentos e conselhos durante esse trabalho. E ao Vicent Baeten e Juan Fernandez-Pierna por gentilmente terem me recebido na Bélgica.

Aos meus amigos do laboratório de análises II, por serem ótima companhia, seja no trabalho de bancada, seja para as boas risadas no café/bolo da tarde. Em especial as alunas de iniciação científica Deborah, Júlia e Letícia por terem ajudado tanto durante a execução desse trabalho. E a Joyce que foi minha companhia do início do mestrado ao fim desse doutorado, obrigada por compartilhar de tantos momentos comigo.

Aos meus queridos José Luan e Lilian, por serem meus amigos em qualquer situação, que grata surpresa da vida me apresentar vocês. Estar com vocês é sempre como estar em casa.

A minha querida amiga Fernanda Damin, por todas as conversas (que não foram poucas), pela companhia, pelas viagens, caronas, cinemas, shows e por fazer o melhor brigadeiro do mundo durante esses mais de dez anos de amizade.

A minha amiga Larissa Margalho, pelas horas dedicadas aos nossos momentos de caridade, por sempre aceitar tomar um sorvete no meio da tarde e caminhar na praça da paz, obrigada pela companhia nessa jornada!

A minha querida Évila Neves, por ser a companhia mais presente mesmo estando longe. Obrigada por tudo!

Aos meus queridos, Thiago Sobral, Kathleen Bouth, Leonardo Ferreira e Paula Almeida, por serem companhia e incentivo em vários momentos dessa caminhada.

Aos meus amigos do GEAE-Barão Geraldo por representarem sempre um momento de paz em meio ao caos.

Ao CNPq (142414/2016-6) pela bolsa concedida e a FAPESP (2018/09759-3) pelo financiamento do projeto. O presente trabalho foi realizado com apoio da Coordenação de

Aperfeiçoamento de Pessoal de Nível Superior - Brasil (CAPES) - Código de Financiamento 001.

RESUMO

Métodos tradicionais (MT) empregados no controle de qualidade (CQ) de alimentos utilizam reagentes químicos, têm elevado custo e tempo de execução. Nesse contexto, a espectroscopia no infravermelho próximo e médio (NIR e MIR) e técnicas de imagem hiperespectral (NIR-HSI) e smartphone (SBI), são alternativas verdes aos MT. Sendo assim, objetivou-se avaliar o potencial de técnicas analíticas verdes associadas a quimiometria para CQ, aspectos nutricionais e bioativos de repolho roxo, polpa de açaí e arroz integral. Inicialmente, 60 amostras de repolho roxo tiveram os parâmetros relacionados aos compostos bioativos (antocianinas e polifenóis totais, ORAC, DPPH e TEAC) determinados por MT, os espectros NIR e MIR coletados e os dados foram empregados para a obtenção de modelos de calibração multivariada. Os modelos de calibração construídos, baseados em NIR e MIR, apresentaram performance satisfatória na predição dos parâmetros avaliados. Para polpas de açaí, espectros de NIR e MIR também foram obtidos para verificar a possibilidade de utilização das técnicas para detecção de amostras adulteradas, com farinha de tapioca, mandioca, trigo e emulsificante. Determinou-se cartas de controle multivariada e modelos PLS-DA e KNN. Como resultado, ambas técnicas foram capazes de detectar amostras adulteradas com 100% de precisão através dos modelos PLS-DA. Além disso, 96 amostras de polpa de açaí liofilizadas foram utilizadas para obtenção de modelos PLS, baseados em NIR e SBI, para a determinação dos parâmetros bioativos obtidos através de MT. Os modelos PLS obtidos por NIR e SBI se mostraram satisfatórios para todos os parâmetros avaliados, com exceção do modelo ORAC-SBI. Em adição, verificou-se a possibilidade de utilização de minerais essenciais como marcadores de adulterações. Para essa fase do trabalho, polpa de açaí liofilizada autêntica e adulterada, com beterraba, suco de uva, maltodextrina, farinhas de tapioca e mandioca, tiveram os teores de Ca, Mn, Fe e K determinados por FAAS e baseado nesses valores foram construídos modelos de classificação por PLS-DA, OCPLS e SIMCA, onde obteve-se 90% de precisão na detecção de polpas adulteradas através do modelo OCPLS, demonstrando que a composição mineral pode ser útil para a detecção de fraudes em açaí. Na etapa seguinte, os teores de Ca, Mn, Fe e K, determinados via FAAS, de polpas de açaí liofilizadas e NIR foram utilizados para a construção de modelos PLS para predição indireta do teor desses minerais. Exceto para o Ca, os modelos obtidos por PLS apresentaram desempenho insatisfatório. A seleção de variáveis (iPLS) foi realizada, as porções do espectro selecionadas resultaram em modelos PLS satisfatórios para Mn, Fe e K. Amostras de arroz integral orgânico e convencional foram analisadas por instrumentos NIR-bancada, NIR-portátil e NIR-HSI, para a construção de modelos discriminativos entre os grãos. Todos modelos PLS-DA mostraram-se capazes de discriminar as amostras (85% de precisão), sendo o NIR-bancada a técnica de melhor desempenho. Sendo assim, foi possível concluir que as técnicas analíticas verdes, conhecidas como rápidas e não destrutivas, associadas a quimiometria, foram consideradas adequadas como alternativas para CQ, nutricional, bioativo e detecção de adulteração em alimentos diferentes alimentos de origem vegetal, com alto valor agregado.

Palavras-chave: NIR; MIR; infravermelho; aprendizagem de máquina; quimiometria; alimentos.

ABSTRACT

Traditional methods (TM) applied in food quality control (QC) use chemical reagents, present high cost and time consuming. In this context, the near and mid infrared spectroscopy (NIR e MIR), hyperspectral imaging system (NIR-HSI) and smartphones (SBI) are green alternatives for TM. Therefore, it is intended to evaluate the potential of green analytical techniques associated to chemometric for QC, nutritional and bioactive aspects of red cabbage, açai pulp and brown rice. Initially, 60 red cabbage samples had parameters related to bioactive compounds (anthocyanins and phenolics content, ORAC, DPPH and TEAC) determined by TM, the NIR and MIR spectra collected and chemical data were implemented to obtain models of multivariate calibration. The calibration models built, based on NIR and MIR, provided satisfactory performance in the prediction of the evaluated parameters. Regard açaí pulp, NIR and MIR spectra were also obtained to verify the possibility of utilization of techniques that aimed to detect adulterated samples, with tapioca flour, cassava and wheat and emulsifier. It was stablished multivariate control charts and PLS-DA and KNN models. The outcome showed that both techniques were capable to detect adulterated samples with 100% precision through PLS-DA models. Furthermore, 96 freeze-dried açaí pulp samples were employed to obtain PSL models, based on NIR and SBI, in order to determined bioactive parameters acquired through TM. The PLS models collected by NIR and SBI had a satisfactory result to all the evaluated parameters, with an exception of ORAC-SBI model. In addition, it was found the possibility of the utilization of essential minerals as adulterations markers. In this stage, authentic and adulterated freeze-dried açaí pulp, with beet pulp, grape juice, maltodextrin, tapioca flour and cassava presented contents of Ca, Mn, Fe and K determined by FAAS and based on these amounts were built models of classification by PLS-DA, OCPLS and SIMCA, attaining 90% of precision on the detection of adulterated pulps via OCPLS model, revealing that the mineral composition can be useful to expose fraud in açai. In the next stage, the contents of Ca, Mn, Fe and K, determined by FAAS, of freeze-dried açai pulp samples and NIR were used to build PLS models for the indirect prediction of the content of these minerals. Except for Ca, the models acquired by PLS presented unsatisfactory performance. The selection of variables (iPLS) was executed, the portions of spectra selected resulted in satisfactory PLS models for Mn, Fe and K. Samples of organic and conventional brown rice were analyzed by NIR-benchtop, NIR-portable and NIR-HIS instruments, in order to build discriminative models among grains. All the PLS-DA models were able to discriminate the samples (85% of precision) and NIR-benchtop achieved the best performance. Accordingly, it was possible to conclude that green analytical techniques, known as fast and non-destructive, associated with chemometric, were considered suitable as alternatives for QC, nutritional, bioactive and detection of adulterations in different food of plant origin, with high value-added.

Keywords: NIR; MIR; infrared; machine learning; chemometrics; foods.

SUMÁRIO

CAPÍTULO I
Introdução Geral e Objetivos

1. INTRODUÇÃO GERAL

O estilo de vida saudável tem sido uma busca constante nas últimas décadas, o setor de alimentos saudáveis e sustentáveis tem se solidificado como um segmento de mercado com cada vez mais importância, principalmente entre os jovens adultos. Nesse sentido, as escolhas alimentares têm mudado significativamente, para um contexto onde alimentos funcionais desempenham papel principal em uma dieta equilibrada (KÜSTER; VILA; SARABIA, 2019)

Nesse contexto, frutas, vegetais e grãos são componentes importantes dentro de uma dieta balanceada, pois são considerados fontes de fibras e nutrientes essenciais, como minerais, além de outros compostos bioativos, que quando ingeridos regularmente, são associados a diversos efeitos benéficos na saúde (SCHAUSS, 2016).

Dentre os principais compostos bioativos que podem ser encontrados em matrizes alimentares estão os fenólicos e os minerais essenciais, entre outros. Os compostos fenólicos são classificados de acordo com a sua estrutura química. Sendo assim, as classes mais comumente observadas nos alimentos são os ácidos fenólicos (como ácido cafeico, ácido ferrúlico, ácido clorogênico, entre outros), flavonóides (como antocianinas, luteonina, quercetina, miricertina), carotenóides (como beta caroteno, luteína e licopeno) e fitoesteróis (VERMA; SRIVASTAV, 2020). A essas classes de compostos fenólicos são associadas propriedades anti-inflamatórias, anticancerígenas, preventivas em relação a doenças crônicas e cardiovasculares (SCHAUSS, 2016; VERMA; SRIVASTAV, 2020).

Os minerais também desempenham um papel fundamental para a manutenção de um bom funcionamento do corpo humano. Cálcio e ferro são minerais essenciais e a deficiência desses está ligada ao surgimento de doenças como a anemia, que atingiu mais de 1 bilhão de pessoas entre 1993 e 2005, e osteoporose, respectivamente (SHAMAH; VILLALPANDO; DE LA CRUZ, 2016). O potássio trabalha sinergicamente com o sódio, exercendo uma importante função para o processo de transporte através da membrana celular (REBELLATO et al., 2020).

Ainda no âmbito de alimentação saudável é válido ressaltar também a preferência que têm se dado nas últimas décadas para o consumo de alimentos orgânicos, que são cultivados livres da utilização de fertilizantes, herbicidas, antibióticos, pesticidas ou alimentos geneticamente modificados (KATT; MEIXNER, 2020). Essa preferência está relacionada a diversos fatores que variam principalmente entre sabor, valor nutricional,

preocupações com saúde e preservação do meio ambiente e priorizar o comércio com produtores locais (KUSHWAH et al., 2019). O mercado de produtos orgânicos, incluindo bebidas e alimentos, movimentou um montante de aproximadamente 92 bilhões de euros em 2017 (KATT; MEIXNER, 2020). Por serem produtos cada vez mais valorizados, se tornam vulneráveis a adulteração (TEYE et al., 2019).

Nesse contexto, entre os principais grãos produzidos está o arroz (*Oryza sativa* L.) que é consumido por cerca 3,5 bilhões de pessoas no mundo, o que é equivalente a quase metade da população mundial, e por isso tem grande influência na nutrição humana e na segurança alimentar, especialmente na Ásia, América do Sul e países da África, portanto, o arroz é responsável por uma importante porção dos carboidratos e, consequentemente, da energia consumida pelos habitantes dessas regiões. Por isso, é um dos produtos mais consumidos também na sua forma orgânica, especialmente na forma integral que têm sido cada vez mais preferido pelo seu perfil nutricional, devido ao seu elevado teor de fibras (PASTORELLI et al., 2018; TEYE et al., 2019).

Já dentre as frutas e vegetais produzidas no Brasil, que apresentam potencial bioativo, encontram-se o repolho roxo e o açaí. O repolho roxo, a hortaliça economicamente mais relevante do gênero *Brassica oleracea*, apresenta um alto valor nutricional, sendo fonte de vitamina C e E, rico em minerais, como o cálcio, oligossacarídeos e compostos bioativos, como as antocianinas, carotenoides, glicosinolatos e flavonoides (WICZKOWSKI; TOPOLSKA; HONKE, 2014). O açaí (*Euterpe oleracea*), por sua vez, também apresenta um excelente perfil nutricional, contendo fibras, proteínas, minerais, ótimo perfil de ácidos graxos e grande presença de compostos bioativos (DE OLIVEIRA; SCHWARTZ, 2018; ROGEZ, 2000).

Açai e o repolho roxo, tem na sua cor um dos seus principais atrativos, que é conferida graças a alta concentração de antocianinas. Sendo uma classe de compostos bioativos, as antocianinas, são os mais importantes corantes hidrossolúveis naturais, podem ser encontradas não somente em frutas e vegetais, mas também em flores e cereais. Mais de 500 tipos de antocianinas já foram identificadas na natureza, dentre elas as mais relevantes são as cianidinas, delfinidinas, peonidinas, petunidinas e malvidinas. Vários estudos apontam grande correlação entre as antocianinas e efeitos benéficos, como propriedades antioxidantes, antimicrobianas, anti-inflamatória, anti-proliferativo, anti-carcinogênicas, anti-obesidade,

habilitando aplicações desses compostos para diversos fins, como fármacos, suplementos alimentares, corantes naturais, embalagens, etc (YONG; LIU, 2020).

A mudança de estilo de vida dos consumidores aliada aos excelentes perfis nutricionais e potencial bioativo do açaí e do repolho roxo aumentaram a produção e consumo desses produtos. O consumo do açaí até meados da década de 90 limitava-se a região amazônica, sendo uma cultura essencialmente extrativista, no entanto, no início dos anos 2000, a polpa de açaí conquistou mercado em outras regiões do Brasil, e na última década já é consumida nos grandes centros globais, como a União Europeia, Estados Unidos e Japão, gerando renda equivalente a mais de 400 milhões de reais em 2015, com taxa de aumento de 37 % ao ano, o que classifica o açaí um produto de alto valor, tanto no mercado nacional como internacional, e com isso se tornou alvo de adulterações (CONAB, 2016; LOBATO et al., 2018).

O repolho roxo também tem apresentado aumento nos volumes comercializados. Segundo a Companhia de Entrepostos e Armazéns Gerais de São Paulo, maior estado produtor da hortaliça, em 2007 comercializou-se cerca de 4 toneladas de repolho roxo, enquanto que em 2017 esse número saltou para 47 toneladas. Além do aumento da produção e demanda do produto, é válido ressaltar que esse é um produto de alto valor agregado, uma vez que, é vendido em mercados varejistas por até quatro vezes mais que o repolho verde, por exemplo (CEAGESP, 2020).

Os compostos responsáveis pelo potencial bioativo de açaí e repolho roxo são sensíveis a luz, umidade, altas temperaturas e exposição ao oxigênio. Com a degradação desses compostos o produto final perde propriedades bioativas, valor nutricional e também econômico. Nesse sentido, as análises de controle de qualidade desempenham papel fundamental. Para a quantificação de classes específicas de compostos bioativos como antocianinas, flavonois, taninos, entre outros, a cromatografia líquida de alta eficiência (HPLC) é um dos métodos mais utilizados, para a separação, identificação e quantificação de compostos individuais pertencentes a essas classes de compostos. Enquanto, que para a quantificação dos mesmos de forma mais geral, como compostos fenólicos totais ou antocianinas totais, entre outros, são utilizadas técnicas de espectrofotometria no visível. Já para a determinação da capacidade antioxidante atribuída a esses compostos são utilizadas técnicas como: ORAC (Oxygen Radical Absorbance Capacity), baseada em propriedade de transferência de hidrogênio, TEAC (Trolox Equivalent Antioxidant Capacity), baseada em

propriedade de transferência de elétron, ou técnicas que agem por ambos mecanismos como DPPH (2,2-diphenyl-picrylhydrazyl) (PALLONE; CARAMÊS; ALAMAR, 2018; SCHAICH; TIAN; XIE, 2015). Já para o controle de qualidade e autenticidade de arroz, os métodos mais utilizados são a cromatografia líquida de alta eficiência e cromatografia a gás (HPLC e CG), testes enzimáticos e técnicas de DNA são as técnicas analíticas classicamente empregadas (HUSSAIN; SUN; PU, 2019).

Apesar dessas técnicas serem tradicionalmente usadas para controle de qualidade de alimentos, elas envolvem processo de extração, que demanda uma quantidade relevante de reagentes químicos, muitas vezes nocivos tanto ao ambiente quanto ao analista, equipamentos que podem ter custo elevado, como as leitoras de microplacas, necessidade de um manipulador treinado, além de um elevado tempo para obtenção de resultados. Para a determinação tradicional do teor de compostos fenólicos e de antocianinas totais e capacidade antioxidante, a amostra passa por uma extração inicial que geralmente é feita com solvente orgânicos polares (ex.: etanol, metanol e acetona), que pode variar entre diferentes amostras, acidificados ou não (ex.: ácido trifluoracético, ácido acético). Os solventes utilizados nessa etapa apresentam diferentes níveis de toxicidade que podem causar risco ao manipulador e gerar resíduos tóxicos ao ambiente que necessitarão de posterior tratamento adequado. Seguindo a etapa de extração, a determinação dos compostos e da capacidade antioxidante é geralmente feita em espectrofotômetro/fluorímetro, sendo muitas vezes empregada a uma leitora de microplacas ou em cromatógrafo à líquido de alta eficiência (HPLC), equipamentos que podem exigir um alto grau de treinamento por parte do operador, além de um alto investimento na aquisição de alguns dos equipamentos (GIULIANI; CERRETANI; CICHELLI, 2016; SHIBAMOTO; BJELDANES, 2014).

Situação similar é encontrada para a quantificação de minerais em alimentos, onde é necessário um extenso processo de preparo de amostra, incluindo a mineralização, onde são utilizados ácidos fortes, como o ácido nítrico, agentes oxidantes, como peróxido de hidrogênio, e elevadas temperaturas. Além de gerar resíduos tóxicos, alto risco ao operador e consumir um elevado tempo durante a mineralização, a quantificação de minerais demanda a utilização de equipamento específico, como o espectrofotômetro de absorção atômica com chamas (Flame Atomic Absorption Spectrometry - FAAS), que exige alto grau de treinamento do analista (COSTA et al., 2019).

Nesse âmbito, opções alternativas, como a possibilidade de realização de análises referentes ao potencial antioxidante de alimentos, com emprego de espectroscopia no infravermelho (IV), imagens hiperespectral e digital, associada à quimiometria, em substituição aos métodos tradicionais pode ser avaliada. A espectroscopia no infravermelho pode ser realizada como ferramenta analítica com utilização da região do infravermelho médio (MIR) e infravermelho próximo (NIR).

As técnicas de espectroscopia vibracional, como MIR e NIR, de maneira geral, se destacam como técnica verde, com possibilidade de aplicação no controle de qualidade e avalição da capacidade antioxidante, em substituição os métodos tradicionais, podem ser avaliadas. Entre as vantagens da técnica se destacam ainda a rapidez, possibilidade de avaliação de vários parâmetros, não necessitam de preparo de amostra e não geram resíduos. A espectroscopia no infravermelho também tem sido cada vez mais aplicada em avaliações de casos de fraudes em alimentos, demonstrando eficiência e aplicabilidade tanto na detecção quanto na quantificação de substâncias fraudulentas, assim como na quantificação de minerais.(PALLONE; CARAMÊS; ALAMAR, 2018).

Já as imagens são derivadas da radiação do espectro eletromagnético, tanto na faixa do visível quanto do não visível. Análises visuais são uma das formas mais exploradas de determinar-se parâmetros de qualidade e aspectos importantes de um alimento dentro da indústria, tradicionalmente parâmetros que pudessem ser avaliados visualmente eram determinados por pessoas treinadas, mas isso vem sendo modificado com o advento dos sistemas de imagem eletrônicos, e hoje podem ser realizadas visualmente por pessoas ou através da análise de imagens. As imagens podem ser adquiridas em duas dimensões (2D), onde a coordenada x e y formam um pixel, ou em três dimensões (3D), onde as coordenadas x, y e z formam um voxel, independentemente disso cada imagem tem uma informação espectral específica que pode consistir em uma medida única como em sistemas RGB (red-green-blue) ou em vários canais espectrais como em sistemas hiperespectrais. Nesse sentido, sistemas de imagens hiperespectrais normalmente coletam dados na faixa de 11000 cm-1 – 4000 cm-1, quando combinado com técnicas espectroscópicas a sensibilidade desses sistemas é potencializada, uma vez que informações sobre a superfície da amostra se tornam mais acessíveis, permitindo a visualização da distribuição de componentes químicos da amostra. Já as imagens digitais, a partir da década de 80, começaram a ser processadas em cores, normalmente utilizando três coordenadas: vermelho-verde-azul (RGB, Red-Green-Blue) por cada pixel constituinte da imagem, com o advento da revolução tecnológica e

desenvolvimento da capacidade de processamento dos computadores a análise de imagens se tornou possível, representando a imagem através de valores numéricos ou gráficos que permitem que essas informações sejam utilizadas para a construção de modelos matemáticos utilizados para classificações ou predição de parâmetros de qualidade do produto/objeto fotografado (ARAÚJO et al., 2018; PALLONE; CARAMÊS; ALAMAR, 2018; PRATS-MONTALBÁN; DE JUAN; FERRER, 2011).

Assim, tendo em vista a elevada importância nutricional e potencial bioativo do repolho roxo e do açaí em função dos compostos bioativos presentes, relevância econômica dos produtos, a aplicação da técnica verde de espectroscopia no infravermelho e de imagens digitais, associadas a ferramentas quimiométricas, para a construção de modelos de classificação e calibração multivariadas que demonstrem o desempenho das técnicas para aplicação pode contribuir para a substituição de métodos tradicionais. Além disso, a avaliação da viabilidade de uso da espectroscopia no infravermelho para a predição não convencional de minerais essenciais (cálcio, potássio, manganês e ferro) em polpa de açaí, pode fornecer ferramentas para o rápido controle de qualidade nutricional do produto. Ademais, considerando a crescente valorização de arroz integral orgânico e polpa de açaí, a avaliação da viabilidade de uso de espectroscopia no infravermelho e imagens hiperespectrais, para a detecção de adulterações nos produtos, poderia contribuir para a segurança no consumo da polpa e arroz integral, com aplicação de método rápido e não destrutivo, para a detecção de não conformidade do produto.

2. OBJETIVOS

2.1. OBJETIVO GERAL

Esta tese tem como objetivo geral avaliar a possibilidade de emprego da espectroscopia vibracional, nas regiões do infravermelho próximo e médio, além de imagens digitais, para estimar o potencial bioativo, capacidade antioxidante em alimentos e detecção de fraude, como alternativa aos métodos tradicionais.

2.2. OBJETIVOS ESPECÍFICOS

- Desenvolver modelos de calibração para a determinação de antocianinas e polifenóis totais, ORAC, DPPH e TEAC de repolho roxo, com uso de dados espectrais obtidos por espectroscopia no infravermelho próximo (NIR) e médio (MIR) e aplicação do método de regressão PLS (Partial Least Square).

-Construção de cartas de controle multivaradas e modelos de classificação através dos métodos de PLS-DA (Partial Least Square- Discriminant Analysis) e KNN (K-Nearest Neighbor), baseados nos dados espectrais de NIR e MIR, para a detecção fraudes por adulteração em polpas de açaí adulteradas.

-Utilização dos dados espectrais NIR e imagens digitais para a criação de modelos de calibração para a predição de antocianinas e polifenóis totais, ORAC, DPPH e TEAC de polpa de açaí liofilizada, através do método de regressão PLS.

- Quantificação de minerais essenciais, com emprego de método tradicional de análise de FAAS (Flame Atomic Absorption Spectroscopy) e utilização dos dados obtidos para o desenvolvimento de modelos de classificação para a verificação da possibilidade de uso da técnica para a detecção de adulteração em polpas de açaí liofilizadas.

-Construção de modelos de regressão PLS, baseados nas informações de espectros obtidos no NIR, para a predição de minerais essenciais majoritários em polpa de açaí, como alternativa ao rápido controle de qualidade nutricional do produto.

-Utilização de espectros NIR e imagens hiperespectrais para a determinação de modelos PLS-DA para a discriminação entre arroz integral orgânico e convencional, como alternativa verde e rápida para a garantia de qualidade do produto.

3. REFERÊNCIAS

ARAÚJO A, MARINHO W, DE ARAÚJO GOMES A: A Fast and Inexpensive Chemometric-Assisted Method to Identify Adulteration in Acai (*Euterpe oleracea*) Using Digital Images. **Food Anal Methods** 2017, doi:10.1007/s12161-017-1127-4.

CEAGESP. **Guia da CAGESP**. 2020. Disponível em: http://www.ceagesp.gov.br/guia-ceagesp/repolho-roxo/.

CONAB. **Conjuntura mensal do açai**. 2016. Disponível em: http://www.conab.gov.br/conteudos.php?a=526&ordem=titulo. Acesso em: 24 mar. 2017.

COSTA, Maria Cristina A.; MORGANO, Marcelo A.; FERREIRA, Marcia Miguel C.; MILANI, Raquel F. Quantification of mineral composition of Brazilian bee pollen by near infrared spectroscopy and PLS regression. **Food Chemistry**, *[S. l.]*, v. 273, n. July 2017, p. 85–90, 2019. DOI: 10.1016/j.foodchem.2018.02.017. Disponível em: https://doi.org/10.1016/j.foodchem.2018.02.017.

DE OLIVEIRA, Maria do S. P.; SCHWARTZ, Gustavo. Açaí— Euterpe oleracea. *In*: **Exotic Fruits**. [s.l.] : Elsevier, 2018. p. 1–5. DOI: 10.1016/B978-0-12-803138-4.00002-2. Disponível em: http://linkinghub.elsevier.com/retrieve/pii/B9780128031384000022. Acesso em: 17 abr. 2018.

GIULIANI, A.; CERRETANI, L.; CICHELLI, A. Colors: Properties and Determination of Natural Pigments A2 - Caballero, Benjamin. *In*: FINGLAS, Paul M.; TOLDRÁ, Fidel (org.). Oxford: Academic Press, 2016. p. 273–283. Disponível em: http://www.sciencedirect.com/science/article/pii/B9780123849472001896. Acesso em: 11 mar. 2016.

HUSSAIN, N.; SUN, Da Wen; PU, Hongbin. Classical and emerging non-destructive technologies for safety and quality evaluation of cereals: A review of recent applications. **Trends in Food Science and Technology**, *[S. l.]*, v. 91, n. February, p. 598–608, 2019. DOI: 10.1016/j.tifs.2019.07.018. Disponível em: https://doi.org/10.1016/j.tifs.2019.07.018.

KATT, Felix; MEIXNER, Oliver. A systematic review of drivers influencing consumer willingness to pay for organic food. **Trends in Food Science and Technology**, *[S. l.]*, v. 100, n. July 2019, p. 374–388, 2020. DOI: 10.1016/j.tifs.2020.04.029. Disponível em: https://doi.org/10.1016/j.tifs.2020.04.029.

KUSHWAH, Shiksha; DHIR, Amandeep; SAGAR, Mahim; GUPTA, Bhumika. Determinants of organic food consumption. A systematic literature review on motives and barriers. **Appetite**, *[S. l.]*, v. 143, n. October 2018, p. 104402, 2019. DOI: 10.1016/j.appet.2019.104402. Disponível em: https://doi.org/10.1016/j.appet.2019.104402.

KÜSTER, Inés; VILA, Natalia; SARABIA, Francisco. Food packaging cues as vehicles of healthy information: Visions of millennials (early adults and adolescents). **Food Research International**, *[S. l.]*, v. 119, n. November 2018, p. 170–176, 2019. DOI: 10.1016/j.foodres.2019.01.051. Disponível em: https://doi.org/10.1016/j.foodres.2019.01.051.

LOBATO, Kleidson Brito de Sousa; ALAMAR, Priscila Domingues; CARAMÊS, Elem Tamirys dos Santos; PALLONE, Juliana Azevedo Lima. Authenticity of freeze-dried açai pulp by near-infrared spectroscopy. **Journal of Food Engineering**, *[S. l.]*, v. 224, p. 105–111, 2018. DOI: 10.1016/j.jfoodeng.2017.12.019.

PALLONE, Juliana Azevedo Lima; CARAMÊS, Elem Tamirys dos Santos; ALAMAR,

Priscila Domingues. Green analytical chemistry applied in food analysis: alternative techniques. **Current Opinion in Food Science**, *[S. l.]*, v. 22, n. Figure 1, p. 115–121, 2018. DOI: 10.1016/j.cofs.2018.01.009.

PASTORELLI, Augusto Alberto; ANGELETTI, Roberto; BINATO, Giovanni; MARIANI, Maurizio Boccacci; CIBIN, Veronica; MORELLI, Stefania; CIARDULLO, Silvia; STACCHINI, Paolo. Exposure to cadmium through Italian rice (Oryza sativa L.): Consumption and implications for human health. **Journal of Food Composition and Analysis**, *[S. l.]*, v. 69, n. April 2017, p. 115–121, 2018. DOI: 10.1016/j.jfca.2018.02.005. Disponível em: https://doi.org/10.1016/j.jfca.2018.02.005.

PRATS-MONTALBÁN, J. M.; DE JUAN, A.; FERRER, A. Multivariate image analysis: A review with applications. **Chemometrics and Intelligent Laboratory Systems**, *[S. l.]*, v. 107, n. 1, p. 1–23, 2011. DOI: 10.1016/j.chemolab.2011.03.002.

REBELLATO, Ana Paula; CARAMÊS, Elem Tamirys dos Santos; MORAES, Priscila Probio De; PALLONE, Juliana Azevedo Lima. Minerals assessment and sodium control in hamburger by fast and green method and chemometric tools. **Lwt**, *[S. l.]*, v. 128, n. October 2019, p. 109438, 2020. DOI: 10.1016/j.lwt.2020.109438. Disponível em: https://doi.org/10.1016/j.lwt.2020.109438.

ROGEZ, Hervé. **Açaí- Preparo, Composição, Melhoramento da consevação**. Belém: Editora da Universidade Federal do Pará, 2000.

SCHAICH, K. M.; TIAN, X.; XIE, J. Hurdles and pitfalls in measuring antioxidant efficacy: A critical evaluation of ABTS, DPPH, and ORAC assays. **Journal of Functional Foods**, *[S. l.]*, v. 14, p. 111–125, 2015. DOI: 10.1016/j.jff.2015.01.043.

SCHAUSS, Alexander G. Chapter 10 - Advances in the study of the health benefits and mechanisms of action of the pulp and seed of the Amazonian palm fruit, Euterpe oleracea Mart., known as “Açai”. *In*: WATSON, Ronald Ross; PREEDY, Victor R. (org.). [s.l.] : Academic Press, 2016. p. 179–220. Disponível em: http://www.sciencedirect.com/science/article/pii/B978012802972500010X. Acesso em: 24 mar. 2017.

SHAMAH, Teresa; VILLALPANDO, Salvador; DE LA CRUZ, Vanessa. Anemia. **International Encyclopedia of Public Health**, *[S. l.]*, v. 1, p. 103–112, 2016. DOI: 10.1016/B978-0-12-803678-5.00018-7.

SHIBAMOTO, Takayuki; BJELDANES, Leonard F. Capítulo 2 - Determinação de Agentes Tóxicos Presentes nos Alimentos. *In*: Rio de Janeiro: Elsevier Editora Ltda., 2014. p. 31–50. Disponível em: http://www.sciencedirect.com/science/article/pii/B9788535271188000026. Acesso em: 11 mar. 2016.

TEYE, Ernest; AMUAH, Charles L. Y.; MCGRATH, Terry; ELLIOTT, Christopher. Innovative and rapid analysis for rice authenticity using hand-held NIR spectrometry and chemometrics. **Spectrochimica Acta - Part A: Molecular and Biomolecular Spectroscopy**, *[S. l.]*, v. 217, p. 147–154, 2019. DOI: 10.1016/j.saa.2019.03.085. Disponível em: https://doi.org/10.1016/j.saa.2019.03.085.

VERMA, Deepak Kumar; SRIVASTAV, Prem Prakash. Bioactive compounds of rice (Oryza sativa L.): Review on paradigm and its potential benefit in human health. **Trends in Food Science and Technology**, *[S. l.]*, v. 97, n. January, p. 355–365, 2020. DOI: 10.1016/j.tifs.2020.01.007. Disponível em: https://doi.org/10.1016/j.tifs.2020.01.007.

WICZKOWSKI, Wieslaw; TOPOLSKA, Joanna; HONKE, Joanna. Anthocyanins profile and antioxidant capacity of red cabbages are influenced by genotype and vegetation period. **Journal of Functional Foods**, *[S. l.]*, v. 7, p. 201–211, 2014. DOI: 10.1016/j.jff.2014.02.011. Disponível em: http://www.sciencedirect.com/science/article/pii/S1756464614000619. Acesso em: 13 mar. 2017.

YONG, Huimin; LIU, Jun. Recent advances in the preparation, physical and functional properties, and applications of anthocyanins-based active and intelligent packaging films. **Food Packaging and Shelf Life**, *[S. l.]*, v. 26, n. April, p. 100550, 2020. DOI: 10.1016/j.fpsl.2020.100550. Disponível em: https://doi.org/10.1016/j.fpsl.2020.100550.

CAPÍTULO II
Revisão Bibliográfica

O aumento da preocupação da população com a escolha de um estilo de vida mais saudável têm feito com que a demanda por alimentos que se encaixem em uma dieta balanceada aumente. Nesse cenário, entende-se por dieta balanceada a ingestão regular de alimentos que provenham energia suficiente para a manutenção das atividades diárias do indivíduo, assim como, os nutrientes necessários para as atividades biológicas do corpo (BVENURA; SIVAKUMAR, 2017).

Sendo assim, é inquestionável o papel fundamental exercido pelos grãos e vegetais dentro da nutrição humana. Arroz integral, repolho roxo e açaí, se mostram como relevantes opções de alimentos com qualidades nutricionais capazes de agregar positivamente ao corpo humano através de efeitos benéficos a saúde produzidos pelos compostos bioativos presentes nesses produtos (DELSHADI et al., 2020).

A coloração roxa característica marcante do açaí e do repolho roxo são consequência da concentração elevada de antocianinas, uma classe de composto fenólico que tem efeito antioxidante, antimutagênico, antiproliferativo e antimicrobiano (KLJUSURIĆ et al., 2016). Ademais, repolho roxo tem em sua composição vitaminas, glicosinolatos e sulfurosos (RADZIEJEWSKA-KUBZDELA; BIEGAŃSKA-MARECIK, 2015). Já o açaí apresenta um bom perfil de ácidos graxos insaturados e minerais, com destaque para os essenciais magnésio e cálcio, mas também merecem destaque as concentrações de cobre e manganês (DA SILVA SANTOS; DE ALMEIDA TEIXEIRA; BARBOSA, 2014).

O arroz é um dos cereais mais consumidos no mundo, é considerado um alimento base por estar presente na alimentação básica de vários países. A busca por alimentos mais saudáveis tem impulsionado o aumento do consumo desse grão na versão orgânica e integral, uma vez que o arroz apresenta vitaminas (tiamina, riboflavina, niacina e vitamina E), minerais (ferro e zinco), aminoácidos (lisina, metionina, triptofano) e fibras (SEN; CHAKRABORTY; KALITA, 2020).

A maioria dos compostos bioativos, no entanto, podem ser degradados durante a cadeia de produção, desde o pós colheita até as condições de armazenamento (ALAMAR et al., 2016a). Além disso, a valorização desses produtos têm feito com que eles se tornem cada vez mais suscetíveis a fraudes, casos já foram relatados em polpa de açaí e arroz (CARAMÊS; ALAMAR; PALLONE, 2019; TEYE et al., 2019). Nesse cenário, a necessidade de métodos analíticos capazes de garantir a qualidade desses alimentos tem sido cada vez mais urgente (WADOOD et al., 2020).

Informações referentes à legislação para a garantia da qualidade desses produtos torna obrigatória a realização de análises físico-químicas, como avaliação de proteínas, lipídeos, sólidos totais, açúcares totais, acidez. No caso do açaí, há ainda a necessidade de análises específicas para determinação antocianinas e fenólicos totais como parte das análises do padrão de identidade e qualidade de polpa de açaí (BRASIL, 2000; BRASIL, 2018). No caso de alimentos orgânicos, que devem ser produzidos livres da utilização de fertilizantes, agrotóxicos e outros produtos químicos (ou fazendo uso somente dos previstos em lei), faz-se necessários métodos analíticos capazes de detectar resíduos do uso desses produtos ou capazes de diferenciar orgânicos de convencionais (BRASIL, 2014).

Geralmente, as técnicas analíticas mais utilizadas no controle de qualidade e detecção de fraude de alimentos nos últimos anos incluem cromatografia líquida e gasosa de alta eficiência (HPLC e CG*)*, testes enzimáticos (como ELISA), técnicas baseadas no DNA e análises elementares, baseadas em titulação, partição, secagem, entre outros (WADOOD et al., 2020). Apesar dessas técnicas serem eficientes e sensíveis, apresentam as desvantagens de serem invasivas e destrutivas, demoradas e utilizarem diversos reagentes químicos durante processos de *clean-up*, derivatização e/ou extração, que podem resultar na produção de resíduos tóxicos (PALLONE; CARAMÊS; ALAMAR, 2018a).

Considerando a crescente preocupação com conceitos de sustentabilidade e química analítica verde, a indústria 4.0 (ou quarta revolução industrial) busca o desenvolvimento de novas tecnologias capazes de melhorar a produção e, simultaneamente, diminuam os efeitos adversos ao meio ambiente, através da implementação de ferramentas mecanizadas, rápidas, verdes e com boa adaptação para processos on-line (KAKANI et al., 2020).

Nesse sentido, técnicas como a espectroscopia no infravermelho (próximo e médio), associado ou não a imagem hiperespectral, além de imagem de *smartphone*, surgem como alternativas aos métodos tradicionalmente utilizados no controle de qualidade da indústria de alimentos, uma vez que apresentam vantagens como mínimo (ou nenhum) preparo de amostra, não geração de resíduos e por permitirem, em sua maioria, tanto a aplicação *in situ* quanto para sistemas on-line (HUSSAIN; SUN; PU, 2019). Sendo assim, nas últimas décadas fez-se necessária a realização de estudos que avaliem a aplicabilidade dessas técnicas em substituição aos métodos tradicionais nas mais diversas possibilidades dentro do segmento alimentício (HUSSAIN; SUN; PU, 2019; KAKANI et al., 2020; PALLONE; CARAMÊS; ALAMAR, 2018c).

1. ALIMENTOS DE ALTO VALOR AGREGADO

1.1. REPOLHO ROXO

O repolho (*Brassica oleracea* var *rubra*) pertence a família Brassicaceae, é originária da costa norte do Mediterrâneo, da Ásia menor e da cos Ocidental Europeia. Naturalmente a espécie se adapta melhor ao clima temperado, no entanto, hibridizações permitiram a adaptação da espécie a regiões com temperaturas elevadas (KUSTER et al., 2018).

Os maiores produtores mundiais são China, Rússia e Índia (FAOSTAT, 2017). A produção brasileira é de cerca de 420 toneladas ao ano, com mais de 20 mil hectares de área cultivada, os maiores estados produtores são São Paulo, Paraná e Minas Gerais. Essa hortaliça é facilmente encontrada nos cinturões verdes de todas as capitais nacionais, uma vez que apresenta um baixo custo de produção (KIST et al., 2018).

O repolho roxo é uma fonte de vitaminas C e E, carotenoides, fibras e minerais, como o cálcio. Apresenta ainda alta concentração de antocianinas, que é uma classe flavonoides hidrofilicos. Esses compostos, no repolho roxo, estão tipicamente presentes na forma de cianidinas glicosiladas que podem ser mono ou di aciladas com ácidos hidroxicinâmicos, conferindo um excelente perfil nutricional (STRAUCH et al., 2019).

Alguns estudos apontam para bons efeitos farmacológicos do repolho roxo, como efeitos antioxidantes, anti inflamatório, a indução a apoptose de células leucêmicas (WICZKOWSKI; TOPOLSKA; HONKE, 2014). O consumo desse vegetal aumenta a concentração de antocianinas no plasma sanguíneo e isso tem sido associado ao aumento da atividade antioxidante plasmática e consequente redução do estresse oxidativo do corpo (WICZKOWSKI; SZAWARA-NOWAK; ROMASZKO, 2016). Enquanto, o extrato desse vegetal já mostrou potencial para reduzir as lesões intestinais causadas pelos efeitos tóxicos decorrentes do tratamento quimioterápico de câncer de cólon (TONG et al., 2017) .

Consequentemente, o repolho roxo tem atraído a atenção de consumidores que buscam maior qualidade nutricional dos alimentos ingeridos diariamente. É um ingrediente que pode ser consumido cru ou cozido, em saladas, mas que também é comumente processado industrialmente, podendo ser fermentado ou liofilizado, e aplicado como suplemento alimentar ou corante natural na preparação de outros produtos, como sucos de frutas (RADZIEJEWSKA-KUBZDELA; BIEGAŃSKA-MARECIK, 2015; WICZKOWSKI; SZAWARA-NOWAK; ROMASZKO, 2016).

No entanto, os compostos presentes no repolho roxo podem sofrer degradação ou alterar a sua biodisponibilidade de acordo com o processamento aplicado industrialmente ou durante preparações domésticas, uma vez que são sensíveis a altas temperaturas, oxigênio e exposição a luz. Por exemplo, durante o cozimento do repolho roxo em vapor a concentração de fenólicos totais diminui, em relação a concentração no vegetal cru, devido a exposição a altas temperaturas. Esse processo de degradação é acentuado quando o cozimento é realizado por fervura, uma vez que o efeito de lixiviação dos compostos na água de cozimento é maior do que no cozimento a vapor (MURADOR; MERCADANTE; DE ROSSO, 2016).

Nesse contexto, apesar de o repolho roxo atender a crescente demanda por um estilo de vida saudável e sustentável, é importante a utilização de métodos analíticos alternativos sustentáveis capazes de avaliar a qualidade nutricional e potencial bioativo do produto (HANSCHEN, 2020; RADZIEJEWSKA-KUBZDELA; BIEGAŃSKA-MARECIK, 2015).

1.2. ARROZ INTEGRAL

O arroz (*Oryza sativa* L.) é um dos grãos mais populares do mundo, considerado como item básico da dieta de diversos países, especialmente da região Asiática, do Caribe e América Latina, onde, na dieta da população, representa uma das principais fontes de energia. Na Ásia encontram-se os maiores produtores mundiais do grão, sendo eles: China (207 milhões de toneladas), que produz cerca de 28% da produção mundial de arroz, seguida por Índia (157 milhões de toneladas) e Indonésia (70 milhões de toneladas). O Brasil, que tem destaque entre os países produtores de arroz na América Latina, é o maior produtor de arroz do Mercado do Cone Sul (Mercosul), com cerca de 12,2 milhões de toneladas produzidas, correspondendo a 42% do arroz produzido na América Latina e Caribe (EMBRAPA, 2016; SEN; CHAKRABORTY; KALITA, 2020).

O gênero *Oryza*, atualmente, é composto por 23 espécies, com diferentes genótipos. Dentre as mais encontradas no mercado estão os: arroz branco polido, parbolizado ou integral, arroz preto, vermelho, moti (próprio para a culinária japonesa), cateto, carnaroli e arbóreo (apropriado para risotos), tipos aromáticos (basmati e jasmim) (FRANCO et al., 2012). O consumo de arroz representa uma importante fonte de carboidratos para os seus consumidores, além de ser uma boa alternativa para a ingestão de nutrientes como as fibras, minerais (zinco e ferro), proteínas, vitaminas (tiamina, riboflavina, niacina e vitamina E) e antioxidantes (fitoesterois, tocoferóis e antocianinas, especialmente nas variedades vermelho e preto) (SEN; CHAKRABORTY; KALITA, 2020).

O mercado brasileiro ainda é pouco variado para o consumo de arroz, os mais procurados são o arroz branco polido, parbolizado e integral, enquanto as outras variedades se configuram como mercados de nicho (FRANCO et al., 2012). O grão de arroz é composto por cariopse, formada pelas camadas pericarpo, tegumento e aleurona, casca, que representa 20% do peso do grão, além de endosperma e gérmen (Figura 1). Durante o processamento do arroz é realizado o descascamento, onde retira-se a casca do grão e é obtido o arroz integral. Após polimento e retirada do farelo (pericarpo, tegumento, camada de aleurona e gérmen) é obtido o arroz branco polido. Para a obtenção do arroz branco parbolizado os grãos polidos são submetidos a um processo hidrotérmico, uma espécie de pré-cozimento, com a intenção de diminuir o tempo de cozimento (WALTER; MARCHEZAN; DE AVILA, 2008).

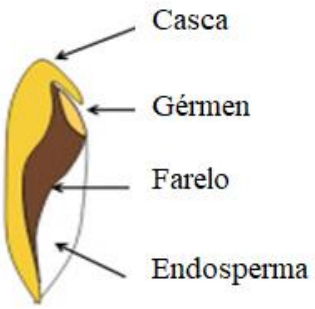

Figura 1. Estrutura do grão de arroz. Fonte: adaptado de PEANPARKDEE; IWAMOTO (2019).

Sendo assim, dentre as variedades de arroz mais consumidos no Brasil, o branco integral tem ganhado bastante destaque pela sua qualidade nutricional, uma vez que, quando comparado ao arroz branco polido, apresenta maiores concentrações de fibras insolúveis e compostos fenólicos, uma vez que os últimos apresentam-se naturalmente ligados aos componentes estruturais, como celulose, lignina e proteínas, que estão presentes nas camadas mas externas dos grãos de arroz, que são retirados durante o processamento do arroz branco polido (GONG et al., 2017).

O arroz integral, devido a sua alta concentração de ácido gama-aminobutírico e compostos fenólicos, atua no controle de índice glicêmico provocado pela ingestão da alta concentração de carboidratos, encontrados no grão. Com isso, o consumo regular de arroz integral tem sido associado a uma diminuição no risco na ocorrência de doenças de desordem metabólica, como a diabetes (NAKAYAMA et al., 2017). Além disso, os compostos fenólicos presentes no arroz integral também são associados a efeitos antioxidantes e hepato-protetivos (SEN; CHAKRABORTY; KALITA, 2020).

Outro fator determinante para o consumidor que busca um estilo de vida mais saudável é a forma com que esse grão foi produzido, com isso, a preferência pelo consumo de produtos orgânicos tem crescido. A ausência da utilização de produtos químicos como fertilizantes, pesticidas e herbicidas que caracteriza a produção de orgânicos, faz com que esse segmento tenha um apelo saudável no mercado (KUSHWAH et al., 2019).

Esse contexto conduz o arroz integral orgânico a uma valorização econômica por aumento de demanda, e nesse sentido, o torna alvo de fraudes, seja por adição de arroz convencional, grãos de menor qualidade ou outros materiais. Com isso, há a necessidade de estratégias analíticas capazes de detectar fraudes e garantir a produção e consumo de produtos de maior qualidade (TEYE et al., 2019).

1.3. AÇAÍ

O açaí é o fruto de uma palmeira (*Euterpe oleracea*) comumente encontrada na região amazônica, particularmente abundante na parte oriental da bacia. O açaizeiro predomina em solos de várzea, mas também são encontrados em terra firme e igapó. A palmeira do açaí produz touceira com até 25 estipes, cujos perfilhos apresentam diferentes estágios de desenvolvimento (OLIVEIRA et al., 2002). A produção dos frutos ocorre a partir do terceiro ano de cultivo da palmeira em cachos contendo centenas de frutos e a produção máxima ocorre no quinto e sexto ano da palmeira. Cada fruto apresenta-se na forma globular, com diâmetro entre 1-2 cm e peso médio de 0,8-2,3g. O epicarpo, porção violácea- púrpura, e o mesocarpo formam a porção comestível do fruto, e, juntos, equivalem a 5-15% do volume total do fruto (COSTA et al., 2017; CUNHA JÚNIOR et al., 2016).

A produção de açaí é predominantemente extrativista, porém desde 1995 o cultivo racional do açaizeiro vem se intensificando. Com isso, o açaizeiro tem sido plantado em terra firme no Norte do Brasil e em estados brasileiros do Nordeste e Centro-Oeste. Contudo, os principais estados produtores de açaí continuam sendo o Acre, Amapá, Amazonas, Maranhão, Pará e Rondônia. Dentre esses, o estado do Pará é o maior produtor de açaí, com cerca de 850 toneladas, gerando um valor aproximado de R$ 677,2 milhões para a economia paraense.(OLIVEIRA et al., 2002; PAGLIARUSSI, 2010).

O principal destino do açaí é a produção de polpa que é o produto da extração da parte comestível do fruto do açaizeiro após amolecimento através de processos tecnológicos adequados. É comumente obtida através de um despolpamento, seguido por filtragem, homogeneização e envase. A polpa de açaí tem alta perecibilidade e por isso é comumente

comercializada congelada, quando destinada ao mercado interno, ou liofilizada, quando destinada ao mercado externo (BEZERRA, 2007; BRASIL, 2018).

A fim de garantir a qualidade das polpas de frutas comercializadas no Brasil, o Ministério da Agricultura, Pecuária e Abastecimento (MAPA) estabeleceu através da instrução normativa nº1, de 7 de janeiro de 2000 o Padrão de Identidade e Qualidade (PIQ) mínimos para a polpa de açaí destinada ao consumo como bebida. Dentre as características físico-químicas regidas pela legislação brasileira estão: sólidos totais, proteínas, lipídios totais, carboidratos totais e pH. Dentre essas o teor de sólidos totais (ST) é a responsável pela classificação de açaí em diferentes em 3 categorias: grosso ou especial (ST>14%), médio ou regular (11-14%) e fino ou popular (8-11%), como apresentado na Tabela 1. Dentre essas três categorias o açaí tipo grosso é o que apresenta o maior valor agregado e a aparência mais densa (BRASIL, 2000; BRASIL, 2018).

Tabela 1. Padrão de Identidade e Qualidade polpa de açaí (Brasil, 2000).

	Sólidos totais (g/100g)	
	Máximo	**Mínimo**
Açaí grosso ou especial	-	14%
Açaí médio ou regular	14%	11%
Açaí fino ou popular	11%	8%

A tendência mundial de consumo de produtos saudáveis vai de encontro ao consumo regular de açaí, tendo em vista, a sua alta qualidade nutricional. No açaí há a presença massiva de compostos bioativos como as antocianinas, principalmente as cianidina-3-glicosídeo e cianidina-3-rutinosídeo, que são as principais responsáveis pela sua alta capacidade antioxidante. O açaí apresenta ainda quantidade significativa de lipídios em sua composição (20-60% em base seca); dentre os principais grupos de ácidos graxos encontrados estão os ômega-9, ômega-6 e ômega-3, com destaque para ácido α-linolênico, linoleico, araquidônico e ácido oleico, que são considerados essenciais para o bom funcionamento do organismo, auxiliando a prevenção de algumas doenças. Além disso, o alto teor lipídico faz com que o açaí seja uma boa fonte de vitaminas lipossolúveis A, D, E e K. É válido destacar ainda o perfil de composição mineral do açaí, rico em cálcio, ferro, magnésio, zinco, ademais há a presença de cobre e manganês (BORGES et al., 2016; SANTOS et al., 2014; YAMAGUCHI et al., 2015).

2. MÉTODOS ANALÍTICOS TRADICIONAIS PARA CONTROLE DE QUALIDADE E IDENTIDADE EM ALIMENTOS

O Brasil começou em meados da década de 70 a determinar regras e regulamentações que dispõem a respeito da qualidade de produtos e serviços, como a estipulação de regras de rotulagem, medidas sanitárias, ingredientes necessários, avaliação de parâmetros que poderiam classificar um produto em uma categoria específica. Essas normas são conhecidas como Padrão de Identidade e Qualidade (PIQ), que representam um conjunto de normas básicas de qualidade para produtos alimentícios no Brasil e têm como objetivo proteger a saúde do consumidor, minimizar possíveis divergências entre produtores e consumidores dos alimentos, além de auxiliar no mais adequado direcionamento dos órgãos fiscalizadores do poder público (DAVID; GUIVANT, 2020).

Com o advento dos anos 2000, o PIQ, sob regulamentação da Agência Nacional de Vigilância Sanitária (ANVISA) e do Instituto Nacional de Meteorologia, Qualidade e Tecnologia (INMETRO), começou a passar por um processo de mudança e flexibilização com o intuito de garantir a harmonização da legislação com os países integrantes do Mercosul, e com isso garantir maior qualidade diante do mercado internacional. O PIQ hoje determina a definição do produto e as suas principais características, como parâmetros físico-químicos (ex: percentual mínimo de sólidos totais ou percentual máximo de açúcares em polpas de frutas), ingredientes obrigatórios em algumas formulações, determina ainda as regras de rotulagem e normas específicas para que produtos possam declarar *diet*, *light* ou “rico em” (BRASIL, 2000; DAVID; GUIVANT, 2020).

No entanto, os parâmetros de qualidade estabelecidos pelo PIQ são comumente realizadas através de métodos analíticos tradicionais. Esses métodos variam entre os mais básicos e simples, como para a determinação de açúcares, proteínas e acidez total, que se baseiam em processos titulométricos, até a necessidade de técnicas mais refinadas, como para a determinação de minerais ou compostos fenólicos, que se baseiam no uso de técnicas de espectrometria e/ou cromatografia de alta eficiência (ALAMAR et al., 2016b).

Esses métodos analíticos, todavia, envolvem uma quantidade relevante de reagentes químicos nocivos tanto ao ambiente quanto ao analista, equipamentos com custo elevado, necessidade de um manipulador treinado, além de um elevado tempo para obtenção de resultados. Por exemplo, a determinação de sólidos totais em polpa de frutas, determinante na classificação de produtos como a polpa de açaí, e essencial para a detecção dos principais

tipos de fraudes alimentares nesse segmento, é usualmente executada pelo método descrito pela AOAC (método 934.06) onde a amostra é seca em estufa a 105ºC até atingir peso constante, esse processo requer um tempo elevado para execução inviabilizando uma fiscalização mais prática, segura, eficiente e *in loco* (AOAC, 1998).

Em outros casos como na determinação de minerais, os métodos analíticos mais comumente utilizados são a espectroscopia de absorção atômica de chama (FAAS), espectrometria de emissão ótica com plasma (ICP-OES) e espectrometria de massa com fonte de plasma (ICP-MS), que apesar de não apresentarem problemas quanto a sensibilidade, necessitam de um trabalhoso processo de preparo de amostra, como a mineralização, que faz uso de ácidos fortes e altas temperaturas, levando risco ao operador, produção de resíduos tóxicos e elevando o custo de análise (REBELLATO et al., 2020).

3. MÉTODOS ANALÍTICOS TRADICIONAIS PARA AVALIAÇÃO DE POTENCIAL BIOATIVO DE POLPA DE AÇAÍ E REPOLHO ROXO

O reflexo positivo do consumo regular de compostos bioativos na saúde, elevou ainda mais a importância desses compostos na indústria de alimentos. Eles são passíveis a degradação através da exposição a luz, ao oxigênio e também a elevadas temperaturas, ocasionando possíveis perdas desses compostos durante o processamento, estocagem e distribuição do alimento (BAO et al., 2019)**.**

Dada essa importância, alguns produtos como a polpa de açaí, já ganharam novos parâmetros de qualidade previstos no PIQ, que asseguram uma concentração mínima de antocianinas totais (0,44 g/100gms) e polifenóis totais (1,80 g/100gms) (BRASIL, 2018). Enquanto outros, como o repolho roxo, ainda não apresentam nenhum parâmetro de qualidade relacionado a composição bioativa.

No entanto, além da determinação antocianinas e polifenóis totais, é também comum a realização de análises relacionadas a capacidade antioxidante. Nesse sentido, análises como ORAC (Oxigen Radical Absorbance Capacity), DPPH (2,2-difenil-1-picril-hidrazila) e TEAC (Trolox Equivalent Antioxidant Capacity), entre outras, são executadas a fim de certificar um produto final com valor agregado maior e grande qualidade funcional.

No geral, para a determinação do teor de compostos fenólicos e de antocianinas totais e capacidade antioxidante, a amostra passa por uma extração inicial que geralmente é feita com solvente orgânicos polares (ex.: etanol, metanol e acetona) acidificados ou não

(ex.: ácido trifluoracético, ácido acético). Os solventes utilizados nessa etapa apresentam diferentes níveis de toxicidade que podem variar para diferentes amostras, causar risco ao manipulador e gerar resíduos tóxicos ao ambiente que necessitarão de tratamento adequado. Seguindo a etapa de extração, a determinação dos compostos e da capacidade antioxidante é geralmente feita em espectrofotômetro/fluorímetro ou em cromatógrafo à líquido de alta eficiência (HPLC), equipamentos que exigem grau de treinamento por parte do manipulador além de um alto investimento na aquisição de equipamentos (GIULIANI; CERRETANI; CICHELLI, 2016; SHIBAMOTO; BJELDANES, 2014). Ademais, todas as etapas de extração e de análise de compostos bioativos descritas demandam tempo (cerca de 2h para análises de capacidade antioxidante), que pode variar de acordo com a matriz alimentar e com o protocolo estabelecido.

4. FRAUDES EM ALIMENTOS E MÉTODOS ANALÍTICOS TRADICIONAIS PARA DETECÇÃO

Adulteração é a adição ou substituição de um ingrediente, elemento ou substância, especialmente, por outra de um valor inferior ou ingredientes inertes. Esse ato caracteriza uma fraude alimentar que é um termo genérico que engloba a substituição, adição, adulteração, ou informação falsa sobre o alimento, ingredientes do alimento ou embalagem e/ou falsas declarações sobre um produto para ganho econômico (SPINK; MOYER, 2011).

Na indústria de alimentos, esse é um problema antigo que permanece existente até os dias de atuais. Buscando aumentar as margens de lucro vários tipos de adulterações são realizadas, entre as mais comuns: mistura de alimentos degradados com frescos, substituição e ingredientes caros por outros de menor valor, introdução fraudulenta de aditivos ou corantes (SHIEBER, 2008).

As fraudes mais comuns estão associadas a falsas informações sobre a variedade e/ou espécie do produto ou dos ingredientes, da região de origem, sobre o processamento do produto, marcas e fraudes industriais- adição e/ou substituição de ingredientes sem declaração e/ou proibidos (ASHURST; DENNIS, 2013).

Nas últimas décadas vários casos de fraude alimentar foram divulgados e se tornaram conhecidos. Casos de diluição, como o de óleo de oliva com outros tipos de óleo, alguns potencialmente tóxicos, de substituição de ingredientes, como a substituição não declarada de óleo de girassol por óleo mineral ou de adição, como no caso da adição

irregular de melamina para repor conteúdo proteico de alimentos como o leite (ROBSON et al., 2020), entre outros.

Posto isso, a garantia da autenticação alimentar, ou seja, a garantia de que o produto foi produzido, transportado e vendido de forma tal que corresponde às expectativas associadas a ele, é uma preocupação constante e objeto de pesquisas. Produtos com designação de origem garantida, resultantes de um processo específico ou de origem exótica, são tidos como produtos de alto valor agregado e por isso são comumente alvos de fraude (DANEZIS et al., 2016; ELZAKKER et al., 2005).

Nesse sentido, o açaí como fruto de origem exótica, somado ao fato de ser um produto sazonal, tem sido alvo de fraudes. No caso das polpas de frutas em geral, a fraude mais recorrente se dá através da adição de água para aumentar o rendimento de polpa ou adição de açúcar para aumento do teor de sólidos solúveis, principalmente após uma diluição. Na polpa de açaí, várias fraudes são relatadas, além da adição de água para aumento do rendimento, há a adição de ingredientes, como farinha de tapioca, mandioca e/ou jornal, que aumentam o teor de sólidos totais e fazem com que polpas de açaí fino sejam classificadas como grosso ou médio (ALAMAR et al., 2016a; G1, 2014).

Outro alimento que vêm sendo alvo de fraudes, é o arroz. Fraudes em relação a origem geográfica, mistura de grãos de maior e menor qualidade e orgânicos com não orgânicos têm sido relatadas para as variedades de arroz branco e integral. A variação de arroz preto já foi fraudado através da adição de corante artificial preto sudão (TEYE et al., 2019; XIAO et al., 2019; ZHAO et al., 2019).

O métodos analíticos mais empregados atualmente para esse fim são os de cromatografia líquida de alta eficiência acoplados ou não a espectrometria de massas, técnicas de DNA e eletroforese capilar, que apesar de serem muito sensíveis e robustos, apresentam desvantagens como o alto custo e complexidade (CARAMÊS; ALAMAR; PALLONE, 2019; ZHAO et al., 2019).

5. MÉTODOS ANALÍTICOS ALTERNATIVOS VERDES NO CONTEXTO DA INDÚSTRIA 4.0 PARA CONTROLE DE QUALIDADE, ESTIMATIVA DE POTENCIAL BIOATIVO E DETECÇÃO DE FRAUDES EM ALIMENTOS

Na última década, a indústria vive um período de quebra de paradigmas que leva a uma inquestionável busca por mudanças nos sistemas de produção, distribuição e consumo

de alimentos, com uma alta tendência a busca pela sustentabilidade, exigida no conceito de quarta revolução industrial (indústria 4.0). A indústria alimentícia tem como novo desafio o desenvolvimento de técnicas que possam aumentar a capacidade de produção, diminuir o desperdício e garantir a qualidade durante a produção de alimentos sustentáveis (KAKANI et al., 2020).

Nesse contexto, a visão computacional tem ganhado destaque na área industrial desde os anos 70. Primeiramente, as indústrias implementaram sistemas automatizados que buscavam mimetizar a visão humana, com isso desenvolveu-se os sistemas de fotometria, aplicada principalmente como forma de detecção e classificação de produtos de acordo com não conformidades. Com o passar dos anos, esses sistemas foram combinados com outras compos de conhecimento como o reconhecimento de padrões, técnicas de imagem, sistemas óticos, entre outros. Essas tecnologias tem como ponto comum a agilidade, confiabilidade, a sustentabilidade e a versatilidade (KAKANI et al., 2020; SAEYS et al., 2019).

Nesse contexto, técnicas vibracionais, como o infravermelho, e/ou de imagens digitais, podem ser classificadas como técnicas ambientalmente amigáveis e que se encaixam no conceito buscado pela indústria 4.0 como técnicas alternativas aos métodos tradicionais.

5.1. ESPECTROSCOPIA NO INFRAVERMELHO

A radiação na região do infravermelho amplifica os níveis vibracionais, quando absorvida por uma molécula orgânica e então, esse processo é quantizado e o espectro vibracional resultante aparece como uma série de bandas, que são características de determinados grupos de átomos que permitem ao analista, através do estudo detalhado do espectro, consulta de tabelas que servem como indicações para informações estruturais, e quimiometria, incluída em ferramentas de aprendizagem de máquina, utilizar os dados espectrais para identificação e/ou quantificação de compostos (ROBERT M. SILVERSTEIN, FRANCIS X. WEBSTER, 2005).

A região espectral que corresponde ao infravermelho (IV) compreende a radiação com números de onda no intervalo de aproximadamente 12800 a 10 cm^{-1}. Do ponto de vista da aplicação, o espectro infravermelho é dividido em infravermelho próximo (NIR – do inglês, Near Infrared), médio (MIR – do inglês, Middle Infrared) e distante (FIR – do inglês, Far Infrared), como pode ser observado na Tabela 2 (SKOOG; HOLLER; CROUCH, 2009).

Tabela 2. Regiões espectrais no infravermelho.

Região no infravermelho	**Intervalos de número de onda (ν)-(cm^{-1})**	**Intervalos de comprimento de onda (λ)-(nm)**
Próximo (NIR)	14000-4000	750-2500
Médio (MIR)	4000-400	2500-25000
Distante (FIR)	400-100	$25x10^3$ - $100x10^3$

Fonte: SKOOG; HOLLER; NIEMAN (2002).

A principal diferença entre as faixas de infravermelho médio e próximo é que a absorção da radiação na região do infravermelho próximo corresponde a sobretons e combinações, resultantes do aumento do nível vibracional das moléculas orgânicas, enquanto na espectroscopia no infravermelho médio, o espectro registrado é resultante das vibrações fundamentais das moléculas. Outra diferença é que o NIR apresenta melhor capacidade de penetração na matéria que o MIR, uma vez que o coeficiente de absorção é muito menor na faixa do NIR, como consequência disso o espectro NIR é mais difícil de ser interpretado, devido a abundância de bandas de combinações e sobretons, quando comparado ao espectro MIR (BELLON-MAUREL; MCBRATNEY, 2011).

Quando a radiação incide sobre a amostra ela pode ser refletida, transmitida ou absorvida, nisso se baseia os quatro tipos básicos de aquisição de espectros no infravermelho: transmitância, reflectância, transflectância e interação (Figura 2). No modo de transmitância (Figura 2A) a luz incidente se propaga através da amostra e é detectada do lado oposto ao de entrada; no modo reflectância (Figura 2B), detector e fonte de luz se encontram do mesmo lado, a luz incide na amostra e reflete; no caso da transflectância (Figura 2C), ocorre a combinação de transmitância e reflectância, onde a amostra é colocada como no modo de reflectância, mas é utilizado um refletor, do lado oposto a fonte de luz, que reflete a luz que é transmitida pela amostra de volta para o detector; também no modo interação (Figura 2D) ocorre a combinação de reflectância e transmitância mas em amostras sólidas, esse método é característico na utilização de fibras óticas, a luz incidente entra em contato direto com a amostra, interage e é detectada pela fibra (ALANDER et al., 2013).

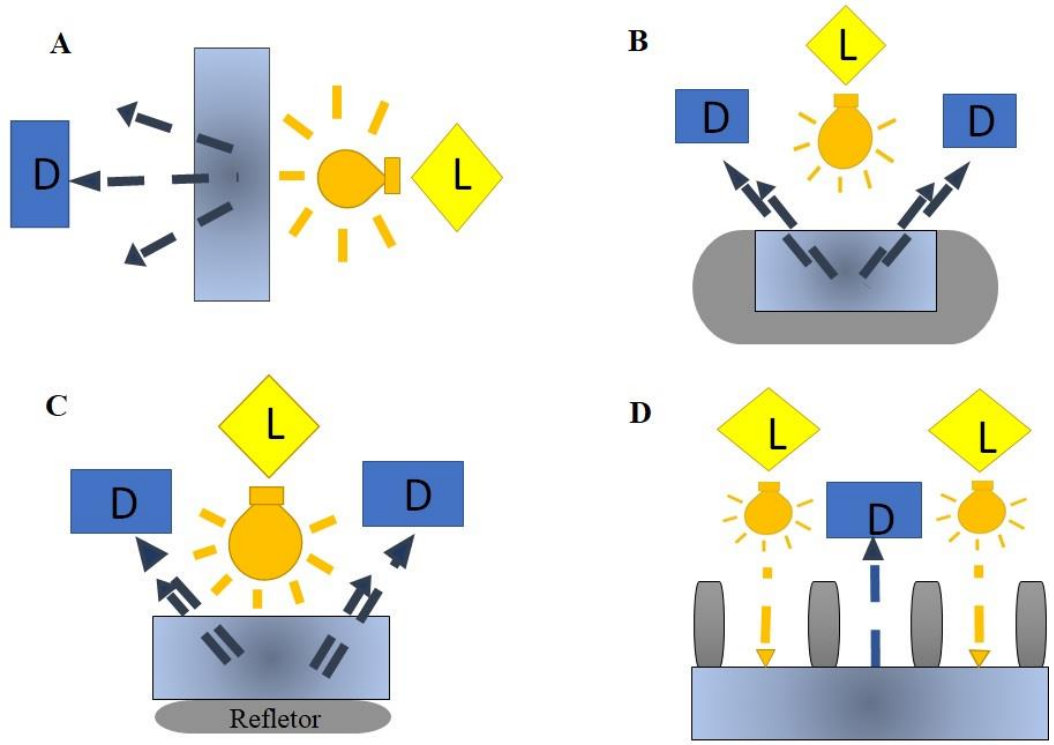

Figura 2. Esquema dos principais formas de medida: (A) transmitância, (B) reflectância, (C) transflectância e (D) interação. Adaptado de Cortés et al. (2019)

A Espectroscopia na região do IV associada a métodos de análise multivariada (quimiometria) fornecem resultados rápidos e confiáveis para quantificação e classificação de diversas amostras, incluindo alimentos. Além disso, é uma técnica não invasiva, não destrutiva, com mínima manipulação de amostra e de baixo custo, pois, dispensa reagentes específicos ou uso de materiais para preparo de amostra, por isso caracterizam-se por ser ambientalmente amigável, alinhada aos princípios de "química verde" (PALLONE; CARAMÊS; ALAMAR, 2018c).

A busca por métodos de análise que se adequem ao conceito de indústria 4.0 foi impulsionada nos últimos anos, com isso diversas pesquisas têm sido realizadas com o objetivo de aplicar análises espectroscópicas no infravermelho próximo e/ou médio para análises de rotina de controle de qualidade de alimentos em substituição as análises tradicionais como a quantificação de parâmetros físico-químicos, detecção de fraudes e também na determinação de parâmetros microbiológicos (Tabela 3) (KAKANI et al., 2020). Ademais, a técnica NIR também tem se mostrado como uma boa alternativa para a determinação de minerais em alimentos, mesmo não apresentando sensibilidade para uma detecção direta de componentes inorgânicos, a ligação entre minerais e moléculas orgânicas presentes nas matrizes alimentares permitem o uso dessa técnica como alternativa também para esse fim (COSTA et al., 2019).

Tabela 3. Aplicações de NIR e MIR para o controle de qualidade de alimentos.

	Categoria	Parâmetros	Matriz alimentar	Referência
NIR	Físico-químico	Umidade, lípidio, proteína e carboidrato	Quinoa	(FERREIRA; PALLONE; POPPI, 2015)
		Proteína	Leite em pó	(CHEN et al., 2018)
		Vitamina C e fenólicos totais	Maçã	(PISSARD et al., 2013)
		Ferro, cálcio, potássio e sódio	Hamburguer	(REBELLATO et al., 2020)
	Autenticidade	Adição de suco sintético ao natural	Suco de limão natural	(SHAFIEE; MINAEI, 2018)
		Origem geográfica e genótipo	Café arábica	(MARQUETTI et al., 2016)
	Microbiológicos	*Escherichia coli* e *Salmonella*	Polpa de abacaxi	(DE SOUSA MARQUES et al., 2013)
		Enterococcus e *Lactococcus*	Leite	(TREGUIER et al., 2019)
MIR	Físico-químico	Álcool, valor energético e grau de fermantação	Cerveja	(POLSHIN et al., 2011)
		Proteínas, lipídios e amido	Feijão preto	(SANTIAGO-RAMOS et al., 2018)
		Capacidade antioxidante e fenólicos totais	Chocolate	(HU et al., 2016)
	Autenticidade	Adição de farinhas de soja, milho, trigo	Farinha de quinoa	(RODRÍGUEZ; ROLANDELLI; BUERA, 2019)
		Origem geográfica	Amêndoas (Espanha)	(CORTÉS et al., 2018)
	Microbiológicos	*Listeria innocua*	Ácido acético	(WU et al., 2013)
		Escherichia coli	Carne moída	(DAVIS et al., 2010)

5.2. IMAGEM DE SMARTPHONE (SBI)

Cor é uma percepção mental de resposta ao espectro da luz na porção do visível quando emitida ou refletida de algum objeto, a luz então entra em contato com os olhos através da retina e chega até o cérebro por sinais conduzidos pelo nervo ótico. A percepção de cores é influenciada por diversos fatores, como a exposição a luz, a fonte da luz e ainda características intrínsecas ao objeto observado (WU; SUN, 2013).

Nos alimentos, as cores são altamente correlacionadas aos parâmetros de qualidade. No caso de frutas e vegetais, as cores são determinadas pela presença das diferentes classes pigmentos, como as clorofilas, carotenos, antocianinas, xantofilas, entre outras. Nesse sentido, a cor é um relevante parâmetro para a aceitação de um produto, uma vez que é relacionada com a maior presença desses compostos bioativos (WALSH et al., 2020).

As cores podem ser representadas por três cores componentes pelos olhos, enquanto que o espaço da cor é uma representação matemática da associação dos valores de cada cor componente, esses espaços são classificados em orientados pelo *hardware*, como o RGB (Red Green Blue), orientados por humano, como o HSV (Hue Saturation Value) ou instrumental, como CIE XYZ (Commission Internationale d'Eclairage XYZ) (WU; SUN, 2013).

Dispositivos eletrônicos que detectam e armazenam imagens RGB são os mais baratos e disseminados pelo mundo. As imagens adquiridas nesse espaço de cor tem ainda a vantagem de ser facilmente convertida a outros espaços, ampliando assim sua versatilidade. Nesse sentido, essas imagens tem sido aplicadas na indústria de alimentos como uma ferramenta poderosa para ajudar em uma rápida tomada de decisão sobre diferentes parâmetros, como cor, textura, forma, entre outros, já durante a linha de produção (DU; SUN, 2006; RODRÍGUEZ-PULIDO et al., 2013).

Nesse âmbito, dentre os dispositivos mais promissores, apresenta-se o smartphone que é um equipamento portátil, ligado a internet, com sistema de localização, considerado uma tecnologia de baixo custo e de fácil operação. O uso das imagens obtidas por um celular tem sido aplicado em diversos campos, como na medicina, meio ambiente e em alimentos (NELIS et al., 2020).

Sendo assim, diversas aplicações práticas na indústria de alimentos têm sido alcançadas com a utilização de imagens digitais. Na Tabela 4 encontram-se alguns exemplos, como a classificação de frutas, a avaliação da heterogeneidade de cor em frutas e legumes, para a detecção de defeitos em presuntos, para a avaliação de corantes em bebidas energéticas e para a detecção de adulterantes em leite de vaca (COSTA et al., 2020; NOWAK, 2020; RODRÍGUEZ-PULIDO et al., 2013; ULRICI et al., 2012; ZHANG et al., 2014).

Tabela 4. Aplicações de imagens digitais para o controle de qualidade de alimentos.

Categoria	Parâmetro	Matriz Alimentar	Referência
Físico-químico	Antocianina e capacidade antioxidante	Suco de uva	(BELTRAME et al., 2019)
	Corantes	Bebidas energéticas	(NOWAK, 2020)
	Corante *sunset yellow*	Refrigerantes	(BOTELHO; DE ASSIS; SENA, 2014)
Autenticidade	Adição de amido, peróxido de hidrogênio e NaClO	Leite	(COSTA et al., 2020)
	Adição de farinha de trigo e mandioca	Polpa de açaí	(ARAÚJO; MARINHO; DE ARAÚJO GOMES, 2018)
Microbiológico	*Escherichia coli* e *Enterococcus*	Alface	(ADKINS et al., 2017)
	Escherichia coli O157:H7	Carne moída e espinafre	(JUNG et al., 2020)

5.3. IMAGEM HIPERESPECTRAL

As imagens são derivadas da radiação do espectro eletromagnético, tanto na faixa do visível quanto do não visível. Análises visuais são uma das formas mais exploradas de determinar-se parâmetros de qualidade e aspectos importantes de um alimento dentro da indústria. Tradicionalmente, parâmetros que pudessem ser avaliados visualmente eram determinados por pessoas treinadas, mas isso vem sendo modificado com o advento dos sistemas de imagem eletrônicos, e hoje podem ser realizadas visualmente por pessoas ou através da análise de imagens (KAKANI et al., 2020).

Imagens podem ser adquiridas em duas dimensões (2D), onde a coordenada x e y formam um pixel, como no caso das imagens digitais, ou em três dimensões (3D), onde as coordenadas x, y e z formam um voxel, independentemente disso cada imagem tem uma

informação espectral específica que pode consistir em uma medida única como em sistemas RGB (red-green-blue) ou em vários canais espectrais, como em sistemas hiperespectrais, onde a matriz de dados obtida é tridimensional e, geralmente, chamada de hipercubo (PRATS-MONTALBÁN; DE JUAN; FERRER, 2011).

A instrumentação de sistemas de imagens hiperespectrais, normalmente, são formados por três itens básicos, uma fonte de luz, um dispersor e um detector. As fontes de luz mais utilizadas são de quartzo-tungstênio-halogênio (QTH), diodos emisores de luz (LED-*Light emitting diodes*) e lasers, onde as fontes de luz QTH são as mais utilizadas para alimentos. Já o dispersor de comprimento de onda pode ser baseado em uma grade de difração ou em filtro eletricamente ajustável (ETF). Existem diversos tipos de detectores, que devem ser escolhidos de acordo com a finalidade de aplicação, dentre os mais comuns estão o dispositivo de carga acoplada (CCD – *Charge-coupled device*), o semi-condutor óxido metálico (CMOS – *Complementary metal-oxide-semiconductor*) e o arseneto de gálio e índio (InGaAs – *indium gallium arsenide*) (LU et al., 2020).

Em sistemas de imagens hiperespectrais há a combinação da imagem com técnicas espectroscópicas, como NIR, Raman, florescência, ultra-violeta, onde a escolha da técnica é realizada de acordo com o analito de interesse. Com isso, a sensibilidade desses sistemas é potencializada, uma vez que informações sobre a superfície da amostra se tornam mais acessíveis, permitindo a visualização da distribuição de componentes químicos e/ou físicos da mesma. (PALLONE; CARAMÊS; ALAMAR, 2018b; PRATS-MONTALBÁN; DE JUAN; FERRER, 2011).

Normalmente, sistemas de imagem acoplados ao NIR (NIR-*Hyperspectral imaging* – NIR-HSI), são sistemas de imagens hiperespectrais mais utilizados em alimentos (Tabela 5). Entre as aplicações, sistema de imagem hiperespectral acoplado ao NIR já foi utilizado com sucesso para a classificação de pepinos de acordo com defeitos internos, onde os modelos matemáticos criados baseado nas informações dadas pelo NIR-HSI apresentaram mais de 80% de precisão na detecção de pepinos defeituosos. Também para a detecção de melamina em leite em pó, onde o NIR-HSI se mostrou capaz de detectar a presença desse adulterante a partir da concentração de 0,02% (ARIANA; LU, 2010; LIM et al., 2016), entre outros empregos.

Tabela 5. Aplicações de imagens hiperespectrais para o controle de qualidade de alimentos.

Categoria	Parâmetro	Matriz Alimentar	Referência
Físico-químico	Defeitos internos	Pepino	(ARIANA; LU, 2010)
	Índice de Maturidade	Mangas	(WENDEL; UNDERWOOD; WALSH, 2018)
Autenticidade	Adição de melamina	Leite em pó	(LIM et al., 2016)
	Adição de porco, rim, coração e pulmão de ovelha	Carne de ovelha moída	(KAMRUZZAMAN et al., 2013)
Microbiológico	Contaminação fecal	Alface	(CHO et al., 2018)
	Aspergillus niger e *Aspergillus flavus*	Milho	(DEL FIORE et al., 2010)

6. ANÁLISE MULTIVARIADAS PARA NIR, MIR E IMAGENS: QUIMIOMETRIA E APRENDIZAGEM DE MÁQUINA E APLICAÇÕES EM MÉTODOS ALTERNATIVOS PARA ALIMENTOS

A inteligência artificial tem suas origens nos ensaios especulativos realizados por Turing em 1950, sobre o poder dos computadores. A partir de então, a inteligência artificial passou a ter como principal objetivo solucionar os mais diversos problemas, como a melhora de performance, interpretação de linguagens, reconhecimento de padrões e imagens, através da criação de modelos ou estruturas matemáticas capazes de mimetizar a inteligência observada no homem (COSTA, 1992). Sendo assim, alguns autores definem a inteligência artificial como um ramo da ciência da computação envolvida na pesquisa, design e aplicação de computadores inteligentes (LU; CHEN; ZHENG, 2012).

A aprendizagem de máquina é um ramo da inteligência artificial, que pode ser definida como a criação de algoritmos capazes de extrair automaticamente informações de um conjunto de dados (SZYMAŃSKA, 2018). Ou também, como as técnicas envolvidas no tratamento de dados de maneira inteligente (através da criação de algoritmos), com essas técnicas se espera que os algoritmos aprendam com o conjunto de dados e aprendam por eles sem serem explicitamente programados (JIMÉNEZ-CARVELO et al., 2019). Ou seja, a

aprendizagem de máquinas busca extrair o máximo de dados possíveis de um conjunto de dados, através da criação de algoritmos capazes de utilizar esses dados para adquirir experiência representada pelos dados e aplicando de forma mais conveniente na solução dos mais diversos problemas.

Na década de 70, surgiu o termo “quimiometria” que é conceituada, pela IUPAC, como a aplicação de estatística à análise de dados químicos e o planejamento de experimentos químicos e simulações (IUPAC, 1997). Os mais detalhadamente por Wold (1991) como a ciência de extração e análise de informações derivadas da química analítica pela aplicação adequada de algoritmos matemáticos e estatísticos. Nesse sentido, a quimiometria abrange a aplicação de métodos matemáticos e/ou estatísticos multivariados capazes de extrair a maior quantidade possível de informação química útil de um conjunto de dados.

Atualmente, os conceitos de aprendizagem de máquina e quimiometria se tornaram muito abrangentes, e por vezes se confundem, alguns pesquisadores citam a quimiometria como a aprendizagem de máquina quando aplicada a dados químicos, enquanto outros defendem que a quimiometria refere-se ao uso de métodos multivariados baseados em fatores e aprendizagem de máquina refere-se ao uso de métodos não baseados em fatores (SANTANA, 2020; TAULER; PARASTAR, 2018).

Independente da nomenclatura utilizada, o fato é que essas ferramentas estatísticas tem ganhado cada vez mais espaço e importância para a análise de dados em campos diversos, como química, medicina, alimentos e agricultura (SZYMAŃSKA, 2018). A revolução tecnológica vivida nas últimas décadas atingiu todos os setores da sociedade, incluindo a química analítica, com o desenvolvimento de equipamentos cada vez mais precisos e com mais recursos, sendo assim, a geração de dados cresceu em volume e se tornou mais rápida, com isso métodos de aprendizagem de máquina e/ou quimiométricos surgiram como uma solução encontrada para a interpretação adequada desses dados (FERREIRA, 2015).

A aliança entre métodos analíticos sustentáveis e quimiometria, tem se mostrado como uma ótima alternativa para o desenvolvimento da indústria de alimentos. Com o advento da quarta revolução industrial (ou indústria 4.0) houve um aumento da demanda por novas alternativas que sejam capazes de reduzir os impactos ambientais negativos gerados pela produção agrícola e industrial nos últimos séculos, ou seja, sejam mais sustentáveis. Hoje, com as tecnologias de inteligência artificial aplicadas na agricultura e em alimentos, há a previsão de aumento de 30% no rendimento de cultivos de alimentos, redução da utilização

de água em mais de 300 bilhões de litros e redução da utilização de combustíveis em 25 milhões de barris até 2030, reduzindo assim os impactos ambientais e atendendo aos pilares trazidos pela indústria 4.0 (CAMARÉNA, 2020).

No entanto, para que isso se torne uma realidade é necessária a aplicação de algoritmos capazes de otimizar a interpretação dos dados gerados, e assim reconhecer padrões e com isso fornecer informações importantes para o melhor controle de qualidade dentro da indústria de alimentos, como a determinação de concentração de compostos, presença de produtos inadequados, perdas durante o processamento, entre outros (KAKANI et al., 2020).

Métodos quimiométricos usados para reconhecimento de padrões, ou seja, para detectar semelhanças e diferenças entre as amostras de agrupá-las de acordo com esses critérios, podem ser divididos entre: métodos supervisionados e não supervisionados (Figura 3). Onde os métodos supervisionados necessitam da informação sobre o pertencimento de cada amostra a uma classe pré-estabelecida, ou seja, requerem um conhecimento prévio das amostras, enquanto os métodos não supervisionados não apresentam essa necessidade, sendo assim, o agrupamento das amostras nesse tipo de análise ocorre naturalmente devido as informações contidas nos dados experimentais (FERREIRA, 2015).

Os principais métodos não supervisionados mais conhecidos são: análise de componentes principais (*Principal Component Analysis* – PCA) e agrupamentos por métodos hierárquicos (*Hierarchical Cluster Analysis* – HCA), sendo o primeiro o mais utilizado (FERREIRA, 2015). O PCA é uma ferramenta de projeção poderosa, que tem como objetivo maximizar a variância dos dados no menor número de componentes possível, mantendo as informações que mais contribuem na similaridade do grupo de amostras estudado (BRO; SMILDE, 2014). Já o HCA é uma técnica aglomerativa que se baseia nas informações intrísecas as amostras para reduzir a dimensionalidade dos dados reunindo amostras que mais se pareçam no mesmo grupo, é geralmente representado por meio de dendogramas que permitem a análise de grupos e sub-grupos formados (JIMÉNEZ-CARVELO et al., 2019).

Já os métodos supervisionados se dividem entre métodos de quantificação (ou de calibração) e de classificação (ou qualitativos) que se diferenciam basicamente pela tipo de resposta que geram, os métodos de calibração resultam em respostas contínuas enquanto os métodos de classificação geram respostas discretas (NTURAMBIRWE; OPARA, 2020).

Na área de alimentos os principais algoritmos utilizados para quantificação são os de regressão por mínimos quadrados parciais (*Partial Least Squares* – PLS) e regressão em componentes principais (*Principal Component Regression* – PCR). O método PLS é o mais

utilizado dentro na área de alimentos por ser um método de lida bem com a linearidade presente em conjunto de dados químicos. Trata-se de um método que projeta a informação contida no conjunto de dados em dimensões das chamadas variáveis latentes, que são obtidas em etapa única de interação onde se maximiza a matriz de covariância entre matriz de dados (x) e valores gerados sobre o analito de interesse (y) (KETTANEH; BERGLUND; WOLD, 2005). Já o método de PCR projeta as informações nas dimensões das componentes principais e é construído em duas etapas, onde em uma ocorre a compressão da matriz x e na segunda ocorre a projeção de y no espaço criado pelas componentes principais (FERREIRA, 2015).

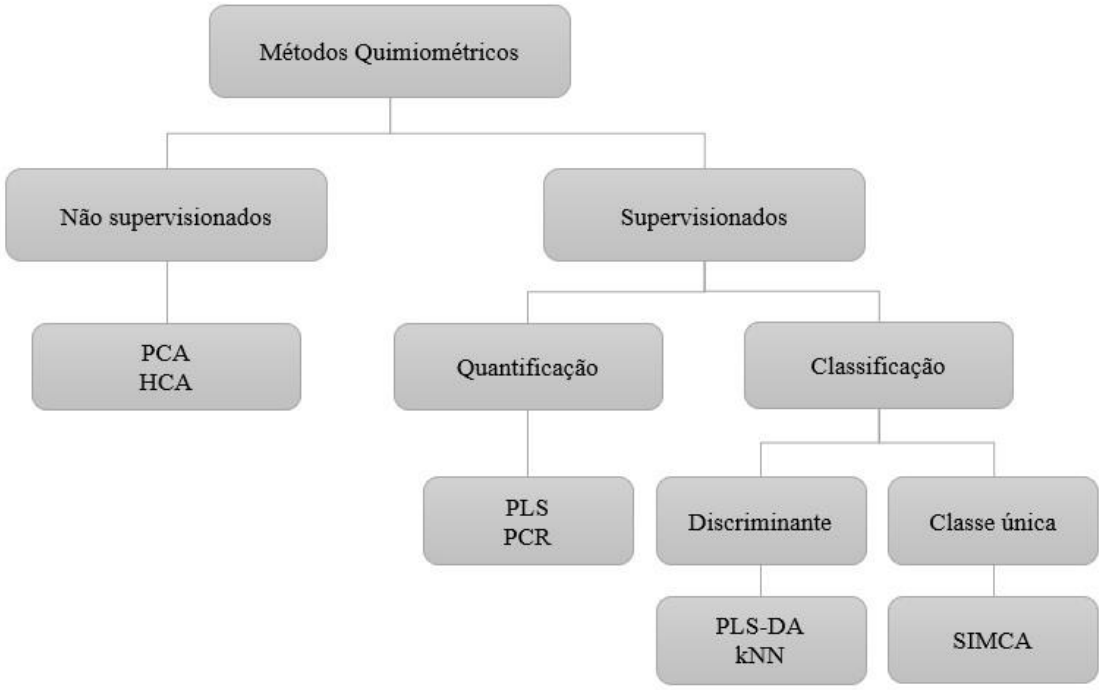

Figura 3. Esquema dos principais algoritmos quimiométricos utilizados em alimentos.- adaptado de (JIMÉNEZ-CARVELO et al., 2019)

Considerando os modelos de classificação há os métodos discriminantes e os modelos de classe única (Figura 3). O modelos discriminantes são caracterizados por classificarem as amostras de acordo com as classes pré definidas, enquanto modelos de classe única analisam se as caraterísticas de uma amostra são ou não compatíveis com a classe de interesse (OLIVERI, 2017).

Dentre os modelos discriminantes aplicados para a área de alimentos encontram-se os métodos de análise discriminante pelo método de quadrados mínimos parciais (*Partial Least Suqare- Discriminant Analysis* - PLS-DA) e o de k-nésimo vizinho mais próximo (*k-nearest neighbours* – kNN) (JIMÉNEZ-CARVELO et al., 2019; OLIVERI, 2017). k-NN é uma metodologia bastante simples, onde durante a construção do modelo uma amostra é

excluída e as distâncias entre ela e todas as demais amostras são calculadas, de acordo com essas medidas então são definidos os vizinho que se apresentam a menor distância (ou vizinhos mais próximos), a amostra excluída é então classificada de acordo com a classe a que pertence os seus k vizinhos mais próximos (FERREIRA, 2015). O PLS-DA é o método discriminante mais utilizado em estudos envolvendo alimentos, propõe uma delimitação linear para realizar a discriminação entre as amostras, aplicando a regressão por mínimos quadrados usando índices binários para cada uma das classes (ex: 0 e 1) (OLIVERI, 2017).

Já dentre os modelos existentes para classe única, o método de modelagem suave independente por analogia de classe (*Soft Independent modelling of class analogy* – SIMCA) é o mais popular. O SIMCA se baseia na direção criada pelas componentes principais, que por definição são determinadas na direção de máxima variância de dados (ou que contém o máximo de informações), para criar modelos para cada classe estudada (OLIVERI, 2017; SANTANA, 2020). Outros métodos como *data-driven SIMCA* (DD-SIMCA) e método de classe única pelo método de quadrados mínimos parciais (*one class PLS – OCPLS*), também tem sido utilizados para classificação supervisionada.

Mais recentemente outros métodos também tem ganhado espaço como alternativas aos métodos mais comumente utilizados, como o máquina de vetores de suporte (*Support Vector Machine* – SVM), especialmente aplicado para dados não lineares, as redes neurais artificiais (*Artificial Neural Networks* – ANN), as árvores de regressão e classificação (*Classification And Regression Tree* – CART) e a floresta aleatória (*Random forest* – RF). Esses métodos podem ser aplicados tanto para a criação de modelos de classificação quanto de calibração (JIMÉNEZ-CARVELO et al., 2019).

Na área de alimentos, esses algoritmos tem atuado no tratamento de dados gerados por vários métodos analíticos, como nas espectroscopias vibracionais (NIR, MIR, Raman), técnicas de imagens digitais ou hiperespectrais, técnicas cromatográficas, língua eletrônica, entre outras (NTURAMBIRWE; OPARA, 2020).

A Tabela 6 apresenta alguns exemplos de aplicações desses algoritmos para diferentes finalidades. Como o estudo feito por Teye et al. (2014) que propôs a criação de métodos de classificação do cacau de acordo com a origem geográfica, para isso utilizou os dados gerados através de língua eletrônica para a construção de métodos qualitativos multivariados através dos algoritmos kNN e SVM, além disso também realizou análise não supervisionada PCA para a observação o agrupamento das amostras de acordo com as informações químicas fornecidas pela língua eletrônica, como resultado o modelo SVM criado apresentou 100% de acertos discriminando cacau de acordo com a origem geográfica.

Teixeira et al. (2020) realizou um estudo para a determinação de modelos multivariados baseados em NIR que fosse capaz de detectar fraudes em leite de cabra, para isso utilizou o PCA como forma de projeção para visualizar os agrupamentos formados entre as amostras e também fez uso desse tipo de projeção para a criação de cartas de controle multivariadas que foram capazes de distinguir as amostras autênticas das adulteradas com água, uréia, soro bovino e leite bovino. Além disso, comparou a performance de três tipos de algoritmos: kNN, PLS-DA e SIMCA, onde PLS-DA apresentou os melhores resultados 100% de acertos ao classificar as amostras dentre as classes pré-estabelecidas durante o estudo.

Tabela 6. Aplicações dos algoritmos de aprendizagem de máquina em alimentos.

Objetivo	Proposta	Matriz alimentar	Algoritmos	Referência
Classificação	Determinação a origem geográfica	Cacau	PCA, kNN, SVM	(TEYE et al., 2014)
	Detecção de adulterantes	Leite de cabra	PCA, kNN, PLS-DA, SIMCA	(TEIXEIRA et al., 2020)
	Determinação de adulteração	Óleo de prímula	SIMCA, PLS-DA, RF	(DE SANTANA; BORGES NETO; POPPI, 2019)
	Detecção de adulterantes	Semolina	SIMCA, PCA	(BADARÓ et al., 2019)
	Detecção de adulterantes	Arroz	PCA, kNN, SVM	(TEYE et al., 2019)
Quantificação	Determinação de níveis de adulteração	Óleo de linhaça	PLS	(DE SOUZA et al., 2015)
	Determinação de microorganismos viáveis (bactérias)	Peixe	PLS, SVM	(CHENG; SUN, 2015)
	Determinação da acidez e vitamina C	Acerola	PLS, SVM	(MALEGORI et al., 2017)
	Determinação da composição centesimal	Trigo	PLS	(HELL et al., 2016)

	Quantificação dos sólidos solúveis totais	Maçã	PLS, PCR	(SAEYS et al., 2019)
	Quantificação de capacidade antioxidante	Grãos sem glúten (trigo sarraceno e aveia)	PLS	(WIEDEMAIR; HUCK, 2018)

De Santana, Borges Neto e Poppi (2019) propuseram o método de árvores aleatórias com MIR e NIR para a detecção da adição ilegal de óleo de soja, milho, girassol, andiroba e rosa mosqueta em óleo de prímula. O método proposto obteve maior precisão ao realizar a classificação das amostras quando comparado com os resultados apresentados pelos modelos de PLS-DA e performance similar ao obtido por SIMCA.

Em relação aos modelos de quantificação, os algoritmos PLS e SVM foram utilizados para a determinação de acidez titulável e concentração de vitamina C em acerola, onde ambos apresentaram boa performance porém SVM teve erros menores quando comparos aos apresentados pelos modelos PLS (MALEGORI et al., 2017). Outro estudo comparativo entre PLS e SVM foi realizado para a determinação de microorganismos viáveis em peixe, onde observou-se resultados similares, com erros menores obtidos pelo método SVM, apesar do PLS também apresentar boa performance (CHENG; SUN, 2015).

Apesar dos bons resultados apresentados por SVM, o método PLS ainda é o método de regressão utilizado na maioria dos estudos em alimentos, por apresentar, em geral, uma performance satisfatória ao ser aplicado para a quantificação dos mais diversos parâmetros como capacidade antioxidante, níveis de adulteração, determinação de composição centesimal em diversas matrizes alimentares (HELL et al., 2016; WIEDEMAIR; HUCK, 2018).

Nesse contexto, é importante ressaltar que esses algoritmos vem se mostrando ser uma ferramenta útil e de sucesso para tornar possível a utilização de métodos alternativos como NIR, MIR e técnicas de imagem em alimentos.

7. REFERÊNCIAS

ADKINS, Jaclyn A.; BOEHLE, Katherine; FRIEND, Colin; CHAMBERLAIN, Briana; BISHA, Bledar; HENRY, Charles S. Colorimetric and Electrochemical Bacteria Detection Using Printed Paper- and Transparency-Based Analytic Devices. **Analytical Chemistry**, *[S. l.]*, v. 89, n. 6, p. 3613–3621, 2017. DOI: 10.1021/acs.analchem.6b05009.

ALAMAR, P. D.; CARAMÊS, E. T. S.; POPPI, R. J.; PALLONE, J. A. L. Quality evaluation of frozen guava and yellow passion fruit pulps by NIR spectroscopy and chemometrics. **Food Research International**, *[S. l.]*, v. 85, 2016. a. DOI: 10.1016/j.foodres.2016.04.027.

ALAMAR, Priscila D.; CARAMÊS, Elem T. S.; POPPI, Ronei J.; PALLONE, Juliana A. L. Quality evaluation of frozen guava and yellow passion fruit pulps by NIR spectroscopy and chemometrics. **Food Research International**, *[S. l.]*, v. 85, p. 209–214, 2016. b. DOI: 10.1016/j.foodres.2016.04.027. Disponível em: http://www.sciencedirect.com/science/article/pii/S0963996916301673. Acesso em: 29 maio. 2016.

ALANDER, Jarmo T.; BOCHKO, Vladimir; MARTINKAUPPI, Birgitta; SARANWONG, Sirinnapa; MANTERE, Timo. A Review of Optical Nondestructive Visual and Near-Infrared Methods for Food Quality and Safety. **International Journal of Spectroscopy**, *[S. l.]*, v. 2013, p. 1–36, 2013. DOI: 10.1155/2013/341402.

AOAC, International. **Association of Official analytical chemists: official methods of analysis**. 17th. ed. Maryland, USA. v. II

ARAÚJO, Alisson; MARINHO, Weverton; DE ARAÚJO GOMES, Adriano. A Fast and Inexpensive Chemometric-Assisted Method to Identify Adulteration in Acai (Euterpe oleracea) Using Digital Images. **Food Analytical Methods**, *[S. l.]*, v. 11, n. 7, p. 1920–1926, 2018. DOI: 10.1007/s12161-017-1127-4.

ARIANA, Diwan P.; LU, Renfu. Evaluation of internal defect and surface color of whole pickles using hyperspectral imaging. **Journal of Food Engineering**, *[S. l.]*, v. 96, n. 4, p. 583–590, 2010. DOI: 10.1016/j.jfoodeng.2009.09.005. Disponível em: http://dx.doi.org/10.1016/j.jfoodeng.2009.09.005.

ASHURST, Philip R.; DENNIS, M. J. **Food Authentication**. [s.l.] : Springer Science &

Business Media, 2013. Disponível em: https://books.google.com.br/books?id=MXTjBwAAQBAJ.

BADARÓ, Amanda Teixeira; MORIMITSU, Fernanda Lie; FERREIRA, Amanda Rios; CLERICI, Maria Teresa Pedrosa Silva; BARBIN, Douglas Fernandes. Identification of fiber added to semolina by near infrared (NIR) spectral techniques. **Food Chemistry**, *[S. l.]*, v. 289, n. March, p. 195–203, 2019. DOI: 10.1016/j.foodchem.2019.03.057. Disponível em: https://doi.org/10.1016/j.foodchem.2019.03.057.

BAO, Cheng et al. The delivery of sensitive food bioactive ingredients: Absorption mechanisms, influencing factors, encapsulation techniques and evaluation models. **Food Research International**, *[S. l.]*, v. 120, n. September 2018, p. 130–140, 2019. DOI: 10.1016/j.foodres.2019.02.024. Disponível em: https://doi.org/10.1016/j.foodres.2019.02.024.

BELLON-MAUREL, Véronique; MCBRATNEY, Alex. Near-infrared (NIR) and mid-infrared (MIR) spectroscopic techniques for assessing the amount of carbon stock in soils - Critical review and research perspectives. **Soil Biology and Biochemistry**, *[S. l.]*, v. 43, n. 7, p. 1398–1410, 2011. DOI: 10.1016/j.soilbio.2011.02.019. Disponível em: http://dx.doi.org/10.1016/j.soilbio.2011.02.019.

BELTRAME, K. K.; GONÇALVES, T. R.; MARÇO, P. H.; GOMES, S. T. M.; MATSUSHITA, M.; VALDERRAMA, P. Application of digital images and multivariate calibration for the quantification of anthocyanin and antioxidant activity in grape juice. **Australian Journal of Grape and Wine Research**, *[S. l.]*, v. 25, n. 2, p. 156–160, 2019. DOI: 10.1111/ajgw.12387.

BEZERRA, Valéria Saldanha. **Açaí congelado**. [s.l.] : Embrapa Amapá, 2007. Disponível em: http://www.infoteca.cnptia.embrapa.br/bitstream/doc/350617/1/AP2007acaicongelado.pdf. Acesso em: 6 mar. 2017.

BORGES, Paulo Rogério Siriano; TAVARES, Evandro Galvão; GUIMARÃES, Isabela Costa; ROCHA, Renata de Paulo; ARAUJO, Ana Beatriz Silva; NUNES, Elisângela Elena; VILAS BOAS, Eduardo Valério de Barros. Obtaining a protocol for extraction of phenolics from açaí fruit pulp through Plackett–Burman design and response surface methodology. **Food Chemistry**, *[S. l.]*, v. 210, p. 189–199, 2016. DOI: 10.1016/j.foodchem.2016.04.077.

Disponível em: http://www.sciencedirect.com/science/article/pii/S0308814616306045. Acesso em: 6 mar. 2017.

BOTELHO, Bruno G.; DE ASSIS, Luciana P.; SENA, Marcelo M. Development and analytical validation of a simple multivariate calibration method using digital scanner images for sunset yellow determination in soft beverages. **Food Chemistry**, *[S. l.]*, v. 159, p. 175–180, 2014. DOI: 10.1016/j.foodchem.2014.03.048. Disponível em: http://dx.doi.org/10.1016/j.foodchem.2014.03.048.

BRASIL. **Regulamento técnico geral para fixação dos padrões de identidade e qualidade para polpa de fruta**Instrução Normativa Nº 01, de 07 de janeiro de 2000, , 2000.

BRASIL. **Instrução Normativa nº 37- Parâmetros Analíticos e Quesitos complementares aos Padrões de Identidade e Qualidade de Polpa de fruta**, 2018.

BRAZIL. **Instrução Normativa Nº17- Regulamento Técnico para os Sistemas Orgânicos de Produção, bem como as listas de substâncias e práticas permitidas para uso no Sistema Orgânicos de Produção.**Ministério da Agricultura, Pecuária e Abastecimento., , 2014.

BRAZIL. **PADRÕES DE IDENTIDADE E QUALIDADE MÍNIMA PARA POLPA DE AÇAÍ-INSTRUÇÃO NORMATIVA Nº37.**, 2018.

BRO, Rasmus; SMILDE, Age K. Principal component analysis. **Analytical Methods**, *[S. l.]*, v. 6, n. 9, p. 2812–2831, 2014. DOI: 10.1039/c3ay41907j.

BVENURA, Callistus; SIVAKUMAR, Dharini. The role of wild fruits and vegetables in delivering a balanced and healthy diet. **Food Research International**, *[S. l.]*, v. 99, n. March, p. 15–30, 2017. DOI: 10.1016/j.foodres.2017.06.046. Disponível em: http://dx.doi.org/10.1016/j.foodres.2017.06.046.

CAMARÉNA, Stéphanie. Artificial intelligence in the design of the transitions to sustainable food systems. **Journal of Cleaner Production**, *[S. l.]*, v. 271, 2020. DOI: 10.1016/j.jclepro.2020.122574.

CARAMÊS, E. T. S.; ALAMAR, P. D.; PALLONE, J. A. L. Detection and identification of açai pulp adulteration by NIR and MIR as an alternative technique: Control charts and classification models. **Food Research International**, *[S. l.]*, v. 123, n. June, p. 704–711, 2019. DOI: 10.1016/j.foodres.2019.06.006.

CHEN, Hui; TAN, Chao; LIN, Zan; WU, Tong. Classification and quantitation of milk powder by near-infrared spectroscopy and mutual information-based variable selection and partial least squares. **Spectrochimica Acta - Part A: Molecular and Biomolecular Spectroscopy**, *[S. l.]*, v. 189, p. 183–189, 2018. DOI: 10.1016/j.saa.2017.08.034. Disponível em: https://doi.org/10.1016/j.saa.2017.08.034.

CHENG, Jun Hu; SUN, Da Wen. Rapid and non-invasive detection of fish microbial spoilage by visible and near infrared hyperspectral imaging and multivariate analysis. **LWT - Food Science and Technology**, *[S. l.]*, v. 62, n. 2, p. 1060–1068, 2015. DOI: 10.1016/j.lwt.2015.01.021. Disponível em: http://dx.doi.org/10.1016/j.lwt.2015.01.021.

CHO, Hyunjeong; KIM, Moon S.; KIM, Sungyoun; LEE, Hoonsoo; OH, Mirae; CHUNG, Soo Hyun. Hyperspectral Determination of Fluorescence Wavebands for Multispectral Imaging Detection of Multiple Animal Fecal Species Contaminations on Romaine Lettuce. **Food and Bioprocess Technology**, *[S. l.]*, v. 11, n. 4, p. 774–784, 2018. DOI: 10.1007/s11947-017-2032-y.

CORTÉS, V.; BLASCO, J.; ALEIXOS, N.; CUBERO, S.; TALENS, P. Monitoring strategies for quality control of agricultural products using visible and near-infrared spectroscopy: A review. **Trends in Food Science and Technology**, *[S. l.]*, v. 85, n. October 2018, p. 138–148, 2019. DOI: 10.1016/j.tifs.2019.01.015. Disponível em: https://doi.org/10.1016/j.tifs.2019.01.015.

CORTÉS, Victoria; BARAT, José Manuel; TALENS, Pau; BLASCO, José; LERMA-GARCÍA, María Jesús. A comparison between NIR and ATR-FTIR spectroscopy for varietal differentiation of Spanish intact almonds. **Food Control**, *[S. l.]*, v. 94, n. June, p. 241–248, 2018. DOI: 10.1016/j.foodcont.2018.07.020. Disponível em: https://doi.org/10.1016/j.foodcont.2018.07.020.

COSTA, Miguel Antonio Bueno Da. Uma abordagem sobre Inteligência Artificial e simulação, com uma aplicação na pecuária de corte nacional. **Production**, *[S. l.]*, v. 2, n. 1, p. 51–59, 1992. DOI: 10.1590/s0103-65131992000100004.

COSTA, Wanessa Almeida Da; OLIVEIRA, Mozaniel Santana De; SILVA, Marcilene Paiva Da; CUNHA, Vânia Maria Borges; PINTO, Rafael Henrique Holanda; JUNIOR, Fernanda Wariss Figueiredo Bezerra and Raul Nunes de Carvalho. Açaí (Euterpe oleracea) and Bacaba (Oenocarpus bacaba) as Functional Food. *[S. l.]*, 2017. DOI: 10.5772/65881. Disponível em:

http://www.intechopen.com/books/superfood-and-functional-food-an-overview-of-their-processing-and-utilization/a-a-euterpe-oleracea-and-bacaba-oenocarpus-bacaba-as-functional-food. Acesso em: 4 mar. 2017.

COSTA, Maria Cristina A.; MORGANO, Marcelo A.; FERREIRA, Marcia Miguel C.; MILANI, Raquel F. Quantification of mineral composition of Brazilian bee pollen by near infrared spectroscopy and PLS regression. **Food Chemistry**, *[S. l.]*, v. 273, n. July 2017, p. 85–90, 2019. DOI: 10.1016/j.foodchem.2018.02.017. Disponível em: https://doi.org/10.1016/j.foodchem.2018.02.017.

COSTA, Rayana A. et al. Quantification of milk adulterants (starch, H2O2, and NaClO) using colorimetric assays coupled to smartphone image analysis. **Microchemical Journal**, *[S. l.]*, v. 156, n. May, p. 104968, 2020. DOI: 10.1016/j.microc.2020.104968. Disponível em: https://doi.org/10.1016/j.microc.2020.104968.

CUNHA JÚNIOR, Luis Carlos; TEIXEIRA, Gustavo Henrique de Almeida; NARDINI, Viviani; WALSH, Kerry Brian. Quality evaluation of intact açaí and juçara fruit by means of near infrared spectroscopy. **Postharvest Biology and Technology**, *[S. l.]*, v. 112, p. 64–74, 2016. DOI: 10.1016/j.postharvbio.2015.10.001. Disponível em: http://www.sciencedirect.com/science/article/pii/S0925521415301459. Acesso em: 25 mar. 2017.

DA SILVA SANTOS, Vivian; DE ALMEIDA TEIXEIRA, Gustavo Henrique; BARBOSA, Fernando. Açaí (euterpe oleracea mart.): A tropical fruit with high levels of essential minerals - Especially manganese - And its contribution as a source of natural mineral supplementation. **Journal of Toxicology and Environmental Health - Part A: Current Issues**, *[S. l.]*, v. 77, n. 1–3, p. 80–89, 2014. DOI: 10.1080/15287394.2014.866923.

DANEZIS, Georgios P.; TSAGKARIS, Aristidis S.; CAMIN, Federica; BRUSIC, Vladimir; GEORGIOU, Constantinos A. Food authentication: Techniques, trends & emerging approaches. **TrAC Trends in Analytical Chemistry**, On-site and In-vivo Instrumentation and Applications. *[S. l.]*, v. 85, Part A, On-site and In-vivo Instrumentation and Applications, p. 123–132, 2016. DOI: 10.1016/j.trac.2016.02.026. Disponível em: http://www.sciencedirect.com/science/article/pii/S0165993615301291. Acesso em: 6 mar. 2017.

DAVID, Marília Luz; GUIVANT, Julia Silvia. Os Padrões de Identidade e Qualidade dos

Alimentos: uma Análise de suas Transformações no Brasil. **Mediações - Revista de Ciências Sociais**, *[S. l.]*, v. 25, n. 1, p. 247, 2020. DOI: 10.5433/2176-6665.2020v25n1p247.

DAVIS, Reeta; IRUDAYARAJ, Joseph; REUHS, Bradley L.; MAUER, Lisa J. Detection of E. coli O157:H7 from ground beef using fourier transform infrared (FT-IR) spectroscopy and chemometrics. **Journal of Food Science**, *[S. l.]*, v. 75, n. 6, 2010. DOI: 10.1111/j.1750-3841.2010.01686.x.

DE SANTANA, Felipe Bachion; BORGES NETO, Waldomiro; POPPI, Ronei J. Random forest as one-class classifier and infrared spectroscopy for food adulteration detection. **Food Chemistry**, *[S. l.]*, v. 293, n. April, p. 323–332, 2019. DOI: 10.1016/j.foodchem.2019.04.073. Disponível em: https://doi.org/10.1016/j.foodchem.2019.04.073.

DE SOUSA MARQUES, Aline; NICÁCIO, Jábine Talitta Nunes; CIDRAL, Tiago André; DE MELO, Maria Celeste Nunes; DE LIMA, Kássio Michell Gomes. The use of near infrared spectroscopy and multivariate techniques to differentiate Escherichia coli and Salmonella Enteritidis inoculated into pulp juice. **Journal of Microbiological Methods**, *[S. l.]*, v. 93, n. 2, p. 90–94, 2013. DOI: 10.1016/j.mimet.2013.02.003. Disponível em: http://dx.doi.org/10.1016/j.mimet.2013.02.003.

DE SOUZA, Letícia Maria; DE SANTANA, Felipe Bachion; GONTIJO, Lucas Caixeta; MAZIVILA, Sarmento Júnior; BORGES NETO, Waldomiro. Quantification of adulterations in extra virgin flaxseed oil using MIR and PLS. **Food Chemistry**, *[S. l.]*, v. 182, p. 35–40, 2015. DOI: 10.1016/j.foodchem.2015.02.081.

DEL FIORE, A.; REVERBERI, M.; RICELLI, A.; PINZARI, F.; SERRANTI, S.; FABBRI, A. A.; BONIFAZI, G.; FANELLI, C. Early detection of toxigenic fungi on maize by hyperspectral imaging analysis. **International Journal of Food Microbiology**, *[S. l.]*, v. 144, n. 1, p. 64–71, 2010. DOI: 10.1016/j.ijfoodmicro.2010.08.001. Disponível em: http://dx.doi.org/10.1016/j.ijfoodmicro.2010.08.001.

DELSHADI, Rana; BAHRAMI, Akbar; TAFTI, Abolfazl Golshan; BARBA, Francisco J.; WILLIAMS, Leonard L. Micro and nano-encapsulation of vegetable and essential oils to develop functional food products with improved nutritional profiles. **Trends in Food Science & Technology**, *[S. l.]*, v. 104, n. July, p. 72–83, 2020. DOI: 10.1016/j.tifs.2020.07.004. Disponível em: https://doi.org/10.1016/j.tifs.2020.07.004.

DU, Cheng Jin; SUN, Da Wen. Learning techniques used in computer vision for food quality evaluation: A review. **Journal of Food Engineering**, *[S. l.]*, v. 72, n. 1, p. 39–55, 2006. DOI: 10.1016/j.jfoodeng.2004.11.017.

ELZAKKER, B. V; TORJUSEN, Hanne; JENSEN, Katherine; BRANDT, Kirsten. **Autenticidade e fraude: informações aos consumidores visando o controlo da qualidade e segurança alimentar em cadeias de produção biológica.** Frick, Switzerlan.

EMBRAPA. **EMBRAPA Arroz e Feijão. Dados de conjuntura da produção de arroz (Oryza sativa L.) no Brasil (1985-2015): área, produção e rendimento.** 2016. Disponível em: http://www.cnpaf.embrapa.br/socioeconomia/index.htm. Acesso em: 12 set. 2020.

FAOSTAT. **Countries by commodities**. 2017.

FERREIRA, D. S.; PALLONE, J. A. L.; POPPI, R. J. Direct analysis of the main chemical constituents in Chenopodium quinoa grain using Fourier transform near-infrared spectroscopy. **Food Control**, *[S. l.]*, v. 48, p. 91–95, 2015. DOI: 10.1016/j.foodcont.2014.04.016. Disponível em: http://dx.doi.org/10.1016/j.foodcont.2014.04.016.

FERREIRA, Márcia M. C. **Quimiometria- conceitos, métodos e aplicações**. 1 st ed. Campinas, SP: Editora UNICAMP, 2015.

FRANCO, Daniel; RICARDO, Paulo; FAGUNDES, Reis; MORAES, Orlando Peixoto De; WICKERT, Ester; NETO, Francisco De Moura; CRISTIANO, Alcides; SEVERO, Morais. Indicação de Tipos Especiais de Arroz para Diversificação de Cultivo 133. *[S. l.]*, p. 1–8, 2012.

G1. **Fiscalização encontra papel higiênico misturado com açaí em Belém.** 2014. Disponível em: http://g1.globo.com/pa/para/noticia/2014/06/fiscalizacao-encontra-papel-higienico-misturado-com-acai-em-belem.html. Acesso em: 17 abr. 2018.

GIULIANI, A.; CERRETANI, L.; CICHELLI, A. Colors: Properties and Determination of Natural Pigments A2 - Caballero, Benjamin. *In*: FINGLAS, Paul M.; TOLDRÁ, Fidel (org.). Oxford: Academic Press, 2016. p. 273–283. Disponível em: http://www.sciencedirect.com/science/article/pii/B9780123849472001896. Acesso em: 11 mar. 2016.

GONG, Er Sheng; LUO, Shunjing; LI, Tong; LIU, Chengmei; ZHANG, Guowen; CHEN,

Jun; ZENG, Zicong; LIU, Rui Hai. Phytochemical profiles and antioxidant activity of processed brown rice products. **Food Chemistry**, *[S. l.]*, v. 232, p. 67–78, 2017. DOI: 10.1016/j.foodchem.2017.03.148. Disponível em: http://dx.doi.org/10.1016/j.foodchem.2017.03.148.

HANSCHEN, Franziska S. Domestic boiling and salad preparation habits affect glucosinolate degradation in red cabbage (Brassica oleracea var. capitata f. rubra). **Food Chemistry**, *[S. l.]*, v. 321, n. March, p. 126694, 2020. DOI: 10.1016/j.foodchem.2020.126694. Disponível em: https://doi.org/10.1016/j.foodchem.2020.126694.

HELL, Johannes; PRÜCKLER, Michael; DANNER, Lukas; HENNIGES, Ute; APPRICH, Silvia; ROSENAU, Thomas; KNEIFEL, Wolfgang; BÖHMDORFER, Stefan. A comparison between near-infrared (NIR) and mid-infrared (ATR-FTIR) spectroscopy for the multivariate determination of compositional properties in wheat bran samples. **Food Control**, *[S. l.]*, v. 60, p. 365–369, 2016. DOI: 10.1016/j.foodcont.2015.08.003.

HU, Yaxi; PAN, Zhi Jie; LIAO, Wen; LI, Jiaqi; GRUGET, Pierre; KITTS, David D.; LU, Xiaonan. Determination of antioxidant capacity and phenolic content of chocolate by attenuated total reflectance-Fourier transformed-infrared spectroscopy. **Food Chemistry**, *[S. l.]*, v. 202, p. 254–261, 2016. DOI: 10.1016/j.foodchem.2016.01.130. Disponível em: http://linkinghub.elsevier.com/retrieve/pii/S0308814616301303. Acesso em: 21 jul. 2017.

HUSSAIN, N.; SUN, Da Wen; PU, Hongbin. Classical and emerging non-destructive technologies for safety and quality evaluation of cereals: A review of recent applications. **Trends in Food Science and Technology**, *[S. l.]*, v. 91, n. February, p. 598–608, 2019. DOI: 10.1016/j.tifs.2019.07.018. Disponível em: https://doi.org/10.1016/j.tifs.2019.07.018.

IUPAC. **Compendium of chemical terminology - the gold book**. 1997. Disponível em: http://goldbook.iupac.org/CT06948.html. Acesso em: 14 set. 2020.

JIMÉNEZ-CARVELO, Ana M.; GONZÁLEZ-CASADO, Antonio; BAGUR-GONZÁLEZ, M. Gracia; CUADROS-RODRÍGUEZ, Luis. Alternative data mining/machine learning methods for the analytical evaluation of food quality and authenticity – A review. **Food Research International**, *[S. l.]*, v. 122, n. March, p. 25–39, 2019. DOI: 10.1016/j.foodres.2019.03.063. Disponível em: https://doi.org/10.1016/j.foodres.2019.03.063.

JUNG, Youngkee; HEO, Yoojung; LEE, Jae Joong; DEERING, Amanda; BAE, Euiwon. Smartphone-based lateral flow imaging system for detection of food-borne bacteria E.coli O157:H7. **Journal of Microbiological Methods**, *[S. l.]*, v. 168, n. December 2019, p. 105800, 2020. DOI: 10.1016/j.mimet.2019.105800. Disponível em: https://doi.org/10.1016/j.mimet.2019.105800.

KAKANI, Vijay; NGUYEN, Van Huan; KUMAR, Basivi Praveen; KIM, Hakil; PASUPULETI, Visweswara Rao. A critical review on computer vision and artificial intelligence in food industry. **Journal of Agriculture and Food Research**, *[S. l.]*, v. 2, n. November 2019, p. 100033, 2020. DOI: https://doi.org/10.1016/j.jafr.2020.100033. Disponível em: http://www.sciencedirect.com/science/article/pii/S2666154320300144.

KAMRUZZAMAN, Mohammed; SUN, Da Wen; ELMASRY, Gamal; ALLEN, Paul. Fast detection and visualization of minced lamb meat adulteration using NIR hyperspectral imaging and multivariate image analysis. **Talanta**, *[S. l.]*, v. 103, p. 130–136, 2013. DOI: 10.1016/j.talanta.2012.10.020. Disponível em: http://dx.doi.org/10.1016/j.talanta.2012.10.020.

KETTANEH, Nouna; BERGLUND, Anders; WOLD, Svante. PCA and PLS with very large data sets. **Computational Statistics and Data Analysis**, *[S. l.]*, v. 48, n. 1, p. 69–85, 2005. DOI: 10.1016/j.csda.2003.11.027.

KIST, Benno Bernardo; SANTOS, Cleiton Evandro Dos; CARVALHO, Cleonice De; BELING, Romar Rodolfo. Anuário Brasileiro de Brazilian Horti 2019. **Editora Gazeta Santa Cruz**, *[S. l.]*, p. 96, 2018. Disponível em: http://www.abcsem.com.br/upload/arquivos/HortiFruti_2019_DUPLA.pdf.

KLJUSURIĆ, J. G.; MIHALEV, K.; BEČIĆ, I.; POLOVIĆ, I.; GEORGIEVA, M.; DJAKOVIĆ, S.; KURTANJEK, Ž. Near-infrared spectroscopic analysis of total phenolic content and antioxidant activity of berry fruits. **Food Technology and Biotechnology**, *[S. l.]*, v. 54, n. 2, p. 236–242, 2016. DOI: 10.17113/ftb.54.02.16.4095.

KUSHWAH, Shiksha; DHIR, Amandeep; SAGAR, Mahim; GUPTA, Bhumika. Determinants of organic food consumption. A systematic literature review on motives and barriers. **Appetite**, *[S. l.]*, v. 143, n. October 2018, p. 104402, 2019. DOI: 10.1016/j.appet.2019.104402. Disponível em: https://doi.org/10.1016/j.appet.2019.104402.

KUSTER, J. B. ..; COSTA, A. F. ..; GALEANO, E. A. V. ..; COSTA, H. ..; ROSSI, D. A. ..;

BARBÁRA, W. P. F. ..; EGGER, V. A. ..; PIASSI, M. Análise de custos da produção de repolho em dois municípios do espírito santo, brasil. **Revista Científica Intelletto**, *[S. l.]*, v. 3, p. 51–58, 2018.

LIM, Jongguk; KIM, Giyoung; MO, Changyeun; KIM, Moon S.; CHAO, Kuanglin; QIN, Jianwei; FU, Xiaping; BAEK, Insuck; CHO, Byoung-Kwan. Detection of melamine in milk powders using near-infrared hyperspectral imaging combined with regression coefficient of partial least square regression model. **Talanta**, *[S. l.]*, v. 151, p. 183–191, 2016. DOI: 10.1016/j.talanta.2016.01.035.

LU, Pengzhen; CHEN, Shengyong; ZHENG, Yujun. Artificial intelligence in civil engineering. **Mathematical Problems in Engineering**, *[S. l.]*, v. 2012, p. 1–23, 2012. DOI: 10.1155/2012/145974.

LU, Yuzhen; SAEYS, Wouter; KIM, Moon; PENG, Yankun; LU, Renfu. Hyperspectral imaging technology for quality and safety evaluation of horticultural products: A review and celebration of the past 20-year progress. **Postharvest Biology and Technology**, *[S. l.]*, v. 170, n. August, p. 111318, 2020. DOI: 10.1016/j.postharvbio.2020.111318. Disponível em: https://doi.org/10.1016/j.postharvbio.2020.111318.

MALEGORI, Cristina; NASCIMENTO MARQUES, Emanuel José; DE FREITAS, Sergio Tonetto; PIMENTEL, Maria Fernanda; PASQUINI, Celio; CASIRAGHI, Ernestina. Comparing the analytical performances of Micro-NIR and FT-NIR spectrometers in the evaluation of acerola fruit quality, using PLS and SVM regression algorithms. **Talanta**, *[S. l.]*, v. 165, n. November 2016, p. 112–116, 2017. DOI: 10.1016/j.talanta.2016.12.035. Disponível em: http://dx.doi.org/10.1016/j.talanta.2016.12.035.

MARQUETTI, Izabele; LINK, Jade Varaschim; LEMES, André Luis Guimarães; SCHOLZ, Maria Brígida dos Santos; VALDERRAMA, Patrícia; BONA, Evandro. Partial least square with discriminant analysis and near infrared spectroscopy for evaluation of geographic and genotypic origin of arabica coffee. **Computers and Electronics in Agriculture**, *[S. l.]*, v. 121, p. 313–319, 2016. DOI: 10.1016/j.compag.2015.12.018. Disponível em: http://dx.doi.org/10.1016/j.compag.2015.12.018.

MURADOR, Daniella Carisa; MERCADANTE, Adriana Zerlotti; DE ROSSO, Veridiana Vera. Cooking techniques improve the levels of bioactive compounds and antioxidant activity in kale and red cabbage. **Food Chemistry**, *[S. l.]*, v. 196, p. 1101–1107, 2016. DOI:

10.1016/j.foodchem.2015.10.037. Disponível em: http://dx.doi.org/10.1016/j.foodchem.2015.10.037.

NAKAYAMA, T.; NAGAI, Y.; UEHARA, Y.; NAKAMURA, Y.; ISHII, S.; KATO, H.; TANAKA, Y. Eating glutinous brown rice twice a day for 8 weeks improves glycemic control in Japanese patients with diabetes mellitus. **Nutrition and Diabetes**, *[S. l.]*, v. 7, n. 5, p. e273-6, 2017. DOI: 10.1038/nutd.2017.26. Disponível em: http://dx.doi.org/10.1038/nutd.2017.26.

NELIS, J. L. D.; TSAGKARIS, A. S.; DILLON, M. J.; HAJSLOVA, J.; ELLIOT, C. T. Smartphone-based optical assays in the food safety field. **Trends in Analytical Chemistry**, *[S. l.]*, v. under revi, p. 115934, 2020. DOI: 10.1016/j.trac.2020.115934. Disponível em: https://doi.org/10.1016/j.trac.2020.115934.

NOWAK, Paweł Mateusz. Simultaneous quantification of food colorants and preservatives in sports drinks by the high performance liquid chromatography and capillary electrophoresis methods evaluated using the red-green-blue model. **Journal of Chromatography A**, *[S. l.]*, v. 1620, 2020. DOI: 10.1016/j.chroma.2020.460976.

NTURAMBIRWE, Jean Frederic Isingizwe; OPARA, Umezuruike Linus. Machine learning applications to non-destructive defect detection in horticultural products. **Biosystems Engineering**, *[S. l.]*, v. 189, p. 60–83, 2020. DOI: 10.1016/j.biosystemseng.2019.11.011. Disponível em: https://doi.org/10.1016/j.biosystemseng.2019.11.011.

OLIVEIRA, Maria do Socorro Padilha De; CARVALHO, José Edmar Urano De; NASCIMENTO, Walnice Maria Oliveira Do; MÜLLER, Carlos Hans. Cultivo do açaizeiro para produção de frutos. *[S. l.]*, 2002. Disponível em: http://www.sifloresta.ufv.br/handle/123456789/7308. Acesso em: 4 mar. 2017.

OLIVERI, Paolo. Class-modelling in food analytical chemistry: Development, sampling, optimisation and validation issues – A tutorial. **Analytica Chimica Acta**, *[S. l.]*, v. 982, p. 9–19, 2017. DOI: 10.1016/j.aca.2017.05.013. Disponível em: http://dx.doi.org/10.1016/j.aca.2017.05.013.

PAGLIARUSSI, Marina. **A cadeia produtiva agroindustrial do açaí: estudo da cadeia e proposta de um modelo matemático.** 2010. São Carlos, 2010.

PALLONE, Juliana Azevedo Lima; CARAMÊS, Elem Tamirys dos Santos; ALAMAR, Priscila Domingues. Green analytical chemistry applied in food analysis: alternative

techniques. **Current Opinion in Food Science**, *[S. l.]*, v. 22, n. Figure 1, p. 115–121, 2018. a. DOI: 10.1016/j.cofs.2018.01.009.

PALLONE, Juliana Azevedo Lima; CARAMÊS, Elem Tamirys dos Santos; ALAMAR, Priscila Domingues. Green analytical chemistry applied in food analysis: alternative techniques. **Current Opinion in Food Science**, *[S. l.]*, v. 22, n. Figure 1, p. 115–121, 2018. b. DOI: 10.1016/j.cofs.2018.01.009.

PALLONE, Juliana Azevedo Lima; CARAMÊS, Elem Tamirys dos Santos; ALAMAR, Priscila Domingues. Green analytical chemistry applied in food analysis: alternative techniques. **Current Opinion in Food Science**, *[S. l.]*, v. 22, p. 115–121, 2018. c. DOI: 10.1016/J.COFS.2018.01.009. Disponível em: https://www.sciencedirect.com/science/article/pii/S2214799317301558. Acesso em: 18 abr. 2018.

PEANPARKDEE, Methavee; IWAMOTO, Satoshi. Bioactive compounds from by-products of rice cultivation and rice processing: Extraction and application in the food and pharmaceutical industries. **Trends in Food Science and Technology**, *[S. l.]*, v. 86, n. July 2018, p. 109–117, 2019. DOI: 10.1016/j.tifs.2019.02.041. Disponível em: https://doi.org/10.1016/j.tifs.2019.02.041.

PISSARD, Audrey; FERNÁNDEZ PIERNA, Juan A.; BAETEN, Vincent; SINNAEVE, Georges; LOGNAY, Georges; MOUTEAU, Anne; DUPONT, Pascal; RONDIA, Alain; LATEUR, Marc. Non-destructive measurement of vitamin C, total polyphenol and sugar content in apples using near-infrared spectroscopy. **Journal of the Science of Food and Agriculture**, *[S. l.]*, v. 93, n. 2, p. 238–244, 2013. DOI: 10.1002/jsfa.5779. Disponível em: http://onlinelibrary.wiley.com/doi/10.1002/jsfa.5779/abstract. Acesso em: 12 out. 2015.

POLSHIN, Evgeny; AERNOUTS, Ben; SAEYS, Wouter; DELVAUX, Filip; DELVAUX, Freddy R.; SAISON, Daan; HERTOG, Maarten; NICOLAÏ, Bart M.; LAMMERTYN, Jeroen. Beer quality screening by FT-IR spectrometry: Impact of measurement strategies, data pre-processings and variable selection algorithms. **Journal of Food Engineering**, *[S. l.]*, v. 106, n. 3, p. 188–198, 2011. DOI: 10.1016/j.jfoodeng.2011.05.003. Disponível em: http://dx.doi.org/10.1016/j.jfoodeng.2011.05.003.

PRATS-MONTALBÁN, J. M.; DE JUAN, A.; FERRER, A. Multivariate image analysis: A review with applications. **Chemometrics and Intelligent Laboratory Systems**, *[S. l.]*, v.

107, n. 1, p. 1–23, 2011. DOI: 10.1016/j.chemolab.2011.03.002.

RADZIEJEWSKA-KUBZDELA, Elżbieta; BIEGAŃSKA-MARECIK, Róża. A comparison of the composition and antioxidant capacity of novel beverages with an addition of red cabbage in the frozen, purée and freeze-dried forms. **LWT - Food Science and Technology**, *[S. l.]*, v. 62, n. 1, p. 821–829, 2015. DOI: 10.1016/J.LWT.2014.07.018. Disponível em: https://www.sciencedirect.com/science/article/pii/S0023643814004496. Acesso em: 8 fev. 2018.

REBELLATO, Ana Paula; CARAMÊS, Elem Tamirys dos Santos; MORAES, Priscila Probio De; PALLONE, Juliana Azevedo Lima. Minerals assessment and sodium control in hamburger by fast and green method and chemometric tools. **Lwt**, *[S. l.]*, v. 128, n. October 2019, p. 109438, 2020. DOI: 10.1016/j.lwt.2020.109438. Disponível em: https://doi.org/10.1016/j.lwt.2020.109438.

ROBERT M. SILVERSTEIN, FRANCIS X. WEBSTER, David J. Kiemle. **Spectrometric identification of organic compounds**. [s.l: s.n.]. DOI: 10.1016/0022-2860(76)87024-X. Disponível em: http://linkinghub.elsevier.com/retrieve/pii/002228607687024X.

ROBSON, Kelsey; DEAN, Moira; HAUGHEY, Simon; ELLIOTT, Christopher. A comprehensive review of food fraud terminologies and food fraud mitigation guides. **Food Control**, *[S. l.]*, v. 120, n. June 2020, p. 107516, 2020. DOI: 10.1016/j.foodcont.2020.107516. Disponível em: https://doi.org/10.1016/j.foodcont.2020.107516.

RODRÍGUEZ-PULIDO, Francisco J.; GORDILLO, Belén; LOURDES GONZÁLEZ-MIRET, M.; HEREDIA, Francisco J. Analysis of food appearance properties by computer vision applying ellipsoids to colour data. **Computers and Electronics in Agriculture**, *[S. l.]*, v. 99, p. 108–115, 2013. DOI: 10.1016/j.compag.2013.08.027.

RODRÍGUEZ, Silvio D.; ROLANDELLI, Guido; BUERA, M. Pilar. Detection of quinoa flour adulteration by means of FT-MIR spectroscopy combined with chemometric methods. **Food Chemistry**, *[S. l.]*, v. 274, n. March 2018, p. 392–401, 2019. DOI: 10.1016/j.foodchem.2018.08.140. Disponível em: https://doi.org/10.1016/j.foodchem.2018.08.140.

SAEYS, Wouter; NGUYEN DO TRONG, N.; VAN BEERS, R.; NICOLAÏ, Bart M. Multivariate calibration of spectroscopic sensors for postharvest quality evaluation: A

review. **Postharvest Biology and Technology**, *[S. l.]*, v. 158, n. July, p. 110981, 2019. DOI: 10.1016/j.postharvbio.2019.110981. Disponível em: https://doi.org/10.1016/j.postharvbio.2019.110981.

SANTANA, FELIPE BACHION DE. **Floresta Aleatória Para Desenvolvimento De Modelos Multivariados De Classificação E Regressão Em Química Analítica**. [s.l: s.n.].

SANTIAGO-RAMOS, David; FIGUEROA-CÁRDENAS, Juan de Dios; VÉLES-MEDINA, José Juan; SALAZAR, Ricardo. Physicochemical properties of nixtamalized black bean (Phaseolus vulgaris L.) flours. **Food Chemistry**, *[S. l.]*, v. 240, n. February 2017, p. 456–462, 2018. DOI: 10.1016/j.foodchem.2017.07.156. Disponível em: https://doi.org/10.1016/j.foodchem.2017.07.156.

SANTOS, Silva; HENRIQUE, Gustavo; TEIXEIRA, De Almeida; JR, Barbosa. Açaí (Euterpe oleracea Mart .): A Tropical Fruit with High Levels of Essential Minerals — Especially Manganese — and its Contribution as a Source of Natural Mineral Supplementation. *[S. l.]*, v. 7394, 2014. DOI: 10.1080/15287394.2014.866923.

SEN, Saikat; CHAKRABORTY, Raja; KALITA, Pratap. Rice - not just a staple food: A comprehensive review on its phytochemicals and therapeutic potential. **Trends in Food Science and Technology**, *[S. l.]*, v. 97, n. February 2019, p. 265–285, 2020. DOI: 10.1016/j.tifs.2020.01.022. Disponível em: https://doi.org/10.1016/j.tifs.2020.01.022.

SHAFIEE, Sahameh; MINAEI, Saeid. Combined data mining/NIR spectroscopy for purity assessment of lime juice. **Infrared Physics and Technology**, *[S. l.]*, v. 91, p. 193–199, 2018. DOI: 10.1016/j.infrared.2018.04.012. Disponível em: https://doi.org/10.1016/j.infrared.2018.04.012.

SHIBAMOTO, Takayuki; BJELDANES, Leonard F. Capítulo 2 - Determinação de Agentes Tóxicos Presentes nos Alimentos. *In*: Rio de Janeiro: Elsevier Editora Ltda., 2014. p. 31–50. Disponível em: http://www.sciencedirect.com/science/article/pii/B9788535271188000026. Acesso em: 11 mar. 2016.

SHIEBER, Andreas. **Modern Techniques for Food Authentication**. First ed. [s.l.] : Da-Wen Sun, 2008.

SKOOG, D. A.; HOLLER, F. J.; CROUCH, S. R. **Princípios de Análise Instrumental**. 6. ed. Porto Alegre: Bookman, 2009.

SKOOG, DA; HOLLER, FJ; NIEMAN, TA. **Princípios de análise instrumental**. 5. ed. São Paulo: Bookman, 2002.

SPINK, John; MOYER, Douglas C. **Backgrounder: defining the public health threat of food fraud**. Michigan, USA. Disponível em: http://foodfraud.msu.edu/wp-content/uploads/2014/07/food-fraud-ffg-backgrounder-v11-Final.pdf. Acesso em: 11 maio. 2017.

STRAUCH, Renee C.; MENGIST, Molla F.; PAN, Kevin; YOUSEF, Gad G.; IORIZZO, Massimo; BROWN, Allan F.; LILA, Mary Ann. Variation in anthocyanin profiles of 27 genotypes of red cabbage over two growing seasons. **Food Chemistry**, *[S. l.]*, v. 301, n. July, p. 125289, 2019. DOI: 10.1016/j.foodchem.2019.125289. Disponível em: https://doi.org/10.1016/j.foodchem.2019.125289.

SZYMAŃSKA, Ewa. Modern data science for analytical chemical data – A comprehensive review. **Analytica Chimica Acta**, *[S. l.]*, v. 1028, p. 1–10, 2018. DOI: 10.1016/j.aca.2018.05.038.

TAULER, Roma; PARASTAR, Hadi. Big (Bio)Chemical Data Mining Using Chemometric Methods: A Need for Chemists. **Angewandte Chemie**, *[S. l.]*, 2018. DOI: 10.1002/ange.201801134.

TEIXEIRA, José Luan da Paixão; CARAMÊS, Elem Tamirys dos Santos; BAPTISTA, Débora Parra; GIGANTE, Mirna Lúcia; PALLONE, Juliana Azevedo Lima. Vibrational spectroscopy and chemometrics tools for authenticity and improvement the safety control in goat milk. **Food Control**, *[S. l.]*, v. 112, n. January, p. 107105, 2020. DOI: 10.1016/j.foodcont.2020.107105. Disponível em: https://doi.org/10.1016/j.foodcont.2020.107105.

TEYE, Ernest; AMUAH, Charles L. Y.; MCGRATH, Terry; ELLIOTT, Christopher. Innovative and rapid analysis for rice authenticity using hand-held NIR spectrometry and chemometrics. **Spectrochimica Acta - Part A: Molecular and Biomolecular Spectroscopy**, *[S. l.]*, v. 217, p. 147–154, 2019. DOI: 10.1016/j.saa.2019.03.085. Disponível em: https://doi.org/10.1016/j.saa.2019.03.085.

TEYE, Ernest; HUANG, Xingyi; HAN, Fangkai; BOTCHWAY, Francis. Discrimination of Cocoa Beans According to Geographical Origin by Electronic Tongue and Multivariate Algorithms. **Food Analytical Methods**, *[S. l.]*, v. 7, n. 2, p. 360–365, 2014. DOI:

10.1007/s12161-013-9634-4.

TONG, Tao; NIU, Yun Hui; YUE, Yuan; WU, Shuang chan; DING, Hong. Beneficial effects of anthocyanins from red cabbage (Brassica oleracea L. var. capitata L.) administration to prevent irinotecan-induced mucositis. **Journal of Functional Foods**, *[S. l.]*, v. 32, p. 9–17, 2017. DOI: 10.1016/j.jff.2017.01.051. Disponível em: http://dx.doi.org/10.1016/j.jff.2017.01.051.

TREGUIER, Sylvain; COUDERC, Christel; TORMO, Helene; KLEIBER, Didier; LEVASSEUR-GARCIA, Cecile. Identification of lactic acid bacteria Enterococcus and Lactococcus by near-infrared spectroscopy and multivariate classification. **Journal of Microbiological Methods**, *[S. l.]*, v. 165, n. August, p. 105693, 2019. DOI: 10.1016/j.mimet.2019.105693. Disponível em: https://doi.org/10.1016/j.mimet.2019.105693.

ULRICI, Alessandro; FOCA, Giorgia; IELO, Maria Cristina; VOLPELLI, Luisa Antonella; LO FIEGO, Domenico Pietro. Automated identification and visualization of food defects using RGB imaging: Application to the detection of red skin defect of raw hams. **Innovative Food Science and Emerging Technologies**, *[S. l.]*, v. 16, p. 417–426, 2012. DOI: 10.1016/j.ifset.2012.09.008. Disponível em: http://dx.doi.org/10.1016/j.ifset.2012.09.008.

WADOOD, Syed Abdul; BOLI, Guo; XIAOWEN, Zhang; HUSSAIN, Imtiaz; YIMIN, Wei. Recent development in the application of analytical techniques for the traceability and authenticity of food of plant origin. **Microchemical Journal**, *[S. l.]*, v. 152, n. July 2019, p. 104295, 2020. DOI: 10.1016/j.microc.2019.104295. Disponível em: https://doi.org/10.1016/j.microc.2019.104295.

WALSH, Kerry B.; BLASCO, José; ZUDE-SASSE, Manuela; SUN, Xudong. Postharvest Biology and Technology Visible-NIR ‘ point ’ spectroscopy in postharvest fruit and vegetable assessment : The science behind three decades of commercial use. **Postharvest Biology and Technology**, *[S. l.]*, v. 168, n. March, p. 111246, 2020. DOI: 10.1016/j.postharvbio.2020.111246. Disponível em: https://doi.org/10.1016/j.postharvbio.2020.111246.

WALTER, Melissa; MARCHEZAN, Enio; DE AVILA, Luis Antonio. Rice: Composition and nutritional characteristics. **Ciencia Rural**, *[S. l.]*, v. 38, n. 4, p. 1184–1192, 2008. DOI: 10.1590/s0103-84782008000400049.

WENDEL, Alexander; UNDERWOOD, James; WALSH, Kerry. Maturity estimation of

mangoes using hyperspectral imaging from a ground based mobile platform. **Computers and Electronics in Agriculture**, *[S. l.]*, v. 155, n. August, p. 298–313, 2018. DOI: 10.1016/j.compag.2018.10.021. Disponível em: https://doi.org/10.1016/j.compag.2018.10.021.

WICZKOWSKI, Wieslaw; SZAWARA-NOWAK, Dorota; ROMASZKO, Jerzy. The impact of red cabbage fermentation on bioavailability of anthocyanins and antioxidant capacity of human plasma. **Food Chemistry**, *[S. l.]*, v. 190, p. 730–740, 2016. DOI: 10.1016/j.foodchem.2015.06.021. Disponível em: http://dx.doi.org/10.1016/j.foodchem.2015.06.021.

WICZKOWSKI, Wieslaw; TOPOLSKA, Joanna; HONKE, Joanna. Anthocyanins profile and antioxidant capacity of red cabbages are influenced by genotype and vegetation period. **Journal of Functional Foods**, *[S. l.]*, v. 7, p. 201–211, 2014. DOI: 10.1016/j.jff.2014.02.011. Disponível em: http://www.sciencedirect.com/science/article/pii/S1756464614000619. Acesso em: 13 mar. 2017.

WIEDEMAIR, Verena; HUCK, Christian W. Evaluation of the performance of three hand-held near-infrared spectrometer through investigation of total antioxidant capacity in gluten-free grains. **Talanta**, *[S. l.]*, v. 189, n. March, p. 233–240, 2018. DOI: 10.1016/j.talanta.2018.06.056. Disponível em: https://doi.org/10.1016/j.talanta.2018.06.056.

WOLD, Svante. Chemometrics, why, what and where to next? **Journal of Pharmaceutical and Biomedical Analysis**, *[S. l.]*, v. 9, n. 8, p. 589–596, 1991. DOI: 10.1016/0731-7085(91)80183-A.

WU, Di; RASCO, Barbara; VIXIE, Kevin R.; ÜNLÜ, Gülhan; SWANSON, Barry; LIU, Yaoyao. Using Fourier transform infrared (FT-IR) spectroscopy to detect sublethally- or lethally-stressed Listeria innocua treated with acetic acid. **LWT - Food Science and Technology**, *[S. l.]*, v. 54, n. 2, p. 456–462, 2013. DOI: 10.1016/j.lwt.2013.06.010.

WU, Di; SUN, Da Wen. Colour measurements by computer vision for food quality control - A review. **Trends in Food Science and Technology**, *[S. l.]*, v. 29, n. 1, p. 5–20, 2013. DOI: 10.1016/j.tifs.2012.08.004.

XIAO, Ran; LIU, Li; ZHANG, Dongjie; MA, Ying; NGADI, Michael O. Discrimination of organic and conventional rice by chemometric analysis of NIR spectra: a pilot study.

Journal of Food Measurement and Characterization, *[S. l.]*, v. 13, n. 1, p. 238–249, 2019. DOI: 10.1007/s11694-018-9937-7. Disponível em: http://dx.doi.org/10.1007/s11694-018-9937-7.

YAMAGUCHI, Klenicy Kazumy De Lima; PEREIRA, Luiz Felipe Ravazi; LAMARÃO, Carlos Vitor; LIMA, Emerson Silva; DA VEIGA-JUNIOR, Valdir Florêncio. Amazon acai: Chemistry and biological activities: A review. **Food Chemistry**, *[S. l.]*, v. 179, p. 137–151, 2015. DOI: 10.1016/j.foodchem.2015.01.055. Disponível em: http://dx.doi.org/10.1016/j.foodchem.2015.01.055.

ZHANG, Yudong; WANG, Shuihua; JI, Genlin; PHILLIPS, Preetha. Fruit classification using computer vision and feedforward neural network. **Journal of Food Engineering**, *[S. l.]*, v. 143, p. 167–177, 2014. DOI: 10.1016/j.jfoodeng.2014.07.001. Disponível em: http://dx.doi.org/10.1016/j.jfoodeng.2014.07.001.

ZHAO, Yubin; YAMAGUCHI, Yoshinori; LIU, Chenchen; LI, Mingda; DOU, Xiaoming. Rapid and quantitative detection of trace Sudan black B in dyed black rice by surface-enhanced Raman spectroscopy (SERS). **Spectrochimica Acta - Part A: Molecular and Biomolecular Spectroscopy**, *[S. l.]*, v. 216, p. 202–206, 2019. DOI: 10.1016/j.saa.2019.03.030. Disponível em: https://doi.org/10.1016/j.saa.2019.03.030.

CAPÍTULO III

Bioactive compounds and antioxidant capacity in freeze-dried red cabbage by FT-NIR and MIR spectroscopy and chemometric tools

Elem Tamirys dos Santos Caramês[a], Priscila Domingues Alamar[a], Juliana Azevedo Lima Pallone[a]

[a]*Department of food science, School of food engineering, University of Campinas, Monteiro Lobato street, 80, Campinas, São Paulo 13083-862, Brazil.*

Artigo publicado em *Food Analytical Methods*.

Reprinted from Caramês, E. T. S., Alamar, P. D., & Lima Pallone, J. A. (2019). Bioactive Compounds and Antioxidant Capacity in Freeze-Dried Red Cabbage by FT-NIR and MIR Spectroscopy and Chemometric Tools. *Food Analytical Methods*. https://doi.org/10.1007/s12161-019-01523-6

Food Analytical Methods
https://doi.org/10.1007/s12161-019-01523-6

Bioactive Compounds and Antioxidant Capacity in Freeze-Dried Red Cabbage by FT-NIR and MIR Spectroscopy and Chemometric Tools

Elem T. S. Caramês[1] · Priscila D. Alamar[1] · Juliana A. Lima Pallone[1]

Received: 12 February 2019 / Accepted: 29 April 2019

Abstract
Red cabbage is a widely consumed vegetable worldwide due to its popularity and affordability. This vegetable has a significant content of bioactive compounds known for their antioxidant properties. Several traditional methodologies are commonly used to measure the total phenolic and anthocyanin content (TPC and TAC) and the antioxidant capacity. However, these methods generate toxic waste, pose a threat to the operator, and are time-consuming. This study determined the potential use of near and mid-infrared (NIR and MIR) spectroscopy, along with chemometric tools to evaluate TPC, TAC, and antioxidant capacity in red cabbage. The PLS models obtained by MIR to predict TAC (RMSEP = 0.35 mg/g), TPC (RMSEP = 0.34 mg GAEq/g), oxygen radical absorbance capacity (ORAC) (RMSEP = 125.31 μMol Eq trolox/g), and trolox equivalent antioxidant capacity (TEAC) (RMSEP = 0.33 μMol Eq trolox/g), and 2,2-diphenyl-picrylhydrazyl (DPPH) (RMSEP = 11.11 μMol Eq trolox/100 g) displayed good parameters of errors of prediction. Models constructed with NIR to predict TAC (RMSEP = 0.47 mg/g), TPC (RMSEP = 0.41 mg GAEq/g), ORAC (RMSEP = 116.34 μMol Eq trolox/g), TEAC (RMSEP = 0.29 μMol Eq trolox/g), and DPPH (RMSEP = 11.47 μMol Eq trolox/100 g) had similar results. These results suggest that the vibrational spectroscopic techniques of NIR and MIR associated with chemometrics could be successfully used for determination of TAC, TPC, and antioxidant capacity. They are sustainable and efficient methods that reduce toxic waste and time when compared to current protocols.

Keywords TAC · TPC · antioxidant capacity · NIR · MIR

Introduction

Vegetables in the genus *Brassica* are extensively consumed worldwide, due to their popularity, availability, and moderate prices. The species *Brassica oleracea* var. *capitata f. rubra* DC. Red cabbage is a popular health food and rich in minerals, oligosaccharides, and bioactive compounds. These include vitamins (C and E), carotenoids, glucosinolates, sulfur organic compounds, phenolic compounds such as flavonoids, and anthocyanins. The application of conservation technologies, such as freezing or freeze-drying, on fresh cabbages may help to preserve and retain the biologically active compounds at their highest content. Therefore, making it possible to use red cabbages as an additive in a variety of products, such as beverages like apple juice (Wiczkowski et al. 2013, 2014; Nogales-Bueno et al. 2015; Radziejewska-Kubzdela and Biegańska-Marecik 2015; Vale et al. 2015; Cruz et al. 2016; Kapusta-Duch et al. 2017).

Bioactive compounds present in red cabbage are known for their beneficial effects to human body. Red cabbage is source of antioxidants is antimutagenic, anti-inflammatory, antiproliferative, and antimicrobial (Kljusurić et al. 2016). Antioxidant compounds are quantified through various assays. Assays that are based on their total content, or on their classes (flavonols, flavanols, anthocyanins, tannins, among others). They can also be quantified through their antioxidant properties, which include assays such as the following: radical scavenging capacity ferric ion reducing antioxidant power (FRAP), 2,2-diphenyl-picrylhydrazyl (DPPH), oxygen radical absorbance capacity (ORAC), and trolox equivalent antioxidant capacity/2,2'-azino-bis-(3-ethylbenzothiazoline-6-sulfonic acid) (TEAC/$ABTS^{+\bullet}$) (Schönbichler et al. 2014; Wu et al. 2015; Li et al. 2016). These antioxidant capacity assays can be classified according to the radical quenching mechanism in hydrogen atom transfer (HAT) or the single electron transfer (SET) mechanism. In this context, TEAC ($ABTS^{+\bullet}$) reacts through the SET mechanism, ORAC reacts through the

✉ Juliana A. Lima Pallone
jpallone@unicamp.br

[1] Department of Food Science, School of Food Engineering, University of Campinas, Monteiro Lobato Street, 80, Campinas, São Paulo 13083-862, Brazil

Published online: 14 May 2019

HAT mechanism, and DPPH reacts through both mechanisms (Schaich et al. 2015). Determining the antioxidant compounds and antioxidant capacity in a food of interest is critical for understanding its potential dietary benefit and/or function in food industry. However, the aforementioned traditional techniques are time-consuming, expensive, and cause damage to the environment. Therefore, a non-destructive technique that is efficient, inexpensive, and harmless is essential.

Infrared (IR) spectroscopy, in association with chemometrics, could be an appropriate alternative to quantify bioactive compounds and antioxidant capacity in food matrices. Functional groups found on these compounds absorb IR radiation, which is then converted into vibrational energy. This feature makes spectroscopic techniques, such as near-infrared spectroscopy (NIR) and mid-infrared spectroscopy (MIR), advantageous over traditional methods used for determination of bioactive compounds. NIR and MIR also have the added benefit of avoiding the use of organic solvents in an extraction process and accelerates quantification (Silva et al. 2014; Alamar et al. 2016; Redaelli et al. 2016). Presently, some studies have focused on the use of infrared spectroscopies (NIR and/or MIR) to create calibration models of bioactive compounds. These models were based on the content of anthocyanins, phenolic compounds, and antioxidant capacity (FRAP, CUPRAC, TEAC, DPPH, and ORAC) in grape juice (Caramês et al. 2016), berries (Kljusurić et al. 2016; Caramês et al. 2016), maize (Redaelli et al. 2016), apple (Schmutzler and Huck 2016), cocoa beans (Batista et al. 2016), Chinese rice wine (Wu et al. 2015), *Radix scutellariae* (Li et al. 2016), and coffee beans (Liang et al. 2016).

The aim of this study was to apply NIR and MIR spectroscopies, combined with chemometrics, to determine total phenolic compounds (TPC), total anthocyanin content (TAC), and antioxidant capacity (TEAC, ORAC and DPPH) in freeze-dried red cabbage samples.

Material and Methods

Chemicals and Red Cabbage Samples

Folin-Ciocalteu's phenol reagent (2 M), gallic acid (≥ 98%), 2,2'-azino-bis-(3-ethylbenzothiazoline-6-sulfonic acid), diammonium salt (ABTS, ≥ 98%), 2,2-diphenyl-1-picrylhydraziyl (DPPH), 2,2'-azobis(2-methylpropionamidine) dihydrochloride (AAPH, 97%), fluorescein sodium salt, and (±)-6-Hydroxy-2,5,7,8-tetramethylchromane-2-carboxylic acid (97%) were purchased from Sigma Aldrich (St. Louis, USA). Sodium acetate, acetic acid, chloridric acid (37%), sodium carbonate (Na_2CO_3, 99.8%), potassium dihydrogen phosphate anhydrous (KH_2PO_4), dipotassium hydrogen phosphate anhydrous (K_2HPO_4), absolute ethanol (99.9%), and methanol (analytical grade) were purchased from Synth (São Paulo, Brazil). Sixty red cabbage samples were sourced from local fairs (Campinas, Brazil).

Sample Preparation and Extraction

Sixty red cabbage samples were freeze-dried for 24 h (Terroni, Brazil, model LS 3000) under 2000 μHg (or less) at a temperature of about − 40 °C. Samples were then ground (Biovera, Brazil, model Ika A11) and sieved through an 80-mesh sieve (180 μm) to standardize particle size.

An exhaustive extraction was then performed, using methanol/water/acetic acid (0.58:0.38:0.04, *v*/*v*/*v*), applied with sonication for 30 s (1400 UltraSonic Clean, Unique, Brazil) and vortexed for 30 s, as described by Wiczkowski et al. (2013). This extraction process was repeated twice. The resulting extract was used for the determination of TPC and antioxidant capacity (TEAC, ORAC, and DPPH).

Total anthocyanin content (TAC) was determined using an extraction of 0.2 g from each sample with 8 mL of HCl 0.1 mol/L and were then exposed to radiation using a household microwave oven (CCE, Brazil, model MW-1580) operating at 1420 W. The extraction was vortexed for 10 s and 2 cycles of 30 s of irradiation with a cooling time of 10 min (until 25 °C) between cycles (in order to avoid thermal degradation) was carried out (Laokuldilok et al. 2016). The samples were then centrifuged at 6000 rpm for 10 min at 4 °C (Solab Cientifica, Brazil, model SL-706). The supernatant was collected and stored at − 22 °C until further analysis.

Total Phenolic Compounds

TPC of red cabbage extracts was determined according to the methodology of Singleton and Rossi (1965). Per sample, 85 μL was used. In a dark room, 43 μL of Folin-Ciocalteau reagent (1 N) and 212 μL of Na_2CO_3 (75 g/L) was added to each sample in a 96-well microplate. The absorbance of the samples was then measured at 725 nm in a multi-mode microplate reader (BMG Labtech, Germany, model Fluostar Omega). The TPC concentrations were obtained from a standard curve of gallic acid (1–50 mg/mL) and the results were expressed as mg of gallic acid/g of red cabbage. The analyses were performed in triplicate.

Total Anthocyanin Content

TAC of red cabbage was quantified according to the reference AOAC (2005-02) method (AOAC) with modifications (Giusti and Wrolstad 2001). The absorbance was recorded with a multi-mode microplate reader (BMG Labtech, Germany, model Fluostar Omega) at wavelengths of 520 and 700 nm, for pH 1.0 and pH 4.5 solutions. The analyses were carried out in triplicate.

Trolox Equivalent Antioxidant Capacity

TEAC was determined as previously described by Cano et al. (1998) with modifications. ABTS radical cations were generated by mixing 7 mM ABTS with 2.45 mM potassium persulfate in distilled water. The mixed solution was kept in the dark at 25 °C for 24 h. An aliquot of ABTS stock solution was diluted in ethanol, to give the working solution an absorbance of around 0.40 ± 0.02 at 734 nm. Trolox was used to obtain a standard curve (3–15 μM). The kinects were recorded with a multi-mode microplate reader (BMG Labtech, Germany, model Fluostar Omega). TEAC of red cabbage extracts were expressed as μM trolox equivalent (TE)/g of red cabbage and all samples were analyzed in triplicate.

Oxygen Radical Absorbance Capacity ($ORAC_{FL}$)

The $ORAC_{FL}$ assay was performed according to Prior et al. (2003) with modifications. Trolox (10 nM), fluorescein (55 nM), AAPH (150 mM), and sample dilutions for $ORAC_{FL}$ were prepared in phosphate buffer solution pH 7.4 (75 nM) and incubated at 37 °C. The intensity of fluorescence was measured at an excitation wavelength of Ex = 493 nm and an emission wavelength of Em = 515 nm, using 96-well black microplates. Kinects, in triplicate, were recorded with a multi-mode microplate reader (BMG Labtech, Germany, model Fluostar Omega). Standard curves were constructed with trolox (0.5 to 4.0 μM) and the results were expressed as μM TE/g of red cabbage.

Antioxidant Capacity Determined by DPPH Radical Scavenging Assay

The DPPH radical scavenging assay of the extracted samples was determined with DPPH radical in methanol (25 mg/L) as described previously by Sánchez-Moreno et al. (1998). The calibration curve was built with trolox (concentration 0.6–20.0 mM) in methanol, with an added 312 μL of DPPH solution under 8 μL of trolox/sample solution. Kinect measurements (515 nm) were carried out using a multi-mode microplate reader (BMG Labtech, Germany, model Fluostar Omega). DPPH values of red cabbage extracts were expressed as μM TE/g and all samples were analyzed in triplicate.

NIR spectroscopy

From each sample, approximately 3 g was placed into a glass vial (Wheaton, USA, Shell vial). Diffuse reflectance measurements were taken using a near-infrared reflectance accessory (Perkin Elmer-Waltham, USA, model NIRA) in a FT-NIR spectrometer (Perkin Elmer-Waltham, USA, model Spectrum 100N) equipped with an integrating sphere and InGaAs detector. Thirty-two scans per sample were made in the range of 10,000 to 4000 cm^{-1} at a spectral resolution of 8 cm^{-1}. The samples were scanned in triplicate and the average spectrum was used in subsequent calculations.

MIR Spectroscopy

The mid-infrared (MIR) spectra were recorded using a FT-MIR spectrometer (Agilent Cary 630, CA, USA) equipped with an attenuated total reflectance (HATR) accessory with a SeZn crystal and deuterated triglycine sulfate detector (DTGS). Sixty-four scans/sample were made at wavenumbers ranging from 4000 to 400 cm^{-1}, at a resolution of 4 cm^{-1}.

Multivariate Analysis

The spectra data were mean centered and preprocessed by MSC (mean scatter correction) and/or first derivative using the Savitzky-Golay algorithm with a smoothing window of 21 points. The calibration models were constructed using the PLS method (partial least squares regression). The internal validation was performed with leave-one-out cross-validation and used to determine the optimal value of latent variables (LV). The original spectra data were randomly divided in two groups: the calibration group (70% of the samples) and the external validation group (30% of the samples).

The calibration models were calculated with PLS-toolbox 8.6 and MatLab version 2017b. The root mean square error of calibration (RMSEC), root mean square error of prediction (RMSEP), and the coefficient of determination (R^2) were used to evaluate the performance of generated models. Samples with the high Student residual values and leverage were considered outliers and removed to improve the quality of the PLS model.

Results and Discussion

Bioactive Compounds and Antioxidant Capacity by Traditional Methods

Total anthocyanin content (TAC) analysis showed that red cabbage is high in TAC percentage and represents the major class of bioactive compounds found in the samples. Therefore, the antioxidant properties of red cabbage are mostly connected to the high TAC value. The average level of TAC (Table 1) determined by this study was 5.16 mg/g dm, similar to that of Wiczkowski et al. (2015) that reported a value of 6.30 mg/g dm in their study using fresh red cabbages and during the fermentation process (Wiczkowski et al. 2015). The variation in results could be attributed to the seasonal conditions during vegetative growth (temperature, precipitation, soil type, and light exposure, for example) and/or the postharvest transport conditions. These same conditions may have also affected the

Table 1 Bioactive compounds and antioxidant capacity results (dry matter)

	Range	Media	CV%
TAC (mg/g)	7.41–3.04	5.16	0.21
TPC[1] (mg GAEq/g)	6.97–3.87	5.30	1.67
ORAC[2] (μMol Eq trolox/g)	1741.18–434.11	852.88	7.96
TEAC[2] (μMol Eq trolox/g)	6.46–3.79	5.16	3.08
DPPH[2] (μMol Eq trolox/100 g)	209.85–94.01	131.78	1.39

[1] Data are expressed in milligrams of gallic acid per gram dry matter of red cabbage

[2] Data are expressed in micromoles of trolox per gram dry matter of red cabbage

total polyphenols content (TPC) values, which varied between 6.97–3.87 mg GAEq/g dm (Wiczkowski et al. 2014; Wiczkowski et al. 2015).

Vicas et al. (2013) developed a study to determine the profile of glucosinolates and antioxidant capacity of Roman *Brassica* vegetables produced using organic and conventional agricultural practices. The conventionally produced red cabbage displayed mean values of 3.02 mg GAE/g dw while organic red cabbage had 3.17 mg GAE/g dw (Vicas et al. 2013). These results corroborate those presented in this study, although below the minimum level described, the variation could also be explained by the environmental factors previously cited and by the different regions of sample origin.

In regard to daily intake, Floegel et al. (2011) investigated the antioxidant capacity of common fruits and vegetables in the USA. Their study determined that red cabbage (fresh) had a DPPH value of 187.4 ± 8.4 mg VCE/100 g and an ABTS value of 2.68 ± 0.13 mg VCE/g. These results were similar to the averages determined in this study (131.78 μMol Eq trolox/100 g and 5.16 μMol Eq trolox/g, respectively).

Wiczkowski et al. (2014) conducted a detailed study to characterize the anthocyanins profile and antioxidant capacity of different genotypes and the vegetative period lengths of red cabbages. They reported ORAC values between 100.00 and 413.33 μmol trolox/g dm. Despite these values being below the average level presented in this study, it highlights how genotype and the length of the vegetative period can influence the variation of ORAC values.

MIR and NIR Spectra Data and Preprocessing

The mean of the raw spectra data obtained from MIR and NIR are presented in Fig. 1 a and b.

Regarding the NIR spectra data obtained, three relevant bands of absorbance was detected. These are the first and the second overtone bands caused by O–H groups (6900 cm^{-1} and 5200 cm^{-1}, respectively). The third peak was detected at 4500 cm^{-1} and is commonly associated with the C–H groups of aromatic groups, especially those phenolic in nature (Xie et al. 2009; Shiroma and Rodriguez-Saona 2009; Frizon et al. 2015).

The sulforaphane compound has the highest importance in *Brassica* species because of their high antioxidant capacity. In the MIR spectra, this compound presents a cumulative bond stretch with an absorbance at 2280–2000 cm^{-1}. It was also relevant to the process of constructing the PLS models of antioxidant capacity. The portion between 3500–3000 cm^{-1} is associated with the O–H band (Silverstein et al. 2005; Dal Prá et al. 2013).

In order to increase the final performance of the PLS calibration models, the spectra data of NIR and MIR were preprocessed (Table 2). Several methods of preprocessing were tested, and the best results were obtained with multiplicative scatter correction (MSC). This was used in NIR and MIR to correct the light scattering, common in the process of obtaining spectra. The first derivative Savitzky-Golay method was also applied to the NIR spectra data that presented spectral off-set. All spectra data used in this study were mean centered.

The selection of variables were done to increase the quality of the PLS models (Table 2). In the NIR spectra the initial portion (10000–7200 cm^{-1}) showed poor chemical information and was considered as the base line and removed from all calibration models. In MIR calibration models of TAC and TPC, the final portion of the spectra displayed significant

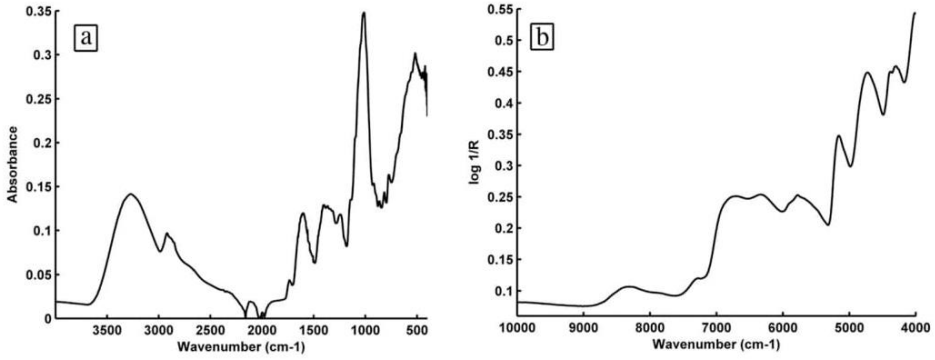

Fig. 1 Raw spectra data means obtained in MIR (**a**) and NIR (**b**)

Table 2 Preprocessing and variables used in MIR and NIR PLS models

	Preprocessing	Wavenumber (cm^{-1})
MIR		
TAC	MSC + mean center	4000–762.24
TPC	MSC + mean center	4000–538.66
ORAC	MSC + mean center	4000–2129.80
TEAC	MSC + mean center	4000–2155.88
DPPH	MSC + mean center	4000–2345.95
NIR		
TAC	1st derivative + MSC + mean center	7228–4000
TPC	1st derivative + MSC + mean center	7200–4000
ORAC	1st derivative + MSC + mean center	7186–4000
TEAC	1st derivative + MSC + mean center	7200–4000
DPPH	1st derivative + MSC + mean center	7214–4000

residuals, hindering the calibration process and were removed. In antioxidant capacity models, the portion of spectra data associated with the O–H band and sulforaphane compounds were used.

MIR and NIR Calibration Models

A summary of parameters for the PLS models are presented in Table 3. The TAC models obtained by MIR and NIR presented in Fig. 2 a and b had similar performance, with comparable values of RMSEP, RSMEC, and R^2. Caramês et al. (2017) determined PLS models using NIR and MIR to predict TAC in grape juice; their results indicated a similar performance of NIR and MIR, with R^2 values of 0.84 and 0.81 respectively. These are very similar to the results reported in this study, which were 0.85 for both NIR and MIR.

Viegas et al. (2016) developed a PLS model using NIR to predict TPC in wax jambu fruit which had RMSEP = 0.22 mg GAEq/g, similar to the value of RMSEP (0.34 mg GAEq/g) reported in this work (Fig. 2d). In another study, Frizon et al. (2015) generated PLS models using NIR to determine TPC in *Ilex paraguariensis* (yerba mate) and had RMSEC = 16.07 mg/g and RMSEP = 12.12 mg/g, values greater than those in this study.

Hu et al. (2016) established a PLS model using ATR FT-IR data to predict TPC in chocolate and reported values (RMSEC = 3.21 mg GAE/g and RMSEP = 5.08 mg GAE/g) higher than those in this paper (Fig. 2c).

Batista et al. (2016) developed a study to determine the antioxidant capacity in cocoa beans using MIR, and in their DPPH model reported RMSEP = 0.2524 μMol Eq trolox/g and in their ABTS model RMSEP = 0.94 μMol Eq trolox/g. These results were also higher than the $RMSEP_{DPPH}$ = 0.11 μMol Eq trolox/g and $RMSEP_{TEAC}$ = 0.33 μMol Eq trolox/g reported in this study (Fig. 3c). Another study also applied NIR to the rapid assessment of antioxidant properties in spent coffee grounds and the developed ABTS model found RMSEC = 13.7 μMol Eq trolox/g and RMSEP = 12.9 μMol Eq trolox/g, greater than those in the red cabbage models (Fig. 3f) (Páscoa et al. 2013).

Hu et al. (2016) determined antioxidant capacity in chocolate using FT-IR, the PLS model obtained for DPPH presented RMSEC = 8.46 μMol Eq trolox/g and RMSEP = 13.07 μMol Eq trolox/g, both values higher than that found in red cabbage models (Fig. 3c). The PLS model developed by Hu et al. (2016) for ORAC had RMSEC = 30.97 μMol Eq trolox/g and RMSEP = 37.92 μMol Eq trolox/g, with these values being lower than those for red cabbage (Fig. 3a). It is important to emphasize that the authors used a larger number of LVs (15), which can result in an overfitting model and/or include too much noise from the *x* and *y* data during the calibration process. Despite this, the range of values of ORAC found in chocolate were smaller than the range found in red cabbage

Table 3 Parameters of MIR and NIR PLS models

	Nc	Nv	LV	R^2	RMSEC	RMSEP
MIR						
TAC (mg/g)	36	20	7	0.85	0.44	0.35
TPC (mg GAEq/g)	40	19	8	0.79	0.32	0.34
ORAC (μMol Eq trolox/g)	40	19	6	0.83	129.09	125.31
TEAC (μMol Eq trolox/g)	40	20	6	0.78	0.32	0.33
DPPH (μMol Eq trolox/100 g)	40	14	7	0.88	8.24	11.11
NIR						
TAC (mg/g)	40	20	7	0.85	0.46	0.47
TPC (mg GAEq/g)	40	19	7	0.78	0.32	0.41
ORAC (μMol Eq trolox/g)	40	18	8	0.87	105.01	116.34
TEAC (μMol Eq trolox/g)	40	18	8	0.85	0.26	0.29
DPPH (μMol Eq trolox/100 g)	40	19	7	0.80	11.57	11.47

Nc number of samples in calibration set, *Nv* number of samples in external validation set, *LV* number of latent variable, R^2 coefficient of regression

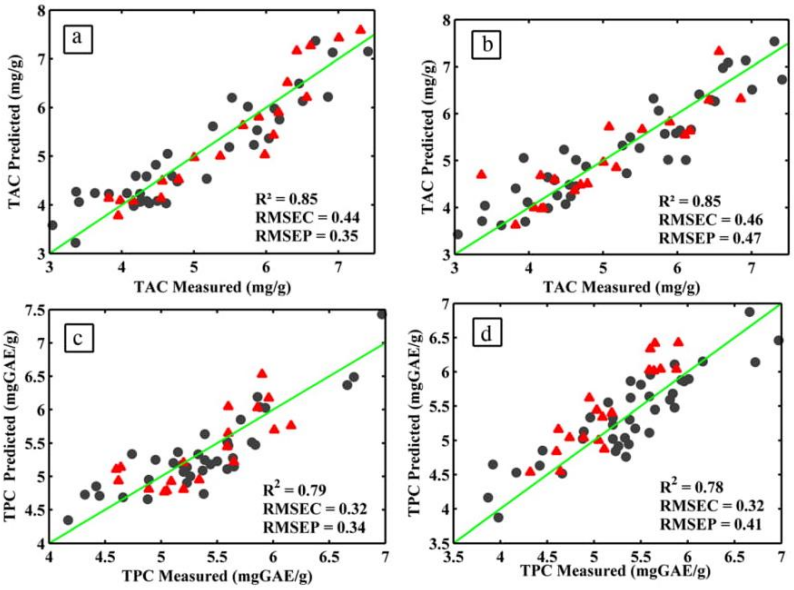

Fig. 2 TAC models by MIR (**a**) and NIR (**b**) and TPC models by MIR (**c**) and NIR (**d**)

samples, 39.67–424.62 μMol Eq trolox/g and 1741.18–434.11 μMol Eq trolox/g, respectively, which consequently, results in smaller values of RMSEC and RMSEP (Burns and Ciurczak 2009).

Considering all the performance parameters of the models determined by NIR and MIR, both resulted in excellent values of error and high values of R^2. Therefore, NIR and MIR could be applied to the proposed aim. However, even though the MIR raw data displayed more chemical information when compared with the NIR raw data, the results achieved from NIR PLS models were slightly better to those of MIR; mainly when observed with the ORAC model. Therefore, considering these factors, and that NIR has a greater variety of portable instruments and on-line devices, NIR has shown itself as the best alternative technique in this case study.

Conclusion

Freeze-dried red cabbage can be classified as a beneficial and affordable source to increase the daily consumption of bioactive compounds that have antioxidant capacity. A main reason why this food should be increasingly valued by consumers. In order to facilitate the efficient, sustainable, and accurate measurement of phenolic compound content and antioxidant capacity present in freeze-dried red cabbage, this study reports the possibility of applying near (NIR) and mid-infrared (MIR) to replace the common methodologies currently used. Both NIR and MIR achieved similar results when compared using the parameters of RMSEC and RMSEP for each PLS model developed. The spectra data obtained in the MIR region also displayed the possibility of interpreting chemical information.

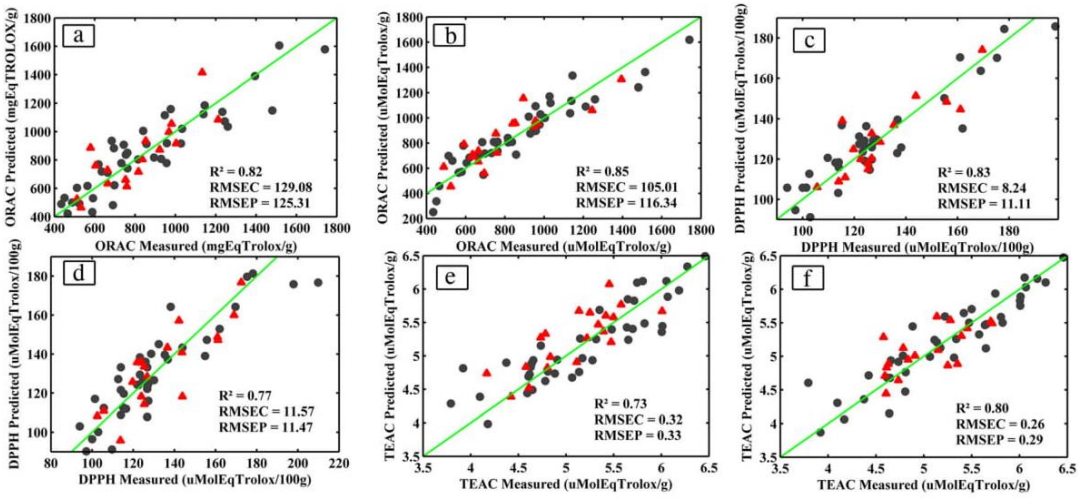

An important and added advantage of both techniques is that they require no toxic reagents. For this reason, there is no generation of toxic waste, danger to the operator, no complicated methods of sample preparation, and are faster methods of analysis. Therefore, NIR and MIR should be considered as a good alternative for the rapid assessment of TAC, TPC, and antioxidant capacity in red cabbage.

Funding This study was financed in part by the Coordenação de Aperfeiçoamento de Pessoal de Nível Superior - Brasil (CAPES) - Finance Code 001.

Compliance with Ethical Standards

Conflict of Interest The authors declare that they have no conflict of interest.

Ethical Approval This article does not contain any studies with animals performed by any of the authors.

Informed Consent Not applicable.

References

Alamar PD, Caramês ETS, Poppi RJ, Pallone JAL (2016) Quality evaluation of frozen guava and yellow passion fruit pulps by NIR spectroscopy and chemometrics. Food Res Int 85:209–214. https://doi.org/10.1016/j.foodres.2016.04.027

AOAC (2005) Official methods of analysis of the Association of Official Analytical Chemists, 17th edn. AOAC, Washington, DC

Batista NN, de Andrade DP, Ramos CL, Dias DR, Schwan RF (2016) Antioxidant capacity of cocoa beans and chocolate assessed by FTIR. Food Res Int 90:313–319. https://doi.org/10.1016/j.foodres.2016.10.028

Burns DA, Ciurczak EW (2009) Handbook of near-infrared analysis, 3rd ed. Anal Bioanal Chem 393:1387–1389

Cano A, Hernández-Ruíz J, García-Cánovas F, Acosta M, Arnao MB (1998) An end-point method for estimation of the total antioxidant activity in plant material. Phytochem Anal 9:196–202. https://doi.org/10.1002/(SICI)1099-1565(199807/08)9:4<196::AID-PCA395>3.0.CO;2-W

Caramês ETS, Alamar PD, Poppi RJ, Pallone JAL (2016) Rapid assessment of total phenolic and anthocyanin contents in grape juice using infrared spectroscopy and multivariate calibration. Food Anal Methods 1–7. https://doi.org/10.1007/s12161-016-0721-1

Caramês ETS, Alamar PD, Poppi RJ, Pallone JAL (2017) Quality control of cashew apple and guava nectar by near infrared spectroscopy. Journal of Food Composition and Analysis, 56:41–46. https://doi.org/10.1016/j.jfca.2016.12.002

Cruz AB, H da S P, Veber B et al (2016) Assessment of bioactive metabolites and hypolipidemic effect of polyphenolic-rich red cabbage extract. Pharm Biol 54:3033–3039. https://doi.org/10.1080/13880209.2016.1200633

Dal Prá V, Dolwitsch CB, da Silveira GD, Porte L, Frizzo C, Tres MV, Mossi V, Mazutti MA, do Nascimento PC, Bohrer D, de Carvalho LM, Viana C, da Rosa MB (2013) Supercritical CO2 extraction, chemical characterisation and antioxidant potential of Brassica oleracea var capitata against OH and ROO. Food Chem 141:3954–3959. https://doi.org/10.1016/j.foodchem.2013.06.098

Floegel A, Kim D-O, Chung S-J, Koo SI, Chun OK (2011) Comparison of ABTS/DPPH assays to measure antioxidant capacity in popular antioxidant-rich US foods. J Food Compos Anal 24:1043–1048. https://doi.org/10.1016/j.jfca.2011.01.008

Frizon CNT, Oliveira GA, Perussello CA, Peralta-Zamora PG, Camlofski AMO, Rossa ÜB, Hoffmann-Ribani R (2015) Determination of total phenolic compounds in yerba mate (Ilex paraguariensis) combining near infrared spectroscopy (NIR) and multivariate analysis. LWT Food Sci Technol 60:795–801. https://doi.org/10.1016/j.lwt.2014.10.030

Giusti MM, Wrolstad RE (2001) Characterization and measurement of anthocyanins by UV-Visible spectroscopy. In: Wrolstad RE, Acree TE, Decker EA et al (eds) Current Protocols in Food Analytical Chemistry. John Wiley & Sons, Inc., Hoboken, NJ, USA

Hu Y, Pan ZJ, Liao W, Li J, Gruget P, Kitts DD, Lu X (2016) Determination of antioxidant capacity and phenolic content of chocolate by attenuated total reflectance-Fourier transformed-infrared spectroscopy. Food Chem 202:254–261. https://doi.org/10.1016/j.foodchem.2016.01.130

Kapusta-Duch J, Kusznierewicz B, Leszczyńska T, Borczak B (2017) The effect of package type on selected parameters of nutritional quality of the chilled stored red sauerkraut. J Food Process Preserv 41:n/a-n/a. https://doi.org/10.1111/jfpp.13105

Kljusurić JG, Mihalev K, Bečić I et al (2016) Near-infrared spectroscopic analysis of total phenolic content and antioxidant activity of berry fruits. Food Technol Biotechnol 54:236–242. https://doi.org/10.17113/ftb.54.02.16.4095

Laokuldilok N, Thakeow P, Kopermsub P, Utama-ang N (2016) Optimisation of microencapsulation of turmeric extract for masking flavour. Food Chem 194:695–704. https://doi.org/10.1016/j.foodchem.2015.07.150

Li H, He J, Li F, Zhang Z, Li R, Su J, Zhang J, Yang B (2016) Application of NIR and MIR spectroscopy for rapid determination of antioxidant activity of Radix Scutellariae from different geographical regions. Phytochem Anal 27:73–80. https://doi.org/10.1002/pca.2602

Liang N, Lu X, Hu Y, Kitts DD (2016) Application of attenuated total reflectance–Fourier transformed infrared (ATR-FTIR) spectroscopy to determine the chlorogenic acid isomer profile and antioxidant capacity of coffee beans. J Agric Food Chem 64:681–689. https://doi.org/10.1021/acs.jafc.5b05682

Nogales-Bueno J, Baca-Bocanegra B, Rodríguez-Pulido FJ, Heredia FJ, Hernández-Hierro JM (2015) Use of near infrared hyperspectral tools for the screening of extractable polyphenols in red grape skins. Food Chem 172:559–564. https://doi.org/10.1016/j.foodchem.2014.09.112

Páscoa RNMJ, Magalhães LM, Lopes JA (2013) FT-NIR spectroscopy as a tool for valorization of spent coffee grounds: application to assessment of antioxidant properties. Food Res Int 51:579–586. https://doi.org/10.1016/j.foodres.2013.01.035

Prior RL, Hoang H, Gu L, Wu X, Bacchiocca M, Howard L, Hampsch-Woodill M, Huang D, Ou B, Jacob R (2003) Assays for hydrophilic and lipophilic antioxidant capacity (oxygen radical absorbance capacity (ORACFL)) of plasma and other biological and food samples. J Agric Food Chem 51:3273–3279. https://doi.org/10.1021/jf0262256

Radziejewska-Kubzdela E, Biegańska-Marecik R (2015) A comparison of the composition and antioxidant capacity of novel beverages with an addition of red cabbage in the frozen, purée and freeze-dried forms. LWT Food Sci Technol 62:821–829. https://doi.org/10.1016/J.LWT.2014.07.018

Redaelli R, Alfieri M, Cabassi G (2016) Development of a NIRS calibration for total antioxidant capacity in maize germplasm. Talanta 154:164–168. https://doi.org/10.1016/j.talanta.2016.03.048

Sánchez-Moreno C, Larrauri JA, Saura-Calixto F (1998) A procedure to measure the antiradical efficiency of polyphenols. J Sci Food Agric

76:270–276. https://doi.org/10.1002/(SICI)1097-0010(199802)76:2<270::AID-JSFA945>3.0.CO;2-9

Schaich KM, Tian X, Xie J (2015) Hurdles and pitfalls in measuring antioxidant efficacy: a critical evaluation of ABTS, DPPH, and ORAC assays. J Funct Foods 14:111–125. https://doi.org/10.1016/j.jff.2015.01.043

Schmutzler M, Huck CW (2016) Simultaneous detection of total antioxidant capacity and total soluble solids content by Fourier transform near-infrared (FT-NIR) spectroscopy: a quick and sensitive method for on-site analyses of apples. Food Control 66:27–37. https://doi.org/10.1016/j.foodcont.2016.01.026

Schönbichler SA, Falser GFJ, Hussain S, et al. (2014) Comparison of NIR and ATR-IR spectroscopy for the determination of the antioxidant capacity of Primulae flos cum calycibus 6:6343–6351. https://doi.org/10.1039/C4AY00669K

Shiroma C, Rodriguez-Saona L (2009) Application of NIR and MIR spectroscopy in quality control of potato chips. J Food Compos Anal 22:596–605. https://doi.org/10.1016/j.jfca.2008.09.003

Silva SD, Feliciano RP, Boas LV, Bronze MR (2014) Application of FTIR-ATR to Moscatel dessert wines for prediction of total phenolic and flavonoid contents and antioxidant capacity. Food Chem 150:489–493. https://doi.org/10.1016/j.foodchem.2013.11.028

Silverstein RM, Webster FX DJK (2005) Spectrometric identification of organic compounds .J Mol Struct https://doi.org/10.1016/0022-2860(76)87024-X

Singleton VL, Rossi JA (1965) Colorimetry of total phenolics with phosphomolybdic-phosphotungstic acid reagents. Am J Enol Vitic 16:144–158

Vale AP, Santos J, Brito NV, Marinho C, Amorim V, Rosa E, Oliveira MBPP (2015) Effect of refrigerated storage on the bioactive compounds and microbial quality of Brassica oleraceae sprouts. Postharvest Biol Technol 109:120–129. https://doi.org/10.1016/j.postharvbio.2015.06.013

Vicas SI, Teusdea AC, Carbunar M, Socaci SA, Socaciu C (2013) Glucosinolates profile and antioxidant capacity of Romanian brassica vegetables obtained by organic and conventional agricultural practices. Plant Foods Hum Nutr 68:313–321. https://doi.org/10.1007/s11130-013-0367-8

Viegas TR, Mata ALML, Duarte MML, Lima KMG (2016) Determination of quality attributes in wax jambu fruit using NIRS and PLS. Food Chem 190:1–4. https://doi.org/10.1016/j.foodchem.2015.05.063

Wiczkowski W, Szawara-Nowak D, Topolska J (2013) Red cabbage anthocyanins: profile, isolation, identification, and antioxidant activity. Food Res Int 51:303–309. https://doi.org/10.1016/j.foodres.2012.12.015

Wiczkowski W, Topolska J, Honke J (2014) Anthocyanins profile and antioxidant capacity of red cabbages are influenced by genotype and vegetation period. J Funct Foods 7:201–211. https://doi.org/10.1016/j.jff.2014.02.011

Wiczkowski W, Szawara-Nowak D, Topolska J (2015) Changes in the content and composition of anthocyanins in red cabbage and its antioxidant capacity during fermentation, storage and stewing. Res Gate. https://doi.org/10.1016/j.foodchem.2014.06.087

Wu Z, Xu E, Long J, Wang F, Xu X, Jin Z, Jiao A (2015) Rapid measurement of antioxidant activity and γ-aminobutyric acid content of Chinese rice wine by Fourier-transform near infrared spectroscopy. Food Anal Methods 8:2541–2553. https://doi.org/10.1007/s12161-015-0144-4

Xie L, Ye X, Liu D, Ying Y (2009) Quantification of glucose, fructose and sucrose in bayberry juice by NIR and PLS. Food Chem 114:1135–1140. https://doi.org/10.1016/j.foodchem.2008.10.076

CAPÍTULO IV

Near infrared spectroscopy and smartphone-based imaging as fast alternatives for the evaluation of bioactive potential of freeze-dried açai.

Elem Tamirys dos Santos Caramês [a], Michel Rocha Baqueta [a], Deborah A. Conceição [a], Juliana Azevedo Lima Pallone [a].

[a] *Department of Food Science, School of Food Engineering, State University of Campinas, Street Monteiro Lobato, 80, CEP: 13.083-862, Campinas, São Paulo, Brazil*

Artigo publicado em *Food Research International*

Reprinted from Tamirys dos Santos Caramês, E., Rocha Baqueta, M., Conceição, D.A., Azevedo Lima Pallone, J., Near infrared spectroscopy and smartphone-based imaging as fast alternatives for the evaluation of the bioactive potential of freeze-dried açai, **Food Research International** (2020), doi: https://doi.org/10.1016/j.foodres.2020.109792

ARTICLE IN PRESS

Food Research International xxx (xxxx) xxx

Contents lists available at ScienceDirect

Food Research International

journal homepage: www.elsevier.com/locate/foodres

Near infrared spectroscopy and smartphone-based imaging as fast alternatives for the evaluation of the bioactive potential of freeze-dried açai

Elem Tamirys dos Santos Caramês, Michel Rocha Baqueta, Deborah Alves Conceição, Juliana Azevedo Lima Pallone *

Department of Food Science, School of Food Engineering, State University of Campinas, Street Monteiro Lobato, 80, CEP: 13.083-862, Campinas, São Paulo, Brazil

ARTICLE INFO

Keywords:
açai pulp
chemometrics
digital image
fruit
near infrared
RGB

ABSTRACT

The development of green analytical techniques for food industry quality control has become an important issue in the context of the fourth industrial revolution. In this sense, near infrared spectroscopy (NIR) and smartphone-based imaging (SBI) were applied to evaluate the bioactive potential of freeze-dried açai pulps. For this purpose, reference results of ninety-six samples were obtained by determining total anthocyanins (TAC), polyphenol content (TPC), and antioxidant capacity (DPPH, ORAC and TEAC) by traditional methods and correlated to NIR spectra and SBI to build predictive models based on partial square least (PLS) regression. In summary, the NIR-PLS models showed better performance for predicting the TAC, TPC and antioxidant capacity of studied samples; considering the parameters of merit, such as coefficient of determination (0.8) and residual prediction deviation (RPD) (2.2) compared to the SBI-PLS models (0.7 and lower 1.5, respectively). The better performance of NIR-PLS could be potentially justified by a higher sensitivity of the NIR equipment than the smartphone images. In conclusion, these results show that the proposed alternative methods are promising tools for the future context of the 4.0 food industry.

1. Introduction

Fruits and fruits products with high nutritional quality have become one of the most important industrial segments in many countries. Nowadays, the consumption of products known as superfood represents one of the main trends in human nutrition. In this respect, several fruits produced in the Amazon rainforest in Brazil, the world's largest intact forest, have been incorporated in diets for their high nutritional quality (Moreda-Piñeiro et al., 2020).

Among the Amazon products in highlight is açai (*Euterpe oleracea*), a fruit that grows typically in the north of the Brazilian Amazon, and that normally is commercialized as juice, puree or powder, including freeze-dried açai pulp. This fruit is well associated with health benefits such as protection against cancer, heart disease, arthritis, better digestion and health in general. Most of these potential effects are attributed to the chemical composition of açai that contains proteins (4%), lipids (12%) - including poly and monounsaturated fatty acids (PUFA and MUFA) as oleic and palmitic acid - as well as dietary fiber (44%) and a high amount of antioxidant compounds such as anthocyanins (mainly cyanindin-3-glucoside and cyanindin-3-rutinoside) that are responsible for the violet color of açai (Çopur & Tamer, 2014).

Due to its nutritional composition, freeze-dried açai pulp has been consumed as a food supplement, being among the 30 best-selling products in the United States in 2015, and has also been widely used in food (gelatin, juice, cookies, powder for shakes, soups, or additive to energy drinks, etc.) and pharmaceutical industries (contrast agent for magnetic resonance or in the composition of some pharmaceutical formulations) (Benatrehina et al., 2018). However, most of these bioactive compounds, present in both açai and other foods, are degrade under exposure to high temperatures, oxygen and light, conditions that could decrease the nutritional value during the processing, storage and product distribution. In this sense, concerned with the intention of assuring the quality of the final product, methods capable of determining the content of bioactive compounds and antioxidant capacity of açai were previously developed (Wurlitzer et al., 2019).

The presence of bioactive compounds in a sample can be ~~is~~ determined through different types of colorimetric assays, with some of them based on the total content of classes of compounds, including tannins, anthocyanins, flavonols, and flavanols. There are also analytical methods that aim to quantify the bioactive compounds with respect to

* Corresponding author.
E-mail address: jpallone@unicamp.br (J.A.L. Pallone).

https://doi.org/10.1016/j.foodres.2020.109792
Received 12 June 2020; Received in revised form 30 September 2020; Accepted 4 October 2020
Available online 29 October 2020
0963-9969/

their antioxidant properties, being often divided based on the radical quenching mechanism: hydrogen atom transfer, such as oxygen radial absorbance capacity method (ORAC), or single electron transfer, such as in the trolox equivalent antioxidant capacity method (TEAC). Other methods can also be classified in both mechanism like 2,2-diphenyl-picrylhydrazyl (DPPH) assay. Even though these methods are well-known and routinely applied in various laboratories, they are time-consuming, expensive, laborious and, in addition, they use toxic reagents, consequently generating toxic waste. Duo to the reagents, these methods can be still be harmful to the operator (Caramês et al., 2019).

Keeping the above in mind, the concept of the fourth industrial revolution (Industry 4.0), especially in food sector, is being developed worldwide promoting the emergence of new technologies for food analysis. With this, the development of alternative analytical methods becomes fundamental, with advantages like quickness, efficient and reliable, while maintaining reliable analysis of the product. Furthermore, alternative methods are more flexible and efficient than conventional methods, even though less sensitive. In this context, the concept of Industry 4.0 is aligned with sustainability, not only in the environmental aspect, but also in the economic factor, encouraging the replacement of traditional chemical analysis for green and low-cost control quality tools, such as near infrared (NIR) spectroscopy and smartphone-based imaging (SBI), both which accomplish also the requirement of being applicable to on-line quality control and allow the use of the final data to build a big data for mathematical modeling (Kakani et al., 2020).

NIR spectroscopy in combination with chemometric tools has been successfully applied to determine total phenolic compounds and antioxidant capacity in food products such as grape juice, passion fruit, red wine, cocoa beans and red cabbage, since the functional groups, found in these foods, can absorb the radiation in infrared region and convert it into a signal, also named spectral data (Pallone et al., 2018). On the other hand, SBI has been calling attention in analytical chemistry due to its portability, low-cost, fast response, and for being environmentally friendly. In this regard, this technology was used in food applications industry to assure to determine color additives in food, to estimate the impurities content in olive oils and cyanides in water (Albizu et al., 2020; Botelho et al., 2014).

Since NIR spectroscopy and SBI provided complex information with large data sets, the use of appropriate techniques of preprocessing is indispensable. After an optimal data collection, preprocessing methods of the spectra is the most important step to achieve successful in multivariate calibration to obtain a model with good performance. In addition, variable selection methods can also be applied to remove spectra portion that are noisy and/or without any relevant chemical information (Rinnan et al., 2009). Regarding the SBI, the use of strategies such as segmentation, cropping and the adequate choice of the best variables that will compose the colourgram can directly impact the calibration model performance and improve the prediction capacity of the models (Giraudo et al., 2018).

Therefore, the aim of this study was to evaluate the bioactive potential of freeze-dried açai pulps and compare the performance of NIR spectroscopy and SBI coupled to chemometric tools to evaluate and predict the bioactive potential of freeze-dried açai pulps. The multivariate calibration models were developed based on based on partial square least (PLS) regression after optimization and subsequent validation.

2. Material and methods

2.1. Chemicals and samples

Ninety-six genuine samples of açai pulp were acquired in Abaetetuba and Igarapé-Miri cities (Pará, Brazil). To a achieve the best homogenization of açai pulp, the samples were standardized based on the total solids content (=14%), once the total solids content can range from 8% to 14%, according to legislation (Brazil, 2018). Then the samples were frozen at −28 °C and freeze dried under pressure of 2000μHg with a condenser temperature of −40 °C (LS 3000, Terroni, Brazil). Thereafter, the particle size of the samples was standardized using a 25 mesh sieve with 0.71 mm and stored in translucent bags under vacuum to avoid light and oxygen exposure. The samples were also stored under −28 °C until the analysis.

During the chemical analysis it was used Folin-Ciocalteu reagent (2 mol/L), gallic acid (≥98%), 2,2′-azino-bis-(3-ethylbenzothiazoline-6-sulfonic acid), diammonium salt (ABTS, ≥98%), 2,2-dyphenil-1-picrylhydrazil (DPPH), 2,2′-azobis(2-methyl-propionamidine) dihydrochloride (AAPH 97%), fluorescein sodium salt and 6-Hydroxy-2,5,7,8-tetramethylchroman-2-carboxylic acid (Trolox) acquired from Sigma Aldrich (St. Louis, USA), were used. Sodium carbonate (Na_2CO_3 98%), sodium acetate, acetic acid, chloride acid (37%), potassium dihydrogen and dipotassium hydrogen phosphate anhydrous (KH_2PO_4 and K_2HPO_4), absolute acetone (99.9%) were obtained from Synth (São Paulo, Brazil).

2.2. Samples extraction methods

2.2.1. Total phenolic content (TPC) and antioxidant analysis

The total phenolic extraction was conducted according to Ou et al. (2001) with some modifications. Each sample (1 g) was added by 9 mL of aqueous acetone solution (1:1 v/v), the samples were agitated with a vortex for 90 s. Then, the extraction was microwave assisted (Panasonic, Japan, model NN-ST654WRUN), with two cycles of 10 s, with 2 min under refrigeration between cycles to avoid thermo degradation of the bioactive compounds, the entire process was repeated twice. Afterwards, the samples were centrifugated at 6000 rpm, under 4 °C for 15 min (Solab Cientifica, Brazil, model SL-706). The supernatant was collected and used for the analysis of total phenolic compounds (TPC), 2,2-dyphenil-1-picrylhydrazil (DPPH), trolox equivalent antioxidant capacity (TEAC) and oxygen radical absorbance capacity (ORAC).

2.2.2. Total anthocyanin extract

The total anthocyanins extraction was conducted according to Caramês et al. (2019) and Laokuldilok et al. (2016) with some modifications. Each sample (0.05 g) was added to 8 mL aqueous solution of HCl (1%). The samples were agitated for 30 s using a vortex, afterwards the samples were extracted with microwave assistance (Panasonic, Japan, model NN-ST25JWRU) during 15 s. This process was repeated for a total of four times. Subsequently, the samples were centrifuged as described in the item 2.2.1. The final extract was stored under −28 °C until the moment to perform the total anthocyanin content analysis (TAC).

2.3. Standard methods

2.3.1. Total phenolic compounds (TPC)

The TPC of açai extracts was determined according to Singleton and Rossi (Singleton & Rossi, 1965). An aliquot of 85 μL of each extract sample was added by 43 μL of Folin-Ciocalteau reagent (1 mol/L) and 212 μL of aqueous solution of Na_2CO_3 (75 g/L). After 25 min of reaction in a dark room, the absorbance was measured at 725 nm in a multi-mode microplate reader (BMG Labtech, Germany, model Fluostar Omega). The calibration curve was determined using gallic acid in different concentrations between 1 and 50 mg/mL, and the final results were expressed in mg of gallic acid equivalent per gram of açai (mg GAEq/g).

2.3.2. Total anthocyanins content (TAC)

The content of total anthocyanins was measured according to AOAC (2016) method 2005–02 with modifications (Giusti & Wrolstad, 2001). The absorbance of each sample diluted separately in solutions of pH = 1 and pH = 4.5 was measured at wavelength of 520 nm and 700 nm in a multi-mode microplate reader (BMG Labtech, Germany, model Fluostar Omega). Through the dimensions of the microplate the equipment adequate the absorbance value according to the optic length, and the final result is expressed in mg/g of açai.

2.3.3. Oxygen radical absorbance capacity ($ORAC_{FL}$)

The ORAC assay was conducted as described by Prior et al. (2003) with modifications. The samples were diluted in phosphate buffer solution 75 nM (pH = 7.4) according to necessity, then 25 μL of the diluted sample were mixed with 150 μL of fluorescein (55 nmol/L), 25 μL of Trolox (10 nmol/L) and 25 μL AAPH (150 mM). The mixture was incubated at 37 °C, the fluorescence intensity was measured at an excitation of 493 nm and emission of 515 nm. The kinect were recorded in a multi-mode microplate reader (BMG Labtech, Germany, model Fluostar Omega). The standard curve was determined with trolox solution with concentrations ranging from 0.5 to 4.0 μmol/L. The final results were expressed in μM of Trolox Equivalent/ g of açai (μMTE/g).

2.3.4. Trolox equivalent antioxidant capacity (TEAC)

TEAC value was determined according to Cano et al. (1998) with some adaptations. Initially, an aqueous solution of potassium persulfate with concentration of 2.45 mmol/L was prepared. Then, the radical ABTS solution was prepared by mixing 10 mL of distilled water, 38.4 mg of ABTS and 1 mL of the potassium persulfate solution. The ABTS solution was stored in dark room at 25 °C during 24 h, then an aliquot of it was diluted in ethanol until absorbance reaches 0.40 ± 0.02 at wavelength of 734 nm. The samples were diluted in ethanol according the necessity, then 10 μL of it was added to 190 μL of the diluted ABTS solution. The kinetic was monitored with a multi-mode microplate reader (BMG Labtech, Germany, model Fluostar Omega). The standard curve was determined with trolox (concentrations from 3 μmol/L to 15 μmol/L) and the final results were expressed in μMol of trolox Equivalent per gram of açai (μMTE/g).

2.3.5. DPPH radical scavenging assay

The antioxidant capacity determined by DPPH radical scavenging was performed according to Sánchez-Moreno et al. (1998). The radical DPPH was diluted in methanol (25 mg/L), then 312 μL of DPPH solution was added to 8 μL of sample (or Trolox standard solution). The kinetic was measured at 515 nm in a multi-mode microplate reader (BMG Labtech, Germany, model Fluostar Omega). The standard curve was built with trolox solution using methanol in concentrations ranging from 0.6 mmol/L to 20 mmol/L. The final results were expressed in μmol/L of Trolox Equivalent per gram of açai (μMTE/g).

2.4. SBI acquisition

In order to acquire the images (Fig. 1), it was built an isolated environment: a closed wood box (100 × 100 × 100 cm) painted in black color to reduce possible effects of light reflection, two LED lamps of 4 W, color 6500 k, 350 lm were used for illumination purposes (OL iluminação, Barueri, Brazil). A cellphone (Xiaomi Mi A2, model M1804D2SG, China) with a double camera of 12 and 20 MP (f/1.8 1/2.8″ 1.0 μm), focal of f/1.8, resolution of 4000 × 3000 pixels was required to obtain the images (Fig. 1). About 6 g of each sample was placed in a glass petri dish (1.1 cm of depth and 3.3 cm of diameter), the cellphone was set above the sample with the distance of 10 cm and programmed with a temporizer. The box was completely closed to avoid external illumination during the acquisition process.

2.5. NIR spectra acquisition

Approximately 2 g of each sample of freeze dried açai was placed into a glass vial (Weathon, USA, Shell vial). The reflectance measurements were acquired using a near infrared reflectance accessory (Perkin Elmer-Walthman, USA, model NIRA) coupled into a FT-NIR spectrometer (Perkin Elmer-Walthman, USA, model Spectrum 100 N) with an InGaAs detector. Each sample was analyzed directly in the NIR using properly cleaned glass cuvette. Additionally, was used one cuvette for each sample to ensure the safety of the samples and that there would be no cross contamination. The samples were scanned once and its resulting spectrum is the average of 32 scans, with a resolution of 4 cm^{-1} in the region from 10,000 cm^{-1} to 4,000 cm^{-1}.

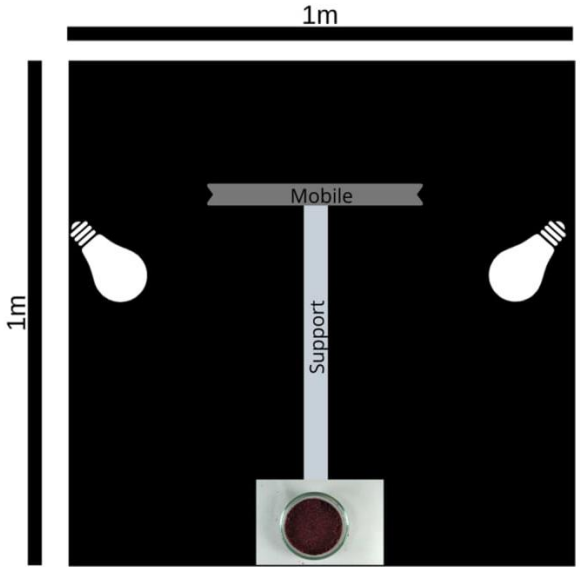

Fig. 1. Illustration of the box used during the acquisition of smartphone-based images.

2.6. Multivariate image analysis

The SBI data were initially cropped to remove the background, reducing the images to 649 × 520 pixels. Based on the cropped images the colourgrams were obtained by the calculation of red (R), green (G), blue (B) histograms, lightness (L). Relative colors (yR, yG and yB), hue (H), saturation (S) and value (V). The lightness (L) was, calculated summing the respective R, G and B parameters, the relative colors were obtained by the ratio between each RGB and L values. Also, the values of R, G and B were converted, with the function rgb2hsv, into HSV space, resulting in a matrix with dimension of 96 × 2560. That dataset was used to determine the sequential Partial Square Least Regression (PLS-R) models (Calvini et al., 2020; Oliveira et al., 2013).

2.7. Data analysis and chemometrics

To determine the standard error of reference methods (SEL or reproducibility), six samples from calibration set were analyzed in three repetitions as performed by Lequeue et al. (2016), the values were standardized trough a normalization in a continuous space (Equation (1)) as described by Prevolnik et al. (2010). The values of SEL were determined as the average of the standard deviation between the triplicates of each one of the six samples (Dardenne, 2010).

$$X_{new} = \frac{(X_{old} - X_{mean})}{SD} \quad (1)$$

All data preprocessing techniques and chemometric process was performed using MatLab 2017b version and PLS toolbox version 8.6.

The NIR spectroscopy data was mean centered and preprocessed with multiplicative scatter correction (MSC) in order to reduce the light scattering effects commonly founded in NIR spectra data and 2nd derivative by Savitsky-Golay method to reduce multiplicative and additive effects. The variables were selected according to the loadings values to improve the multivariate models that presented poor performance using all the spectral range.

In multivariate calibration, PLS regression method was implemented

for modeling. More information on the this method can be found in literature (Calvini et al., 2020; Ferreira, 2015; Oliveira et al., 2013). The reference results (TAC, TPC, DPPH, ORAC, and TEAC) obtained by traditional methods for each sample were used as the dependent variables (**y**) and the preprocessed SBI data or NIR spectra of the studied samples were used as the independent variables to build the PLS models. For modeling, the 96 samples were used. The data was randomly divided with the help of the RAND function from Excel, the list of samples label was placed into a column, at the next column the rand function was applied, after it the values were sorted from the smallest to largest number expanding the process to the samples label column. Then, the first 66 samples (70%) were set as calibration set and the remaining 30 samples (30%) were set as validation set. The models were optimized by a step of detection and elimination of outliers according to the values of Q residuals, T^2 Hoteling and leverage. The cross validation was performed by venetian blinds method (10 split and 1 sample per split), the number of latent variables (LV) was set according to the lowest value of Root Mean Squared Error of Cross-Validation (RMSECV).

The final PLS models obtained were validated according to the Root Mean Squared Errors of Calibration and Prediction (RMSEC and RMSEP, respectively), coefficient of determination (R^2) and correlation, where the ideal model should present low values of RMSEC, RMSEP and bias (Shao & He, 2013). The Residual Prediction Deviation (RPD) is the ratio of standard deviation of reference values and RMSEP and is also used to evaluate PLS regressions, once it is really useful compering models based on distinct datasets or in absolute terms (Beltrame et al., 2019). Values of RPD higher than 2.4 indicates a calibration model with excellent ability of prediction, values between 2.4 and 1.5 are considered with satisfactory performance, while values lower than 1.5 indicate poor performance of the multivariate model (Botelho et al., 2014).

3. Results and Discussions

3.1. Chemical analysis

At Table 1 are described the statical results for each chemical parameter analyzed of the samples, on the calibration and validation set. Comparable ranging and mean values of all parameters were founded in calibration and validation sets, which means that the sets could be used through this study to verify the accuracy of PLS models (Lequeue et al., 2016). The standard errors of reference methods for each method applied were also considered satisfactory and similar to the values achieved by Prevolnik et al. (2010). Additionally, the chemical analysis for all samples used in calibration and validation sets during modeling process were performed in triplicate with maximum relative standard error between replicates of 9.0% for TAC, 7.7% for TPC, 12.8% for ORAC, 10% for DPPH and 12.3% for TEAC.

The values of bioactive compounds and antioxidant capacity were expressive in freeze-dried açai pulps, demonstrating that these Amazon fruits offer a real benefit for human nutrition. Regarding mean values obtained for the samples, the total amount of anthocyanins (6.26 mg/g) and the total phenolic compounds (11.4 mgGAEq/g) correspond as the major class of phenolic compounds present in the açai pulps (Table 1). Previous studies have reported that açai pulp often has a higher anthocyanin content, with prevalence of cyanidin-3-O-glucoside and cyanidin-3-O-rutinoside, that can be used even as an isolated standard in future investigations of anthocyanin content in foods (Gouvêa et al., 2012). Also, other studies (Inácio et al., 2013) have shown that TAC levels were higher for intact açai (*Euterpe oleracea* Mart.) and palmitero-juçara (*Euterpe edulis* Mart) (mean about 20 g/kg) in comparison with the present study. Although this result was superior, it is relevant to point that this study was based in intact fruits compared with the pulps studied here, therefore, this difference was expected.

The average results of the ORAC, DPPH and TEAC methods were 2588.4 μMol trolox eq./g, 5.86 μMol trolox eq./g and 19.88 μMol trolox eq./g, respectively (Table 1). The phenolic content and antioxidant capacity achieved in açai pulp are within the range reported in the literature: about 0.17 μMol trolox eq./g of TEAC (Gordon et al., 2012); and from 133.4 μMol trolox eq./g in *Euterpe oleracea* fruit to 745.3 μMol trolox eq./g in *Euterpe edulis* pulp for DPPH (Bicudo et al., 2014). The ORAC results also are within the reported range, presenting values of 1027 μMol trolox eq./g in samples of freeze dried açai and of 2649 μMol trolox eq./g in freeze dried *Euterpe oleracea* fruit (Benatrehina et al., 2018; Kang et al., 2012).

In general, comparing the previous values obtained analyzing phenolic compounds and antioxidant capacity between themselves, which was presented in Table 1, it is notorious great variability and wide range of values of the mean content of TAC, TPC and antioxidant capacity. This observation can be explained to different reasons, as the season of the year, the cultivate place, the climatic conditions, the specie of the plant and the stage of ripe. Not only the content, but also the profile of the phenolic compounds changes depending of the maturation state of the fruit and the season of the year, therefore, is strictly correlated with the final antioxidant capacity of the freeze dried fruit pulp (Gordon et al., 2012; Rogez et al., 2011; Schulz et al., 2016).

3.2. NIR spectra and SBI evaluation

The NIR spectra data acquired in reflectance mode is presented in Fig. 2. The data presented eight bands of interest (8264 cm^{-1}, 6897 cm^{-1}, 5793 cm^{-1}, 5679 cm^{-1}, 5176 cm^{-1}, 4664 cm^{-1}, 4335 cm^{-1} and 4212 cm^{-1}). At 8264 cm^{-1}, 6897 cm^{-1} and 5176 cm^{-1} the bands are correlated to O-H groups at the first and second overtone, normally from water molecules. The bands at 5793 cm^{-1} and 5679 cm^{-1} are associated with the first overtone of C-H group, usually attributed to the presence of lipids and oils. 4664 cm^{-1} band is associated to C-H groups connected with aromatic structures. Frizon et al., (2015) already correlated this region of NIR spectrawith the phenolic content in yerba mate (*Ilex paraguariensis*). The two peaks at 4335 cm^{-1} and 4212 cm^{-1} are located in a region between 4501 and 5000 cm^{-1} commonly associated to O-H bending or C-O stretching combination (Caramês, Alamar, & Pallone, 2019; Lobato et al., 2018).

The RGB histograms (Fig. 3A) showed great intensity of red, green and blue. Purple is typically the color of açai pulp, due to the high concentration of anthocyanin pigment, this color is the mixture of magenta and green, and magenta is the mixture of blue and red,

Table 1
Bioactive compounds and antioxidant capacity for freeze dried açai samples of calibration and validation sets.

	Calibration set			Validation set			
	Range	Mean ± SD	CV	Range	Mean ± SD	CV	SEL
TAC (mg/g)	11.98–4.11	6.43 ± 1.62	0.25	8.72–4.99	6.31 ± 0.91	0.14	0.14
TPC(mg GAEq/g)	26.72–6.02	11.93 ± 2.68	0.22	13.11–9.31	11.36 ± 1.07	0.10	0.28
ORAC (μMol trolox eq./g)	3854.64–627.53	2549.1 ± 695.5	0.27	3724.46–1490.38	2578.49 ± 478	0.18	0.39
DPPH (μMol trolox eq./g)	11.37–2.74	5.97 ± 1.82	0.30	7.85–3.71	6.16 ± 1.19	0.19	0.66
TEAC (μMol trolox eq./g)	27.36–10.41	20.13 ± 2.82	0.14	22.58–15.91	19.71 ± 1.48	0.07	0.66

TAC: Total Anthocyanins Content; TPC: Total Phenolic Content; ORAC: Oxygen Radial Absorbance Capacity; TEAC: Trolox Equivalent Antioxidant Capacity. SD: Standard Deviation.

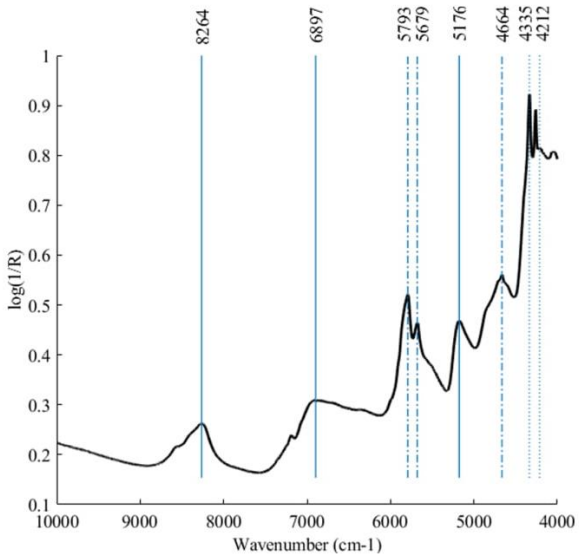

Fig. 2. NIR raw data.

nonetheless it is relevant to emphasize that the red color presented the highest intensity in the samples compared to the blue and green. This highest intensity of red color is even more evident when these histograms are expressed in relative colors (Fig. 3D). Regarding the lightness values, it is important to highlight that the samples presented a dark purple color, confirming the high concentration of pigments (Fig. 3B).

The degradation of the phenolic compounds in açai pulp (by exposition of light, oxygen or enzymes) causes the transformation in the color on account of the polymerization of anthocyanins. This process makes the purple turn into a brownish color (brown = red + green) or colorless (Jiang et al., 2019). Based on this, even though the color changing is visible, it is not simple to measure by naked eye, and this fact easily justifies the use of the system of colors to determine the quality of food products regarding the bioactive content and antioxidant capacity (Herrero-Latorre et al., 2019).

The HSV space is an alternative representation of RGB color, where the hue value appears as a value of color (primary and secondary colors), saturation represents the purity of the color and the value is about the illumination of the colors. This representation could be extremely useful since the RGB space is inspired in human vision and HSV system can project information imperceptible to us (Wallet et al., 2012). Concerning the samples of açai (Fig. 3B), the value (or brightness) spectra agrees that the samples are dark and the hue channel presented high value in channels that correspond to reddish colors.

3.3. PLS regression models

The NIR spectra data was preprocessed with several methods and the best performance was achieved by Multiplicative Scatter Correction (MSC) - to reduce the light scattering effects- second derivative (order: 2, window: 37 points and tails: polyinterp) by Savitzky-Golay - method to correct the multiplicative and additives errors - and the data was mean centered. to predict the parameters TAC, TPC, DPPH, and TEAC PLS models were developed using full spectra range (10000 cm^{-1} –4000 cm^{-1}), but to improve the performance of ORAC method, a variable selection was implemented based on loading values (Figure S1). The variables in the beginning and ending of spectra data did not present elevated values of loadings, in this context, the spectra sections of 10000 cm^{-1}-8858 cm^{-1} and 4471 cm^{-1}-4000 cm^{-1} were excluded. The performance parameters of the PLS models obtained based on NIR are presented in Table 2 and the mathematical models are presented in supplementary material (Figure S2).

Generally, all the NIR models showed good values of errors and coefficient of regression (R^2), and the small number of latent variables used in modeling indicates or suggests that the models were not overfitted. The values of errors for both calibration and test set (RMSEC and RMSEP) were close, indicating that the NIR-PLS models are sufficiently robust. The values of RMSEP, in general, were about 10% of the minimal reference value to each performed analysis indicating also the building of models with proper adjust, as observed in Table 2.

Several studies in the scientific literature have demonstrated the potential of NIR-PLS models for the prediction of bioactive potential of various foods and the performance of the models are within the range obtained in the present study. For example, NIR-PLS models were developed to determine the TPC in maize distinct genotypes with values

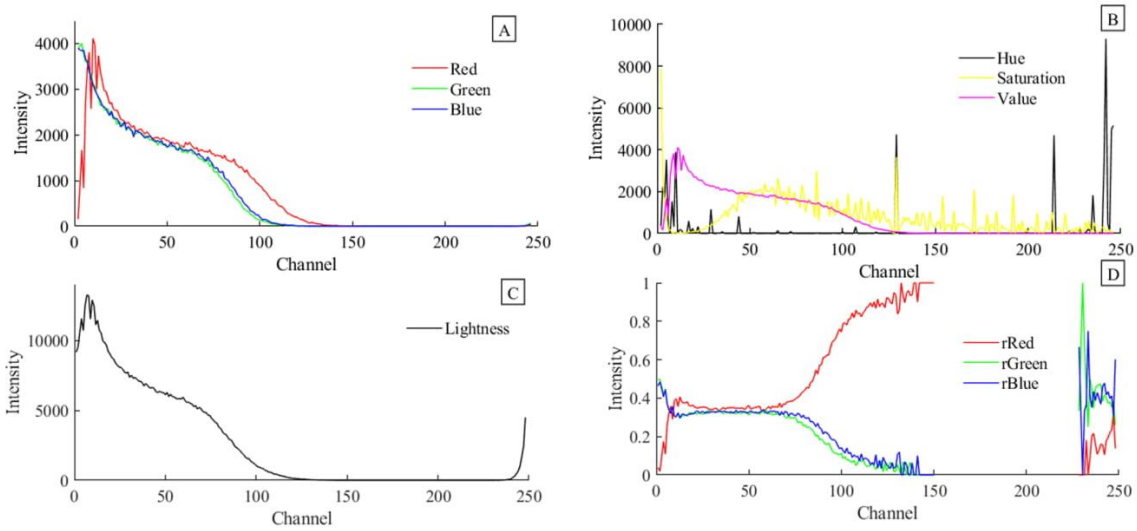

Fig. 3. Average colourgram for freeze dried açai samples. The Red, Green and Blue vectors (A), the colors in HSV space (B), the calculated lightness (C) and relative vectors of red (rRed), green (rGreen) and blue (rBlue) (D). (For interpretation of the references to color in this figure legend, the reader is referred to the web version of this article.)

Table 2
Performance parameters to PLS models based on NIR data.

	NIR								
Parameter	N	Spectral range (cm^{-1})	Variable selection method	LV	RMSEC	Calibration Bias	R^2	RMSEP	RPD
TAC (mg/g)	96	[10000–4000]	none	5	0.43	0	0.89	0.5	2.9
DPPH(μMol trolox eq./g)	96	[10000–4000]	none	4	0.54	1.78E-15	0.86	0.74	2.2
ORAC(μMol trolox eq./g)	92	[8859–4470]	Loadings	4	204.08	0	0.88	245.52	2.6
TEAC(μMol trolox eq./g)	94	[10000–4000]	none	5	0.63	0	0.9	0.89	2.8
TPC(mg GAEq/g)	92	[10000–4000]	none	7	0.76	−1.78E-15	0.8	0.71	3.4

N: Number of samples, TAC: Total Anthocyanins Content; TPC: Total Phenolic Content; ORAC: Oxygen Radial Absorbance Capacity; TEAC: Trolox Equivalent Antioxidant Capacity, LV: Latent Variable, RMSEC: Root Mean Square Error of Calibration; R^2: Coefficient of determination; RMSEP: Root Mean Square Error of Prediction; RPD: Residual Prediction Deviation.

of SEC ranging from 0.06 to 0.10 g GAEq/kg and R^2 between 0.6 and 0.8. These authors also produced a model for predicting total antioxidant capacity using the TEAC method, which presented errors SEC ranging from 0.69 to 1.31 mmol TE/kg and R^2 between 0.77 and 0.82 (Redaelli et al., 2016). Inácio and contributors also investigated the TAC determination via NIR-PLS approach in intact açai fruit, and found errors of prediction equal to 4.8 g/kg (Inácio et al., 2013). Finally, Wiedemair and Huck used NIR combined with PLS to determine TPC with three different handheld NIR spectrometers, showing a variation in RMSEP between 1.02 and 1.86 mgGAEq/g (Wiedemair & Huck, 2018).

Regarding SBI-PLS approach, all models, except for ORAC determination, exhibited satisfactory performance. In general, the models presented R^2 above 0.7 and low values of errors, RMSEC and RMSEP (Table 3 and supplementary material - Figure S3). All the analyzed parameters are correlated to the presence of phenolic compounds, and the majoritarian class of phenolics in açai is the anthocyanins. This class of compounds is a pigment highly delicate and it has its color sensitive to changes as pH, that could range from red in acid pH, to colorless in neutral pH and blue in basic pH. In other cases, this pigment can be degraded giving to açai a brown tone (Pfisterer et al., 2018). In virtue of this variations is possible try to correlate SBI to parameters as TAC, TPC, DPPH, ORAC and TEAC.

Based on this valuable information, Beltrame applied the RGB histograms from smartphone-based images to designed PLS models to quantify total anthocyanins and antioxidant capacity based on DPPH method in grape juice, and achieved RMSEC = 10.8 mg/L and 8.8 μMol and RMSEP = 11.8 mg/L and 12.2 μMol, respectively (Beltrame et al., 2019). The RGB information was also used to build PLS model to quantify different pigments, as chlorophyll, in pesto sauce, the colourgrams were applied and generate good models with $R^2 > 0.6$ using 2 Latent Variables (Foca et al., 2011).

The results of regression coefficient of each NIR and SBI-PLS are represented into supplementary material (Figures S4 and S5). Relevant variables are present into NIR data, mainly at the final portion, 5500–4000 cm^{-1}, regarding TEAC, DPPH, TAC and TPC models, and the region between 5500 and 4400 cm^{-1} in ORAC model. NIR spectra data in this rage brings information about phenolic compounds as described by Frizon et al. (2015). Looking at the coefficients of regression obtained to SBI-PLS, the most important information was present in the portion of colourgram composed by the relative color (yR, yG and yB), confirming an existing correlation between the parameters modeled and the RGB channels (Beltrame et al., 2019).

Multivariate calibration models are typically validated by determining RMSEC and RMSEP, and some additional parameters, like RPD. The RPD is a parameter of merit that has been applied to measure the prediction ability of PLS models, and is defined as the ratio between the standard deviation based on the reference method results and the RMSEP presented by the PLS model. RPD higher than 2.4 indicates good calibration models, whereas RPD smaller than 1.5 indicate an inadequate predictive ability (Beltrame et al., 2019; Botelho et al., 2012, 2015). The results of RPD obtained in the models are displayed in Table 2 and 3.

According to this classification, the NIR-PLS models developed to evaluate directly TAC, TPC, ORAC and TEAC in freeze-dried açai pulps can be considered good models, while the model to predict the DPPH can be considered satisfactory. Regarding the RPD obtained in SBI-PLS models, the results showed that the models could better predict TAC, TPC, and TEAC parameters than ORAC one, which showed an unsatisfactory performance.

Comparing the models developed both NIR spectroscopy and SBI, is notable the advantages of performance obtained by NIR technique, presenting better values of RPD and lower values for RMSEC and RMSEP. This result was expected once the NIR spectroscopy technique is more sensitive, detects vibrational spectra according to organic compounds and presents higher resolution compared to a digital image obtained by smartphone. Nevertheless, it is important to highlight that a smartphone is cheaper than NIR spectrometer and it is portable in comparison to a benchtop NIR. In this sense, even though the SBI-PLS models showed inferior results than those based on NIR-PLS, the smartphone image could be considered as a quick and cheap method to evaluate directly the bioactive potential of freeze dried açai, with exception for ORAC.

Considering the proposed methods and good results achieved in order to directly verify and assure the potential bioactive of freeze dried açai pulps with the demands of the Industry 4.0, the present study, more than the development calibration models, suggests ways for on-line monitoring in açai industries aiming the construction of intelligent food industries (Kakani et al., 2020).

Table 3
Performance parameters to PLS models based on Smartphone-based image data.

	Smartphone-based image						
Parameter	N	Latent Variables	RMSEC	Calibration Bias	R^2	RMSEP	RPD
TAC(mg/g)	91	6	0.59	1.77E-15	0.70	0.64	2.3
DPPH(μMol trolox eq./g)	93	5	0.73	8.88E-16	0.75	1.12	1.5
ORAC(μMol trolox eq./g)	92	7	239.33	−9.09E-13	0.72	527.8	1.2
TEAC(μMol trolox eq./g)	96	4	1.29	−7.1E-15	0.79	1.27	2.0
TPC(mg GAEq/g)	96	6	1.24	1.77E-15	0.76	0.78	3.1

N: Number of samples, TAC: Total Anthocyanins Content; TPC: Total Phenolic Content; ORAC: Oxygen Radial Absorbance Capacity; TEAC: Trolox Equivalent Antioxidant Capacity. RMSEC: Root Mean Square Error of Calibration; R^2: Coefficient of determination; RMSEP: Root Mean Square Error of Prediction; RPD: Residual Prediction Deviation.

4. Conclusion

In this study, the NIR spectroscopy and smartphone-based image (SBI) were combined with the PLS method in models aiming to predict the bioactive potential of freeze-dried açai pulps. The results obtained show that NIR-PLS models presented better performance to evaluate the TAC, TPC, DPPH, ORAC, and TEAC in comparison with SBI-PLS models. The best performance of the NIR-PLS could be potentially justified by a higher sensitivity on the NIR equipment than on the smartphone image. With the exception of the SBI-PLS for the evaluation of ORAC, all remaining PLS models combined with NIR spectroscopy or SBI could be applied as green techniques for the analysis and quality control of freeze-dried açai pulps with advantages under traditional methods, such as simplicity and quickness and in case of smartphone, portability and low cost.

Declaration of Competing Interest

The authors declare that they have no known competing financial interests or personal relationships that could have appeared to influence the work reported in this paper.

Acknowledgments

The authors would like to thank the São Paulo Research Foundation (FAPESP) funding of the research project (project n° 2018/09759-3). The Coordination for the Improvement of Higher Education Personnel (CAPES) (Financial Code 001) and for the PhD scholarship of Michel Baqueta, and the National Council for Scientific and Technological Development (CNPq) for the PhD scholarship of Elem Caramês (scholarship n° 142414/ 2016-6).

Appendix A. Supplementary data

Supplementary data to this article can be found online at https://doi.org/10.1016/j.foodres.2020.109792.

References

Albizu, G., Bordagaray, A., Dávila, S., Garcia-Arrona, R., Ostra, M., & Vidal, M. (2020). Analytical control of nickel coating baths by digital image analysis. *Microchemical Journal, 154*(January), Article 104600. https://doi.org/10.1016/j.microc.2020.104600.

Beltrame, K. K., Gonçalves, T. R., Março, P. H., Gomes, S. T. M., Matsushita, M., & Valderrama, P. (2019). Application of digital images and multivariate calibration for the quantification of anthocyanin and antioxidant activity in grape juice. *Australian Journal of Grape and Wine Research, 25*(2), 156–160. https://doi.org/10.1111/ajgw.12387.

Benatrehina, P. A., Pan, L., Naman, C. B., Li, J., & Kinghorn, A. D. (2018). Usage, biological activity, and safety of selected botanical dietary supplements consumed in the United States. *Journal of Traditional and Complementary Medicine, 8*(2), 267–277. https://doi.org/10.1016/j.jtcme.2018.01.006.

Bicudo, M. O. P., Ribani, R. H., & Beta, T. (2014). Anthocyanins, Phenolic Acids and Antioxidant Properties of Juçara Fruits (Euterpe edulis M.) Along the On-tree Ripening Process. *Plant Foods for Human Nutrition, 69*(2), 142–147. https://doi.org/10.1007/s11130-014-0406-0.

Botelho, B. G., De Assis, L. P., & Sena, M. M. (2014). Development and analytical validation of a simple multivariate calibration method using digital scanner images for sunset yellow determination in soft beverages. *Food Chemistry, 159*, 175–180. https://doi.org/10.1016/j.foodchem.2014.03.048.

Botelho, B. G., Mendes, B. A. P., & Sena, M. M. (2012). Development and Analytical Validation of Robust Near-Infrared Multivariate Calibration Models for the Quality Inspection Control of Mozzarella Cheese. *Food Analytical Methods, 6*(3), 881–891. https://doi.org/10.1007/s12161-012-9498-z.

Botelho, B. G., Reis, N., Oliveira, L. S., & Sena, M. M. (2015). Development and analytical validation of a screening method for simultaneous detection of five adulterants in raw milk using mid-infrared spectroscopy and PLS-DA. *Food Chemistry, 181*, 31–37. https://doi.org/10.1016/J.FOODCHEM.2015.02.077.

Brazil. (2018). PADRÕES DE IDENTIDADE E QUALIDADE MÍNIMA PARA POLPA DE AÇAÍ-INSTRUÇÃO NORMATIVA No37. (pp. 2–4).

Calvini, R., Orlandi, G., Foca, G., & Ulrici, A. (2020). Colourgrams GUI: A graphical user-friendly interface for the analysis of large datasets of RGB images. Chemometrics and Intelligent Laboratory Systems, 196(December 2019), 103915. https://doi.org/10.1016/j.chemolab.2019.103915.

Cano, A., Hernández-Ruíz, J., García-Cánovas, F., Acosta, M., & Arnao, M. B. (1998). An end-point method for estimation of the total antioxidant activity in plant material. *Phytochemical Analysis, 9*(4), 196–202. https://doi.org/10.1002/(SICI)1099-1565(199807/08)9:4<196::AID-PCA395>3.0.CO;2-W.

Caramês, E. T. S., Alamar, P. D., & Pallone, J. A. L. (2019). Detection and identification of açai pulp adulteration by NIR and MIR as an alternative technique: Control charts and classification models. *Food Research International, 123*(June), 704–711. https://doi.org/10.1016/j.foodres.2019.06.006.

Caramês, E. T. S., Alamar, P. D., & Lima Pallone, J. A. (2019). Bioactive Compounds and Antioxidant Capacity in Freeze-Dried Red Cabbage by FT-NIR and MIR Spectroscopy and Chemometric Tools. *Food Analytical Methods*. https://doi.org/10.1007/s12161-019-01523-6.

Çopur, Ö. U., & Tamer, C. E. (2014). Fruit Processing. In A. Malik, Z. Erginkaya, S. Ahmad, & H. Erten (Eds.), *Food Processing: Strategies for Quality Assessment* (pp. 9–35). New York: Springer. https://doi.org/10.1007/978-1-4939-1378-7_2.

Dardenne, P. (2010). Some Considerations about NIR Spectroscopy: Closing Speech at NIR-2009. *NIR News, 21*(1), 8–14. https://doi.org/10.1255/nirn.1165.

Ferreira, M. M. C. (2015). Quimiometria- conceitos, métodos e aplicações (1st ed.). Campinas, SP. Editora UNICAMP.

Foca, G., Masino, F., Antonelli, A., & Ulrici, A. (2011). Prediction of compositional and sensory characteristics using RGB digital images and multivariate calibration techniques. *Analytica Chimica Acta, 706*(2), 238–245. https://doi.org/10.1016/j.aca.2011.08.046.

Frizon, C. N. T., Oliveira, G. A., Perussello, C. A., Peralta-Zamora, P. G., Camlofski, A. M. O., Rossa, Ü. B., & Hoffmann-Ribani, R. (2015). Determination of total phenolic compounds in yerba mate (Ilex paraguariensis) combining near infrared spectroscopy (NIR) and multivariate analysis. *LWT - Food Science and Technology, 60*(2, Part 1), 795–801. https://doi.org/10.1016/j.lwt.2014.10.030.

Giraudo, A., Calvini, R., Orlandi, G., Ulrici, A., Geobaldo, F., & Savorani, F. (2018). Development of an automated method for the identification of defective hazelnuts based on RGB image analysis and colourgrams. *Food Control, 94*(April), 233–240. https://doi.org/10.1016/j.foodcont.2018.07.018.

Giusti, M. M., & Wrolstad, R. E. (2001). Characterization and Measurement of Anthocyanins by UV-Visible Spectroscopy. In R. E. Wrolstad, T. E. Acree, M. H. Penner, D. S. Reid, S. J. Schwartz, C. F. Shoemaker, D. Smith, … P. Sporns (Eds.), *Current Protocols in Food Analytical Chemistry*. John Wiley & Sons Inc.

Gordon, A., Cruz, A. P. G., Cabral, L. M. C., De Freitas, S. C., Taxi, C. M. A. D., Donangelo, C. M., De Andrade Mattietto, R., Friedrich, M., Da Matta, V. M., & Marx, F. (2012). Chemical characterization and evaluation of antioxidant properties of Açaí fruits (Euterpe oleraceae Mart.) during ripening. Food Chemistry, 133(2), 256–263. https://doi.org/10.1016/j.foodchem.2011.11.150.

Gouvêa, A. C. M. S., de Araujo, M. C. P., Schulz, D. F., Pacheco, S., Godoy, R. L. de O., & Cabral, L. M. C. (2012). Anthocyanins standards (cyanidin-3-O-glucoside and cyanidin-3-O-rutinoside) isolation from freeze-dried açaí (Euterpe oleraceae Mart.) by HPLC. *Food Science and Technology, 32*(1), 43–46. https://doi.org/10.1590/s0101-20612012005000001.

Herrero-Latorre, C., Barciela-García, J., García-Martín, S., & Peña-Crecente, R. M. (2019). Detection and quantification of adulterations in aged wine using RGB digital images combined with multivariate chemometric techniques. *Food Chemistry: X, 3*(March), Article 100046. https://doi.org/10.1016/j.fochx.2019.100046.

Inácio, M. R. C., de Lima, K. M. G., Lopes, V. G., Pessoa, J. D. C., & de Almeida Teixeira, G. H. (2013). Total anthocyanin content determination in intact açaí (Euterpe oleracea Mart.) and palmitero-juçara (Euterpe edulis Mart.) fruit using near infrared spectroscopy (NIR) and multivariate calibration. *Food Chemistry* (Vol. 136, Issue 3). https://doi.org/10.1016/j.foodchem.2012.09.046.

Jiang, T., Mao, Y., Sui, L., Yang, N., Li, S., Zhu, Z., Wang, C., Yin, S., He, J., & He, Y. (2019). Degradation of anthocyanins and polymeric color formation during heat treatment of purple sweet potato extract at different pH. *Food Chemistry, 274*(2018), 460–470. https://doi.org/10.1016/j.foodchem.2018.07.141.

Kakani, V., Nguyen, V. H., Kumar, B. P., Kim, H., & Pasupuleti, V. R. (2020). A critical review on computer vision and artificial intelligence in food industry. *Journal of Agriculture and Food Research, 2*(2019). https://doi.org/10.1016/j.jafr.2020.100033.

Kang, J., Thakali, K. M., Xie, C., Kondo, M., Tong, Y., Ou, B., … Wu, X. (2012). Bioactivities of açaí (Euterpe precatoria Mart.) fruit pulp, superior antioxidant and anti-inflammatory properties to Euterpe oleracea Mart. *Food Chemistry, 133*(3), 671–677. https://doi.org/10.1016/j.foodchem.2012.01.048.

Laokuldilok, N., Thakeow, P., Kopermsub, P., & Utama-ang, N. (2016). Optimisation of microencapsulation of turmeric extract for masking flavour. *Food Chemistry, 194*, 695–704. https://doi.org/10.1016/j.foodchem.2015.07.150.

Lequeue, G., Draye, X., & Baeten, V. (2016). Determination by near infrared microscopy of the nitrogen and carbon content of tomato (Solanum lycopersicum L.) leaf powder. *Scientific Reports, 6*(May), 1–9. https://doi.org/10.1038/srep33183.

Lobato, K. B. de S., Alamar, P. D., Caramês, E. T. dos S., & Pallone, J. A. L. (2018). Authenticity of freeze-dried açai pulp by near-infrared spectroscopy. *Journal of Food Engineering, 224*, 105–111. https://doi.org/10.1016/j.jfoodeng.2017.12.019.

Moreda-Piñeiro, J., Sánchez-Piñero, J., Alonso-Rodríguez, E., Turnes-Carou, I., López-Mahía, P., & Muniategui-Lorenzo, S. (2020). Major, minor and trace elements composition of Amazonian foodstuffs and its contribution to dietary intake. *Journal of Food Measurement and Characterization, 0123456789*. https://doi.org/10.1007/s11694-020-00379-3.

Oliveira, L. F., Canevari, N. T., Guerra, M. B. B., Pereira, F. M. V., Schaefer, C. E. G. R., & Pereira-Filho, E. R. (2013). Proposition of a simple method for chromium (VI) determination in soils from remote places applying digital images: A case study from brazilian antarctic station. *Microchemical Journal, 109*, 165–169. https://doi.org/10.1016/j.microc.2012.03.007.

Ou, B., Hampsch-woodill, M., & Prior, R. L. (2001). *Development and Validation of an Improved Oxygen Radical Absorbance Capacity Assay Using Fluorescein as the Fluorescent Probe Development and Validation of an Improved Oxygen Radical Absorbance Capacity Assay Using Fluorescein as the Fluorescent., 49*, 4619–4626. https://doi.org/10.1021/jf010586o.

Pallone, J. A. L., Caramês, E. T. dos S., & Alamar, P. D. (2018). Green analytical chemistry applied in food analysis: alternative techniques. Current Opinion in Food Science, 22(Figure 1), 115–121. https://doi.org/10.1016/j.cofs.2018.01.009.

Pfisterer, K. J., Amelard, R., & Wong, A. (2018). Differential color space analysis for investigating nutrient content in a pureed food dilution-flavor matrix: a step toward objective malnutrition risk assessment. February 2018, 18. https://doi.org/10.1117/12.2289028.

Prevolnik, M., Čandek-Potokar, M., & Škorjanc, D. (2010). Predicting pork water-holding capacity with NIR spectroscopy in relation to different reference methods. *Journal of Food Engineering, 98*(3), 347–352. https://doi.org/10.1016/j.jfoodeng.2009.11.022.

Prior, R. L., Hoang, H., Gu, L., Wu, X., Bacchiocca, M., Howard, L., … Jacob, R. (2003). Assays for hydrophilic and lipophilic antioxidant capacity (oxygen radical absorbance capacity (ORACFL)) of plasma and other biological and food samples. *Journal of Agricultural and Food Chemistry, 51*(11), 3273–3279. https://doi.org/10.1021/jf0262256.

Redaelli, R., Alfieri, M., & Cabassi, G. (2016). Development of a NIRS calibration for total antioxidant capacity in maize germplasm. *Talanta, 154*, 164–168. https://doi.org/10.1016/j.talanta.2016.03.048.

Rinnan, Åsmund, van den Berg, F., & Engelsen, S. B. (2009). Review of the most common pre-processing techniques for near-infrared spectra. *TrAC Trends in Analytical Chemistry, 28*(10), 1201–1222. https://doi.org/10.1016/j.trac.2009.07.007.

Rogez, H., Pompeu, D. R., Akwie, S. N. T., & Larondelle, Y. (2011). Sigmoidal kinetics of anthocyanin accumulation during fruit ripening: A comparison between açai fruits (Euterpe oleracea) and other anthocyanin-rich fruits. *Journal of Food Composition and Analysis, 24*(6), 796–800. https://doi.org/10.1016/j.jfca.2011.03.015.

Sánchez-Moreno, C., Larrauri, J. A., & Saura-Calixto, F. (1998). A procedure to measure the antiradical efficiency of polyphenols. *Journal of the Science of Food and Agriculture, 76*, 270–276.

Schulz, M., da Silva Campelo Borges, G., Gonzaga, L. V., Oliveira Costa, A. C., & Fett, R. (2016). Juçara fruit (Euterpe edulis Mart.): Sustainable exploitation of a source of bioactive compounds. *Food Research International, 89*, 14–26. https://doi.org/10.1016/j.foodres.2016.07.027.

Shao, Y., & He, Y. (2013). Visible/near infrared spectroscopy and chemometrics for the prediction of trace element (Fe and Zn) levels in rice leaf. *Sensors (Switzerland), 13*(2), 1872–1883. https://doi.org/10.3390/s130201872.

Wallet, B. C., Davogustto, O., Daber, R., & Marfurt, K. J. (2012). Using an HSV color map to visualize spectral phase and magnitude information for an incised valley system in the Anadarko Basin, Oklahoma, USA. Society of Exploration Geophysicists International Exposition and 82nd Annual Meeting 2012, SEG 2012, 2008, 1211–1216. https://doi.org/10.1190/segam2012-0497.1.

Wurlitzer, N. J., Dionísio, A. P., Lima, J. R, Garruti, D. S., Silva Araújo, I. M., da Rocha, R. F. J., & Maia, J. L. (2019). Tropical fruit juice: effect of thermal treatment and storage time on sensory and functional properties. *Journal of Food Science and Technology, 56*(12), 5184–5193. https://doi.org/10.1007/s13197-019-03987-0.

Wiedemair, V., & Huck, C. W. (2018). Evaluation of the performance of three hand-held near-infrared spectrometer through investigation of total antioxidant capacity in gluten-free grains. *Talanta, 189*(March), 233–240. https://doi.org/10.1016/j.talanta.2018.06.056.

Supplementary material

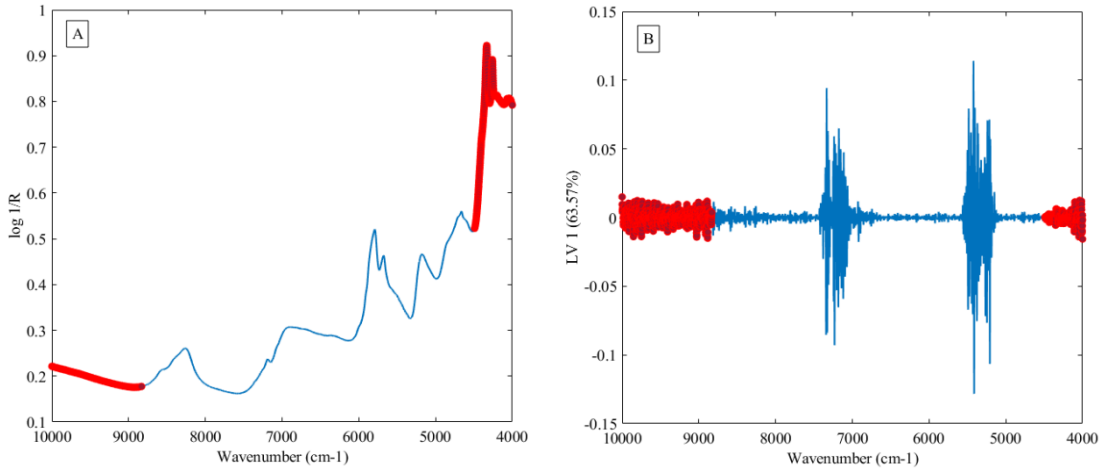

Figure S 1. Mean NIR spectra data (A) and plot of loadings values (B).

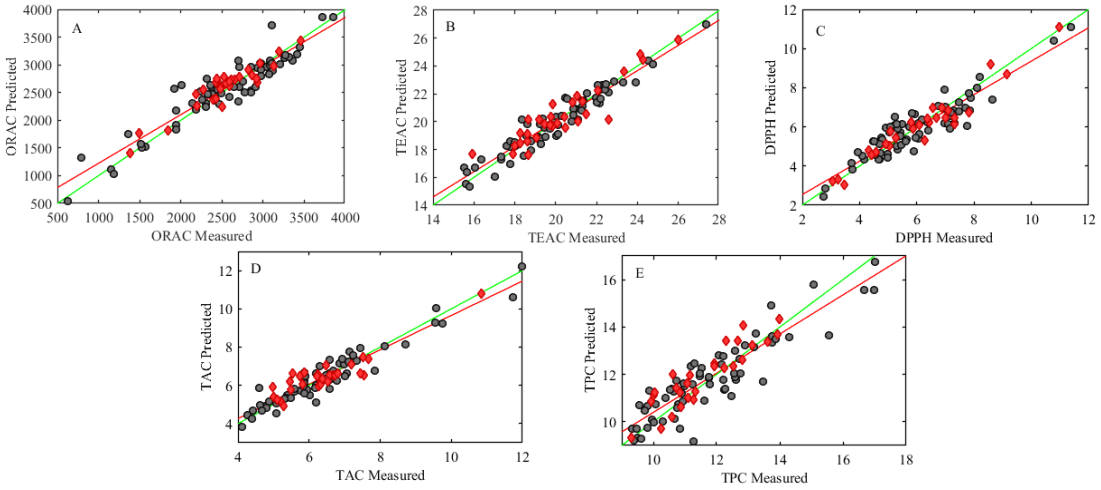

Figure S 2. NIR-PLS models determined to (A) ORAC, (B) TEAC, (C) DPPH, (D) TAC and (E) TPC. ● Calibration set ♦ Test set.

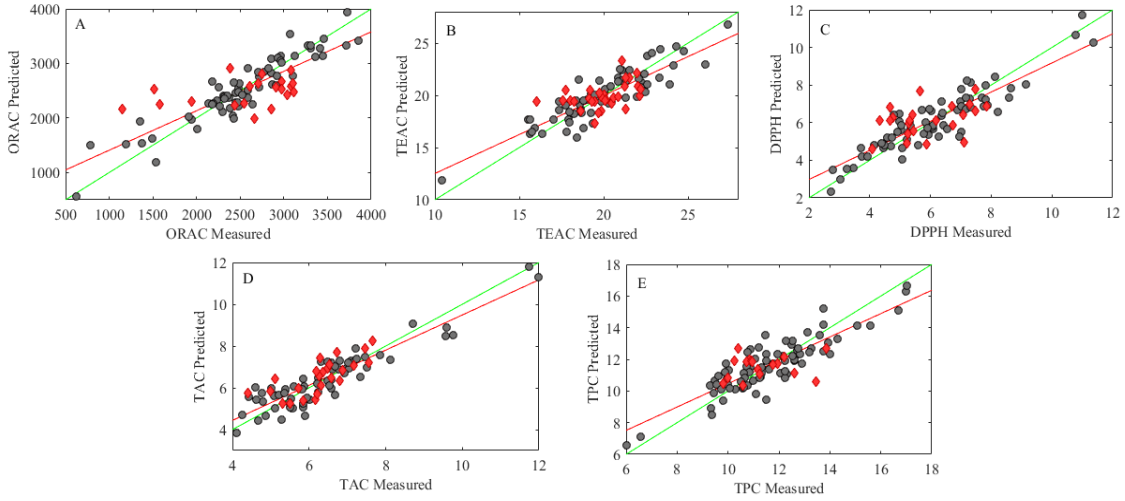

Figure S 3. SBI-PLS models determined to (A) ORAC, (B) TEAC, (C) DPPH, (D) TAC and (E) TPC. ● Calibration set ♦ Test set.

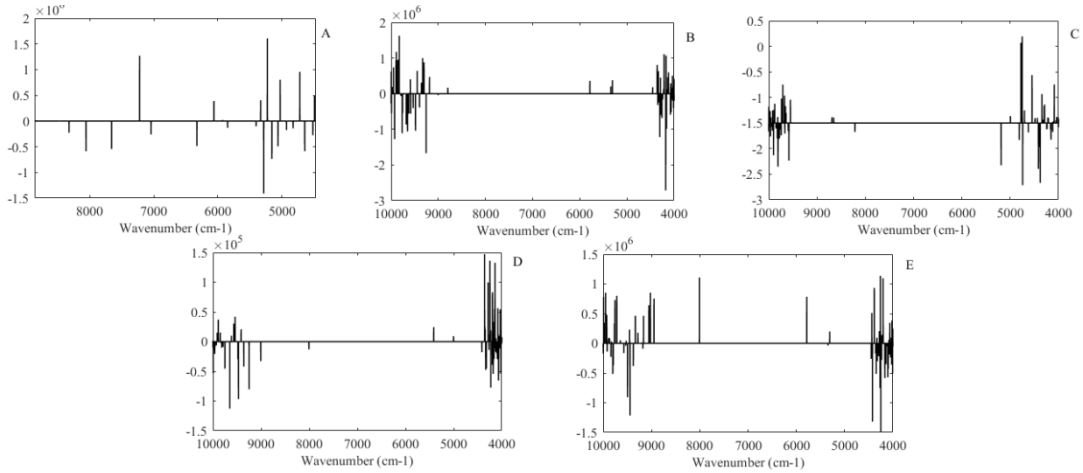

Figure S4. Regression coefficients obtained for the NIR-PLS models developed for (A) ORAC, (B) TEAC, (C) DPPH, (D) TAC and (E) TPC.

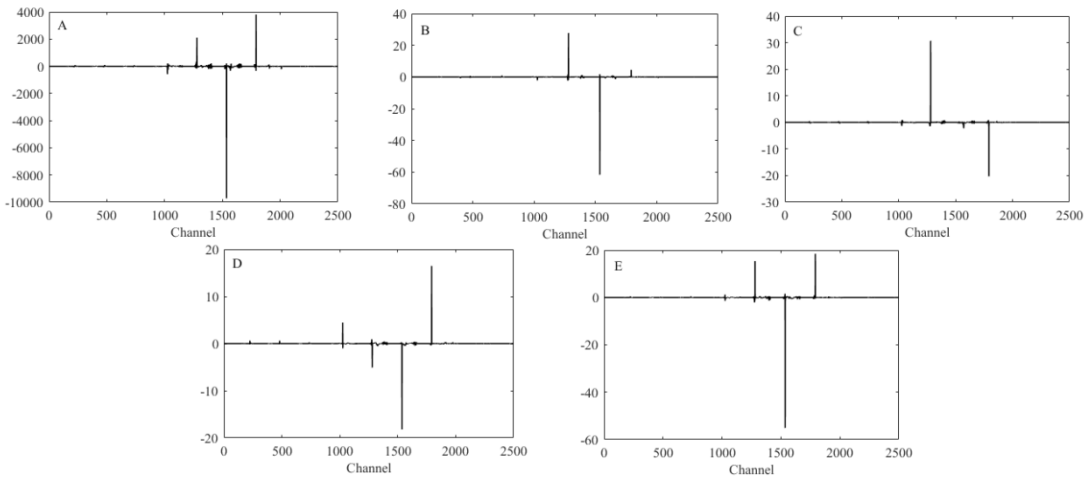

Figure S5. Regression coefficients obtained for the SBI - PLS models developed for (A) ORAC, (B) TEAC, (C) DPPH, (D) TAC and (E) TPC.

CAPÍTULO V

Detection and identification of açai pulp adulteration by NIR and MIR as an alternative technique: Control Charts and classification models

Elem Tamirys dos Santos Caramês[a], Priscila Domingues Alamar[a], Juliana Azevedo Lima Pallone[a]

[a]*Department of food science, School of food engineering, University of Campinas, Monteiro Lobato street, 80, Campinas, São Paulo 13083-862, Brazil.*

Artigo publicado em *Food Research International*.

Reprinted from Caramês, E. T. S., Alamar, P. D., & Pallone, J. A. L. (2019). Detection and identification of açai pulp adulteration by NIR and MIR as an alternative technique: Control charts 711. https://doi.org/10.1016/j.foodres.2019.06.006

Food Research International 123 (2019) 704–711

Contents lists available at ScienceDirect

Food Research International

journal homepage: www.elsevier.com/locate/foodres

Detection and identification of açai pulp adulteration by NIR and MIR as an alternative technique: Control charts and classification models

Caramês E.T.S., Alamar P.D., Pallone J.A.L.*

Department of Food Science, School of Food Engineering, University of Campinas, Monteiro Lobato Street, 80, 13083-862 Campinas, São Paulo, Brazil

1. Introdution

Açai is the fruit of the palm tree *Euterpe oleracea* and is native to the Amazon basin. The fruit are small, between 1 and 2 cm in diameter and only 7% to 25% of the total fruit is consumed. The pulp is obtained through maceration of the açai berries with water and followed with sieving. This pulp has a notable nutritional composition of high lipid content, especially Monounsaturated Fatty Acids (MUFA); polyphenols, as flavonoids and anthocyanins, and consequently high antioxidant capacity; and high fiber and protein content (de Oliveira, Do, & Schwartz, 2018; Pala et al., 2018).

Global consumption of açai has increased in the past decade because its nutritional composition conforms with the growing trend for healthier lifestyles. Apart from its consumption as food, acai pulp is also used in certain sub products, such as in drinks like wine and smoothies, and also for its medicinal purposes in countries other than Brazil; these include Japan, the USA and throughout Europe. Açai has also been used as a natural pigment in the cosmetic and pharmaceutical industries, and for oil extraction. Açai pulp is classified according to dry matter: thin ($\leq$11%), medium (11%$\geq$ and $\leq$14%), and thick ($\geq$14%). The higher the total solids content, the higher the commercial value of the pulp (Pala et al., 2018).

In this context, with the increase of açai pulp production and commercial valorization, cases of fraud have also progressively risen. The state of Pará, the largest producer of açai in Brazil (54% of production), reported cases of açai pulp adulteration with cassava flour, tapioca flour, and other thickeners. The fraudulent practices aim to raise apparent thickness with inexpensive products, since higher total solids content has the highest commercial price (G1, 2014; Lobato, Alamar, Caramês, & Pallone, 2018).

Techniques, such as high/ultra performance liquid chromatography and mass spectroscopy are powerful tools used to detect food adulteration and identify specific adulterants. However, they are relatively slow and expensive, generate toxic residues, and destroy samples. As an alternative, spectroscopic techniques, such as near and mid infrared (NIR and MIR), are fast, non-destructive, safe, produce no toxic residues, are cheaper and environmentally friendly compared to traditional methods. Furthermore, they have been applied successfully to detect food adulteration and control production process in honey, palm oil, turkey meat, soybean meal, glucose fermentation and others (Alamprese, Amigo, Casiraghi, & Engelsen, 2016; Ávila, Poppi, Lunardi, Tizei, & Pereira, 2012; Basri et al., 2017; Bázár et al., 2016; Haughey, Graham, Cancouët, & Elliott, 2013; Lohumi, Lee, Lee, & Cho, 2015).

Efficient classification models have already been developed using NIR to detect and identify adulterants in freeze-dried açai pulp. However, it is relevant to note that the adulterants commonly used in fresh and freeze-dried açai pulp are distinct from the açai pulp. The main form of açai consumption is the pulp and the presence of a high water content is a challenge for the successful use of infrared spectroscopic techniques. In this context, the aim of this research is to detect and distinguish adulterated from authentic açai pulp, identify the adulterant used, and compare NIR and MIR performance for this application (Caramês, Alamar, Poppi, & Pallone, 2017a, 2017b; Lobato et al., 2018; Xie, Ye, Liu, & Ying, 2009).

2. Material and methods

2.1. Adulterant standard solution preparations

Cassava and tapioca flour samples were obtained from Ananindeua-PA, Brazil. The commercial emulsifier (Marvi, Ourinhos, Brazil) composed of monoglyceride and diglyceride fatty acids, sorbitan monostearate, propylene glycol and potassium stearate, along with wheat flour (Tia Ofélia, Sertanópolis, Brazil) were obtained from a market in Campinas-SP, Brazil. In order to ensure solubilization of all flour adulterants, adulterant standard solutions were prepared using 126.72 g of cassava flour in 400 mL of distilled water, 181.18 g of tapioca flour in 400 mL of distilled water, and 160.29 g of wheat flour in 400 mL of distilled water. Solutions were under constant agitation and heat (90 °C) until they resulted in a homogeneous solution.

The resulting adulterant standard solutions were used in the açai pulp adulteration procedure.

2.2. Açai pulp adulteration procedure

Thin açai pulp was obtained from Ananindeua-PA. The adulteration

* Corresponding author.
E-mail address: jpallone@fea.unicamp.br (J.A.L. Pallone).

https://doi.org/10.1016/j.foodres.2019.06.006
Received 26 November 2018; Received in revised form 30 May 2019; Accepted 4 June 2019
Available online 07 June 2019
0963-9969/

procedure is described in Fig. S1 in the Supplementary Materials and was carried out in a laboratory setting.

The samples of thin açai pulp were altered to 5%, 10%, 20%, and 40% *w*/w using the cassava, tapioca, and wheat flour solutions (as described in item 2.1). The adulteration levels were determined according to the increasing thickness in appearance and in the total solids content of the adulterated samples. Levels above 40% were not used because the discrepancy could be detected visually. Regarding the emulsifier, the samples of açai were altered using lower values (1%, 2.5%, 5%, and 10% *w*/w), since this adulterant required less to produce the same effects in appearance. Levels above 10% w/w were tested and the samples noticeably blended.

In order to control the level of total solids (TS) increased during production of adulterated samples, an analysis of TS was performed by placing about 5 g of each sample in a drying oven (105 °C) to achieve constant weight, according to AOAC (A.O.A.C, 1998). Samples with cassava flour had an increased TS average of 10.86% to 15.20%, samples with tapioca flour from 10.80% to 15.06%, samples with wheat flour from 10.20% to 12.30% and with the emulsifier from 10.57% to 11.92%.

2.3. Spectra data acquisition

For the acquisition of NIR spectra data, about 2 g of each sample was placed into a petri dish, and the liquid reflector (PerkinElmer, Walthman, USA, part number L118–0503) was placed above the sample and slowly placed against the glass before scanning. The near infrared reflectance accessory (PerkinElmer, Walthman, USA, model NIRA) was coupled in the FT-NIR spectrometer (PerkinElmer, Walthman, USA, model Spectrum 100 N) using indium gallium arsenide (InGaAs) as detector and diffuse reflectance, to acquire the mean spectra of 32 scans with the transflectance measurements in the range of 10,000–4000 cm^{-1}, with a resolution of 4 cm^{-1}.

To obtain MIR spectra data, a drop of each sample was placed directly into the crystal of an Attenuated Total Reflectance and Fourier transformation mid-infrared (ATR-FTIR) spectrometer (Cary630FTIR Spectrometer, Agilent Technologies, USA) using diffuse reflectance and deuterated triglycine sulfate (dTGS) detector cooled thermoelectrically with 1.3 mm of diameter. All data was collected in range of 4000–400 cm^{-1}, with a resolution of 4 cm^{-1} and with 32 scans.

2.4. Chemometrics

Chemometrics analyses were performed using the software MatLab R2018 and PLS-toolbox version 8.6 (*Eingevector Research Inc, 2010*). Preprocessing methods were applied in order to improve the performance of the classification models, Multiplicative Scatter Correction (MSC) or Standard Normal Variate (SNV) were used to reduce the light scattering effects of raw spectra data. The offset correction was minimized by applying the first derivative of Savitzky-Golay (filter width: 37, polynomial order: 2). Raw data were mean centered (MC).

Samples were randomly separated and about 70% were used in a calibration set and 30% used as an external validation set. The k-Nearest Neighbors (KNN) and Partial Least Squares-Discriminant Analysis (PLS-DA) methods were used for determination of classification models to assure best performance. Models were evaluated by figures of merit:sensitivity and specificity, according to Eqs. (1) and (2) (where TP is true positive, FN is false negative, TN is true negative, and the FP is false positive) (Barra, Mansouri, Cherrah, Kharbach, & Bouklouze, 2019; Miaw, Sena, de Souza, Callao, & Ruisanchez, 2018).

$$Sensitirvity\ (\%) = \frac{TP}{TP + FN} * 100 \quad (1)$$

$$Specificity\ (\%) = \frac{TN}{TN + FP} * 100 \quad (2)$$

Sample outliers were detected using the Student residual values and leverage to reach the best performance for the classification models.

Unsupervised exploratory techniques like Principal Component Analysis (PCA) are usually used in the food and drug industry for quality control and process monitoring. In this context, multivariate control charts are the plots of distinct parameters, such as, the Hotelling's T^2 and $Q_{residuals}$ of PCA and the samples. The $Q_{residuals}$ are a lack-of-fit statistic that can be used, in this case, as an indicative of how well the sample are being described by the model pre-established (Eq. (3)). Whereas the values of $Q_{residuals}$ represents the variation remaining in each sample after projected by the model, the Hotelling's T^2 values (Eq. (4)) represent the variation of each sample within the model, that is how far the sample is from the center of the model (scores = 0) (Mason, Tracy, & Young, 2018; *the Math Works Inc, 2009*).

$$Q_i = e_i e_i^T = x_i (I - P_k P_k^T) x_i^T \quad (3)$$

$$T_i^2 = t_i \lambda^{-1} t_i^T = x_i P_k \lambda^{-1} P_k^T x_i^T \quad (4)$$

where e_i is the i^{th} row of the matrix of samples, P_k is the matrix of the k loadings vectors retained by the model and I is the identity matrix, t_i represents the i^{th} row of the matrix of score's samples T (m × k) and λ represents the diagonal matrix of eigenvalues according to k principal components choose in the model.

These multivariate control charts are based on calibrations using authentic samples, which define the normal limits of the charts; and consequently, the differentiation of adulterated samples using this alteration in residual values. These multivariate control charts were already performed by Lobato et al. (2018) to discriminate adulterated samples of freeze-dried açai and by Clavaud, Roggo, Von Daeniken, Liebler, and Schwabe (2013) monitoring biopharmaceutical Chinese hamster ovary cell culture and by Xiong, Gong, and Qu (2012) monitoring batch-to-batch reproducibility of liquid-liquid extraction process. In this paper, multivariate control charts were developed with sample residues (Q) in the PCA model.

The Interval Partial Least-Squares Regression (iPLS), removal of baseline range, and Variable Importance in Projection (VIP) scores were used as methods to select variables, when needed, to improve performance. VIP scores relates to the importance and influence of the variables used in the models constructed. In this context, variables that were below the significance threshold were removed and the iPLS method was used to develop PLS models in equal width intervals of the full spectra data. Therefore, intervals of 250 variables were used and an automatic number of intervals were set, the sub-intervals that gave the lowest values of Root Mean Square Error of Calibration (RMSEC) and Root Mean Square Error of Cross-Validation (RMSECV) were then used then used (Galindo-Prieto, Trygg, & Geladi, 2017; Rahman, Kondo, Ogawa, Suzuki, & Kanamori, 2016).

3. Results and discussion

3.1. IR spectra data and multivariate Q control charts

The raw spectra data obtained by NIR and MIR spectroscopy are presented in Fig. S2 in the supplementary material. The MIR spectra displayed similar behavior for both adulterated and authentic samples. Two large peaks are noticeable, one peak at 3500 cm^{-1} to 3000 cm^{-1} and another at 1640 cm^{-1}. Both peaks are associated with O—H stretching and bending vibration mode respectively, resulting from the high water content in the samples. The region from 1200 cm^{-1} to 900 cm^{-1} showed peaks that are correlated with C—O and C—C stretching; and C—O—C and C—O—H, which could be for esters, carbohydrates, and organic acids typical to the sample. The region between 1700 cm^{-1} - 1000 cm^{-1} are correlated to the presence of phenolic compounds, such as, C═C—C aromatic ring stretching and the C—O stretching of phenol (Miaw et al., 2018). Similar results were observed in NIR spectra data collected. Two large peaks were detected

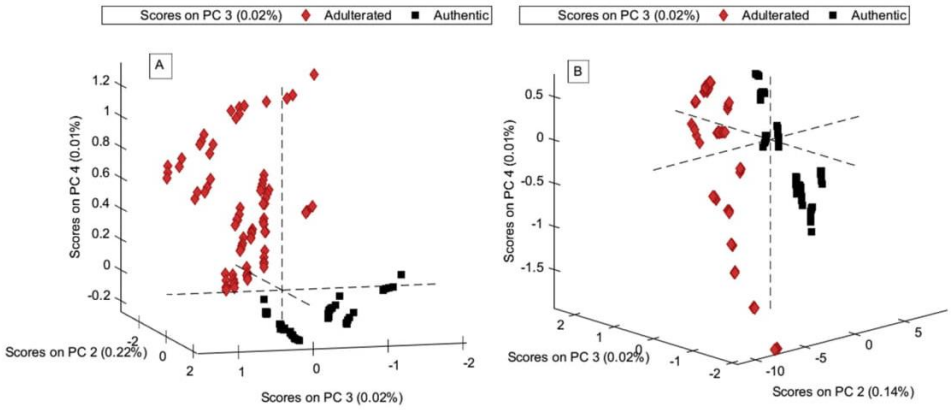

Fig. 1. Plot of scores in PC 2 × PC 3 × PC 4 by MIR data (A) and NIR data (B).

at ≈6900 cm^{-1} and 5200 cm^{-1}, these peaks represent the O−H first overtone and combination, and are also related to the high water content in açai pulp (Caramês et al., 2017a, 2017b; Musingarabwi, Nieuwoudt, Young, Eyéghè-Bickong, & Vivier, 2016).

The PCA analysis was performed using the NIR data range 10,000 cm^{-1} - 4000 cm^{-1}. The mean centered data was preprocessed with SNV, other methods of preprocessing were tested but did not improve the results. Four Principal Components (PC) were used representing 99.99% of cumulative variance. The PCA model performed using MIR data, used the portion of the spectra data from 3747.02 cm^{-1} - 2794.95 cm^{-1} and 2422.31 cm^{-1} - 452.955 cm^{-1}, this represented the highest contribution in $Q_{residuals}$ values. Since these $Q_{residuals}$ values were chosen to build the control chart, the other sections that had values below the significance threshold were removed and SNV applied at the mean centered data. Other methods were tested with no improvement to the final results. Five PCs were used to build this model, representing 100% of cumulative variance (Fig. 1).

The two PCA models did not show any significant separation between authentic and adulterated samples in PC1. Most likely because this PC contained a greater amount of information, and only the amount of water found was used to represent this information, therefore this PC was not sufficient for differentiation. In both models, the use of plots with 3 PCs (PC2 × PC3 × PC4) assisted in better visualization of the sample's distribution, and in both cases adequate separation was observed.

Control charts are another effective method of projection, and in this case, were used to discriminate adulterated from authentic açai pulp samples. To develop this type of projection, the preprocessing (SNV- for NIR and MIR- and variable selection- for MIR) used to perform the PCA models previously presented were repeated. Using only authentic samples in the calibration set and authentic and adulterated samples in the experimental set. The experimental set were plotted using $Q_{residuals}$ values × Samples (Fig. 2) and both charts were successful and efficient in discriminating between adulterated and authentic samples with 99% confidence.

In regression data analysis, plot data using the residual values are commonly used to detect anomalous samples. Each regression model originates a set of residuals, therefore, any sample that is significantly different from the residuals of the multivariate analysis calibration set samples are anomalous. When this concept is applied to analyze fraudulent cases, the presence of adulterated samples in the experimental set is identified through the high residual values found for these samples (Fig. 2). Therefore, the spectra data used is successful in detecting the chemical information necessary to determine adulteration in açai pulp (Ferreira, 2015).

In this context, other research has also been conducted using this concept. For example, Ávila et al. (2012) developed Q control charts using Raman spectroscopy data for on-line control of glucose fermentation by *Saccharomyces cerevisiae*. The Q charts were efficient in detecting fault-batches with 95% confidence. Lobato et al. (2018) developed Q control charts based on NIR spectra data that were able to successfully detect grape juice, beet pulp, maltodextrin, cassava starch, and corn starch in adulterated freeze-dried açai pulp with; proving the efficiency of this type of projection.

3.2. MIR spectroscopy

3.2.1. KNN and PLS-DA classification models

Since the addition of any of these substances (emulsifier, cassava flour, tapioca flour, and wheat flour) is prohibited and characterized as adulteration, this study developed methods to detect adulteration. Classifying the sample as authentic and adulterated (2 classes); as well as identifying the type of adulterant, by classifying the samples as authentic and adulterated by commercial emulsifier, cassava, tapioca, and wheat flour (5 classes).

All models used spectra data (4000 cm^{-1}- 400 cm^{-1}), and the results for 2 classes (authentic and adulterated) are shown in Table 1. Several preprocessing methods were applied in order to improve the performance. The ones with better results were first derivative by Savitzky-Golay algorithm (1DV), MC, SNV and MSC. KNN models were performed using three neighbors (k = 3) and the PLS-DA models were all performed using 8 latent variables (LV), this number was chosen according to the lowest values obtained from Root Mean Square Error of Cross Validation (RMSECV) and Cross Validation (CV) class error average. The cross validation was performed using leave-one-out method. Both, KNN and PLS-DA methods presented desirable performances with high values of sensitivity and specificity. Comparing the preprocessing techniques in KNN, the best results were found for SNV with 100% specificity and sensitivity in prediction. For PLS-DA, all preprocessing presented 100% specificity and sensitivity in discriminating adulterated from authentic samples.

The results of models constructed to identify the type of adulterant are presented in Table 2. In KNN models for the 5 classes, the use of SNV also showed the best results for prediction, with 3 neighbors showing 100% specificity and sensitivity in all classes. In PLS-DA multiclass models, using 12 LVs, SNV and MSC preprocessing methods gave maximum values of specificity and sensitivity. Both techniques, SNV and MSC, have the same concept of reducing the negative effects caused by light scattering, which is recurrent in samples that present solid particles of different sizes. SNV and MSC were proved to be efficient in this case, presenting exactly the same parameters of performance. In this case, the PLS-DA algorithm also showed great performance, much like the study by Miaw et al. (2018), which aimed to perform a multiclass classification to detect adulteration in grape juice,

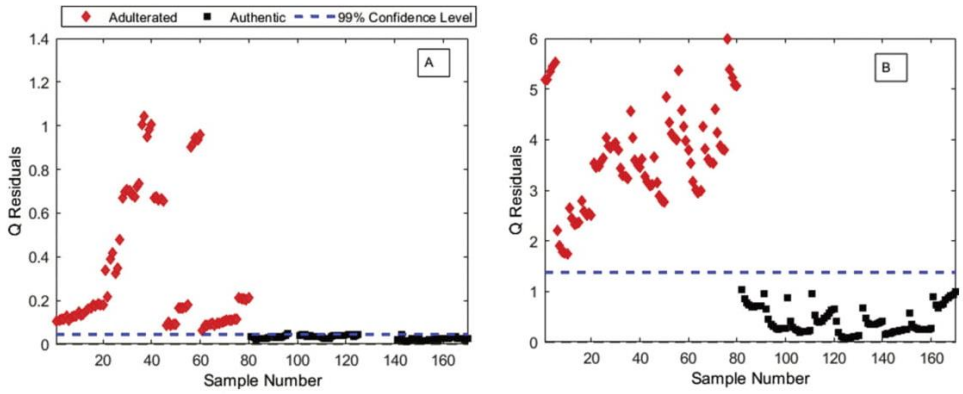

Fig. 2. Q control chart by MIR (A) and NIR (B).

the PLS-DA algorithm was successfully applied presenting no false negatives (classifying an adulterated sample as authentic). The results of this study and Miaw et al. (2018), support the desirable ability of PLS-DA models to classify samples in more than two classes (Miaw et al., 2018).

3.3. NIR spectroscopy

3.3.1. KNN and PLS-DA classification models

NIR spectra data between 10,000 cm^{-1} - 4000 cm^{-1} were pre-processed with various preprocessing algorithms. MC and SNV presented the best values for specificity and sensitivity (Table 3). The KNN model, considering 2 classes with preprocessing techniques of MC and 3 neighbors, showed 100% sensitivity and specificity in predicting açai pulp adulteration. When the spectra data are mean centered, all the variables are subtracted by the mean value, generally, this act is evidence for the largest internal variance of the data. In this case, it presented excellent results for KNN's applicability. PLS-DA models, considering 2 classes were constructed using 6 LVs and had 100% sensitivity and specificity for the SNV preprocessing method. Commonly, samples that have a large number of solid particles with different sizes can cause the physical phenomenon of light scattering. These signals are registered by the detector of FT-NIR but do not represent real chemical information. Once açai pulp has between 8 and 14% of total solids, the SNV method was successfully applied, minimizing these multiplicative errors in the two-class and multiclass models (Ferreira, 2015).

Regarding the models considering all 5 classes, the KNN models used 3 neighbors and had 100% specificity and sensitivity when MC was applied to all classes. PLS-DA models also presented best results when applied with MC, giving values of specificity above 90% and sensitivity above 85% (considering prediction values and using 15 LVs for all models). Nevertheless, none of preprocessing methods applied could give 100% correct prediction in all classes (Table 4).

In order to improve the performance obtained in PLS-DA models, the preprocessing method with the best results (MC) were applied with different types of variable selection. Such as iPLS in intervals of 250 variables, removal of baseline, and VIP scores (Table 5). The model developed using the spectrum portion of 6177 cm^{-1}- 4000 cm^{-1} selected with VIP scores (Fig. S3 in Supplementary Material) and preprocessed with MC had the better results than models obtained with full spectra data. Using 13 LVs, results were 100% sensitivity and specificity for calibration and validation sets. Regarding the cross validation, results varied between 91.7% and 100% of sensitivity and 96.7% and 100% of specificity.

VIP is a method for finding significant variables in large and complex data, and consists of select variables from PLS models. VIP scores for each variable used in the analysis were calculated, and all variables that had VIP scores below the defined threshold (in this case, value = 1) were excluded. The PLS-DA model was reprocessed using

Table 1
Results of classification methods in 2 classes obtained by MIR spectra data.

Pre-processing	Class	MIR- 2 classes					
		KNN					
		Sensitivity cal (%)	Specificity cal (%)	Sensitivity CV (%)	Specificity CV (%)	Sensitivity pred (%)	Specificity pred (%)
1DV	Authentic	100	87.5	100	87.5	100	96.87
	Adulterated	87.5	100	87.5	100	96.87	100
MC	Authentic	100	91.67	100	91.67	100	100
	Adulterated	91.67	100	91.67	100	100	100
SNV	Authentic	100	93.75	100	93.75	100	100
	Adulterated	93.75	100	93.75	100	100	100
Pre-processing	Class	PLS-DA					
		Sensitivity cal (%)	Specificity cal (%)	Sensitivity CV (%)	Specificity CV (%)	Sensitivity pred (%)	Specificity pred (%)
MSC	Authentic	100	100	100	100	100	100
	Adulterated	100	100	100	100	100	100
SNV	Authentic	100	100	100	100	100	100
	Adulterated	100	100	100	100	100	100

Table 2
Results of classification methods in 5 classes obtained by MIR spectra data.

Pre-processing	Class	MIR- 5 classes					
		KNN					
		Sens. cal (%)	Spec. cal (%)	Sens. CV (%)	Spec. CV (%)	Sens. pred (%)	Spec. pred (%)
1DV	Emulsifier	100	100	100	100	100	100
	Cassava flour	100	100	50	100	75	100
	Tapioca flour	100	100	100	100	100	100
	Wheat flour	100	100	100	100	100	100
	Authentic	100	100	100	87.50	100	93.75
MC	Emulsifier	100	100	100	100	100	100
	Cassava flour	66.67	100	66.67	100	91.67	100
	Tapioca flour	100	100	100	100	100	100
	Wheat flour	100	100	100	100	100	100
	Authentic	100	91.67	100	91.67	100	97.92
SNV	Emulsifier	100	100	100	100	100	100
	Cassava flour	75	100	75	100	100	100
	Tapioca flour	100	100	100	100	100	100
	Wheat flour	100	100	100	100	100	100
	Authentic	100	93.75	100	93.75	100	100
Pre-processing	Class	PLS-DA					
		Sens. cal (%)	Spec. cal (%)	Sens. CV (%)	Spec. CV (%)	Sens. pred (%)	Spec. pred (%)
MSC	Emulsifier	100	100	100	100	100	100
	Cassava flour	100	100	100	99.59	100	100
	Tapioca flour	100	100	91.67	100	100	100
	Wheat flour	100	100	100	100	100	100
	Authentic	100	100	100	100	100	100
SNV	Emulsifier	100	100	100	100	100	100
	Cassava flour	100	100	100	99.59	100	100
	Tapioca flour	100	100	91.67	100	100	100
	Wheat flour	100	100	100	100	100	100
	Authentic	100	100	100	100	100	100

only the variables that contained the most significant contributions to the classification model. Comparing the spectra range selected by VIP scores, iPLS and removal of the baseline, is notable that the model based on VIP scores selection used fewer variables. Therefore, it is correct to affirm that iPLS and baseline removal variable selection methods still used undue variables that undermined the performance (Medina, Perestrelo, Silva, Pereira, & Câmara, 2019).

Lobato et al. (2018) used NIR to perform a multiway class classification and identified five adulterants (corn starch, beet, cassava starch, maltodextrin and grape juice) in freeze-dried açai pulp. KNN models determined using preprocessed data with MSC or SNV showed 100% of sensitivity and 0% of false positives. In the PLS-DA model using data preprocessed with MSC or SNV all classes presented 100% of sensitivity except for one class that was 80%. It is important to highlight that even though both food matrices are açai pulp, the presence and/or absence of water interferes in the success of classification methods. A high amount of water in açai pulp could mask important bands and overtones, making the identification of adulterated samples difficult. Moreover, each adulterant has different spectral data; and fresh and freeze-dried açai pulp have distinct typical adulterants, making it relevant to develop models for açai pulp.

Araújo, Marinho, and de Araújo Gomes (2017) reported another

Table 3
Results of classification methods in 2 classes obtained by FT-NIR spectra data.

Pre-processing	Class	FT-NIR- 2 classes					
		KNN					
		Sens. cal (%)	Spec. cal (%)	Sens. CV (%)	Spec. CV (%)	Sens. pred (%)	Spec. pred (%)
MC	Authentic	100	100	100	100	100	100
	Adulterated	100	100	100	100	100	100
SNV	Authentic	100	100	100	100	88.89	100
	Adulterated	100	100	100	100	100	88.89
Pre-processing	Class	PLS-DA					
		Sens. cal (%)	Spec. cal (%)	Sens. CV (%)	Spec. CV (%)	Sens. pred (%)	Spec. pred (%)
MC	Authentic	100	100	99.52	100	100	100
	Adulterated	100	100	100	99.52	100	100
SNV	Authentic	100	100	100	100	100	100
	Adulterated	100	100	100	100	100	100

Table 4
Results of classification methods in 5 classes obtained by FT-NIR spectra data.

Pre-processing	Class	FT-NIR- 5classes					
		KNN					
		Sens. cal (%)	Spec. cal (%)	Sens. CV (%)	Spec. CV (%)	Sens. pred (%)	Spec. pred (%)
MC	Emulsifier	100	100	100	100	100	100
	Cassava flour	100	100	100	100	100	100
	Tapioca flour	100	100	100	100	100	100
	Wheat flour	100	100	100	100	100	100
	Authentic	100	100	100	100	100	100
SNV	Emulsifier	100	100	100	100	100	91.23
	Cassava flour	75	98.78	75	99.19	100	95.61
	Tapioca flour	66.67	98.38	75	98.37	37.5	100
	Wheat flour	91.67	99.59	91.67	99.59	100	100
	Authentic	100	100	100	100	88.89	100
Preprocessing	Class	PLS-DA					
		Sens. cal (%)	Spec. cal (%)	Sens. CV (%)	Spec. CV (%)	Sens. pred (%)	Spec. pred (%)
MC	Emulsifier	100	100	100	100	100	100
	Cassava flour	100	100	75	99.59	87.5	99.12
	Tapioca flour	100	100	83.33	98.78	87.5	99.12
	Wheat flour	100	100	100	99.19	100	91.23
	Authentic	100	100	99.52	100	88.88	100
SNV	Emulsifier	100	100	100	100	100	100
	Cassava flour	91.67	100	83.33	100	100	95.61
	Tapioca flour	100	100	91.67	99.19	50	99.12
	Wheat flour	100	99.6	100	99.19	75	99.12
	Authentic	100	100	99.52	100	98.89	100

Table 5
Results of classification methods using variable selection in 5 classes obtained by FT-NIR spectra data.

PLS-DA 5 classes							
Pre-processing	Range (cm^{-1})	Variable selection	Class	Sensitivity cal (%)	Specificity cal (%)	Sensitivity pred (%)	Specificity pred (%)
MC	7750-7501; 6000-5501; 4750-4501	iPLS	Emulsifier	100	100	100	100
			Cassava flour	100	100	87.5	100
			Tapioca flour	100	100	100	99.04
			Wheat flour	100	100	100	100
			Authentic	100	100	100	100
MC	6177- 4000	VIP scores	Emulsifier	100	100	100	100
			Cassava flour	100	100	100	100
			Tapioca flour	100	100	100	100
			Wheat flour	100	100	100	100
			Authentic	100	100	100	100
MC	7864-4000	Baseline	Emulsifier	100	100	100	100
			Cassava flour	100	100	100	97.15
			Tapioca flour	100	100	62.5	99.04
			Wheat flour	100	100	87.5	100
			Authentic	100	100	100	100

Table 6
Confusion matrix and precision rate of best models to FT-NIR and MIR with 2 classes.

		MIR		FT-NIR	
Method		PLS-DA		KNN	
Preprocessment		SNV		Mean center	
		Authentic	Adulterated	Authentic	Adulterated
Actual class	Authentic	90	0	90	0
	Adulterated	0	32	0	32
Precision rate%		100	100	100	100
Average precision rate%		100		100	

Table 7
Confusion matrix and precision rate of best models to FT-NIR and MIR with 5 classes.

						MIR
Method						PLS-DA
Preprocessment						SNV
		Authentic	Emulsifier	Cassava flour	Tapioca flour	Wheat flour
Actual class	Authentic	81	0	0	0	0
	Emulsifier	0	8	0	0	0
	Cassava flour	0	0	8	0	0
	Tapioca flour	0	0	0	8	0
	Wheat flour	0	0	0	0	8
Precision rate%		100	100	100	100	100
Average precision rate%		100				
						FT-NIR
Method						KNN
Preprocessment						Mean center
		Authentic	Emulsifier	Cassava flour	Tapioca flour	Wheat flour
Actual class	Authentic	90	0	0	0	0
	Emulsifier	0	8	0	0	0
	Cassava flour	0	0	8	0	0
	Tapioca flour	0	0	0	8	0
	Wheat flour	0	0	0	0	8
Precision rate%		100	100	100	100	100
Average precision rate%		100				

technique to detect adulteration in açai pulp. They used RBG images as a base to develop DD-SIMCA and OC-PLS models to detect açai pulp mixed with cassava and wheat (with 10% of adulterant). The OC-PLS model did not show satisfactory results with 31% of error rate and 78.69% specificity. The model developed using DD-SIMCA had a better performance with 2% error rate and 98.14% specificity. Both models were one-class way, meaning that, they were efficient in distinguishing authentic from adulterated samples. However, this technique was not capable of discriminating the type of adulterant used. This method had a worse performance when compared to the models using NIR and MIR spectral data.

A summary of the best classification models and the matrix of confusion in question, considering the sample validation subsets, and precision data are shown in Tables 6 and 7 (for classification models with two and five classes, respectively). According to the performance indicators for precision, all models are reliable in detecting tampered samples of açai pulp and identifying possible adulterants. SNV and PLS-DA methods presented the best results with MIR data, and the KNN method applied with mean center as preprocessing method showed the best results in NIR data.

4. Conclusion

This paper presents the application of NIR and MIR techniques to detect adulteration and identify the type of adulterant used in açai pulp. MIR and NIR validated models presented high percentage of specificity and sensitivity. MIR models constructed using PLS-DA presented 100% specificity and sensitivity in two of five classes, and the same performance was observed for NIR models using KNN and PLS-DA. In this context, it is important to note that both spectroscopic techniques (-NIR and MIR) presented good results, with high percentage of accurate differentiation between classes. Both techniques succeeded in distinguishing authentic from adulterated samples and also capable of identifying the type of all adulterants in samples, however the emulsifier was the more successful adulterant detectable probably because of its composition, regarding the classification methods, KNN and PLS-DA, when they were applied within MIR spectra data PLS-DA presented a better performance than KNN, considering NIR spectra data both methods presented similar results. Cases using a mixture of adulterants are not common, as the main aim of this practice is to reduce production cost and use of more than one would cause an increase. However, if this does occur, the control chart is still able to classify this as an adulterated açai pulp product. Therefore, the methods studied can be applied for identifying adulterants and adulterated acai pulp products.

Supplementary data to this article can be found online at https://doi.org/10.1016/j.foodres.2019.06.006.

Acknowledgements

The authors would like to acknowledge the Foundation for Research Support of the State of São Paulo (FAPESP- Grant number: 2018/09759-3) for funding the research. The Coordination for the Improvement of Higher Education Personnel (CAPES- Grant number: 001) and the National Council for Scientific and Technological Development (CNPq) for awarding a PhD scholarship to Priscila D. Alamar and Elem T. S. Caramês.

References

A.O.A.C (1998). *Association of official analytical chemists: Official methods of analysis.* (16th ed.).

Alamprese, C., Amigo, J. M., Casiraghi, E., & Engelsen, S. B. (2016). Identification and quantification of Turkey meat adulteration in fresh, frozen-thawed and cooked minced beef by FT-NIR spectroscopy and chemometrics. *Meat Science, 121*, 175–181. https://doi.org/10.1016/j.meatsci.2016.06.018.

Araújo, A., Marinho, W., & de Araújo Gomes, A. (2017). A fast and inexpensive chemometric-assisted method to identify adulteration in Acai (*Euterpe oleracea*) using digital images. *Food Analytical Methods,* 1–7. https://doi.org/10.1007/s12161-017-1127-4 (Canto 2001).

Ávila, T. C., Poppi, R. J., Lunardi, I., Tizei, P. A. G., & Pereira, G. A. G. (2012). Raman spectroscopy and chemometrics for *on-line* control of glucose fermentation by *Saccharomyces cerevisiae*. *Biotechnology Progress, 28*(6), 1598–1604. https://doi.org/10.1002/btpr.1615.

Barra, I., Mansouri, M. A., Cherrah, Y., Kharbach, M., & Bouklouze, A. (2019). FTIR fingerprints associated to a PLS-DA model for rapid detection of smuggled non-compliant diesel marketed in Morocco. *Vibrational Spectroscopy, 101*, 40–45. https://

doi.org/10.1016/j.vibspec.2019.02.001.
Basri, K. N., Hussain, M. N., Bakar, J., Sharif, Z., Khir, M. F. A., & Zoolfakar, A. S. (2017). Classification and quantification of palm oil adulteration via portable NIR spectroscopy. *Spectrochimica Acta Part A: Molecular and Biomolecular Spectroscopy, 173*, 335–342. https://doi.org/10.1016/j.saa.2016.09.028.
Bázár, G., Romvári, R., Szabó, A., Somogyi, T., Éles, V., & Tsenkova, R. (2016). NIR detection of honey adulteration reveals differences in water spectral pattern. *Food Chemistry, 194*, 873–880. https://doi.org/10.1016/j.foodchem.2015.08.092.
Caramês, E. T. S., Alamar, P. D., Poppi, R. J., & Pallone, J. A. L. (2017a). Rapid assessment of total phenolic and anthocyanin contents in grape juice using infrared spectroscopy and multivariate calibration. *Food Analytical Methods, 10*(5), https://doi.org/10.1007/s12161-016-0721-1.
Caramês, E. T. S., Alamar, P. D., Poppi, R. J., & Pallone, J. A. L. (2017b). Quality control of cashew apple and guava nectar by near infrared spectroscopy. *Journal of Food Composition and Analysis, 56*, 41–46. https://doi.org/10.1016/j.jfca.2016.12.002.
Clavaud, M., Roggo, Y., Von Daeniken, R., Liebler, A., & Schwabe, J. O. (2013). Chemometrics and in-line near infrared spectroscopic monitoring of a biopharmaceutical Chinese hamster ovary cell culture: Prediction of multiple cultivation variables. *Talanta, 111*, 28–38. https://doi.org/10.1016/j.talanta.2013.03.044.
Eingevector Research Inc (2010). *Manson, USA*.
Ferreira, M. M. C. (2015). *Quimiometria conceitos, métodos e aplicações.* (Campinas, SP).
G1, D. P. (2014). Fiscalização encontra papel higiênico misturado com açaí em Belém. Retrieved March 6, 2017, From http://g1.globo.com/pa/para/noticia/2014/06/fiscalizacao-encontra-papel-higienico-misturado-com-acai-em-belem.html.
Galindo-Prieto, B., Trygg, J., & Geladi, P. (2017). A new approach for variable influence on projection (VIP) in O2PLS models. *Chemometrics and Intelligent Laboratory Systems, 160*, 110–124. https://doi.org/10.1016/j.chemolab.2016.11.005.
Haughey, S. A., Graham, S. F., Cancouët, E., & Elliott, C. T. (2013). The application of Near-Infrared Reflectance Spectroscopy (NIRS) to detect melamine adulteration of soya bean meal. *Food Chemistry, 136*(3–4), 1557–1561. https://doi.org/10.1016/J.FOODCHEM.2012.01.068.
Lobato, K. B.d. S., Alamar, P. D., Caramês, E. T.d. S., & Pallone, J. A. L. (2018). Authenticity of freeze-dried açai pulp by near-infrared spectroscopy. *Journal of Food Engineering, 224*, 105–111. https://doi.org/10.1016/J.JFOODENG.2017.12.019.
Lohumi, S., Lee, S., Lee, H., & Cho, B.-K. (2015). A review of vibrational spectroscopic techniques for the detection of food authenticity and adulteration. *Trends in Food Science & Technology, 46*(1), 85–98. https://doi.org/10.1016/j.tifs.2015.08.003.
Mason, R. L., Tracy, N. D., & Young, J. C. (2018). Decomposition of T 2 for multivariate control chart interpretation. *Journal of Quality Technology, 27*(2), 99–108. https://doi.org/10.1080/00224065.1995.11979573.
Medina, S., Perestrelo, R., Silva, P., Pereira, J. A. M., & Câmara, J. S. (2019). Current trends and recent advances on food authenticity technologies and chemometric approaches. *Trends in Food Science and Technology, 85*, 163–176. https://doi.org/10.1016/j.tifs.2019.01.017.
Miaw, C. S. W., Sena, M. M., de Souza, S. V. C., Callao, M. P., & Ruisanchez, I. (2018). Detection of adulterants in grape nectars by attenuated total reflectance Fourier-transform mid-infrared spectroscopy and multivariate classification strategies. *Food Chemistry, 266*, 254–261. https://doi.org/10.1016/j.foodchem.2018.06.006.
Musingarabwi, D. M., Nieuwoudt, H. H., Young, P. R., Eyéghè-Bickong, H. A., & Vivier, M. A. (2016). A rapid qualitative and quantitative evaluation of grape berries at various stages of development using Fourier-transform infrared spectroscopy and multivariate data analysis. *Food Chemistry, 190*, 253–262. https://doi.org/10.1016/j.foodchem.2015.05.080.
de Oliveira, M., Do, S. P., & Schwartz, G. (2018). Açaí— Euterpe oleracea. *Exotic fruits* (pp. 1–5). . https://doi.org/10.1016/B978-0-12-803138-4.00002-2.
Pala, D., Barbosa, P. O., Silva, C. T., de Souza, M. O., Freitas, F. R., Volp, A. C. P., ... de Freitas, R. N. (2018). Açai (Euterpe oleracea Mart.) dietary intake affects plasma lipids, apolipoproteins, cholesteryl ester transfer to high-density lipoprotein and redox metabolism: A prospective study in women. *Clinical Nutrition, 37*(2), 618–623. https://doi.org/10.1016/J.CLNU.2017.02.001.
Rahman, A., Kondo, N., Ogawa, Y., Suzuki, T., & Kanamori, K. (2016). Determination of K value for fish flesh with ultraviolet-visible spectroscopy and interval partial least squares (iPLS) regression method. *Biosystems Engineering, 141*, 12–18. https://doi.org/10.1016/j.biosystemseng.2015.10.004.
the Math Works Inc (2009). *Natick, USA*.
Xie, L., Ye, X., Liu, D., & Ying, Y. (2009). Quantification of glucose, fructose and sucrose in bayberry juice by NIR and PLS. *Food Chemistry, 114*(3), 1135–1140. https://doi.org/10.1016/j.foodchem.2008.10.076.
Xiong, H., Gong, X., & Qu, H. (2012). Monitoring batch-to-batch reproducibility of liquid-liquid extraction process using in-line near-infrared spectroscopy combined with multivariate analysis. *Journal of Pharmaceutical and Biomedical Analysis, 70*, 178–187. https://doi.org/10.1016/j.jpba.2012.06.028.

Supplementary Material

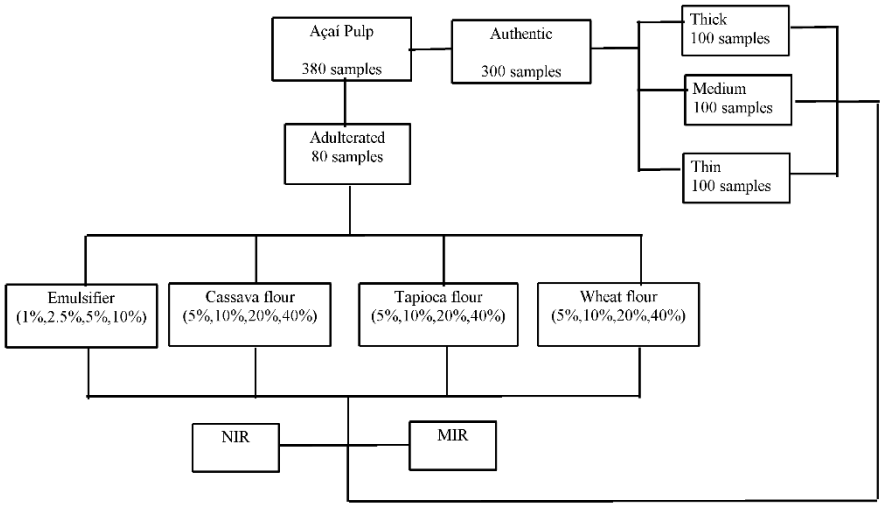

Figure S 1. Adulteration of açai pulp scheme.

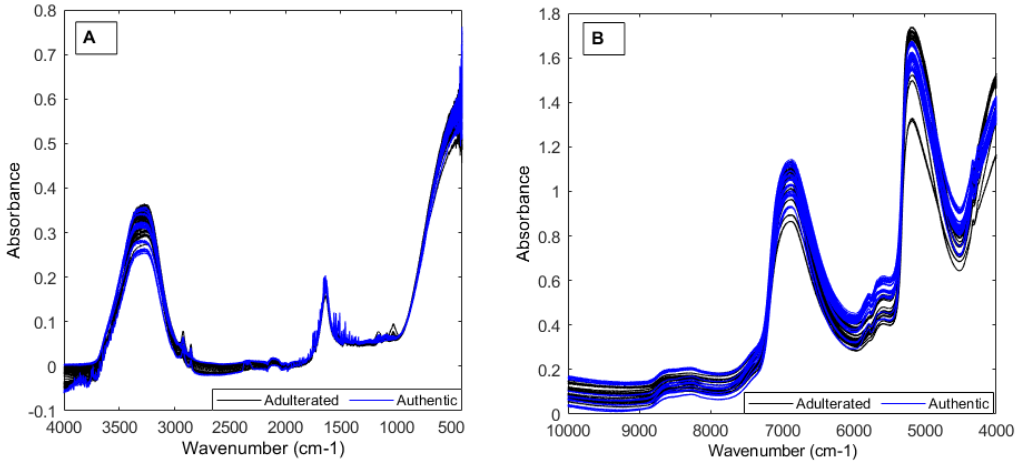

Figure S 2. Raw spectra data by MIR (A) and NIR (B).

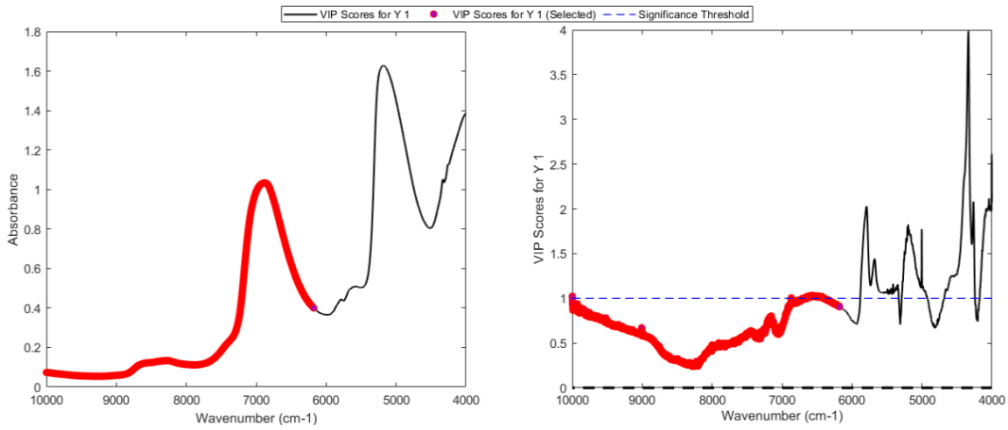

Figure S 3. Region of NIR spectra data excluded by VIP scores selection**.**

CAPÍTULO VI

Multiple element analysis in freeze-dried açai pulp – an efficient method to adulteration detection

Caramês, E.T.S.[1], Schilling, L.C.[1], Silva, J.G.S.[1], Teixeira, J.L.P.[1], Pallone, J.A.L[1]*.

[1] Department of Food Science, School of Food Engineering, State University of Campinas, Monteiro Lobato Street, 80, CEP: 13.083-862, Campinas, São Paulo, Brazil.

Manuscrito submetido em *Food Analytical Methods*

ABSTRACT

In this study, freeze-dried açai were analyzed by FAAS to determine the performance of multiple element evaluation to detect adulteration. Samples were composed by 94 authentic and 75 adulterated with beet pulp, maltodextrin, grape juice, cassava and tapioca flour. It was observed that iron, calcium, potassium and manganese were identified as possible target for adulteration detection. Principal Component Analysis (PCA) was performed to observe the data information and it was also performed the supervised classification methods, partial least square discriminant analysis (PLS-DA), one-class modeling partial least square (OCPLS) and soft independent modeling of class analogy (SIMCA). PCA demonstrated that the data information provided by the iron, calcium, potassium and manganese were useful to group the authentic and adulterated samples. Looking the classification method results, all presented satisfactory results, but the SIMCA and OCPLS showed high values of sensibility and sensitivity (above 80% and 90%). In this context, the use of the FAAS for evaluation of iron, calcium, potassium and manganese coupled to chemometric classification tool showed promising results distinguishing authentic and adulterated freeze-dried açai.

Keywords: mineral; authenticity; fraud; fruit; *Euterpe oleracea.*

1. INTRODUCTION.

The interesting for a healthy life style has been increasing the consumption of fruits and its consumption is highly recommended due to the supply of micronutrients and bioactive compounds to the human diet. In this sense, several fruits have been listed as “super foods” according to its composition, among these açai has highlighted because of the large concentration of bioactive compounds, the high antioxidant and anti-inflammatory properties, valuable fat composition with unsaturated fat acids and essential minerals as calcium, iron, magnesium and zinc, but also for the presence of cupper and manganese (RUZIK; WOJCIESZEK, 2016; SANTOS et al., 2014).

Regarding the micronutrients, the essential minerals present in açai pulp has an important role to an adequate function of human body, these minerals participate in several metabolic reactions. The insufficient or absence intake of it changes the metabolism and results in illness development after a period of time, as anemia, osteoporosis, diabetes mellitus and others (RODRÍGUEZ-SOLANA et al., 2014; SILVA et al., 2017).

In this context, as a relevant source of bioactive compounds, açai evolved from a regional food and gained the status of popularity as an exported fruit, once it has been

consumed into Europe Union, USA and Japan since the mid of 1990s. Although the increasing participation in market, the demand of production had the same behavior, however. açai has a seasonal harvest and it implies in high prices between crops. In order to supply the market during all the year, açai has been exported as frozen and/or freeze-dried pulp. As a profitable market and high price product, freeze dried açai has been a target to frauds that aim elevate the thickness (ex: wheat, cassava and tapioca flour) and modify the color (ex: grape juice and beet pulp) (LOBATO et al., 2018; SANTOS et al., 2014).

There are recent developments applying multi elemental methods coupled to chemometric tools to assure the authenticity of different food products as Italian porcine, Chinese apples, white asparagus and polished rice (LIU et al., 2019; MOTTESE et al., 2020; RICHTER et al., 2019; ZHANG et al., 2019). Although, the mostly applied multi elemental method used in these cases are applying inductively coupled plasma atomic emission spectroscopy (ICP-AES) or inductively coupled plasma mass spectroscopy (ICP-MS) that are high sensitivity but also high price methods. In this sense, flame atomic absorption spectroscopy (FAAS) presents itself as a low cost, simple and robust method to determine mineral elementals (SILVA et al., 2017).

Near infrared (NIR) was already successfully tested to detect adulteration in freeze-dried açai, although it has many advantages NIR it is not a daily method in control quality of freeze-dried acai and other for analytical methods can be proposed. In this context, the aim of this study was developing a simple, robust, traditional and low cost multi elemental method coupled to chemometric tools for verified the performance to detect adulteration in freeze-dried açai. In the best of our knowledge this propose an unpublished research.

2. MATERIALS AND METHODS

2.1. SAMPLES

Açai pulps were obtained by fruits collected at Abaetetuba and Igarapé-Miri (Pará, Brazil). A total of 94 samples constituted the authentic set, and the other 25 samples were adulterated in triplicate, summing 75 adulterated samples. The cassava starch (Yoki, General Mills Brasil Alimentos, São Bernardo do Campo, SP, Brazil), the cornstarch (Maizena, Unilever Bestfoods, Mogi Guaçu, SP, Brazil) and the maltodextrin (Cargill, Uberlândia, MG, Brazil), the beet roots and grape fruit were obtained from local market at Campinas-SP, Brazil. The beet roots and grape were, separately, crushed in processor (Phillips Walita, model RI7761, Varginha, MG, Brazil) until homogeneous beet pulp and grape juice.

To prepare the adulterated samples, it was mixed açai pulp with increasing thickness adulterants – cassava starch, cornstarch and maltodextrin – and modifiers color adulterants – beet pulp and grape juice, in concentrations of 1, 5, 10, 25 and 50% (w/w). After this procedure, all the samples were freeze-dried under 2000μHg with temperature of condenser temperature of -40 °C (Terroni, Brazil, model LS 3000). The freeze-dried samples were size standard (25 mesh) in order to homogenize it.

2.2. MINERAL EVALUATION BY FAAS AND METHOD VALIDATION

Samples were mineralized according to Silva et al. (2017), with modifications. After homogenization, 0.5 g of each sample was added of 4 mL of nitric acid (65%) and left to stand overnight, then it was added 2 mL of hydrogen peroxide (30%) and digested for 2 h at 140ºC. After cooling, the samples were added of more 2 mL of nitric acid (65%) and 2 mL of hydrogen peroxide (30%) and digested for 2 h at 140ºC. After mineralization, samples were filtered with filter ash free (Nalgon), transferred to a volumetric flask of 25 mL and the volume completed with ultrapure water. For calcium evaluation, it was added lanthanum oxide solution up to a concentration of 0.5% w/v to avoid possible interferences. Blanks were obtained following the same procedure and dilution.

To guarantee the reliability of the analytical results, validation studies were carried out by evaluating the parameters of linearity, sensitivity, limit of detection (LOD), limit of quantification (LOQ), precision (intermediate and repeatability) and recovery, according the guidelines on validation (Brazil, 2016; AOAC, 2016).

The linearity of the method was evaluated by the equation of linear regression of analytical curves, analysis of variance (ANOVA) of the regression, and the linear correlation coefficient (r). Analytical curves for each element were obtained and ranged from 0.25 to 3 mg/L for iron (Fe), 0.10 to 1.22 mg / L for potassium (K), 0.50 to 5 for calcium (Ca) and 0.05 to 0.60 to magnesium (Mg). The limits of detection (LOD) and quantification (LOQ) were calculated by measuring ten (10) analytical blanks. The precision was evaluated by repeatability and intermediate precision; repeatability was assessed by the simultaneous analysis of nine (9) replicates on the same day. The maximum value for the CV considered was 10%. The intermediate precision was evaluated through repetitions in three different days, and evaluated if differences were observed by ANOVA tests. The accuracy was

evaluated by recovery tests, then samples were fortified with 100% of the initial value present in the sample. All the tests were performed in triplicate.

The mineral was quantified by flame atomic absorption spectroscopy (FAAS), model AAnalyst 200, with a deuterium lamp for background correction radiation and hollow cathode lamps for determination of iron (248.3 nm), calcium (422.67 nm), magnesium (285.21 nm) and manganese (279.50 nm). Each sample was introduced into the nebulizer and mixed with an air/acetylene flame (2.5 L h^{-1}/10 L h^{-1}) at approximately 2000 °C.

2.3. STATISTICAL TREATMENTS AND CHEMOMETRICS.

The statistical treatments as analysis of variance (ANOVA) and Tukey test were performed using an extension of Microsoft Office Excel. The chemometrics analysis were made using MATLAB version R2019a (MathWorks, USA), PLS-toolbox version 8.6 (2010) and the toolbox described by (Xu et al. 2013).

In order to analyze the data, it was performed an unsupervised method of principal component analysis (PCA) and the supervised methods of Partial Least Square-Discriminant Analysis (PLS-DA), One Class Partial Least Square (OCPLS) and Soft Independent Modeling of Class Analogy (SIMCA). The data obtained were auto scaled and the cross-validation was performed using the method leave-one-out. The final model's performance was measured according to the sensitivity and specificity values (Equation 1 and 2).

$$Sensibility(\%) = \frac{TP}{TP+FN} * 100 \qquad (1).$$

$$Specificity(\%) = \frac{TN}{TN+FP} * 100 \qquad (2).$$

Where TP means True Positive, TN means True Negative, FN is False Negative, and FP is False Positive.

3. RESULTS AND DISCUSSION.

3.1. DEFINITION OF POSSIBLE TARGET MINERALS

To define the target minerals as possible markers to detect the adulteration in freeze-dried açai it was evaluated in a screening text two authentic samples and ten adulterated samples with each one of the 5 types of adulterants (corn starch, beet pulp, cassava flour, maltodextrin and grape juice) in the minimum (1%) and maximum (50%) levels of adulteration tested in this paper. It was determined the concentration of essential minerals

calcium (Ca), magnesium (Mg), potassium (K), iron (Fe), zinc (Zn), cupper (Cu) and manganese (Mn) and the results are presented in Table 1.

In this step the aim was observe the variation of minerals content in freeze-dried açai promoted by the adulterations. In order to quantify this variation, it was determined the percentual variation (PV) of each one, according to the equation 3, where x is the content obtained to authentic samples and y is the content of adulterated samples to each mineral.

$$Percentual\ Variation(\%) = \frac{|x-y|}{x} \times 100 \quad (3)$$

According the mineral content, K highlighted, being the mineral with the highest content between all the analyzed samples, followed by Ca, Mg, Mn, Fe and Zn. Previously, the contents of Ca, Fe, K and Mn were pointed as surprisingly high when compared to other food in human diet, since these minerals profile are typical of açai pulp (Rogez 2000; Da Silva Santos et al. 2014).

Regarding, the values of PV obtained in respect to the authentic samples in concentrations of 1% and 50% of adulteration, we observed that the addition of adulterants even in the lowest percentual (1%) had a high impact in the content of the respective mineral. Ca, Mn and Fe were the minerals that presented the highest results of PV, 51.37%, 52.45% and 42.96%, respectively. While PV adulteration of Cu, Mg and Zn were not so expressive, with 36.06% and 36.70% and 32.11% in average, respectively. In this context we considered that the minerals which had the highest impact on its concentration was the most important to evaluate the mineral profile of authentic samples. Then, Ca, Mn, Fe and K, were the four minerals choose as indicator of adulteration in freeze-dried açai, thus these minerals were analyzed in all the other samples. K did not present a high PV compared to the other minerals, but it is the most abundant mineral in açai, so it is considered important for the mineral profile.

.

Table 1. Minerals content to determine the target mineral.

	Adulteration (%)	Ca		Mg		K		Fe		Zn		Cu		Mn	
		mg/100g	PV (%)	mg/100g	PV (%)	mg/100g	PV (%)	mg/100g	PV (%)	mg/100g	PV (%)	mg/100g	PV (%)	mg/100g	PV (%)
Grape juice	1	158.10	39.00	110.13	31.90	1045.55	18.27	4.73	24.05	0.45	7.99	0.29	18.96	36.67	44.59
Corn starch	1	190.63	26.45	146.33	9.52	1026.67	19.75	4.83	22.52	0.54	10.33	0.33	7.23	52.59	20.54
Beet pulp	1	178.01	31.32	147.76	8.64	1161.59	9.20	4.48	28.05	0.53	8.06	0.33	6.96	48.39	26.88
Cassava flour	1	204.16	21.23	168.61	4.25	1027.98	19.64	3.90	37.39	0.28	43.13	0.31	14.32	55.36	16.35
Maltodextrin	1	175.93	32.12	155.74	3.71	1342.29	4.92	4.73	24.06	0.45	7.34	0.32	9.50	47.45	28.31
Grape juice	50	111.96	56.80	81.44	49.65	859.75	32.79	3.71	40.47	0.36	26.56	0.21	40.88	24.35	63.21
Corn starch	50	23.99	90.74	21.65	86.62	668.54	47.74	1.21	80.57	0.14	72.19	0.07	81.58	6.94	89.51
Beet pulp	50	126.59	51.16	165.08	2.07	950.00	25.74	4.63	25.67	0.44	10.51	0.29	18.10	27.83	57.95
Cassava flour	50	56.61	78.16	21.95	86.43	101.55	92.06	2.32	62.79	0.16	67.05	0.06	82.60	7.24	89.06
Maltodextrin	50	34.53	86.68	25.56	84.19	768.16	39.95	0.99	84.08	0.16	67.92	0.07	80.46	7.90	88.07
Authentic	-	261.88		163.20		1389.39		5.53		0.58		0.36		67.09	
Authentic	-	256.49		160.27		1169.18		6.94		0.40		0.36		65.28	
Authentic means (mg/100g)		259.18		161.73		1279.29		6.23		0.49		0.36		66.18	
Mean of PV(%)			51.37		36.70		31.01		42.96		32.11		36.06		52.45

3.2. METHOD VALIDATION FOR THE DETERMINATION FE, CA, K AND MN IN AUTHENTIC AND ADULTERATED FREEZE-DRIED ACAI AND CONTENTS IN FREEZE-DRIED AÇAI PULP

Analytical curves of each mineral were constructed using five distinct concentrations of external standard solution to evaluate the linearity. Fe ranged from 0.25 mg/L to 3 mg/L, Ca from 0.5 mg/L to 5 mg/L, K from 0.1 mg/L to 1.22 mg/L and to Mn from 0.05 mg/L to 0.6 mg/L. The linearity was evaluated according to the r values, to all minerals r > 0.99 was considered appropriate. The LOQ and LOD were calculated according to the blanks, for K LOQ and LOD were 0.84 mg/L and 0.25 mg/L, for Fe 0.97 mg/L and 0.29 mg/L, for Ca 2.04 mg/L and 0.62 mg/L and for Mn 0.10 mg/L and 0.03 mg/L, respectively (Table 2).

Table 2. Regression equations for analytical curves obtained by external standards, limits of quantification and detection to evaluate K, Fe, Ca and Mn.

Mineral	Mean content ± SD (mg/L)	Regression equation	r	Limit of Quantification	Limit of Detection
K	0.23±0.06	y = 20933,21x + 1809,87	0.9902	0.8391	0.2543
Fe	0.05±0.09	y = 0,050x + 0,0057	0.9969	0.9681	0.2934
Ca	0.44±0.16	y = 0,058x + 0,003	0.9996	2.0450	0.6197
Mn	0.007±0.01	y = 0,116x - 0,0008	0.9977	0.1045	0.0317

Values expressed as means ± standard deviation (SD).

The observed coefficients of variation (CV) were considered suitable according to the values established by INMETRO (2016) to K (2.67<2.7), Fe (1.62<7.3), Ca (2.33<3.7) and to Mn (2.38<5.3), then the CVs calculated were lower than the reference CV, so the repeatability was considered suitable. For the intermediate precision, the results of ANOVA showed that there was no significant difference between the days of analysis with 95% confidence. The accuracy was evaluated by recovery tests for each mineral. The results were a recovery rate of 101,21% for K, 101.26% for Fe, 102.83% for Ca, and 97.29% for Mn. And these values were considered suitable according to standard guidelines (Brazil, 2016).

With the validated method, the content of Fe, Ca, K and Mn in all the samples authentic and adulterated were determined (Table 3). Potassium is the majoritarian mineral in freeze-dried açai, regarding the authentic samples, it was detected a mean value of 12162.02

mg/kg in authentic samples. Manganese, calcium and iron mean content (685.08 mg/kg, 3495.23 mg/kg and 32.75 mg/kg) determined in this study were superior to the values previously determined by Rogez (2000) to Ca (286 mg/100g) and according to the values determined by Santos et al. (2014) to Fe (32.8mg/100g).

Fe, Ca and K are considered essential elements, their diary intake is about milligrams per day, and manganese is also needed to an adequate functioning of human body, but in trace concentration per day. Iron plays an important hole in human body and the deficient of this mineral is commonly detect in pregnant women causing anemia; calcium is crucial for the correct development of the human skeleton and correctly muscular and nerve function and potassium has an important sodium control effect, once its act as an antagonist to the high blood pressure and the manganese deficient can conduct to a poor growth and reproductive problems (Da Silva Santos et al. 2014; Mir-Marqués et al. 2016). In this sense, it is important detect the levels of açai consumption could contribute to an adequate diary intake of these essential minerals and maintenance of the human health.

Regarding the range of the mineral content between the authentic samples, it is remarkable the great variability probably associated to the climatic conditions during the cultivar, the soil, period of the harvest and others (Da Silva Santos et al. 2014).The açai fruit is a recognized Mn source. Da Silva Santos et al. (2014) determined the Mn content in 12 samples of freeze-dried açai obtained at São Paulo-Brazil and found mean of 45 mg/100g lower than the value determined in this study (68.51 mg/100g). The samples evaluated in this study were collected in distinct regions of Brazil (Southwest and North), in this sense, the climatic, temperature could be responsible for this difference in Mn content. Nevertheless, the number of samples analyzed in this study was lager (94 authentic samples) than 12 samples.

Table 3. Mineral content, mean and range, of authentic and adulterated samples.

	Fe		Ca		K		Mn	
Samples	Mean (mg/kg)	Range (mg/kg)	Mean (mg/kg)	Range (mg/kg)	Mean (mg/kg)	Range (mg/kg)	Mean (mg/kg)	Range (mg/kg)
Authentic	32.75^{b}	63.16-19.69	3495.23^{b}	5059.68-1557.58	12162.02^{c}	17286.85-6176.14	685.08^{b}	2361.66-223.76
Adulterated Grape juice	$33.55^{b,c}$	50.15-28.60	1580.97^{a}	1878.46-1119.61	6748.29^{b}	8163.28-5136.07	406.86^{a}	474.95-243.52
Adulterated Corn Starch	29.17^{a}	43.54-8.79	1106.87^{a}	1906.25-239.91	$6400.52^{a,b}$	8598.49-1117.83	305.08^{a}	525.88-69.43

Adulterated Beet Pulp	40.85[c]	43.80-38.90	1780.12[a]	1939.14-1265.91	12241.33[c]	27162.21-3040.00	475.32[a,b]	519.06-278.28
Adulterated Cassava flour	26.67[a]	35.99-1.53	1220.50[a]	2141.27-566.12	1360.90[a]	6601.17-531.33	309.92[a]	553.61-72.42
Adulterated Maltodextrin	27.46[a]	42.74-8.82	1127.09[a]	1759.25-345.35	5831.43[a,b]	9719.81-1034.48	304.22[a]	474.45-78.96

Values expressed as means ± standard deviation. Values followed by the same letters in the same column do not presented significative difference by Tukey test at 95% of confidence for the classes of samples.

Generally looking to the values of minerals content between authentic and adulterated samples, there is a decrease in the mean values of all mineral contents, indicating that these parameters are a potential mark to detect freeze-dried açai pulp adulteration.

The mean contents of Fe were different between authentic group of samples for all the adulterated one but that adulterated with grape juice, the contents of K were not able to differ the authentic sample from those added by beet pulp, same observed to Mn content means, on the other hand Ca contents were able to distinguish authentic samples from all the others adulterated samples. Corn starch, maltodextrin and cassava flour presented similar means of all the analyzed minerals and easily differing to the authentic group, although the samples adulterated by grape juice and beet pulp did not differ in the means content of iron and potassium and manganese, presenting as adulterants with the minerals profile most similar to the authentic ones.

3.3.PCA ANALYSIS

The data was auto scaled and it was set three principal components representing 91.20% of cumulative variance. The PC1, represented 56.12% of the explained variance, it showed a good grouping tendence between authentic and adulterated samples (Figure 1A). According to the loading plots (Figure 1B) we observed that the grouping formation was mainly due the great variation observed in Ca concentration of adulterated samples, presenting lower values of calcium content than authentic samples.

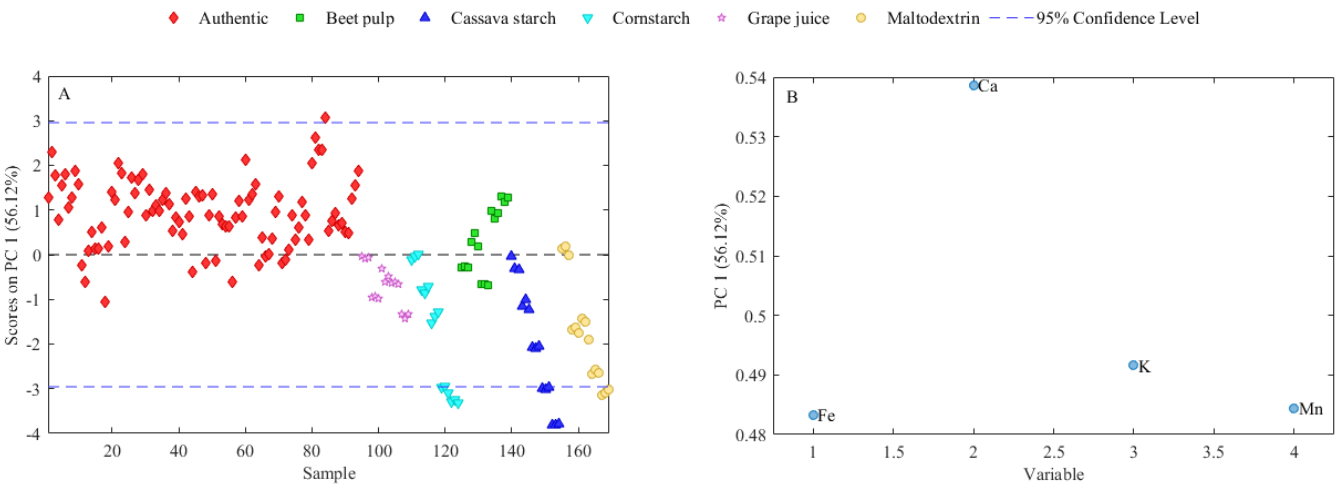

Figure 1. Scores (A) and Loadings (B) in PC1.

Although, the samples adulterated with beet pulp overlapped to the authentic group, and were grouped with the other adulterated samples only in percentages higher than 25% of adulteration. In concentrations under 25% of adulteration, samples added with beet pulp could not be easily distinguished from the authentic ones, once their mineral concentration was very similar.

Samples adulterated with beet pulp presented the mineral profile more similar to the authentic ones. Moreover, these samples presented higher content of Fe than the authentic samples, this information is represented in PC3 helping to distinguish it. Regarding to the loadings plot, the Ca and Fe content were the minerals with the more relevant contribution to discriminating process of the adulterated samples.

The adulterants used in this study are low cost, and do not have in their composition the same mineral profile of açai. Açai has high content of calcium, however the adulterants do not. Then, the minerals evaluated could be explored as good markers to detect adulteration in açai, considering the tested adulterants. Studies using minerals as markers to assure the authenticity were developed by Valentin and Watling (2013); in their study it was developed a method applying ICP-MS and ICP-AES to establish the origin of coffee where Mn was one of the minerals responsible for the correctly classification of the coffee by origin.

3.4. DISCRIMINATION AND ONE-CLASS MODELING MODELS: PLS-DA, OCPLS AND SIMCA

The relevance of performing three different classification methods is about to compare between discriminant (PLS-DA) and class modeling (SIMCA and OCPLS). PLS-DA is a discriminant method, that develops the method performing a multivariate regression and determining numeric values for each different class. The one-class partial least square (OCPLS) is a class modeling technique based in PLS, where the residue values of samples are used to detect outliers. On the other hand, SIMCA determine a region of acceptance for each class based on PCA values (Xu et al. 2013; Jiménez-Carvelo et al. 2019).

Regarding the efficient of these methods, some authors argue that class modeling methods present some advantage against the discriminant ones because once the region of acceptance is determined future sample only will assigned into a class if it fits inside the predetermined region, for example, if one sample is adulterated with a unknown ingredient distinct from these studied during the building process of the classification model, this sample will not be assigned in the target class (Rodionova et al. 2016). In this sense, the drawback of discriminant methods is the need of an exhaustive representation for all classes (Fidelis et al. 2017).

In this context, to detect the freeze-dried açai adulterated using Fe, Ca, K and Mn as marker, it was performed PLS-DA, OCPLS and SIMCA. During the modeling process, it was set 3 latent variables to PLS-DA model, 4 latent variables to OCPLS model and 3 principal components to SIMCA model determination. The results of sensitivity and specificity are presented in Table 4, since the OCPLS model demands only authentic samples at training set these parameters were expressed only to authentic class. PLS-DA, OCPLS and SIMCA results showed adequate parameters above 70% of right assignments, but looking at the confusion matrix it is possible to notice that PLS-DA model presented the lower rates of right assignments compared to the SIMCA and OCPLS. Regarding the SIMCA results only five authentic samples was assigned as adulterated increasing the sensitivity and specificity from test to above 80%. While OCPLS presented seven authentic samples assigned as adulterated, but all adulterated samples were right assigned, presenting sensitivity and specificity above 90%.

Even thought, all methods have presented satisfactory performance, considering the number of samples for each class that is limited and the advantages of class modelling method, is possible to affirm that in this particular study that the OCPLS and SIMCA model are suitable, with values of sensitivity and specificity above 90% and 80%, respectively, into calibration and test sets.

Table 4. Confusion matrix and figure of merits of OCPLS, PLS-DA and SIMCA models.

OCPLS				
	Calibration set		Test set	
Class	Authentic	Adulterated	Authentic	Adulterated
Authentic	61	0	24	0
Adulterated	2	0	7	75
Sensitivity (%)	100	-	100	91.46
Specificity (%)	96.8	-	91.46	100
PLS-DA				
Class	Authentic	Adulterated	Authentic	Adulterated
Authentic	63	2	23	1
Adulterated	0	48	8	24
Sensitivity (%)	96	100	96	74
Specificity (%)	100	96	74	96
SIMCA				
Class	Authentic	Adulterated	Authentic	Adulterated
Authentic	63	0	26	0
Adulterated	0	50	5	25
Sensitivity (%)	100	100	100	83
Specificity (%)	100	100	83	100

Although, PLS-DA method is widely used and it was successfully applied with mineral data obtained by ICP-OES to assure the authenticity of honey. In this study the content values of K, Ca, Mg, Na, Zn, Fe, Cu, Mn, Co, Cr, Ni and Cd were used during the discriminant analysis and was obtained good parameters of classification (Jovetić et al. 2017). The determination of

K, Na, Mg, P and Ca were also applied in classification methods to distinguish the origin of Greek wine, the PCA was effective in correlating the mineral profile to the origin of the Greek wine (Pasvanka et al. 2019).

In this sense, it is possible to affirm that microelements, such as minerals, could represent good markers to detect food frauds and it could a potential tool to assure the authenticity in different samples.

4. CONCLUSIONS

In this paper it was verified that the content of K, Fe, Ca and Mn for authentic and adulterated freeze-dried açai presented potential to be used for adulteration detection, when compared to others essential minerals. The K, Fe, Ca and Mn were determined by FAAS, using a validate method. The content of these minerals was considered relevant to human nutrition and the variation between the contents of these minerals, regarding authentic and adulterated samples, were a factor that allowed a well-being discrimination between the samples applying unsupervised methods of classification (PCA) and the supervised methods (PLS-DA, OCPLS and SIMCA). Comparing the methods performance, it is possible to conclude that SIMCA and OCPLS showed a slightly better result than PLS-DA. In this sense, the use of FAAS, for monitoring K, Fe, Ca and Mg coupled to chemometrics classification tools show itself as a valuable and low-cost option to assure the authenticity of freeze-dried açai.

Acknowledgments

The authors would like to thank the São Paulo Research Foundation (FAPESP) funding of the research project (project nº 2018/09759-3) and the PhD scholarship of José Teixeira (nº2018/08864-8). The Coordination for the Improvement of Higher Education Personnel (CAPES) (Financial Code 001). And the National Council for Scientific and Technological Development (CNPq) for the PhD scholarship of Elem Caramês (scholarship nº 142414/ 2016-6) and Joyce Silva (scholarship nº142415/2016-2).

5. REFERENCES

AOAC. **Association of Official Analytical Chemists International. Appendix F: Guidelines for Standard Method Performance Requirements**, 2016.

DA SILVA SANTOS, Vivian; DE ALMEIDA TEIXEIRA, Gustavo Henrique; BARBOSA, Fernando. Açaí (euterpe oleracea mart.): A tropical fruit with high levels of essential minerals - Especially manganese - And its contribution as a source of natural mineral supplementation. **Journal of Toxicology and Environmental Health - Part A: Current Issues**, *[S. l.]*, v. 77, n. 1–3, p. 80–89, 2014. DOI: 10.1080/15287394.2014.866923.

Eingevector Research Inc. Manson, USA, 2010.

FIDELIS, Marina; SANTOS, Jânio Sousa; COELHO, Ana Letícia Kincheski; RODIONOVA, Oxana Ye; POMERANTSEV, Alexey; GRANATO, Daniel. Authentication of juices from antioxidant and chemical perspectives: A feasibility quality control study using chemometrics. **Food Control**, *[S. l.]*, v. 73, p. 796–805, 2017. DOI: 10.1016/j.foodcont.2016.09.043.

INMETRO. **INMETRO. Instituto Nacional de Metrologia, Normalização e Qualidade Industrial.Orientações sobre Validação de Métodos de Ensaios Químicos, DOQ-CGCRE-008.**, 2016.

JIMÉNEZ-CARVELO, Ana M.; GONZÁLEZ-CASADO, Antonio; BAGUR-GONZÁLEZ, M. Gracia; CUADROS-RODRÍGUEZ, Luis. Alternative data mining/machine learning methods for the analytical evaluation of food quality and authenticity – A review. **Food Research International**, *[S. l.]*, v. 122, n. March, p. 25–39, 2019. DOI: 10.1016/j.foodres.2019.03.063. Disponível em: https://doi.org/10.1016/j.foodres.2019.03.063.

JOVETIĆ, Milica; TRIFKOVIĆ, Jelena; STANKOVIĆ, Dalibor; MANOJLOVIĆ, Dragan; MILOJKOVIĆ-OPSENICA, Dušanka. Mineral content as a tool for the assessment of honey authenticity. **Journal of AOAC International**, *[S. l.]*, v. 100, n. 4, p. 862–870, 2017. DOI: 10.5740/jaoacint.17-0145.

LIU, Zhi; ZHANG, Weixing; ZHANG, Yongzhi; CHEN, Tianjin; SHAO, Shengzhi; ZHOU, Li; YUAN, Yuwei; XIE, Tongzhou; ROGERS, Karyne M. Assuring food safety and traceability of polished rice from different production regions in China and Southeast Asia using chemometric models. **Food Control**, *[S. l.]*, v. 99, n. April 2018, p. 1–10, 2019. DOI:

10.1016/j.foodcont.2018.12.011. Disponível em: https://doi.org/10.1016/j.foodcont.2018.12.011.

LOBATO, Kleidson Brito de Sousa; ALAMAR, Priscila Domingues; CARAMÊS, Elem Tamirys dos Santos; PALLONE, Juliana Azevedo Lima. Authenticity of freeze-dried açai pulp by near-infrared spectroscopy. **Journal of Food Engineering**, *[S. l.]*, v. 224, p. 105–111, 2018. DOI: 10.1016/j.jfoodeng.2017.12.019.

MIR-MARQUÉS, Alba; CERVERA, M. Luisa; DE LA GUARDIA, Miguel. Mineral analysis of human diets by spectrometry methods. **TrAC - Trends in Analytical Chemistry**, *[S. l.]*, v. 82, p. 457–467, 2016. DOI: 10.1016/j.trac.2016.07.007. Disponível em: http://dx.doi.org/10.1016/j.trac.2016.07.007.

MOTTESE, Antonio Francesco; FEDE, Maria Rita; CARIDI, Francesco; SABATINO, Giuseppe; MARCIANÒ, Giuseppe; CALABRESE, Giorgio; ALBERGAMO, Ambrogina; DUGO, Giacomo. Chemometrics and innovative multidimensional data analysis (MDA) based on multi-element screening to protect the Italian porcino (Boletus sect. Boletus) from fraud. **Food Control**, *[S. l.]*, v. 110, n. November 2019, p. 107004, 2020. DOI: 10.1016/j.foodcont.2019.107004. Disponível em: https://doi.org/10.1016/j.foodcont.2019.107004.

PASVANKA, Konstantina; TZACHRISTAS, Alexandros; KOSTAKIS, Marios; THOMAIDIS, Nikolaos; PROESTOS, Charalampos. Geographic characterization of Greek wine by inductively coupled plasma–mass spectrometry macroelemental analysis. **Analytical Letters**, *[S. l.]*, v. 52, n. 17, p. 2741–2750, 2019. DOI: 10.1080/00032719.2019.1596118. Disponível em: https://doi.org/10.1080/00032719.2019.1596118.

RICHTER, Bernadette; GURK, Stephanie; WAGNER, Deniz; BOCKMAYR, Michael; FISCHER, Markus. Food authentication: Multi-elemental analysis of white asparagus for provenance discrimination. **Food Chemistry**, *[S. l.]*, v. 286, n. January, p. 475–482, 2019. DOI: 10.1016/j.foodchem.2019.01.105. Disponível em: https://doi.org/10.1016/j.foodchem.2019.01.105.

RODIONOVA, Oxana Ye; TITOVA, Anna V.; POMERANTSEV, Alexey L. Discriminant

analysis is an inappropriate method of authentication. **TrAC - Trends in Analytical Chemistry**, *[S. l.]*, v. 78, p. 17–22, 2016. DOI: 10.1016/j.trac.2016.01.010. Disponível em: http://dx.doi.org/10.1016/j.trac.2016.01.010.

RODRÍGUEZ-SOLANA, Raquel; SALGADO, José Manuel; DOMÍNGUEZ, José Manuel; CORTÉS, Sandra. Assessment of minerals in aged grape marc distillates by FAAS/FAES and ICP-MS. Characterization and safety evaluation. **Food Control**, *[S. l.]*, v. 35, n. 1, p. 49–55, 2014. DOI: 10.1016/j.foodcont.2013.06.031. Disponível em: http://dx.doi.org/10.1016/j.foodcont.2013.06.031.

ROGEZ, Hervé. **Açaí- Preparo, Composição, Melhoramento da consevação**. Belém: Editora da Universidade Federal do Pará, 2000.

RUZIK, Lena; WOJCIESZEK, Justyna. In vitro digestion method for estimation of copper bioaccessibility in Ac ¸ aı. **Monatshefte für Chemie - Chemical Monthly**, *[S. l.]*, v. 147, n. 8, p. 1429–1438, 2016. DOI: 10.1007/s00706-016-1798-3.

SANTOS, Silva; HENRIQUE, Gustavo; TEIXEIRA, De Almeida; JR, Barbosa. Açaí (Euterpe oleracea Mart .): A Tropical Fruit with High Levels of Essential Minerals — Especially Manganese — and its Contribution as a Source of Natural Mineral Supplementation. *[S. l.]*, v. 7394, 2014. DOI: 10.1080/15287394.2014.866923.

SILVA, Joyce Grazielle Siqueira; ORLANDO, Eduardo Adilson; REBELLATO, Ana Paula; PALLONE, Juliana Azevedo Lima. Optimization and Validation of a Simple Method for Mineral Potential Evaluation in Citrus Residue. **Food Analytical Methods**, *[S. l.]*, v. 10, n. 6, p. 1899–1908, 2017. DOI: 10.1007/s12161-016-0748-3.

VALENTIN, Jenna L.; WATLING, R. John. Provenance establishment of coffee using solution ICP-MS and ICP-AES. **Food Chemistry**, *[S. l.]*, v. 141, n. 1, p. 98–104, 2013. DOI: 10.1016/j.foodchem.2013.02.101. Disponível em: http://dx.doi.org/10.1016/j.foodchem.2013.02.101.

ZHANG, Jianyi; NIE, Jiyun; KUANG, Lixue; SHEN, Youming; ZHENG, Haidong; ZHANG, Hui; FAROOQ, Saqib; ASIM, Syed. Geographical origin of Chinese apples based on multiple element analysis. **Journal of the Science of Food and Agriculture**, *[S. l.]*, v. 99, n. 14, p.

6182–6190, 2019. DOI: 10.1002/jsfa.9890.

CAPÍTULO VII

Rapid indirect assessment of major essential elements of Brazilian açai pulp through NIR and machine learning approaches

Caramês, E.T.S.[1], Schilling, L.C.[1], Silva, J.G.S.[1], Teixeira, J.L.P.[1], Pallone, J.A.L[1].

[1] Department of Food Science, School of Food Engineering, State University of Campinas, Monteiro Lobato Street, 80, CEP: 13.083-862, Campinas, São Paulo, Brazil.

ABSTRACT

Brazilian açai pulp has been commercialized all around the world, due mainly to its nutritional profile. In this sense, the quantification of essential elements is relevant for evaluation of the nutritional quality of açai pulp; and the consequent health benefits of its consumption. This research aimed to study the performance of NIR as a green alternative; and as a rapid and indirect method to quantify essential elements (Fe, Ca, K and Mn) using partial least square regression (PLS) and other machine learning algorithms. The resulting regression models presented coefficient of regression (R^2) above 0.7, the values of RPD were higher than 2, ranging from 2 to 2.5, indicating a suitable ability for mineral prediction. In this context, the results indicate that NIR is a promising technique for quantification of these minerals in açai pulp and could be used as a rapid indirect analytical method.

1. INTRODUCTION

Açai is the fruit from the palm tree Euterpe oleracea Mart.; and native to the Amazon region. Açai is a dark purple, spherical fruit that can reach 1-2 cm in diameter and about 1 g each. Commonly, these fruits are macerated with water and followed with sieving to produce pulp; which can be applied in the food (ex: ice cream, açai powder) or pharmaceutical industry (ex: as a contrast agent for magnetic resonance) (BENATREHINA ET AL., 2018; OLIVEIRA & SCHWARTZ, 2018).

During the last decades açai has grown in global attention, due mainly to its nutritional composition; with a high content of monounsaturated fatty acids (MUFA), bioactive compounds such as flavonoids and anthocyanins, fiber, proteins and essential elements or minerals, especially manganese (Mn). These features, together with the trend of adopting healthier lifestyle habits, has boosted açai consumption. It is now exported from Brazil to Europe, Japan and USA; where in 2015, açai was ranked amongst the 30 best-selling diet supplement products (BENATREHINA et al., 2018; PALA et al., 2018).

Minerals, such as essential micronutrients, play an important role in a healthy human body. An example is calcium (Ca) and iron (Fe), which are essential for good development of bones and teeth during skeletal growth, and is also relevant to blood coagulation functions. The deficiency of Ca could lead to osteoporosis and growth arrest, while iron deficiency could lead to anemia; which affected 1.62 billion people between 1993 and 2005 (REBELLATO et al.,

2020; SHAMAH; VILLALPANDO; DE LA CRUZ, 2016). Potassium (K) is essential to maintain normal blood pressure and muscle contractions; deficiency leads to gastrointestinal disorders and depression. Trace elements such as Mn, which is essential for good brain function and bone structure, are also important (NOSRATPOUR; JAFARI, 2018). Regarding all the special functions of minerals, from the analytical point of view, it is essential to monitor the content of these elements in food.

Analytical methods such as Flame Atomic Absorption Spectrometry (FAAS), Inductively Coupled Plasma Atomic Emission and Inductively Coupled Plasma Mass Spectrometry (ICP OES and ICP-MS) are widely used to determine the mineral content of food (LIU et al., 2019; REBELLATO et al., 2020). However, all these traditional techniques demand a complex sample preparation step; involving mineralization, that requires high temperatures and strong acids, followed by dissolution and filtration, all of which are time consuming (COSTA et al., 2019; SILVA et al., 2017).

On the other hand, the food industry has been initiating a paradigm shifting process within the last decades; known as the fourth industrial revolution or industry 4.0. Under this, there is an increased urgency to search for sustainable methods, capable of modernizing and optimizing food production and processing. In this sense, several artificial intelligence technologies coupled to machine learning techniques have been applied; to maximize the performance and minimize the negative impacts to the environment (KAKANI et al., 2020). In this context, Near Infrared (NIR) spectroscopy is a fast, cheap, non-destructive and green alternative for quality control; and has largely been used in multiples scenarios to assure the quality and authenticity of food products (PALLONE; CARAMÊS; ALAMAR, 2018).

However, based on chemical principles, it is believed that NIR has a lack of sensitivity in detecting inorganic components, such as essential elements that not presents vibrations detectable in NIR region. In this sense, this technique relies on the inorganic components associated to organic compounds to make its application in this scenario possible (COSTA et al., 2019) as an indirect determination. Through this association, NIR has been successfully applied for mineral determination and detection in several food matrices, such as pollen, hamburgers and beans (COSTA et al., 2019; PLANS et al., 2012; REBELLATO et al., 2020).

Regarding the growing consumption of açai, the key roles performed by minerals and the versatility of NIR; this study aimed to evaluate the performance of vibrational NIR

spectroscopy coupled to multivariate calibration models in promote indirect quantification of Ca, Fe, Mn and K from açai pulp samples.

2. MATERIAL AND METHODS

2.1.SAMPLES

Ninety-four açai pulps were acquired at Iguarapé-Mirim and Abaetetuba (Pará, Brazil). Thus, the samples were freeze-dried under 2000 μHg with the condenser at -40 ºC (Terroni, Brazil, model LS 3000) and the resulting lyophilized pulp used into all the analysis. This process was used as a strategy to eliminate the water influence in NIR spectra data (overtone and combination vibration of O-H) (DE OLIVEIRA et al., 2014). In order to standardize the particle size, the samples were sieved in 25 mesh.

2.2. Ca, Fe, Mn AND K DETERMINATION BY FAAS (REFERENCE METHOD)

All the samples were mineralized according to Silva et al. (2017) with adaptions. After homogenization, 0.5 g for each açai pulp sample was placed into a glass tube and added by 4 mL of nitric acid (HNO_3, 65%, Sigma Aldrich) and left overnight. After, the samples were added of 2 mL of hydrogen peroxide (H_2O_2 30%, Merck) and the tubes were mineralized for 2h at 140ºC. After the mineralization step, the samples were transferred to a volumetric flask of 25 mL, the volume completed with ultrapure water and filtered using qualitative filter paper (Nalgon). To calcium evaluation, it was added lanthanum oxide solution (10%) to avoid interferences. The dilutions were performed according to the necessity with nitric acid solution (4%).

The analytical curves were determined with external standard into 5 equidistant concentrations, for each evaluated mineral. For Fe, the curve ranged from 0.25 mg/L to 3 mg/L, for Ca from 0.5 mg/L to 5 mg/L, for K from 0.1 mg/L to 1.22 mg/L and for Mn from 0.05 mg/L to 0.6 mg/L. The coefficient of determination of all analytical curves were higher than 0.99 (R^2>0.99), then they were considered linear.

FAAS (model AAnalyst 200, Perkin Elmer) was used to quantify the mineralized samples. A deuterium lamp for background correction radiation and hollow cathode lamps for determination of iron (248.3 nm), calcium (422.67 nm), and manganese (279.50 nm) were used. To determine potassium (K), the equipment operated in emission mode (766.49 nm, slit

1.8/0.6). Each sample was introduced by a nebulizer and mixed with air and acetylene flame (2.5 L h^{-1}/10 L h^{-1}) at about 2000ºC.

2.3. NIR SPECTRA ACQUISITION

About 2 g of each sample was placed into a glass vial (Weathon, USA, Shell vial) a reflectance measurement was taken using a FT-NIR spectrometer (Perkin Elmer-Walthman, USA, model Spectrum 100N) coupled to an accessory for reflectance measurement (Perkin Elmer-Walthman, USA, model NIRA) with an InGaAS detector. The spectra data were measured with 4 cm^{-1} of resolution, 32 scans and ranging from 10,000 cm^{-1} to 4,000 cm^{-1}. The spectra were expressed in log(1/R).

2.4. MACHINE LEARNING ALGORITHM (CHEMOMETRICS)

All the multivariate analysis was carried out using MatLab 2017b coupled to PLS toolbox version 8.6. The spectra data was mean centered and preprocessing methods were tested according to the necessity, aiming the best performance of the final model. Standard Normal Variate (SNV) was applied to correct the light scattering effects normally presented by NIR, 1st and 2nd derivatives by Savitsky-Golay method (order 2, window: 37 pt, tails: polyinterp) were used in order to reduce the multiplicative and additive effects. The variables were selected according to the needing applying the interval Partial Least Square (iPLS) method with 750, 500 and 250 variables for window and automatic number of windows. The outliers were detected by the values of Q residual, T^2 Hoteling and leverage.

The data were divided into calibration (70%) and test (30%) sets using the Kennard-Stone algorithm. Then, it was developed Partial Least Square Regression (PLS-R) to quantify the content of majority essential elements Ca, Mn, Fe and K in freeze dried açaí pulp. A cross validation was also performed using venetian blinds method. The number of Latent Variables (LV) was set according to the lowest value of Root Mean Squared Error of Cross Validation (RMSECV), to avoid lack of fit or overfitting. To evaluate the final performance of each PLS-R model, it was calculated the Standard Error of Calibration and Prediction (SEC and SEP), the value of Residual Prediction Deviation (RPD) and the coefficient of determination from calibration and test sets (R^2_c and R^2_t).

3. RESULTS AND DISCUSSIONS

3.1.MINERALS CONTENTS IN AÇAI PULP.

The average of essential elements content and range for each mineral analyzed (Fe, Ca, K and Mn) is presented in Table 1. Potassium was the most abundant mineral found in freeze-dried açai pulp, followed by calcium, manganese and iron. The total K values range from 1728.7 to 617.6 mg/100gdw, while the calcium variation was 506.0 to 155.8 mg/100gdw. Comparing the K levels with several authors reported in the literature (Table 1), it is observed that Da Silva Santos et al., (2014) and Schauss et al., (2006) did not determine K concentrations in their studies, while the other authors cited contents of this mineral within the range presented by the freeze-dried açai pulp characterized in our study. On the other hand, Pedro et al., (2019) determined higher potassium content in organic (2200 mg/100g) and conventional (2120 mg/100g) goji berry samples comparing to açai levels, even this mineral being the most abundant one at açai samples. Açai presented higher levels of calcium than kuki fruits cultivated in Spain (about 42 mg/100gdw) and cocona, a wild Brazilian fruit, that presented 1.8 mg/100gdw, but lower than typical calcium sources, such as coalho (654.8 mg/100g) (MATERA et al., 2018; MIR-MARQUÉS et al., 2015; SERENO et al., 2018).

Table 1. Content of Fe, Ca, K and Mn (range and average) in comparison with other studies about açai.

Element	Range (mg/100gdw)	Average (mg/100gdw)	Gordon et al., 2012	Da Silva Santos et al., 2014	Schauss et al., 2006	Rogez, 2000	Menezes, Torres, & Srur, 2008
Fe	6.3-1.9	3.4	7.8	17.8	4.4	1.5	4.5
Ca	506.0-155.8	340.1	423	462	260	286	330
K	1728.7-617.6	1196.2	930	ND	ND	932	900
Mn	99.2-22.4	63.8	13.3	45	ND	32.3	10.71

*ND: Not Determined by the authors.

Manganese presented a substantial content, ranging from 99.2 to 22.4 mg/100gdw of açai pulp and average of 63.8 mg/100g dw. This value was superior of the Mn content of other berries, such as, blackberry (2.87 mg/100gdw), raspberry (0.43 mg/100g dw), blueberry (0.22 mg/100gdw) and strawberry (0.41 mg/100g dw) (Pereira et al., 2018).

The average iron content of açai pulp (Table 1) is higher than the average values founded into other amazon fruits, such as bacuri azedo (1.13 mg/100gdw), biribá (1.21

mg/100gdw) and ingá-açu (1.18 mg/100gdw) and comparable to the iron content of pajurá (2.85 mg/100gdw) and sorvinha (3.53 mg/100gdw) (BERTO et al., 2015).

Table 1 also presents the average content of Ca, Mn and Fe by other studies previously performed with acai using traditional methods. Regarding the results of Ca founded by the authors listed at Table 1, all the values are covered in the range analyzed by the present study. On the other hand, Gordon et al. (2012) and Menezes, Torres, & Srur (2008) determined lower levels than the minimum of Mn founded in the samples analyzed. While, Gordon et al., (2012) and Da Silva Santos et al., (2014) presented higher levels of Fe than the maximum values found in our study.

The variation in the content of K, Ca, Mn and Fe is commonly observed when fruits and vegetables have the chemical profiles analyzed, once variables, such as the conditions of cultivar, climatic condition, postharvest conditions and the stage of ripe can directly influence in the composition of the samples (GORDON et al., 2012; ROGEZ et al., 2011; SCHULZ et al., 2016).

Therefore, the evaluation of the performance of alternative method, as NIR spectroscopy, to predict majority essential elements in açai pulp can be indicated the potential use for a rapid response about nutritional quality control of this product.

3.2. NIR SPECTRA DATA OVERVIEW AND PLS-R MODELS TO QUANTIFY Ca, Fe, Mn AND K.

The raw NIR spectra data obtained from the açai samples are represented in Figure 1. The region between 4000 cm^{-1} and 4500 cm^{-1} is characteristic of C-H combination bands from carbohydrates, protein and lipids absorptions. The bands that appears at 4311 cm^{-1} and 4239 cm^{-1} (Figure 1) is probably correlated to the lipids and polysaccharides present in the chemical composition of açai (RÉBUFA; PANY; BOMBARDA, 2018).

The bounds of C=O and C-H of aromatic groups are normally correlated to the range from 4500 cm^{-1} to 4900 cm^{-1}. In this context, the band that appeared at 4672 cm^{-1} is the result of the high content of phenolic compounds in açai samples. The same band was founded in freeze-dried yerba mate (4670 $cm^{-1)}$ also associated to the phenolic compounds (FRIZON et al., 2015).

The bands at 5173 cm^{-1}, 6892 cm^{-1} and 8264 cm^{-1} are normally due to the presence of O-H bounds, first and second overtones, combinations and stretching from the molecules of water (FRIZON et al., 2015; LOBATO et al., 2018).

Between 5400 cm^{-1} and 6050 cm^{-1} is the range of C-H stretching from CH_2 and CH_3 groups (RÉBUFA; PANY; BOMBARDA, 2018). In this context, the bands at 5810 cm^{-1} and 5682 cm^{-1} is probably due to the groups C-H typically founded into proteins and lipids.

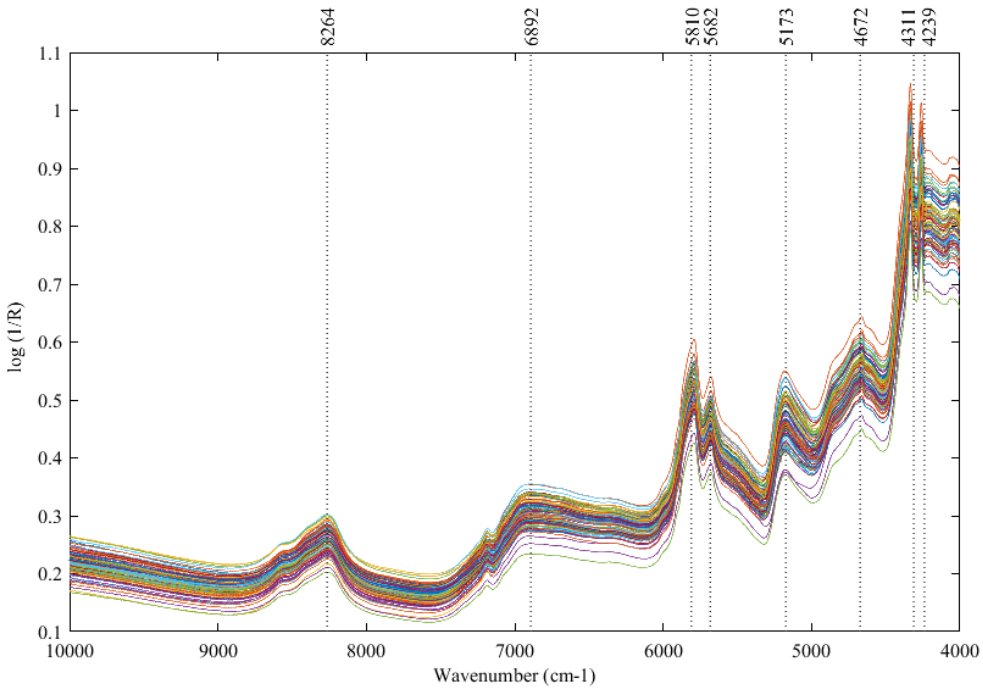

Figure 1. Raw NIR spectra data obtained from freeze dried açai pulp samples.

Looking at the raw data (Figure 1), it is possible to observe the occurrence of the light scattering phenomenon, off-set and slope problems that had negative effects during the modeling process. In order to solve these problems, after mean centering the data, first and second derivative by Savitsky-Golay (order 2, window: 37 pt, tails: polyinterp) and Standard Normal Variate (SNV) were applied in different combinations, to correct the additives and multiplicative errors and to smooth the light scattering. The final results of the Partial Least Square (PLS) models to Fe, Ca, K and Mn are presented in Table 3, the best models were set according the lowest value of SEC and SEP.

All the models with best performance were determined after the combination of three preprocessing methods applied. Regarding Fe and K models, the best results were achieved after

SNV, 2nd derivative and MC. Otherwise, Ca and Mn had the best performance with the combination of SNV, 1st derivative and MC.

The noise presented in raw data leads to a systematic variation, that when mixed with the chemical information have negative effects during the spectra appliance. Light scattering is a high common problem analyzing solid samples with NIR, even after of standardize the particle size (RINNAN, 2014). Thus, 1st or 2nd derivatives and SNV are the natural preprocessing to be used when the untreated NIR data presents these kinds of problems and it shows a high impact at the quality into the performance of PLS models as it could be observed in Table 3.

However, even with the definition of the most appropriated preprocessing, only Ca model achieved a good performance, SEC and SEP values were low, the coefficient of determination (R^2=0.88) was suitable and comparable to the one presented by Plans et al., (2012) (R^2=0.821) analyzing Ca in seed coats of beans.

RPD is an indicative of performance widely used by researchers in food and agricultural fields. This parameter categorizes the quality of regression models into excellent models (RPD > 2), fair models (1.4 < RPD < 2.0) and non-reliable models (RPD < 1.4) (BELLON-MAUREL et al., 2010). Thus, the Ca model reached RPD = 2.5, indicating an excellent power of prediction, as the result determined by Costa et al., (2019) to determine Ca in Brazilian bee pollen by NIR (RPD = 2.1).

The models determined for quantification of iron and potassium presented a really poor performance with low values of coefficient of determination indicating lack of linearity and high values of SEC and SEP. Regarding the best Mn PLS model, the parameters were better compared to the achieved by Fe and K models, but presented a relative low value of R^2 in prediction set, high values of SEP and for these reasons the performance was considered not satisfactory.

Table 21. Summary of the results from PLS regression models to quantify Fe, Ca, K and Mn.

Fe						
Preprocessing	**LV**	**R^2_c**	**R^2_v**	**SEC (mg /kg)**	**SEP (mg /kg)**	**RPD**
1DV+MC	6	0.42	0.01	5.72	6.35	1.3
2DV+MC	5	0.57	0.1	4.92	7.71	0.9
SNV+1DV+MC	7	0.63	0.02	4.52	6.25	1.1
SNV+2DV+MC	**6**	**0.8**	**0.015**	**3.34**	**6.92**	**1.1**
Ca						
Preprocessing	**LV**	**R^2c**	**R^2v**	**SEC (mg /kg)**	**SEP (mg /kg)**	**RPD**
1DV+MC	8	0.82	0.75	339.20	363.46	2.3
2DV+MC	6	0.86	0.54	304.56	501.93	1.7
SNV+1DV+MC	**8**	**0.88**	**0.8**	**276.29**	**343.29**	**2.5**
SNV+ 2DV+MC	6	0.87	0.6	290.29	440.63	1.8
K						
Preprocessing	**LV**	**R^2c**	**R^2v**	**SEC (mg /kg)**	**SEP (mg /kg)**	**RPD**
1DV+MC	7	0.57	0.59	873.86	790.22	1.7
2DV+MC	6	0.86	0.4	504.57	1364.34	1.2
SNV+1DV+MC	6	0.57	0.62	879.42	757.53	1.7
SNV+2DV+MC	**5**	**0.73**	**0.58**	**695.28**	**695.28**	**1.5**
Mn						
Preprocessing	**LV**	**R^2c**	**R^2v**	**SEC (mg /kg)**	**SEP (mg /kg)**	**RPD**
1DV+MC	6	0.73	0.65	85.64	81.12	2.0
2DV+MC	6	0.81	0.46	72.37	107.30	1.5
SNV+1DV+MC	**8**	**0.82**	**0.60**	**70.54**	**101.38**	**2.2**
SNV+2DV+MC	6	0.84	0.46	65.41	338.20	2.1

LV: Latent Variable; R^2_c: coefficient of determination from calibration set; R^2_v: coefficient of determination from test set; SEC: standard error of calibration; SEP: Standard Error of Prediction; RPD: Residual Prediction Deviation, 1DV: First derivative; 2DV: second derivative; MC: mean center; SNV: Standard Normal Variate.

To promote an improvement of the PLS models, the best preprocessing method, observed in Table 3, was maintained and the variable selection was performed by iPLS algorithm, it was tested three sizes of window: 500, 250 and 150 variables with automatic number of intervals. The final results are expressed in Table 4.

Table 32. Summary of the results of PLS regression models with variables selected by iPLS to quantify Fe, K and Mn

Fe								
Preprocessing	**Variable selection**	**Range (cm^{-1})**	**LV**	**R^2c**	**R^2v**	**SEC (mg/kg)**	**SEP (mg/kg)**	**RPD**
SNV+2DV +MC	**iPLS (150)**	**[9550-9401; 6700-6551; 6100-5951]**	**7**	**0.76**	**0.74**	**3.69**	**3.90**	**2.5**
	iPLS (250)	[8250-8001; 6250-6001]	7	0.78	0.11	3.47	3.41	1.1
	iPLS (500)	[10000-9501; 5500-4001]	4	0.31	0.025	6.23	7.28	1.1
K								
Preprocessing	**Variable selection**	**Range (cm^{-1})**	**LV**	**R^2c**	**R^2v**	**SEC (mg/kg)**	**SEP (mg/kg)**	**RPD**
SNV+2DV +MC	iPLS (150)	[7500-7301]	3	0.51	0.28	933.69	1146.46	1.2
	iPLS (250)	**[8000-7750; 7500-7251]**	**6**	**0.78**	**0.7**	**627.99**	**685.58**	**2.0**
	iPLS (500)	[8500-8001; 7000-6501; 5500-5001]	4	0.57	0.32	878.68	1089.28	1.3
Mn								
Preprocessing	**Variable selection**	**Range (cm^{-1})**	**LV**	**R^2c**	**R^2v**	**SEC (mg/kg)**	**SEP (mg/kg)**	**RPD**
SNV+1DV +MC	iPLS(150)	[8780-8501; 7000-6551; 6250-5951; 4300-4151]	8	0.86	0.72	60.82	101.31	1.9
	iPLS(250)	**[8750-8501; 7000-5751; 4750-4001]**	**8**	**0.81**	**0.74**	**70.72**	**70.97**	**2.3**
	iPLS(500)	[8750-8501; 7000-5751; 4750-4001]	9	0.87	0.69	58.76	75.00	2.1

LV: Latent Variable; R^2_c: coefficient of determination from calibration set; R^2_v: coefficient of determination from test set; SEC: standard error of calibration; SEP: Standard Error of Prediction; RPD: Residual Prediction Deviation, 1DV: First derivative; 2DV: second derivative; MC: mean center; SNV: Standard Normal Variate, iPLS: interval Partial Least Square.

Spectroscopic data is generally large and it could contain a lot of redundant information and/or noises that can result into a reduced predictive power. In this context, the iPLS algorithm is a really helpful tool that allows, trough the definition of a local PLS model

in each subinterval, a wisely choose of the best spectral subsection based on the lowest Root Mean Square Error of Cross-Validation (RMSECV) (NØRGAARD et al., 2000). In this context, the iPLS algorithm allowed an improvement of performance for all models in comparison to the same models when determined based on the full spectra range.

The subintervals selected by iPLS helped to highlight the relevant chemical information to quantify Fe, K and Mn, since the NIR technique has a lack of sensibility to directly detect mineral components. For example, the subintervals selected to iron PLS model are related to carbohydrates information and this mineral in açai is bounded to fibers, phytate and bioactive compounds (OLIVEIRA et al., 2019; RÉBUFA; PANY; BOMBARDA, 2018; SCHULZ et al., 2017). While, the Mn was calibrated based on subintervals that contains information of proteins, reinforcing the hypothesis made by Oliveira et al. (2019) that manganese in açai pulp can be bounded to it, since this fruit presents a reasonable protein content. It is known that K has a key role during the translocation of sugars in fruits during the ripening process, therefore, analyzing the NIR spectra data, the K models were determined based on subintervals that are usually correlated to the carbohydrate content, proving that the bounds between these minerals and the organic elements of açai is good solution to allow the use of NIR indirect mineral quantification (LEQUEUE; DRAYE; BAETEN, 2016; SCHULZ et al., 2016).

Looking to the performance parameters, Fe calibration model with the best results was achieved after the variable selection by iPLS with window of 150 variables, the values of R^2 considerable increased comparing to the models based on full range and reached 0.74 to test set, value comparable to the $R^2 = 0.73$ determined by Rebellato et al. (2020) quantifying iron in hamburger meat. To determine K content in tea leaf by NIR hyperspectral imaging, Wang et al. (2020) founded values of RMSEC = 0.42 mg/gdw and RMSEP = 0.49 mg/g dw comparable to the values presented (RMSEC = 0.62 mg/gdw and RMSEP = 0.68 mg/gdw). The values of RPD also increased in Fe (2.5), K (2.0) and Mn (2.3) models presenting now values higher than 2, in other words, presenting an excellent ability of indirect prediction.

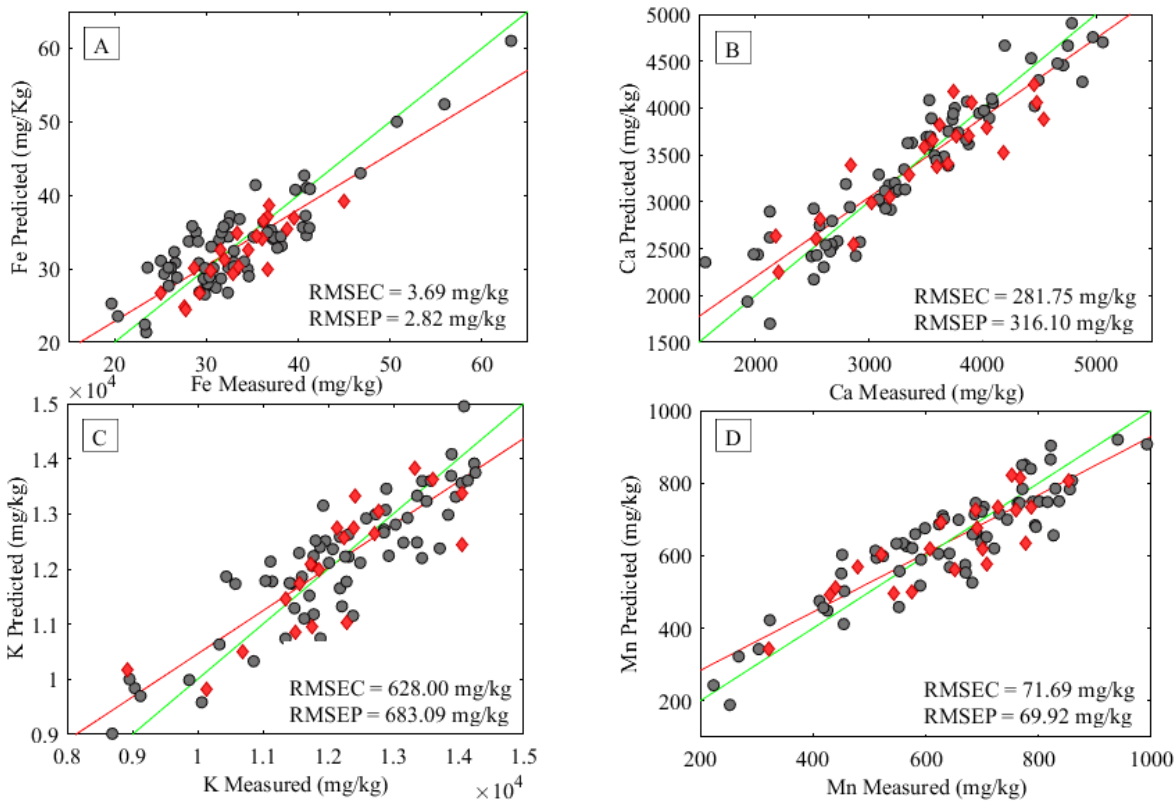

Figure 2. The best PLS regression model to quantify Fe (A), Ca (B), K (C) and Mn (D).

The final PLS regression models obtained to quantify Fe, Ca, K and Mn are presented at Figure 2. It is important to highlight that the process to set the most adequate preprocessing is vital to extract the chemical information contained into NIR spectra data. Also, that the according to the necessity of improvement, to perform a variable selection is relevant to exclude information that are not contributing with the right chemical information or noise that could possibly hide the relevant information in the middle of a such huge data as the spectroscopic.

Looking at the final results, it is possible to affirm that NIR could be considerable a satisfactory alternative to the traditional methods applied during the indirect determination of Fe, Ca, K and Mn content in açai pulp, since it generates no residual and is classified as a multi parameters and fast analysis.

4. CONCLUSIONS

This study investigated the possibility to use NIR spectroscopy to quantify Fe, Ca, K and Mn in açai pulp, since the fruit has a relevant content of these inorganic compounds. In this context, it was tested several preprocessing methods, such as SNV, 1DV and 2DV, in order to optimize the spectra data and the resulting PLS regression models. According to the necessity, the iPLS algorithm was also applied in order to highlight the most important subsections of the spectra to assure the best fitting of the PLS model. In this sense, the prediction of Fe, K and Mn contents had the models determined based on selected variables that highlighted the importance of the bounding between minerals and organic compounds to achieve satisfactory results. The final four PLS models obtained using spectra data of the samples and iPLS to quantify Fe, Ca, K and Mn presented suitable parameters of performance, proving that through the bounds between essential elements evaluated and organic compounds in the pulp açai samples, NIR could be successfully applied to a quick and non-destructive assessment of these minerals content. The relation between evaluated essential elements (no bands in NIR) and organic compounds in the açai pulp samples indicated NIR could be successfully applied as a rapid and indirect assessment of major mineral contents

Acknowledgments

The authors would like to thank the São Paulo Research Foundation (FAPESP) funding of the research project (project nº 2018/09759-3) and the PhD scholarship of José Teixeira (nº 2018/08864-8). The Coordination for the Improvement of Higher Education Personnel (CAPES) (Financial Code 001). And the National Council for Scientific and Technological Development (CNPq) for the PhD scholarship of Elem Caramês (scholarship nº 142414/ 2016-6) and Joyce Silva (scholarship nº 142415/2016-2).

5. REFERENCES

BELLON-MAUREL, Véronique; FERNANDEZ-AHUMADA, Elvira; PALAGOS, Bernard; ROGER, Jean Michel; MCBRATNEY, Alex. Critical review of chemometric indicators commonly used for assessing the quality of the prediction of soil attributes by NIR spectroscopy. **TrAC - Trends in Analytical Chemistry**, *[S. l.]*, v. 29, n. 9, p. 1073–1081, 2010. DOI: 10.1016/j.trac.2010.05.006. Disponível em:

http://dx.doi.org/10.1016/j.trac.2010.05.006.

BENATREHINA, P. Annécie; PAN, Li; NAMAN, C. Benjamin; LI, Jie; KINGHORN, A. Douglas. Usage, biological activity, and safety of selected botanical dietary supplements consumed in the United States. **Journal of Traditional and Complementary Medicine**, *[S. l.]*, v. 8, n. 2, p. 267–277, 2018. DOI: 10.1016/j.jtcme.2018.01.006.

BERTO, Alessandra; DA SILVA, Alex Fiori; VISENTAINER, Jesuí Vergilio; MATSUSHITA, Makoto; DE SOUZA, Nilson Evelázio. Proximate compositions, mineral contents and fatty acid compositions of native Amazonian fruits. **Food Research International**, *[S. l.]*, v. 77, p. 441–449, 2015. DOI: 10.1016/j.foodres.2015.08.018. Disponível em: http://dx.doi.org/10.1016/j.foodres.2015.08.018.

COSTA, Maria Cristina A.; MORGANO, Marcelo A.; FERREIRA, Marcia Miguel C.; MILANI, Raquel F. Quantification of mineral composition of Brazilian bee pollen by near infrared spectroscopy and PLS regression. **Food Chemistry**, *[S. l.]*, v. 273, n. July 2017, p. 85–90, 2019. DOI: 10.1016/j.foodchem.2018.02.017. Disponível em: https://doi.org/10.1016/j.foodchem.2018.02.017.

DA SILVA SANTOS, Vivian; DE ALMEIDA TEIXEIRA, Gustavo Henrique; BARBOSA, Fernando. Açaí (euterpe oleracea mart.): A tropical fruit with high levels of essential minerals - Especially manganese - And its contribution as a source of natural mineral supplementation. **Journal of Toxicology and Environmental Health - Part A: Current Issues**, *[S. l.]*, v. 77, n. 1–3, p. 80–89, 2014. DOI: 10.1080/15287394.2014.866923.

DE OLIVEIRA, Gabrieli Alves; DE CASTILHOS, Fernanda; RENARD, Catherine Marie-Geneviève Claire; BUREAU, Sylvie. Comparison of NIR and MIR spectroscopic methods for determination of individual sugars, organic acids and carotenoids in passion fruit. **Food Research International**, Authenticity, Typicality, Traceability and Intrinsic Quality of Food Products. *[S. l.]*, v. 60, Authenticity, Typicality, Traceability and Intrinsic Quality of Food Products, p. 154–162, 2014. DOI: 10.1016/j.foodres.2013.10.051. Disponível em: http://www.sciencedirect.com/science/article/pii/S0963996913005991. Acesso em: 4 jun. 2016.

DE OLIVEIRA, Maria do S. P.; SCHWARTZ, Gustavo. Açaí— Euterpe oleracea. *In*: **Exotic**

Fruits. [s.l.] : Elsevier, 2018. p. 1–5. DOI: 10.1016/B978-0-12-803138-4.00002-2. Disponível em: http://linkinghub.elsevier.com/retrieve/pii/B9780128031384000022. Acesso em: 17 abr. 2018.

FRIZON, Cátia N. T.; OLIVEIRA, Gabrieli A.; PERUSSELLO, Camila A.; PERALTA-ZAMORA, Patrício G.; CAMLOFSKI, Ana M. O.; ROSSA, Überson B.; HOFFMANN-RIBANI, Rosemary. Determination of total phenolic compounds in yerba mate (Ilex paraguariensis) combining near infrared spectroscopy (NIR) and multivariate analysis. **LWT - Food Science and Technology**, *[S. l.]*, v. 60, n. 2, Part 1, p. 795–801, 2015. DOI: 10.1016/j.lwt.2014.10.030. Disponível em: http://www.sciencedirect.com/science/article/pii/S0023643814006653. Acesso em: 27 jan. 2016.

GORDON, André et al. Chemical characterization and evaluation of antioxidant properties of Açaí fruits (Euterpe oleraceae Mart.) during ripening. **Food Chemistry**, *[S. l.]*, v. 133, n. 2, p. 256–263, 2012. DOI: 10.1016/j.foodchem.2011.11.150.

KAKANI, Vijay; NGUYEN, Van Huan; KUMAR, Basivi Praveen; KIM, Hakil; PASUPULETI, Visweswara Rao. A critical review on computer vision and artificial intelligence in food industry. **Journal of Agriculture and Food Research**, *[S. l.]*, v. 2, n. November 2019, p. 100033, 2020. DOI: https://doi.org/10.1016/j.jafr.2020.100033. Disponível em: http://www.sciencedirect.com/science/article/pii/S2666154320300144.

LEQUEUE, Gauthier; DRAYE, Xavier; BAETEN, Vincent. Determination by near infrared microscopy of the nitrogen and carbon content of tomato (Solanum lycopersicum L.) leaf powder. **Scientific Reports**, *[S. l.]*, v. 6, n. May, p. 1–9, 2016. DOI: 10.1038/srep33183.

LIU, Zhi; ZHANG, Weixing; ZHANG, Yongzhi; CHEN, Tianjin; SHAO, Shengzhi; ZHOU, Li; YUAN, Yuwei; XIE, Tongzhou; ROGERS, Karyne M. Assuring food safety and traceability of polished rice from different production regions in China and Southeast Asia using chemometric models. **Food Control**, *[S. l.]*, v. 99, n. April 2018, p. 1–10, 2019. DOI: 10.1016/j.foodcont.2018.12.011. Disponível em: https://doi.org/10.1016/j.foodcont.2018.12.011.

LOBATO, Kleidson Brito de Sousa; ALAMAR, Priscila Domingues; CARAMÊS, Elem Tamirys dos Santos; PALLONE, Juliana Azevedo Lima. Authenticity of freeze-dried açai pulp by near-infrared spectroscopy. **Journal of Food Engineering**, *[S. l.]*, v. 224, p. 105–111, 2018. DOI: 10.1016/J.JFOODENG.2017.12.019. Disponível em: https://www.sciencedirect.com/science/article/pii/S0260877417305460. Acesso em: 21 mar. 2018.

MATERA, Juliana et al. Brazilian cheeses: A survey covering physicochemical characteristics, mineral content, fatty acid profile and volatile compounds. **Food Research International**, *[S. l.]*, v. 108, n. March, p. 18–26, 2018. DOI: 10.1016/j.foodres.2018.03.014. Disponível em: https://doi.org/10.1016/j.foodres.2018.03.014.

MENEZES, Ellen Mayra Da Silva; TORRES, Amanda Thiele; SRUR, Armando Ubirajara Sabaa. Valor nutricional da polpa de açaí (Euterpe oleracea Mart) liofilizada. **Acta Amazonica**, *[S. l.]*, v. 38, n. 2, p. 311–316, 2008. DOI: 10.1590/S0044-59672008000200014.

MIR-MARQUÉS, Alba; DOMINGO, Ana; CERVERA, M. Luisa; DE LA GUARDIA, Miguel. Mineral profile of kaki fruits (Diospyros kaki L.). **Food Chemistry**, *[S. l.]*, v. 172, p. 291–297, 2015. DOI: 10.1016/j.foodchem.2014.09.076. Disponível em: http://dx.doi.org/10.1016/j.foodchem.2014.09.076.

NØRGAARD, L.; SAUDLAND, A.; WAGNER, J.; NIELSEN, J. P.; MUNCK, L.; ENGELSEN, S. B. Interval partial least-squares regression (iPLS): A comparative chemometric study with an example from near-infrared spectroscopy. **Applied Spectroscopy**, *[S. l.]*, v. 54, n. 3, p. 413–419, 2000. DOI: 10.1366/0003702001949500.

NOSRATPOUR, Mitra; JAFARI, Seid Mahdi. **Bioavailability of minerals (Ca, Mg, Zn, K, Mn, Se) in food products**. [s.l.] : Elsevier, 2018. v. 1 DOI: 10.1016/B978-0-08-100596-5.21618-1. Disponível em: http://dx.doi.org/10.1016/B978-0-08-100596-5.21618-1.

OLIVEIRA, Silvana Ruella; CHACÓN-MADRID, Katherine; ARRUDA, Marco Aurélio Zezzi; BARBOSA JÚNIOR, Fernando. In vitro gastrointestinal digestion to evaluate the total, bioaccessible and bioavailable concentrations of iron and manganese in açaí (Euterpe oleracea Mart.) pulps. **Journal of Trace Elements in Medicine and Biology**, *[S. l.]*, v. 53, n. January, p.

27–33, 2019. DOI: 10.1016/j.jtemb.2019.01.016. Disponível em: https://doi.org/10.1016/j.jtemb.2019.01.016.

PALA, Daniela; BARBOSA, Priscila Oliveira; SILVA, Carla Teixeira; DE SOUZA, Melina Oliveira; FREITAS, Fatima Rodrigues; VOLP, Ana Carolina Pinheiro; MARANHÃO, Raul Cavalcante; FREITAS, Renata Nascimento De. Açai (Euterpe oleracea Mart.) dietary intake affects plasma lipids, apolipoproteins, cholesteryl ester transfer to high-density lipoprotein and redox metabolism: A prospective study in women. **Clinical Nutrition**, *[S. l.]*, v. 37, n. 2, p. 618–623, 2018. DOI: 10.1016/J.CLNU.2017.02.001. Disponível em: https://www.sciencedirect.com/science/article/pii/S0261561417300511. Acesso em: 17 abr. 2018.

PALLONE, Juliana Azevedo Lima; CARAMÊS, Elem Tamirys dos Santos; ALAMAR, Priscila Domingues. Green analytical chemistry applied in food analysis: alternative techniques. **Current Opinion in Food Science**, *[S. l.]*, v. 22, n. Figure 1, p. 115–121, 2018. DOI: 10.1016/j.cofs.2018.01.009.

PEDRO, Alessandra Cristina; SÁNCHEZ-MATA, María Cortes; PÉREZ-RODRÍGUEZ, María Luisa; CÁMARA, Montaña; LÓPEZ-COLÓN, José Luis; BACH, Fabiane; BELLETTINI, Marcelo; HAMINIUK, Charles Windson Isidoro. Qualitative and nutritional comparison of goji berry fruits produced in organic and conventional systems. **Scientia Horticulturae**, *[S. l.]*, v. 257, n. May, p. 108660, 2019. DOI: 10.1016/j.scienta.2019.108660. Disponível em: https://doi.org/10.1016/j.scienta.2019.108660.

PEREIRA, Camila Corrêa; DO NASCIMENTO DA SILVA, Emanueli; DE SOUZA, Alexander Ossanes; VIEIRA, Mariana Antunes; RIBEIRO, Anderson Schwingel; CADORE, Solange. Evaluation of the bioaccessibility of minerals from blackberries, raspberries, blueberries and strawberries. **Journal of Food Composition and Analysis**, *[S. l.]*, v. 68, p. 73–78, 2018. DOI: 10.1016/j.jfca.2016.12.001. Disponível em: http://dx.doi.org/10.1016/j.jfca.2016.12.001.

PLANS, Marçal; SIMÓ, Joan; CASAÑAS, Francesc; SABATÉ, José. Near-infrared spectroscopy analysis of seed coats of common beans (Phaseolus vulgaris L.): A potential tool for breeding and quality evaluation. **Journal of Agricultural and Food Chemistry**, *[S. l.]*, v. 60, n. 3, p. 706–712, 2012. DOI: 10.1021/jf204110k.

REBELLATO, Ana Paula; CARAMÊS, Elem Tamirys dos Santos; MORAES, Priscila Probio De; PALLONE, Juliana Azevedo Lima. Minerals assessment and sodium control in hamburger by fast and green method and chemometric tools. **Lwt**, *[S. l.]*, v. 128, n. October 2019, p. 109438, 2020. DOI: 10.1016/j.lwt.2020.109438. Disponível em: https://doi.org/10.1016/j.lwt.2020.109438.

RÉBUFA, Catherine; PANY, Inès; BOMBARDA, Isabelle. NIR spectroscopy for the quality control of Moringa oleifera (Lam.) leaf powders: Prediction of minerals, protein and moisture contents. **Food Chemistry**, *[S. l.]*, v. 261, n. March, p. 311–321, 2018. DOI: 10.1016/j.foodchem.2018.04.066. Disponível em: https://doi.org/10.1016/j.foodchem.2018.04.066.

RINNAN, Åsmund. Pre-processing in vibrational spectroscopy-when, why and how. **Analytical Methods**, *[S. l.]*, v. 6, n. 18, p. 7124–7129, 2014. DOI: 10.1039/c3ay42270d.

ROGEZ, H.; POMPEU, D. R.; AKWIE, S. N. T.; LARONDELLE, Y. Sigmoidal kinetics of anthocyanin accumulation during fruit ripening: A comparison between açai fruits (Euterpe oleracea) and other anthocyanin-rich fruits. **Journal of Food Composition and Analysis**, *[S. l.]*, v. 24, n. 6, p. 796–800, 2011. DOI: 10.1016/j.jfca.2011.03.015. Disponível em: http://dx.doi.org/10.1016/j.jfca.2011.03.015.

ROGEZ, Hervé. **Açaí: preparo, composição e melhoramento da conservação**. Belém: Editora da Universidade Federal do Pará, 2000.

SCHAUSS, Alexander G.; WU, Xianli; PRIOR, Ronald L.; OU, Boxin; PATEL, Dinesh; HUANG, Dejian; KABABICK, James P. Phytochemical and nutrient composition of the freeze-dried amazonian palm berry, Euterpe oleraceae Mart. (Acai). **Journal of Agricultural and Food Chemistry**, *[S. l.]*, v. 54, n. 22, p. 8598–8603, 2006. DOI: 10.1021/jf060976g.

SCHULZ, Mayara et al. Bioaccessibility of bioactive compounds and antioxidant potential of juçara fruits (Euterpe edulis Martius) subjected to in vitro gastrointestinal digestion. **Food Chemistry**, *[S. l.]*, v. 228, p. 447–454, 2017. DOI: 10.1016/j.foodchem.2017.02.038. Disponível em: http://dx.doi.org/10.1016/j.foodchem.2017.02.038.

SCHULZ, Mayara; DA SILVA CAMPELO BORGES, Graciele; GONZAGA, Luciano

Valdemiro; OLIVEIRA COSTA, Ana Carolina; FETT, Roseane. Juçara fruit (Euterpe edulis Mart.): Sustainable exploitation of a source of bioactive compounds. **Food Research International**, *[S. l.]*, v. 89, p. 14–26, 2016. DOI: 10.1016/j.foodres.2016.07.027. Disponível em: http://dx.doi.org/10.1016/j.foodres.2016.07.027.

SERENO, Aiane Benevide; BAMPI, Marlene; DOS SANTOS, Isabela Eloise; FERREIRA, Sila Mary Rodrigues; BERTIN, Renata Labronici; KRÜGER, Claudia Carneiro Hecke. Mineral profile, carotenoids and composition of cocona (Solanum sessiliflorum Dunal), a wild Brazilian fruit. **Journal of Food Composition and Analysis**, *[S. l.]*, v. 72, n. June, p. 32–38, 2018. DOI: 10.1016/j.jfca.2018.06.001. Disponível em: https://doi.org/10.1016/j.jfca.2018.06.001.

SHAMAH, Teresa; VILLALPANDO, Salvador; DE LA CRUZ, Vanessa. Anemia. **International Encyclopedia of Public Health**, *[S. l.]*, v. 1, p. 103–112, 2016. DOI: 10.1016/B978-0-12-803678-5.00018-7.

SILVA, Joyce Grazielle Siqueira; ORLANDO, Eduardo Adilson; REBELLATO, Ana Paula; PALLONE, Juliana Azevedo Lima. Optimization and Validation of a Simple Method for Mineral Potential Evaluation in Citrus Residue. **Food Analytical Methods**, *[S. l.]*, v. 10, n. 6, p. 1899–1908, 2017. DOI: 10.1007/s12161-016-0748-3.

WANG, Yu Jie; JIN, Ge; LI, Lu Qing; LIU, Ying; KIANPOOR KALKHAJEH, Yusef; NING, Jing Ming; ZHANG, Zheng Zhu. NIR hyperspectral imaging coupled with chemometrics for nondestructive assessment of phosphorus and potassium contents in tea leaves. **Infrared Physics and Technology**, *[S. l.]*, v. 108, n. May, p. 103365, 2020. DOI: 10.1016/j.infrared.2020.103365. Disponível em: https://doi.org/10.1016/j.infrared.2020.103365.

CAPÍTULO VIII

Discriminant analysis of intact organic and conventional brown rice by hyperspectral imaging, benchtop and hand-held NIRS coupled to machine learning.

Elem Tamirys dos Santos Caramês[1], Michel Rocha Baqueta[1], Juan Antonio Fernández Pierna[2], Juliana Azevedo Lima Pallone,[1]Vincent Baeten[2]

[1] Department of Food Science, School of Food Engineering, University of Campinas, Monteiro Lobato Street, 80, Zip Code: 13083-862, Campinas, São Paulo, Brazil.

[2] Quality and authentication of products Unit, Knowledge and valorization of agricultural products Department, Walloon Agricultural Research Centre (CRA-W), Gembloux, Belgium

ABSTRACT

The rice crop is one of the most important in the world and it is considered as a staple food in Asia, Africa and some countries of Latin America. As a result of the increasing search for a healthier lifestyle, the market for organic brown rice has been growing and with it has emerged the concern for development of green analytical methodologies able to discriminate between organic and conventional rice grains. This study therefore applied spectral data from near infrared spectroscopy (NIRS) using three different devices: hand-held, hyperspectral imaging and benchtop in the development of partial least square discriminant analysis (PLS-DA) models to distinguish intact grains of organic and conventional brown rice. The final performance of the three instruments were considered satisfactory presenting 100% and 87.5% sensitivity and specificity, respectively, for the hand-held NIR and NIR-HSI and 100% for the benchtop for both parameters. Based on the results obtained it is possible to affirm that NIRS is a potential technique that could be applied to classify conventional and organic brown rice with the advantages of being quick and non-destructive, with the benchtop presenting the best performance.

1. INTRODUCTION

The world's rapid population growth requires bigger crop production yields. This urgency with bad agricultural practices therefore generally leads farmers to use larger quantities of pesticides, fungicides, herbicides and fertilizers (LYU et al., 2020). Sometimes, due to these bad practices, there are chemical residues in rice affecting its quality and putting the environment and the human health at risk, since these chemicals are intrinsically toxic (PAREJA et al., 2011).

In this context, organic products have become part of a new pattern of global food consumption, where people are more concerned about the negative effects that ingestion of regular chemical residues could cause the human organism. In addition, consumers believe that buying organic food is environmentally friendly and helps local producers (TANDON et al., 2020). This has heated up the organic food industry, which had profits of more than 90 billion euros in 2017 (KATT; MEIXNER, 2020).

Rice (*Oryza sativa* L.) is one of the most popular grains in the world. It is considered a staple food in parts of Africa and Asia and is highly consumed in America and Europe. China is the biggest producer of this cereal (about 207 million tons) and responsible for 28% of the total production of this crop (SEN; CHAKRABORTY; KALITA, 2020). Regarding Latin America, Brazil is the most relevant producer of rice with 12.2 million tons, representing 42% of crop production in this region (EMBRAPA, 2016).

The consumption of organic brown rice is increasing because of the search for natural products with a good nutritional profile. This cereal is a good alternative to ingesting fibres, minerals, vitamins and phenolic compounds, as phytosterol and phenolic acids, since most of these bioactive compounds are in the rice bran, a part that is lost during the polishing process from which white rice is obtained (PEANPARKDEE; IWAMOTO, 2019).

Thus, with the organic food industry becoming a solidly profitable market, the development of green analytical methods capable of discriminating conventional from organic products has been a new challenge for product guarantees, since the main traditional analytical methods applied to control pesticide residues – liquid and gas chromatography with tandem mass spectrometry (LC- MS and GC-MS) – involve clean-up and/or extraction steps, applying toxic reagents, and besides are time consuming and expensive (PAREJA et al., 2011).

Emerging as an alternative, near infrared spectroscopy (NIRS) is a green method that has been successfully applied in the food industry to quantify macro and micro parameters, classify samples according geographical origin, detect adulteration and detect spoilage processes (PALLONE; CARAMÊS; ALAMAR, 2018). Since this technique has been widely used in recent years, new instruments have been developed, such as in-line, sensors and hand-held devices, presenting advantages such as lower cost and higher mobility compared to benchtop devices (WALSH et al., 2020). Another successful way of applying NIR is coupled it to image systems, as in NIR- hyperspectral imaging systems (NIR-HSI), that allow recording chemical data with images, showing more details about the spatial information of the samples (LIU; PU; SUN, 2017).

Considering that explained above, this study aims to evaluate the potential of benchtop, hand-held and HSI NIRS and machine learning tools in discriminating intact grains of brown rice.

2. MATERIAL AND METHODS

2.1.SAMPLES

For this study, 80 samples of brown rice (40 organic and 40 conventional samples) were acquired of 8 distinct brands and batches, at local markets from Campinas (São Paulo, Brazil) and Gembloux (Walloon, Belgium) in October and November of 2019. The samples (10 g) were collected and stored in plastic containers at room temperature until the moment of analysis.

2.2.INSTRUMENTATION

Three devices were used to record the spectral information of brown rice, the handheld MicroNIR 1700 (Viavi Solution-Milpitas, CA, USA), operating in the 908 nm - 1676 nm range, with resolution of 6.2 nm, the benchtop XDS Rapid Content Analyzer (FOSS, Hilleroed, Denmark), in the 800 nm - 2498 nm range, with resolution of 2 nm, and the push-broom NIR-HSI system (SWIR Hyperspectral ImSpector N25E Burgermetrics, Riga, Latvia), with a spectral range of 1100 nm – 2400 nm and spectral resolution of 6.3 nm.

During the spectral acquisition, the handheld and benchtop devices operated in room conditions (25ºC and 50% relative humidity). All intact samples were placed in a small quartz sample cup (FOSS, Hilleroed, Denmark, part number 60053059). The spectra were taken in duplicate and the average spectra used during model development and analysis.

For hyperspectral image acquisition of brown rice, the system was calibrated with a dark reference, by closing the lens entrance, and white reference, using a white Teflon plate. Each sample (10g), separately and randomly, were placed on the white Teflon plate, up the conveyor belt, that ran with a speed of 1.1 m/s while the image was recorded. The final image was the average of 32 scans.

2.3. DATA ACQUISITION AND TREATMENT

Regarding the NIR-HIS, spectral data were selected from the raw image by hand using a tool of the Hyper See program (Burgermetrics, Riga, Latvia) to assure that the spectral information was from the grain and not from shadows or background, resulting in a library with 5 spectra for each sample (5 spectra x 80 samples = 400 spectra). MatLab R2017b version

(Mathworks, Natick, MA) with the multivariate image analysis (MIA) toolbox (Eigenvector Research, Manson, WA, USA) was used to perform a principal component analysis (PCA) of the images to build a spectra collection from background and shadows (7909 spectra). In this way, it was used to build a partial least square discriminant analysis (PLS-DA) used as a mask to discriminate the rice grains from the background and shadows. After the segmentation, the mean spectrum of each image was obtained and used in a further modelling process.

The spectral data, for all devices, were mean centred and preprocessed according to the need. A first derivative by the Savitsky-Golay method (filter width: 7pts, polynomial order: 2) was applied to correct baseline offset and the standard normal variate (SNV) was used to minimize the negative impact cause by the light scattering phenomenon, avoiding external interferences (RINNAN, 2014).

Using MatLab R2017b version (Mathworks, Natick, MA) coupled to the PLS toolbox (Eigenvector Research, Manson, WA, USA) the final library of spectral data, for the three devices, was divided into 66% of the samples for the calibration set and 33% for the test set (prediction), applying the Kennard-Stone algorithm, ensuring that the samples used during the modelling process were not the same as those used in the external validation process.

The PCA was performed to observe the grouping of samples according to the spectral information. The parameters of Q residual and T^2 hoteling were also observed to detect and exclude outliers in order to improve the model's robustness.

The discriminant models were performed by the PLS-DA algorithm. PLS-DA is a discriminant method with a regression approach where the discrimination rule is based on the comparison between the predicted values and the value established as the threshold (ZONTOV et al., 2020). It has been widely applied in food industry because it is a quick method to build and the results were very successful (JIMÉNEZ-CARVELO et al., 2019). During the PLS-DA modelling process cross-validation was also performed using the leave-one-out method, the number of latent variable (LV) being set according to the evaluation of sensitivity and specificity parameters (Eq. 1 and Eq. 2) of cross-validation. These parameters were also used to evaluate the model's performance (CRUZ-TIRADO et al., 2020), beyond the external validation (test set).

$$Sensibility\ (\%) = \frac{TP}{TP+FN} * 100 \quad (1).$$

$$Specificity\ (\%) = \frac{TN}{TN+FP} * 100 \quad (2).$$

Where TP is true positive, FN is false negative, TN is true negative and FP is false positive.

To construct the chemical map using NIR-HIS, the samples that were pre-selected by Kennard-Stone to compose the test set were placed together on the Teflon plate and new images were acquired. The PLS-DA determined by NIR-HIS with the best results was tested in two prediction modes directly from the image: (a) pixel by pixel and (b) majority of pixel per rice grain.

3. RESULTS AND DISCUSSION

3.1.SPECTRA OVERVIEW AND PRINCIPAL COMPONENT ANALYSIS (PCA)

The raw spectra of all samples and the mean spectra of each class (organic and conventional brown rice) obtained by the three devices are represented in Figure 1. All of them presented spectral data with baseline offset and light scattering phenomenon. That was expected since it was obtained from intact rice grains, that is, big and irregular solid particles, that are the main cause for the its occurrence (RINNAN; BERG; ENGELSEN, 2009).

Regarding the spectral data of the handheld device (Figure 1A and 1B), it is possible to observe the same profile obtained by Teye et al. (2019), with three main bands. The first at 1000 nm correlates to the second N-H overtone, the second at 1200 nm relates to C-H stretching of CH_2 group, and the third at 1470 nm corresponds to the first overtone of O-H and N-H stretching (SAMPAIO et al., 2018). These molecular groups are typically present in the spectral data due to the fibre, moisture and protein content of brown rice (BAGCHI; SHARMA; CHATTOPADHYAY, 2016).

Looking at the information presented by NIR-HSI (Figure 1C and 1D), the bands at 1222 nm and 1470 nm are the same detected by the hand-held device, the band at 1794 nm could be related to the stretching of group O-H, characteristic of amylose. At 1960 nm and 2331 nm, the band corresponds to C=O stretch, O-H and N-H stretch being associated with the protein, fibre or ash content (BAGCHI; SHARMA; CHATTOPADHYAY, 2016). The same information could be measured by the benchtop NIR (Figure 1E and 1F), since both profiles, from NIR-HIS and benchtop NIR, presented a similar spectral overview.

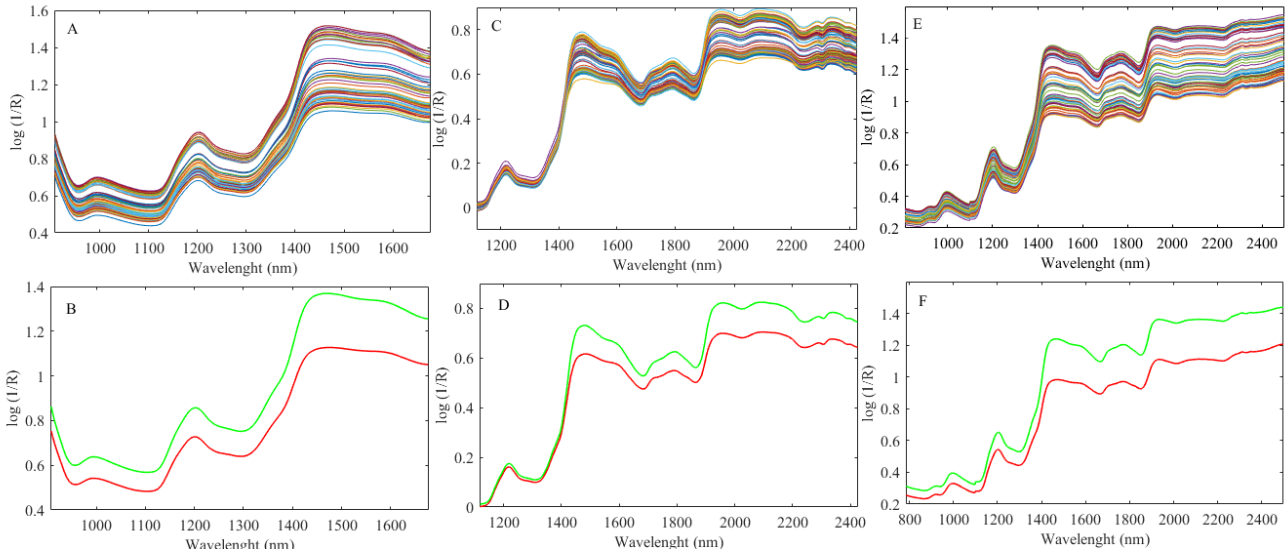

Figure 1. Raw spectral data and mean spectral data from organic (--) and conventional (--) brown rice by handheld NIR (A and B), NIR-HSI (C and D) and benchtop (E and F).

Overall, all devices presented the same shape of spectra for organic and conventional brown rice, pointing up that it would not be easy to distinguish between these types of brown rice by organic and conventional classes using only the analysis of untreated spectral data, justifying the needing of preprocessing to use other approaches such as PCA and PLS-DA models.

The spectral data was then mean centred and principal component analysis then performed. For PCA models based on benchtop and NIR-HSI, four principal components were used representing 99% of the cumulative variance, while for PCA based on handheld NIR five principal components were set also representing 99% of cumulative variance.

The score plots for the three PCAs are presented in Figure 2. In all cases, there is a grouping formed by the organic and conventional brown rice, confirming that there is a relevant chemical information present in NIR data that allows distinguishing between these types of brown rice. The same conclusion arose from another study that was conducted using a benchtop NIR to discriminate organic and conventional ground white rice, where it was possible to observe similar behaviour during PCA analysis (XIAO et al., 2019).

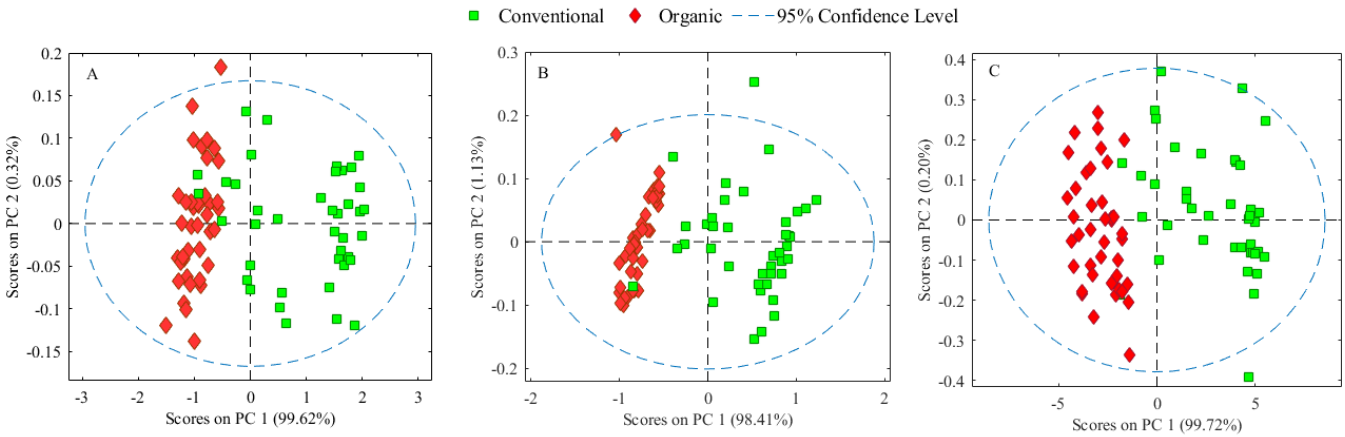

Figure 2. PCA models based on data information obtained from handheld (A), NIR-HSI (B) and benchtop (C) devices.

3.2. PLS-DA MODELS AND PERFORMANCE PARAMETERS

Due to the relevance of the chemical information of NIR, detected by unsupervised analysis (PCA), development of the discriminant model for the distinguishing organic and conventional brown rice was possible.

The three datasets were preprocessed with SNV and first derivative by the Savitsky-Golay method (filter width: 7pts, polynomial order: 2) to correct the baseline shift and offset and minimize the light scattering phenomenon. The values of sensitiveness and specificity of the three models are presented in Table 1.

Regarding the performance achieved by PLS-DA models, it is possible to assume that NIRS was capable of discriminating the brown rice grains into organic and conventional classes with a minimum of 87.5% specificity, which was considered a satisfactory result. Xiao et al. (2019), who conducted a study discriminating organic and conventional ground white rice based on NIR spectral data from a benchtop device, achieved the lower value (87.5%) of right assignments compared to this study (100%).

Teye et al. (2019) used a handheld NIR to estimate the quality of rice by geographical origin and according to quality grades (high, mid and low quality). Classification models were then developed using k-nearest neighbour (kNN) and support vector machine (SVM) algorithms. The kNN model presented the best performance for classifying the rice due to its quality grades, with 91.62% and 91.81% correct assignments. Regarding the classification

model that aimed to discriminate the samples according the origin, the SMV and kNN algorithms present the same performance, with 100% correct assignments. This is slightly better performance than that achieved using a handheld device in this study (100% sensitivity and 87.5% specificity), that could be attributed to the higher resolution (1 nm) used by Teye et al. (2019).

Table 1. Results of the PLS-DA models developed based on handheld, benchtop and NIR-HSI devices.

			Calibration		Cross-Validation		Prediction	
Device	LV	Class	Sen (%)	Spec (%)	Sen (%)	Spec (%)	Sen (%)	Spec (%)
Handheld	5	Organic	100	93.7	100	90.6	100	87.5
		Conventional	93.7	100	90.6	100	87.5	100
Benchtop	6	Organic	100	100	96.7	100	100	100
		Conventional	100	100	100	96.7	100	100
NIR-HSI	3	Organic	100	96.9	100	93.7	100	87.5
		Conventional	96.9	100	93.7	100	87.5	100

Sen: Sensitivity; Spec: specificity; LV: Latent Variable.

Qiu et al. (2018) developed discriminant models to distinguish four varieties of rice based on hyperspectral imaging with SVM and convolutional neural network (CNN), where CNN models presented better performance than SVM, achieving 89.6% and 87% accuracy in training and test sets, respectively, similar to the results obtained by NIR-HSI discriminating between organic and conventional brown rice.

Comparing the results obtained for each device (Table 1), it is possible to assume that the benchtop device provided the best parameters of sensitivity and specificity (100%) in the calibration and prediction set. A comparative study was developed to evaluate the performance of a benchtop Vis-NIR and NIR-HSI device detecting deoxynivalenol (DON) in wheat kernel and wheat flour, where Vis-NIR presented the best performance analysing the kernels and NIR-HSI was the best at analysing wheat flour (LIANG et al., 2020). On the other hand, the handheld device presented the worst results looking at the sensitivity and specificity in the calibration set (100% and 93.7%). In the last few years the development of technology has allowed miniaturization and consequently handheld NIR devices have been built, although they

still present lower performance scores than benchtop and NIR-HSI, mainly due to technical aspects such as resolution (MALEGORI et al., 2017).

Above all, it is important point out that even the performance presented by NIR-HSI was not the best in comparison to the others. This instrument allows the determination of a chemical map (Figure 3) that can return to the original image for better visualization of the model prediction in the case of mixed organic and conventional brown rice grains. In this sense, NIR-HSI could be used in the development of systems that help rough detection of the presence of rice grains with agrochemical residues among organic ones. This approach has already been done to provide an automatic method to detect defects in green coffee (OLIVERI et al., 2019).

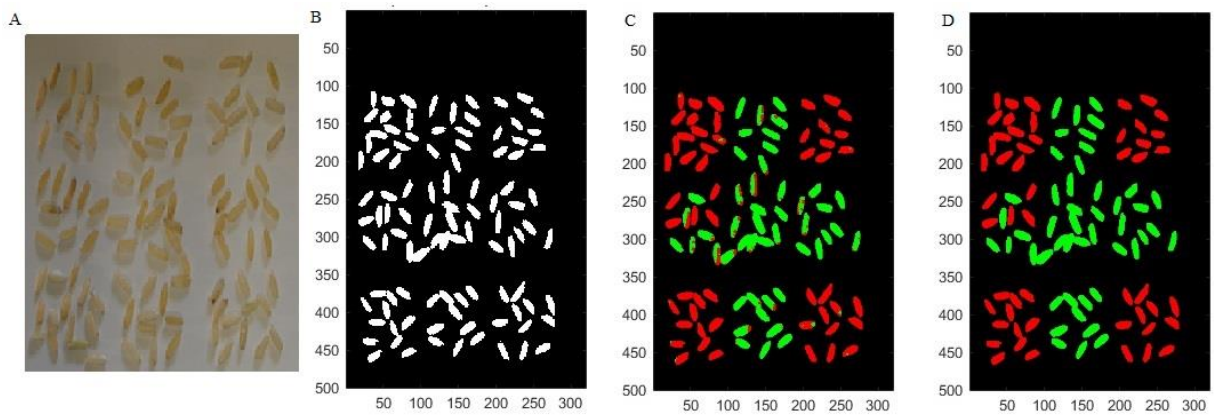

Figure 3. Digital image of conventional and organic rice grains (A), image after the mask processing (B), most probable prediction pixel by pixel (C) and according to the majority of pixel by grain (D). Organic (●) and conventional (●).

The variable importance in projection or variable influence on projection (VIP) scores is a very useful tool to understand the chemical data (X), once it shows which variable best explains the variance present in the results (Y), in this case, the assigned class (FARRÉS et al., 2015). In other words, the VIP scores provide valuable information about the importance of each variable of X to obtain Y. Generally, the variables that present a value greater than 1 (VIP score value > 1) are considered to have the most influence on the results (CARAMÊS et al., 2020).

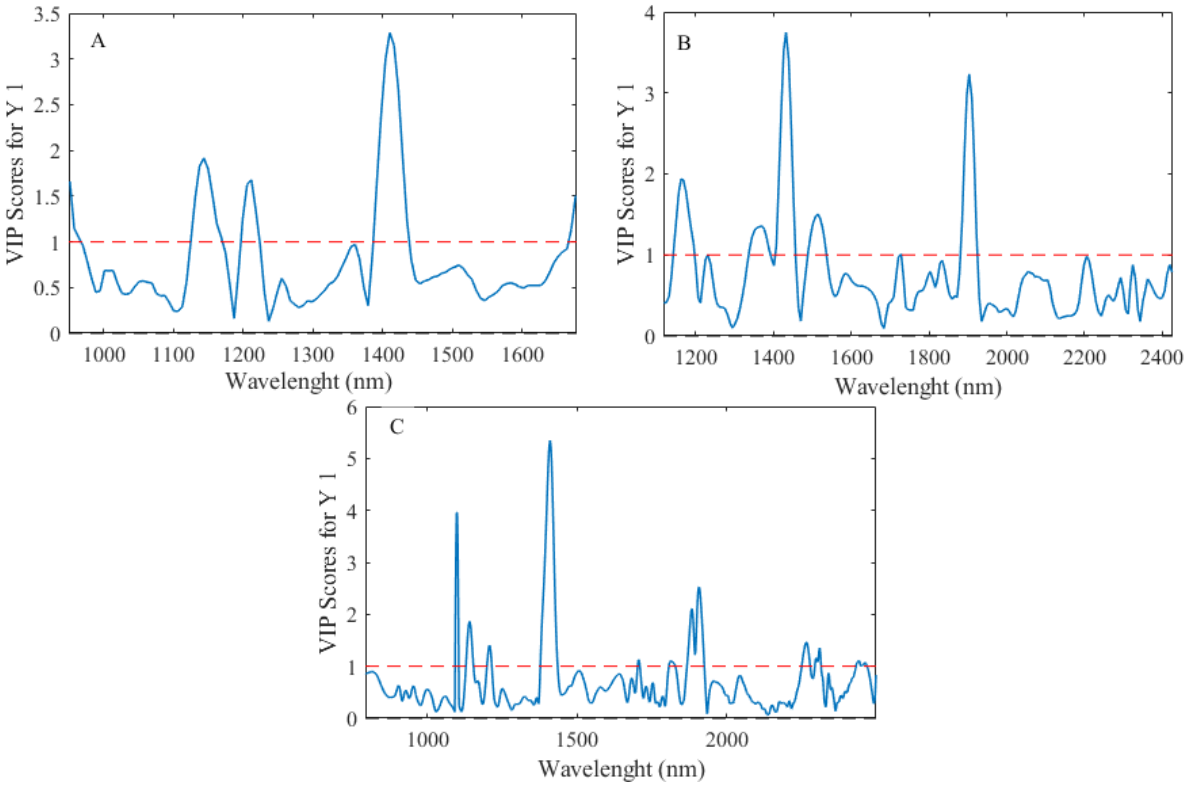

Figure 41. VIP scores of the PLS-DA models developed based on spectral data obtained for brown rice by handheld (A), NIR-HSI (B) and benchtop(C) devices.

In this context, the VIP scores plot of the PLS-DA models presented in Table 1 are represented in Figure 4, for a better understanding of the most important variables to discriminate organic and conventional brown rice. Looking at VIP plots on the PLS-DA model based on handheld NIR (Figure 4A) the bands at 1150 nm, 1220 nm and 1470 nm were those mainly responsible for the discrimination, related to the second overtone of N-H and C-H and first overtone of N-H (XIAO et al., 2019). In addition, the VIP score plots generated by the PLS-DA model of NIR-HSI (Figure 4B) also presented a significant importance at 1920 nm related to stretching of C=O from a structure CONH (BURNS; CIURCZAK, 2009). The information provided by VIP scores of benchtop NIR PLS-DA model (Figure 4C), presented the same important bands previously observed and one more at 2242 nm corresponding to NH stretching from the amino acid structure (BURNS; CIURCZAK, 2009).

Improper management of rice crops results in the excessive use of chemical products, such as fungicides, fertilizers and mainly herbicides (PAREJA et al., 2011). The use of herbicides is very common in rice crops, and consequently this is the class of residues most

often detected in rice crops around the world in countries such as Brazil, Uruguay, the Philippines and Bangladesh (PAREJA et al., 2011; VIEIRA et al., 2016). Among the herbicides more commonly used are bentazon, quinclorac, glyphosate, nominee and others that have in common the presence of nitrogen in their chemical structure. Considering this context and the importance of the variables (VIP scores), it is interesting to highlight that all three models pointed to a great importance of the band at 1470 nm that corresponds to the first overtone of N-H, a fact that could really explain how NIR spectroscopy achieved good results discriminating organic and conventional brown rice.

Looking at the results obtained by all devices tested, it is possible to notice the great applicability potential of NIR spectroscopy to discriminating organic and conventional brown rice samples. The benchtop instrument presented the best results for sensitivity and specificity, but also has a higher cost and lower mobility when compared to the handheld device that also achieved a satisfactory performance. While the NIR-HSI opens the possibility of using image systems to build chemical maps and/or automatic selection models, conditioning the instrument choice to the interests of the user.

4. CONCLUSION

Regarding the relevance of controlling the presence of chemical residues in rice crops, the challenge associated with detection of these residues and with the need of alternative analytical methods for organic and conventional product discrimination, NIR spectroscopy emerges as a possible alternative to help in this problem. The results indicated a high potential of NIR spectroscopy in discriminating between organic and conventional brown rice, with 100% and 87.5% sensitivity and specificity respectively in prediction achieved by the handheld device and NIR-HSI; and 100% sensitivity and specificity by benchtop NIR. In this context, all the devices tested showed good performance and with it opened new possibilities to discriminating brown rice grains into organic and conventional ones, with the advantages of being rapid and non-destructive, and with no production of chemical residues, with the benchtop NIR presenting the best performance.

5. REFERENCES

BAGCHI, Torit Baran; SHARMA, Srigopal; CHATTOPADHYAY, Krishnendu. Development of NIRS models to predict protein and amylose content of brown rice and proximate compositions of rice bran. **Food Chemistry**, *[S. l.]*, v. 191, p. 21–27, 2016. DOI: 10.1016/j.foodchem.2015.05.038. Disponível em: http://dx.doi.org/10.1016/j.foodchem.2015.05.038.

BURNS, Donald A.; CIURCZAK, Emil W. **Handbook of near-infrared analysis, 3rd ed.Analytical and Bioanalytical Chemistry**, 2009. DOI: 10.1021/ja015320c. Disponível em: http://books.google.com/books?hl=en&lr=&id=XkALgZVXxQQC&pgis=1%5Cnhttp://uotechnology.edu.iq/eretc/books/Handbook of Near-Infrared Analysis 084937393X.pdf%5Cnhttp://link.springer.com/10.1007/s00216-008-2580-0.

CARAMÊS, Elem Tamirys; PIACENTINI, Karim C.; ALVES, Lucas Teixeira; PALLONE, Juliana Azevedo Lima; ROCHA, Liliana de Oliveira. NIR spectroscopy and chemometric tools to identify high content of deoxynivalenol in barley. **Food Additives and Contaminants - Part A Chemistry, Analysis, Control, Exposure and Risk Assessment**, *[S. l.]*, v. 00, n. 00, p. 1–11, 2020. DOI: 10.1080/19440049.2020.1778189. Disponível em: https://doi.org/10.1080/19440049.2020.1778189.

CRUZ-TIRADO, J. P.; FERNÁNDEZ PIERNA, Juan Antonio; ROGEZ, Hervé; BARBIN, Douglas Fernandes; BAETEN, Vincent. Authentication of cocoa (Theobroma cacao) bean hybrids by NIR-hyperspectral imaging and chemometrics. **Food Control**, *[S. l.]*, v. 118, n. May, 2020. DOI: 10.1016/j.foodcont.2020.107445.

EMBRAPA. **EMBRAPA Arroz e Feijão. Dados de conjuntura da produção de arroz (Oryza sativa L.) no Brasil (1985-2015): área, produção e rendimento.** 2016. Disponível em: http://www.cnpaf.embrapa.br/socioeconomia/index.htm. Acesso em: 12 set. 2020.

FARRÉS, Mireia; PLATIKANOV, Stefan; TSAKOVSKI, Stefan; TAULER, Romà. Comparison of the variable importance in projection (VIP) and of the selectivity ratio (SR) methods for variable selection and interpretation. **Journal of Chemometrics**, *[S. l.]*, v. 29, n. 10, p. 528–536, 2015. DOI: 10.1002/cem.2736.

JIMÉNEZ-CARVELO, Ana M.; GONZÁLEZ-CASADO, Antonio; BAGUR-GONZÁLEZ, M. Gracia; CUADROS-RODRÍGUEZ, Luis. Alternative data mining/machine learning methods for the analytical evaluation of food quality and authenticity – A review. **Food Research International**, *[S. l.]*, v. 122, n. March, p. 25–39, 2019. DOI: 10.1016/j.foodres.2019.03.063. Disponível em: https://doi.org/10.1016/j.foodres.2019.03.063.

KATT, Felix; MEIXNER, Oliver. A systematic review of drivers influencing consumer willingness to pay for organic food. **Trends in Food Science and Technology**, *[S. l.]*, v. 100, n. July 2019, p. 374–388, 2020. DOI: 10.1016/j.tifs.2020.04.029. Disponível em: https://doi.org/10.1016/j.tifs.2020.04.029.

LIANG, Kun; HUANG, Jiani; HE, Ruiyin; WANG, Qiujin; CHAI, Yinyin; SHEN, Mingxia. Comparison of Vis-NIR and SWIR hyperspectral imaging for the non-destructive detection of DON levels in Fusarium head blight wheat kernels and wheat flour. **Infrared Physics and Technology**, *[S. l.]*, v. 106, n. 40, p. 103281, 2020. DOI: 10.1016/j.infrared.2020.103281. Disponível em: https://doi.org/10.1016/j.infrared.2020.103281.

LIU, Yuwei; PU, Hongbin; SUN, Da-Wen. Hyperspectral imaging technique for evaluating food quality and safety during various processes: A review of recent applications. **Trends in Food Science & Technology**, *[S. l.]*, v. 69, p. 25–35, 2017. DOI: 10.1016/j.tifs.2017.08.013. Disponível em: http://linkinghub.elsevier.com/retrieve/pii/S0924224416305052.

LYU, Yanfeng et al. Performance assessment of rice production based on yield, economic output, energy consumption, and carbon emissions in Southwest China during 2004–2016. **Ecological Indicators**, *[S. l.]*, v. 117, n. May, p. 106667, 2020. DOI: 10.1016/j.ecolind.2020.106667. Disponível em: https://doi.org/10.1016/j.ecolind.2020.106667.

MALEGORI, Cristina; NASCIMENTO MARQUES, Emanuel José; DE FREITAS, Sergio Tonetto; PIMENTEL, Maria Fernanda; PASQUINI, Celio; CASIRAGHI, Ernestina. Comparing the analytical performances of Micro-NIR and FT-NIR spectrometers in the evaluation of acerola fruit quality, using PLS and SVM regression algorithms. **Talanta**, *[S. l.]*, v. 165, n. November 2016, p. 112–116, 2017. DOI: 10.1016/j.talanta.2016.12.035. Disponível em: http://dx.doi.org/10.1016/j.talanta.2016.12.035.

OLIVERI, Paolo; MALEGORI, Cristina; CASALE, Monica; TARTACCA, Edoardo; SALVATORI, Gianni. An innovative multivariate strategy for HSI-NIR images to automatically detect defects in green coffee. **Talanta**, *[S. l.]*, v. 199, n. October 2018, p. 270–276, 2019. DOI: 10.1016/j.talanta.2019.02.049. Disponível em: https://doi.org/10.1016/j.talanta.2019.02.049.

PALLONE, Juliana Azevedo Lima; CARAMÊS, Elem Tamirys dos Santos; ALAMAR, Priscila Domingues. Green analytical chemistry applied in food analysis: alternative techniques. **Current Opinion in Food Science**, *[S. l.]*, v. 22, n. Figure 1, p. 115–121, 2018. DOI: 10.1016/j.cofs.2018.01.009.

PAREJA, Lucía; FERNÁNDEZ-ALBA, A. R.; CESIO, Verónica; HEINZEN, Horacio. Analytical methods for pesticide residues in rice. **TrAC - Trends in Analytical Chemistry**, *[S. l.]*, v. 30, n. 2, p. 270–291, 2011. DOI: 10.1016/j.trac.2010.12.001.

PEANPARKDEE, Methavee; IWAMOTO, Satoshi. Bioactive compounds from by-products of rice cultivation and rice processing: Extraction and application in the food and pharmaceutical industries. **Trends in Food Science and Technology**, *[S. l.]*, v. 86, n. July 2018, p. 109–117, 2019. DOI: 10.1016/j.tifs.2019.02.041. Disponível em: https://doi.org/10.1016/j.tifs.2019.02.041.

QIU, Zhengjun; CHEN, Jian; ZHAO, Yiying; ZHU, Susu; HE, Yong; ZHANG, Chu. Variety identification of single rice seed using hyperspectral imaging combined with convolutional neural network. **Applied Sciences (Switzerland)**, *[S. l.]*, v. 8, n. 2, p. 1–12, 2018. DOI: 10.3390/app8020212.

RINNAN, Åsmund. Pre-processing in vibrational spectroscopy-when, why and how. **Analytical Methods**, *[S. l.]*, v. 6, n. 18, p. 7124–7129, 2014. DOI: 10.1039/c3ay42270d.

RINNAN, Åsmund; BERG, Frans Van den; ENGELSEN, Søren Balling. Review of the most common pre-processing techniques for near-infrared spectra. **TrAC Trends in Analytical Chemistry**, *[S. l.]*, v. 28, n. 10, p. 1201–1222, 2009. DOI: 10.1016/j.trac.2009.07.007. Disponível em: http://linkinghub.elsevier.com/retrieve/pii/S0165993609001629. Acesso em: 6 ago. 2017.

SAMPAIO, Pedro Sousa; SOARES, Andreia; CASTANHO, Ana; ALMEIDA, Ana Sofia; OLIVEIRA, Jorge; BRITES, Carla. Optimization of rice amylose determination by NIR-spectroscopy using PLS chemometrics algorithms. **Food Chemistry**, *[S. l.]*, v. 242, p. 196–204, 2018. DOI: https://doi.org/10.1016/j.foodchem.2017.09.058.

SEN, Saikat; CHAKRABORTY, Raja; KALITA, Pratap. Rice - not just a staple food: A comprehensive review on its phytochemicals and therapeutic potential. **Trends in Food Science and Technology**, *[S. l.]*, v. 97, n. February 2019, p. 265–285, 2020. DOI: 10.1016/j.tifs.2020.01.022. Disponível em: https://doi.org/10.1016/j.tifs.2020.01.022.

TANDON, Anushree; JABEEN, Fauzia; TALWAR, Shalini; SAKASHITA, Mototaka; DHIR, Amandeep. Facilitators and inhibitors of organic food buying behavior. **Food Quality and Preference**, *[S. l.]*, p. 104077, 2020. DOI: 10.1016/j.foodqual.2020.104077. Disponível em: https://doi.org/10.1016/j.foodqual.2020.104077.

TEYE, Ernest; AMUAH, Charles L. Y.; MCGRATH, Terry; ELLIOTT, Christopher. Innovative and rapid analysis for rice authenticity using hand-held NIR spectrometry and chemometrics. **Spectrochimica Acta - Part A: Molecular and Biomolecular Spectroscopy**, *[S. l.]*, v. 217, p. 147–154, 2019. DOI: 10.1016/j.saa.2019.03.085. Disponível em: https://doi.org/10.1016/j.saa.2019.03.085.

VIEIRA, Danielle Cristina; NOLDIN, José Alberto; DESCHAMPS, Francisco C.; RESGALLA, Charrid. Ecological risk analysis of pesticides used on irrigated rice crops in southern Brazil. **Chemosphere**, *[S. l.]*, v. 162, p. 48–54, 2016. DOI: 10.1016/j.chemosphere.2016.07.046.

WALSH, Kerry B.; BLASCO, José; ZUDE-SASSE, Manuela; SUN, Xudong. Postharvest Biology and Technology Visible-NIR ‘ point ’ spectroscopy in postharvest fruit and vegetable assessment : The science behind three decades of commercial use. **Postharvest Biology and Technology**, *[S. l.]*, v. 168, n. March, p. 111246, 2020. DOI: 10.1016/j.postharvbio.2020.111246. Disponível em: https://doi.org/10.1016/j.postharvbio.2020.111246.

XIAO, Ran; LIU, Li; ZHANG, Dongjie; MA, Ying; NGADI, Michael O. Discrimination of

organic and conventional rice by chemometric analysis of NIR spectra: a pilot study. **Journal of Food Measurement and Characterization**, *[S. l.]*, v. 13, n. 1, p. 238–249, 2019. DOI: 10.1007/s11694-018-9937-7. Disponível em: http://dx.doi.org/10.1007/s11694-018-9937-7.

ZONTOV, Y. V.; RODIONOVA, O. Ye; KUCHERYAVSKIY, S. V.; POMERANTSEV, A. L. PLS-DA – A MATLAB GUI tool for hard and soft approaches to partial least squares discriminant analysis. **Chemometrics and Intelligent Laboratory Systems**, *[S. l.]*, v. 203, n. May, p. 104064, 2020. DOI: 10.1016/j.chemolab.2020.104064. Disponível em: https://doi.org/10.1016/j.chemolab.2020.104064.

DISCUSSÃO GERAL

Os casos de obesidade e outras doenças crônicas não transmissíveis, como doenças cardiovasculares, diversas formas de câncer, diabetes tipo II e hipertensão arterial, são comumente correlacionadas a um estilo de vida sedentário aliados a uma dieta desiquilibrada (SAMOGGIA; RIEDEL, 2020). Nesse sentido, identificou-se nas últimas décadas, uma tendência ao aumento da preocupação social por um estilo de vida mais saudável, incluindo uma alimentação balanceada e atividades físicas regulares (WALLS et al., 2019).

Além da preocupação com a composição dos alimentos presentes na dieta, os consumidores têm aumentado também a procura por produtos orgânicos, uma vez que, em alimentos produzidos de forma convencional, trazem consigo o risco da utilização inadequada de produtos químicos intrinsecamente tóxicos, como herbicidas e fungicidas, durante o cultivo podendo ocasionar efeitos deletérios às pessoas que os consomem regularmente (GONG et al., 2017; KUSHWAH et al., 2019).

Sendo assim, sabe-se que o consumo regular de frutas, vegetais e grãos têm efeito benéfico para a saúde a longo prazo, devendo ser incentivado desde a infância, uma vez que, esses alimentos possuem diversos nutrientes, como vitaminas, minerais e compostos bioativos, que são essenciais ao desenvolvimento humano e também relacionados à redução do risco de desenvolvimento de doenças crônicas não transmíssiveis no decorrer da vida (TUURI et al., 2009).

Nesse contexto, alimentos como o açaí, repolho roxo e arroz integral, se tornaram ótimas opções para consumo dentro de uma dieta saudável. O reflexo da associação desses alimentos a aspectos de saudabilidade pode ser medido pelo aumento da produção dos mesmos. O repolho é produzido em todas as capitais nacionais, somando mais de 400 toneladas ao ano. Enquanto o açaí, que tem sua produção concentrada dos estados do Norte do Brasil, teve produção superior a 200 mil toneladas em 2019 gerando mais de 588,6 milhões de reais para a economia (KIST et al., 2018; PAGLIARUSSI, 2010; IBGE, 2019). Já o arroz é um alimento básico na dieta de diversos países do mundo, tendo a China como principal produtor mundial (207 milhões de tonelada) e o Brasil como o maior produtor da América Latina (12,2 milhões de

toneladas), dentre as variedades desse grão o arroz integral, principalmente orgânico, tem sido cada vez mais procurado (EMBRAPA, 2016).

Considerando o atual cenário de mercado os produtos orgânicos são cada vez mais procurados e valorizados, movimentando cerca de 90 bilhões de euros em 2017, a utilização de métodos que sejam capazes de distinguir alimentos produzidos de forma orgânica e convencional têm sido necessária (KATT; MEIXNER, 2020). Os métodos mais utilizados para a detecção de resíduos de produtos agroquímicos se baseiam na utilização de cromatografia líquida ou gasosa de alta eficiência, geralmente, acoplada a espectrometria de massas. Essas metodologias são extremamente eficientes, sensíveis e robustas, no entanto, fazem uso de reagentes tóxicos durante um extenso processo de *clean-up* e extração da amostra. Além disso, demandam a utilização de equipamentos de alto custo de aquisição e manutenção (PAREJA et al., 2011).

Situação similar é observada para o açaí e o repolho roxo, alimentos reconhecidos pelo potencial bioativo decorrente da presença de compostos bioativos, porém são compostos instáveis e por isso a realização de um controle de qualidade que assegure a preservação desses compostos é essencial. Várias técnicas analíticas foram desenvolvidas e aplicadas para essa situação, como a cromatografia líquida de alta eficiência, técnicas espectrofotométricas e/ou por fluorescência. Assim como no caso de produtos orgânicos, essas técnicas são confiáveis e reprodutíveis, mas demandam refinados métodos de extração, em alguns casos seguidos de partições, derivatizações, entre outros passos necessários ao preparo de amostra que geram resíduos e perigos ao operador. (FIBIGR; ŠATÍNSKÝ; SOLICH, 2018).

Em contrapartida, o conceito de técnicas analíticas sustentáveis e verdes promovidas pela quarta revolução industrial tem implicado no aumento da demanda pela substituição das técnicas tradicionalmente utilizadas por técnicas que possibilitem a aplicação com menores custos, maior praticidade para a tomada de decisões, ou seja, tecnologias adaptáveis a linha de produção e que, principalmente, respeitem ao princípio de sustentabilidade (KAKANI et al., 2020).

Nesse contexto, técnicas analíticas vibracionais, como o infravermelho próximo e médio (*Near Infrared* - NIR e *Mid infrared* - MIR), e de imagem, como as de imagem digitais

de smartphone e hiperespectral, têm sido cada vez mais utilizadas como alternativa verde aos procedimentos tradicionalmente adotados na indústria de alimentos (PALLONE; CARAMÊS; ALAMAR, 2018). Logo, nesse trabalho aplicou-se as técnicas de NIR e MIR para a determinação de antocianinas totais (AT), polifenóis totais (PT), DPPH, ORAC e TEAC em repolho roxo, e também para a detecção de fraudes em polpa de açaí. Desenvolveu-se também modelos de calibração para a determinação de AT, PT, DPPH, ORAC e TEAC em polpa de açaí liofilizado aplicando-se NIR e imagens digitais obtidas por smartphone, além da detecção de fraudes em polpa de açaí liofilizado utilizando o conteúdo de minerais como marcador de fraude. A concentração dos minerais cálcio, potássio, ferro e manganês foi determinada através da utilização de NIR, como alternativa a espectrometria atômica e modelos multivariados foram utilizados para a classificação de amostras. Ademais, técnicas de imagem hiperespectral e NIR foram utilizadas para o desenvolvimento de modelos capazes de discriminar arroz integral orgânico e convencional.

Para a primeira etapa do trabalho, 60 repolhos roxos foram adquiridos no comércio de Campinas-SP, triturados e liofilizados. Após padronização de partícula, espectros no infravermelho próximo e médio foram obtidos. Em seguida, os dados espectrais obtidos foram aplicados para a criação de modelos de calibração multivariada que tinham por objetivo a determinação dos parâmetros de AT, PT, DPPH, ORAC e TEAC. Um modelo de regressão para cada um dos parâmetros analisados foi determinado sendo selecionado o método PLS (*Partial Least Square*). A concentração média de AT encontrada nas amostras foi de 5,16 mg/gbs e de PT foi de 5,30 mg/gbs. Esses valores permitem afirmar que a concentração de AT encontrada nas amostras é alta em comparação aos valores médios determinados em PT, o que confirma que antocianinas é a classe marjoritária de compostos fenólicos presentes no repolho roxo. Ao comparar as concentrações médias de AT e PT determinadas nesse estudo com outras pesquisas notou-se variações. Wiczkowski (2014) e colaboradores determinaram uma média de AT igual a 6,30mg/gbs para um estudo conduzido sobre a oscilação da concentração de antocioaninas durante o processo fermentativo do repolho roxo. Enquanto, Vicas et al. (2013) comparou a concentração de PT em repolhos roxos orgânicos e convencionais e encontrou médias de 3,17 e 3,02 mgEAG/gbs, respectivamente. No entanto, as variações encontradas eram esperadas uma vez que a presença desses compostos é influenciada diretamente pelas condições climáticas

durante o cultivo, além das condições pós colheita (WICZKOWSKI; SZAWARA-NOWAK; TOPOLSKA, 2013).

A presença desses compostos confere ao repolho roxo capacidade antioxidante que foi avaliada pelos métodos de ORAC, TEAC e DPPH, onde foram determinados os valores médios de 852,88 µMol Eq. Trolox/g, 5,16 µMol Eq. Trolox/g e 131,78 µMol Eq. Trolox/100g, respectivamente. Como a capacidade antioxidante de um alimento é diretamente relacionada com a presença de compostos bioativos, determinantes como as condições de cultivo e pós colheita aqui também se aplicam para a variação encontrada entre o estudo aqui desenvolvido e outros como o de WICZKOWSKI (2014) e colaboradores que encontraram valor ORAC médio de 256,66 µMol Eq. Trolox/gbs. Os métodos PLS desenvolvidos por NIR e MIR apresentaram bons indicativos de performance. Os modelos PLS baseados em dados MIR apresentaram valores de R^2 entre 0,78 e 0,88, com destaques para os modelos de AT e PT com valores de erros de predição (*Root Mean Square Erros of Prediction* – RMSEP) de 0,35 mg/gbs e 0,34 mgEAG/gbs, respectivamente. Já dentre os modelos PLS baseados nos dados espectrais obtidos na faixa do infravermelho próximo, os valores de R^2 variaram de 0,78 a 0,87, com destaque para os modelos de PT e TEAC com valores de RMSEP de 0,41 mgEAG/gbs e 0,29 µMol Eq. Trolox/g, respectivamente. Nesse contexto, pode-se afirmar que as técnicas NIR e MIR obtiveram bons resultados para a determinação dos parâmetros propostos, e ambas poderiam ser utilizadas para tais fins.

Na etapa seguinte do trabalho, dados espectrais nas faixas do infravermelho próximo e médio foram obtidos a partir de polpa de açaí autêntica e adulterada. Para isso, a polpa de açaí fina (teor de sólidos totais ≤ 8%) foi adulterada com farinhas de trigo, mandioca ou tapioca nos percentuais de 5 %, 10 %, 20 % e 40 % m/m. Emulsificante também foi utilizado como um adulterante, nos percentuais de 1 %, 2,5 %, 5% e 10%, uma vez que maiores percentuais desse adulterante tornavam-se evidentes visualmente. Os dados espectrais, NIR e MIR, foram utilizados para a criação de cartas de controle multivariadas e modelos de classificação através dos métodos de PLS-DA (*Partial Least Square-Discriminant Analysis*) e KNN (*K Nearest Neighbor*). As cartas de controle multivariadas, NIR e MIR, foram construídas com base no valor de Q residual. Ambas foram eficientes na detecção de polpas de açaí adulteradas, com níveis de confiança de 99%. Esse tipo de projeção é muito útil, uma vez que facilita a tomada de

decisão em uma possível aplicabilidade durante produção em escala (LOBATO et al., 2018; PERES et al., 2019). Semelhante abordagem foi realizada por Teixeira et al. (2020), que desenvolveu carta de controle multivariada baseada nos valores de Q resíduo, utilizando dados espectrais NIR, para a detecção de adulteração em leite de cabra com água, ureia, soro ou leite bovino em diferentes percentuais (1%, 5%, 10%, 15% e 20% v/v), onde foi possível detectar as adulterações propostas com 95% de confiança.

Os modelos KNN e PLS-DA desenvolvidos baseado em MIR, foram aplicados tanto para a detecção de amostras de polpas de açaí adulteradas quanto para a detecção do tipo de adulterante utilizado. Nos modelos PLS-DA e KNN que consideraram apenas duas classes, autênticas e adulteradas, atingiu-se 100% de sensibilidade e especificidade. No entanto, nos modelos que objetivaram identificar o tipo de adulterante somente o PLS-DA atingiu 100% de sensibilidade e especificidade para todas as classes. Em relação aos modelos baseados nas informações do NIR, ambos, PLS-DA e KNN, atingiram 100% de acerto, considerando duas classes. Ao considerarmos cinco classes, para identificação dos adulterantes, ambos métodos também atingiram 100% de acerto, porém se fez necessário seleção de variáveis para melhorar a performance do modelo PLS-DA. Araújo; Marinho e De Araújo Gomes (2017) determinaram um método para detecção de adulteração de polpa de açaí com farinha de trigo e de mandioca com adição de 10%, usaram imagens RGB e determinaram modelos DD-SIMCA e OC-PLS. A metodologia DD-SIMCA apresentou os melhores resultados, com 98,14% de especificidade. Apesar dos bons resultados obtidos, as técnicas de NIR e MIR apresentaram um melhor desempenho por serem equipamento mais robustos, podendo assim detectar fraudes presentes em percentuais menores, além da possibilidade de distinguir os adulterantes, uma vez que alguns dos materiais utilizados podem causar risco a saúde se ingeridos por pessoas alérgicas ou celíacas (RIBEIRO; NUNES, 2019).

Uma vez que as técnicas de imagem RGB são caracterizadas por baixo custo e versatilidades, na próxima etapa do trabalho aplicamos as informações adquiridas através de imagens digitais obtidas por um smartphone e também os dados espectrais NIR de polpas de açaí liofilizadas, para a determinação de modelos de calibração multivariada afim de quantificar os parâmetros químicos relacionados aos compostos bioativos: AT, PT, DPPH, ORAC e TEAC. Nesse cenário, as 96 amostras de polpa de açaí, previamente liofilizadas, apresentaram elevados

teores de antocianinas e polifenóis totais, 6,26 mg/g e 11,4 mgEAG/g, respectivamente. Dentre os compostos fenólicos presentes no açaí, as antocianinas compõem a classe de maior destaque, no açaí são majoritariamente cianidinas-3-glicosídeo e cianidina-3-rutinosídeo, as mesmas juntas com outros compostos bioativos conferem ao produto elevada capacidade antioxidante. Nesse estudo, as análises antioxidantes confirmaram essa informação. ORAC, DPPH e TEAC apresentaram valores de 2588,4 µMol trolox eq./g, 5,86 µMol trolox eq./g e 19,88 µMol trolox eq./g, respectivamente. Conhecido por seu alto valor bioativo, o açaí, já teve esses parâmetros determinados em diversos estudos, que corroboram com os dados aqui determinados. Valores de ORAC entre 1027 µMol trolox eq./g em amostras de açaí liofilizado e 2649 µMol trolox eq./g em amostras de frutos de açaí liofilizados foram encontrados, similares aos determinados nas amostras de polpas analisadas nessa etapa do trabalho. (BENATREHINA et al., 2018; KANG et al., 2012).

Histogramas dos parâmetros RGB (*Red Green Blue*), HSV (*Hue Saturation Value*), brilho e cores relativas, compuseram um colorograma aplicado durante a construção de modelos de calibração PLS. Espectros do infravermelho próximo foram obtidos e pré processados da forma mais conveniente a boa performance do modelo final, e utilizados para o mesmo fim. Como resultado, os modelos PLS desenvolvidos com os espectros NIR apresentaram bons indicativos de qualidade, com $R^2 \geq 0,8$ e RPD > 2. Os modelos PLS gerados a partir dos colorogramas apresentaram indicativos de qualidade inferiores aos gerados pelo NIR, com $R^2 \geq 0,7$ e somente três dos cinco modelos construídos com RPD ≥ 2.Comparando os resultados obtidos por NIR e pelas imagens de smartphone, o desempenho do NIR foi notavelmente superior. No entanto, apesar disso, o desempenho das imagens foi adequado para a quantificação de todos parâmetros avaliados, com exceção do ORAC. Nesse sentido, ambas técnicas podem ser consideradas alternativas válidas para o estudado fim, deve-se ainda considerar o baixo custo e alta versatilidade para a obtenção de imagens digitais para caso de necessidade de uma análise rápida de compostos bioativos em polpa de açaí.

Além dos compostos fenólicos, os minerais essenciais presentes no açaí também elevam a qualidade nutricional desse produto. Sendo assim, a seguir, investigou-se a possibilidade da utilização do teor de alguns dos minerais naturalmente presentes no açaí como marcadores de fraude. Para isso, inicialmente 2 amostras autênticas e 10 amostras adulteradas

de polpas de açaí liofilizadas tiveram os teores de Ca, Mg, K, Fe, Zn, Cu e Mn determinados via FAAS (*Flame Atomic Absorption Spectroscopy*) para avaliação da alteração das adulterações nas concentrações desses minerais. Baseado nos maiores valores percentuais de alteração, cálcio (51,37%), manganês (52,45%), ferro (42,96%) e potássio (31,01%), foram os minerais escolhidos como marcadores para adulteração. Sendo assim, esses quatro minerais foram determinados em 94 amostras autênticas e 75 amostras adulteradas com polpa de beterraba, maltodextrina, suco de uva, farinhas de tapioca e trigo, os dados resultantes foram utilizados para análise exploratória PCA (*Principal Component Analysis*) e para a construção de modelos de classificação pelos métodos PLS-DA, método de classe única por mínimos quadrados parciais (OCPLS) e SIMCA. O PCA mostrou que dentre os minerais analisados o Ca e o Fe se destacaram como os que mais evidenciaram o agrupamento entre adulteradas e autênticas.

Observando os modelos finais de PLS-DA, OCPLS e SIMCA, pode-se afirmar que apesar do bom desempenho apresentado por todos, o modelo SIMCA e OCPLS foram considerados os mais aplicáveis a situação uma vez que todos os parâmetros de sensibilidade e especificidade foram ≥ 80%. Nesse cenário, é possível afirmar que os minerais junto com técnicas quimiométricas representam uma alternativa a detecção de fraudes em polpas liofilizadas de açaí.

Considerando ainda a importância desses minerais presentes no açaí, na etapa seguinte de estudo, NIR foi avaliado como um método alternativo para a determinação da concentração de ferro, cálcio, potássio e manganês em polpa de açaí. Noventa e seis amostras de polpa de açaí foram liofilizadas, em seguida, foram determinados os teores de Ca, Fe, Mn e K via FAAS e os dados espectrais no NIR foram obtidos. As concentrações médias para Fe, Ca, K e Mn foram 3,4 mg/100gbs, 340,1 mg/100gbs, 1196,2 mg/100gbs e 63,8 mg/100gbs, respectivamente. Essas médias de Fe, Ca e K foram comparáveis com as médias já encontradas por Rogez (2000) durante a determinação desses minerais em polpa de açaí, no entanto, o valor médio de Mn foi inferior (32,3 mg/100gbs) ao encontrado nesse estudo. Porém essas variações são esperadas, uma vez que frutas podem apresentar alterações em sua composição devido a diversos fatores, como as práticas de cultivo, intensidade das chuvas, exposição ao sol, dentre outros fatores (GORDON et al., 2012). Os dados espectrais foram então pré-processados com primeira ou segunda derivada pelo método de Savitsky-Golay e *Standard Normal Variate* (SNV) para a

correção da linha de base e diminuição dos efeitos de espalhamento de luz. Após a determinação do melhor preprocessamento, o algoritmo PLS foi utilizado para a construção de modelos de calibração. O modelo para a quantificação de Ca, apresentou um ótimo desempenho com R^2=0,88 e *Residual Prediction Deviation* (RPD) =2,5, comparável com a performance alcançada por Plans et al. (2012) (R^2=0.82) na determinação de modelos PLS para a predição de Ca em sementes de feijão.

Os modelos obtidos para Fe, K e Mn não apresentaram desempenho satisfatório quando utilizado toda a faixa espectral (10000 cm^{-1} – 4000 cm^{-1}). O algoritmo de seleção de variáveis *interval partial least square* (iPLS) foi utilizado com diferentes tamanhos de janela: 500, 250 e 150 variáveis e número de intervalos automático. Os modelos PLS para a quantificação de Fe, K e Mn resultante das variáveis selecionadas pelo iPLS (janela: 150, 250 e 250 variáveis, respectivamente) apresentaram um desempenho final satisfatório. O modelo PLS para Fe apresentou R^2=0,74 e RPD=2,5; o modelo para quantificação de K obteve R^2=0,7 e RPD=2 e o modelo para a determinação de Mn apresentou R^2=0,74 e RPD=2,3. Desempenho similar foi encontrado durante a aplicação de dados NIR para a determinação de Fe em hambúrguer com R^2=0,73 (REBELLATO et al., 2020). Nesse contexto, apesar da técnica NIR não detectar diretamente a presença de minerais, a ligação desses compostos a outros compostos orgânicos das matrizes alimentares (ex: proteínas, fibras) justifica o bom desempenho dessa técnica quando aplicada para esse fim. Ademais, as técnicas de seleção de variáveis, como o iPLS, ajudam a manter as informações espectrais mais úteis para a construção de um modelo PLS com melhor desempenho.

Para a última etapa do trabalho foram adquiridas 80 amostras de arroz integral, sendo 40 amostras orgânicas e 40 amostras convencionais. Foram utilizados os dados espectrais obtidos por um espectrômetro NIR de bancada, um portátil e um acoplado ao sistema de imagem (*NIR-Hyperspectral imaging* – NIR-HSI) para a construção de modelos discriminantes PLS-DA. Durante análise não supervisionada PCA, os resultados obtidos pelo emprego das três técnicas analíticas mostraram tendência natural ao agrupamento entre amostras orgânicas e convencionais de arroz integral, essa mesma tendência já havia sido observada quando se determinou PCA baseado na informação NIR de amostras de arroz branco triturado cultivados de forma orgânica e convencional (XIAO et al., 2019). Os modelos supervisionados PLS-DA

apresentaram performance adequada para o NIR de bancada (100% de sensibilidade e especificidade), portátil (100% de sensibilidade e 87,5% de especificidade) e NIR-HSI (100% de sensibilidade e 87,5% de especificidade), sendo que o melhor desempenho para essa aplicação foi obtido com utilização do NIR de bancada. Qiu et al. (2018) desenvolveu modelos para discriminar quatro variedades de arroz baseado na informação obtida através de NIR-HSI, e obteve performance similar, 89,6% e 87% de precisão ao utilizar o algoritmo SVM e CNN, respectivamente. Analisando a contribuição das variáveis envolvidas no desenvolvimento dos modelos (*variable influence on projection* - VIP scores) é possível observar a grande importância da banda presente em 1470 nm, nos três modelos PLS-DA, que é associada ao primeiro sobretom de N-H. O nitrogênio eh um composto presente em diversos herbicidas (insumo agrícola mais utilizado em cultivos de arroz) como bentazon, quinclorac e outros, o que pode explicar a sensibilidade do NIR em discriminar amostras de arroz integral orgânico e convencional (PAREJA et al., 2011).

CONCLUSÃO GERAL

As técnicas tradicionalmente utilizadas no controle de qualidade na indústria de alimentos fazem uso de equipamentos específicos e de alto custo, como cromatógrafos de alta eficiência, espectros UV e/ou fluorescência. Na maioria das vezes essas análises exigem ainda etapas adicionais de extração e *clean up* que envolvem reagentes tóxicos com consequente geração de resíduos. Nesse cenário, além dos custos para aquisição e manutenção desses equipamentos e de um profissional treinado para a operação dos mesmos, ainda é necessário gastos com tratamento dos resíduos gerados.

Na última década, a quarta revolução industrial estabeleceu diretrizes que buscam diminuir os impactos ambientais durante a cadeia produtiva dos alimentos, priorizando técnicas analíticas que promovam maior velocidade na tomada de decisão com menor custo. Nesse cenário, técnicas vibracionais e de imagem se tornam ótimas alternativas as metodologias tradicionais, uma vez que são tecnologias de custo baixo, sem geração de resíduos tóxicos e com possibilidade de uso *on-line* na produção.

Sendo assim, as técnicas vibracionais, NIR e MIR, foram aplicadas para a avaliação da qualidade dos compostos bioativos presentes no repolho roxo, com a geração de modelos PLS capazes de determinar com eficiência antocianinas e polifenóis totais, DPPH, TEAC e ORAC. Mesmo resultado pode ser observado quando aplicamos os dados espectrais NIR e imagens digitais de um smartphone para a determinação desses parâmetros em polpa de açaí liofilizada, o que indica que todas as técnicas aplicadas podem ser empregadas como métodos alternativos para esse fim.

Para casos de fraude em polpa de açaí, cartas de controle e modelos de classificação, baseadas nas informações espectrais na faixa NIR e MIR, foram criadas com sucesso. Ambas as técnicas permitiram a detecção da fraude em polpa de açaí em diferentes percentuais, além de detectaram com sucesso o adulterante.

Já no caso de adulteração em polpa de açaí liofilizado, a análise de minerais via FAAS, permitiu o uso de K, Mn, Ca e Fe como marcadores para a detecção das fraudes mais comuns nesse produto. Modelos SIMCA, PLS-DA e OCPLS, foram determinados e apresentaram excelente performance, com altos valores de sensibilidade e especificidade.

A técnica NIR também apresentou resultados positivos quando aplicada para a construção de modelos PLS para a determinação da concentração de K, Mn, Ca e Fe em polpa de açaí liofilizada. Apesar do NIR não apresentar sensibilidade para detectar diretamente minerais, a ligação desses compostos com outras moléculas orgânicas presentes na matriz alimentar, torna o NIR uma ferramenta útil para essa finalidade.

Espectrômetro NIR de bancada, portátil e um NIR-HSI, foram utilizados para obtenção de dados espectrais de grãos de arroz integral, orgânicos e convencionais. Esses dados foram utilizados para a construção de modelos discriminantes PLS-DA, que apresentaram bons resultados de sensibilidade e especificidade, principalmente o NIR de bancada que foi o mais eficiente entre os três instrumentos avaliados. Além disso, com os dados de imagem obtidos, foi possível a criação de um mapa químico para a distinção automática de grãos orgânicos e convencionais misturados.

Observando os resultados apresentados é possível afirmar que as técnicas vibracionais, NIR e MIR, assim como a técnica de imagem de smartphones e hiperespectrais, tiveram sua eficiência comprovada no controle de qualidade e na detecção de fraudes em repolho roxo, açaí e arroz integral orgânico. A utilização da análise minerais, associada a ferramentas de quimiometria, também se mostrou adequada para a detecção de fraudes em açaí. Nesse sentido, pode-se verificar que tanto análises tradicionais, como FAAS, quanto vibracionais e de imagem, podem se beneficiar e serem aplicadas para diversos fins quando aliadas a quimiometria, tornando-as mais versáteis e adequadas para o contexto industrial atual.

Concluiu-se, finalmente, que é possível a utilização de técnicas analíticas limpas e verdes, associadas a ferramentas quimiométricas para o controle de qualidade, autenticidade e potencial bioativo para os alimentos avaliados no trabalho, além de ser possível a utilização de um método simples e barato como FAAS, com o monitoramento de minerais para controle de fraudes em açaí e ainda, NIR demonstrou capacidade para a predição de minerais essenciais, como análise indireta.

REFERÊNCIAS

ARAÚJO, Alisson; MARINHO, Weverton; DE ARAÚJO GOMES, Adriano. A Fast and Inexpensive Chemometric-Assisted Method to Identify Adulteration in Acai (Euterpe oleracea) Using Digital Images. **Food Analytical Methods**, *[S. l.]*, n. Canto 2001, p. 1–7, 2017. DOI: 10.1007/s12161-017-1127-4.

BENATREHINA, P. Annécie; PAN, Li; NAMAN, C. Benjamin; LI, Jie; KINGHORN, A. Douglas. Usage, biological activity, and safety of selected botanical dietary supplements consumed in the United States. **Journal of Traditional and Complementary Medicine**, *[S. l.]*, v. 8, n. 2, p. 267–277, 2018. DOI: 10.1016/j.jtcme.2018.01.006.

EMBRAPA. **EMBRAPA Arroz e Feijão. Dados de conjuntura da produção de arroz (Oryza sativa L.) no Brasil (1985-2015): área, produção e rendimento.** 2016. Disponível em: http://www.cnpaf.embrapa.br/socioeconomia/index.htm. Acesso em: 12 set. 2020.

FIBIGR, Jakub; ŠATÍNSKÝ, Dalibor; SOLICH, Petr. Current trends in the analysis and quality control of food supplements based on plant extracts. **Analytica Chimica Acta**, *[S. l.]*, v. 1036, p. 1–15, 2018. DOI: 10.1016/j.aca.2018.08.017.

GONG, Er Sheng; LUO, Shunjing; LI, Tong; LIU, Chengmei; ZHANG, Guowen; CHEN, Jun; ZENG, Zicong; LIU, Rui Hai. Phytochemical profiles and antioxidant activity of processed brown rice products. **Food Chemistry**, *[S. l.]*, v. 232, p. 67–78, 2017. DOI: 10.1016/j.foodchem.2017.03.148. Disponível em: http://dx.doi.org/10.1016/j.foodchem.2017.03.148.

GORDON, André et al. Chemical characterization and evaluation of antioxidant properties of Açaí fruits (Euterpe oleraceae Mart.) during ripening. **Food Chemistry**, *[S. l.]*, v. 133, n. 2, p. 256–263, 2012. DOI: 10.1016/j.foodchem.2011.11.150.

INSTITUTO BRASILEIRO DE GEOGRAFIA E ESTATÍSTICA. Produção da extração vegetal e da silvicultura 2019. **Produção da extração vegetal e da silvicultura**, *[S. l.]*, v. 34, p. 1–8, 2019.

KAKANI, Vijay; NGUYEN, Van Huan; KUMAR, Basivi Praveen; KIM, Hakil; PASUPULETI, Visweswara Rao. A critical review on computer vision and artificial

intelligence in food industry. **Journal of Agriculture and Food Research**, *[S. l.]*, v. 2, n. November 2019, p. 100033, 2020. DOI: https://doi.org/10.1016/j.jafr.2020.100033. Disponível em: http://www.sciencedirect.com/science/article/pii/S2666154320300144.

KANG, Jie et al. Bioactivities of açaí (Euterpe precatoria Mart.) fruit pulp, superior antioxidant and anti-inflammatory properties to Euterpe oleracea Mart. **Food Chemistry**, *[S. l.]*, v. 133, n. 3, p. 671–677, 2012. DOI: 10.1016/j.foodchem.2012.01.048. Disponível em: http://dx.doi.org/10.1016/j.foodchem.2012.01.048.

KATT, Felix; MEIXNER, Oliver. A systematic review of drivers influencing consumer willingness to pay for organic food. **Trends in Food Science and Technology**, *[S. l.]*, v. 100, n. July 2019, p. 374–388, 2020. DOI: 10.1016/j.tifs.2020.04.029. Disponível em: https://doi.org/10.1016/j.tifs.2020.04.029.

KIST, Benno Bernardo; SANTOS, Cleiton Evandro Dos; CARVALHO, Cleonice De; BELING, Romar Rodolfo. Anuário Brasileiro de Brazilian Horti 2019. **Editora Gazeta Santa Cruz**, *[S. l.]*, p. 96, 2018. Disponível em: http://www.abcsem.com.br/upload/arquivos/HortiFruti_2019_DUPLA.pdf.

KUSHWAH, Shiksha; DHIR, Amandeep; SAGAR, Mahim; GUPTA, Bhumika. Determinants of organic food consumption. A systematic literature review on motives and barriers. **Appetite**, *[S. l.]*, v. 143, n. October 2018, p. 104402, 2019. DOI: 10.1016/j.appet.2019.104402. Disponível em: https://doi.org/10.1016/j.appet.2019.104402.

LOBATO, Kleidson Brito de Sousa; ALAMAR, Priscila Domingues; CARAMÊS, Elem Tamirys dos Santos; PALLONE, Juliana Azevedo Lima. Authenticity of freeze-dried açai pulp by near-infrared spectroscopy. **Journal of Food Engineering**, *[S. l.]*, v. 224, p. 105–111, 2018. DOI: 10.1016/J.JFOODENG.2017.12.019. Disponível em: https://www.sciencedirect.com/science/article/pii/S0260877417305460. Acesso em: 21 mar. 2018.

PAGLIARUSSI, Marina. **A cadeia produtiva agroindustrial do açaí: estudo da cadeia e proposta de um modelo matemático.** 2010. São Carlos, 2010.

PALLONE, Juliana Azevedo Lima; CARAMÊS, Elem Tamirys dos Santos; ALAMAR, Priscila

Domingues. Green analytical chemistry applied in food analysis: alternative techniques. **Current Opinion in Food Science**, *[S. l.]*, v. 22, n. Figure 1, p. 115–121, 2018. DOI: 10.1016/j.cofs.2018.01.009.

PAREJA, Lucía; FERNÁNDEZ-ALBA, A. R.; CESIO, Verónica; HEINZEN, Horacio. Analytical methods for pesticide residues in rice. **TrAC - Trends in Analytical Chemistry**, *[S. l.]*, v. 30, n. 2, p. 270–291, 2011. DOI: 10.1016/j.trac.2010.12.001.

PERES, Fernanda Araujo Pimentel; PERES, Thiago Neves; FOGLIATTO, Flávio Sanson; ANZANELLO, Michel Jose. Fault detection in batch processes through variable selection integrated to multiway principal component analysis. **Journal of Process Control**, *[S. l.]*, v. 80, p. 223–234, 2019. DOI: 10.1016/j.jprocont.2019.06.002. Disponível em: https://doi.org/10.1016/j.jprocont.2019.06.002.

PLANS, Marçal; SIMÓ, Joan; CASAÑAS, Francesc; SABATÉ, José. Near-infrared spectroscopy analysis of seed coats of common beans (Phaseolus vulgaris L.): A potential tool for breeding and quality evaluation. **Journal of Agricultural and Food Chemistry**, *[S. l.]*, v. 60, n. 3, p. 706–712, 2012. DOI: 10.1021/jf204110k.

QIU, Zhengjun; CHEN, Jian; ZHAO, Yiying; ZHU, Susu; HE, Yong; ZHANG, Chu. Variety identification of single rice seed using hyperspectral imaging combined with convolutional neural network. **Applied Sciences (Switzerland)**, *[S. l.]*, v. 8, n. 2, p. 1–12, 2018. DOI: 10.3390/app8020212.

REBELLATO, Ana Paula; CARAMÊS, Elem Tamirys dos Santos; MORAES, Priscila Probio De; PALLONE, Juliana Azevedo Lima. Minerals assessment and sodium control in hamburger by fast and green method and chemometric tools. **Lwt**, *[S. l.]*, v. 128, n. October 2019, p. 109438, 2020. DOI: 10.1016/j.lwt.2020.109438. Disponível em: https://doi.org/10.1016/j.lwt.2020.109438.

RIBEIRO, Miguel; NUNES, Fernando M. We might have got it wrong: Modern wheat is not more toxic for celiac patients. **Food Chemistry**, *[S. l.]*, v. 278, n. July 2018, p. 820–822, 2019. DOI: 10.1016/j.foodchem.2018.12.003. Disponível em: https://doi.org/10.1016/j.foodchem.2018.12.003.

ROGEZ, Hervé. **Açaí- Preparo, Composição, Melhoramento da consevação**. Belém: Editora da Universidade Federal do Pará, 2000.

SAMOGGIA, Antonella; RIEDEL, Bettina. Assessment of nutrition-focused mobile apps' influence on consumers' healthy food behaviour and nutrition knowledge. **Food Research International**, *[S. l.]*, v. 128, n. November 2019, p. 108766, 2020. DOI: 10.1016/j.foodres.2019.108766. Disponível em: https://doi.org/10.1016/j.foodres.2019.108766.

TEIXEIRA, José Luan da Paixão; CARAMÊS, Elem Tamirys dos Santos; BAPTISTA, Débora Parra; GIGANTE, Mirna Lúcia; PALLONE, Juliana Azevedo Lima. Vibrational spectroscopy and chemometrics tools for authenticity and improvement the safety control in goat milk. **Food Control**, *[S. l.]*, v. 112, n. January, p. 107105, 2020. DOI: 10.1016/j.foodcont.2020.107105. Disponível em: https://doi.org/10.1016/j.foodcont.2020.107105.

TUURI, Georgianna; ZANOVEC, Michael; SILVERMAN, Linda; GEAGHAN, James; SOLMON, Melinda; HOLSTON, Denise; GUARINO, Annrose; ROY, Heli; MURPHY, Ellen. "Smart Bodies" school wellness program increased children's knowledge of healthy nutrition practices and self-efficacy to consume fruit and vegetables. **Appetite**, *[S. l.]*, v. 52, n. 2, p. 445–451, 2009. DOI: 10.1016/j.appet.2008.12.007.

VALENTIN, Jenna L.; WATLING, R. John. Provenance establishment of coffee using solution ICP-MS and ICP-AES. **Food Chemistry**, *[S. l.]*, v. 141, n. 1, p. 98–104, 2013. DOI: 10.1016/j.foodchem.2013.02.101. Disponível em: http://dx.doi.org/10.1016/j.foodchem.2013.02.101.

VICAS, Simona I.; TEUSDEA, Alin C.; CARBUNAR, Mihai; SOCACI, Sonia A.; SOCACIU, Carmen. Glucosinolates Profile and Antioxidant Capacity of Romanian Brassica Vegetables Obtained by Organic and Conventional Agricultural Practices. **Plant Foods for Human Nutrition**, *[S. l.]*, v. 68, n. 3, p. 313–321, 2013. DOI: 10.1007/s11130-013-0367-8. Disponível em: https://link.springer.com/article/10.1007/s11130-013-0367-8. Acesso em: 13 mar. 2017.

WALLS, H.; BAKER, Phillip; CHIRWA, Ephraim; HAWKINS, Benjamin. Food security, food safety & healthy nutrition: are they compatible? **Global Food Security**, *[S. l.]*, v. 21, n. April, p. 69–71, 2019. DOI: 10.1016/j.gfs.2019.05.005.

WICZKOWSKI, Wieslaw; SZAWARA-NOWAK, Dorota; TOPOLSKA, Joanna. Red cabbage anthocyanins: Profile, isolation, identification, and antioxidant activity. **Food Research International**, *[S. l.]*, v. 51, n. 1, p. 303–309, 2013. DOI: 10.1016/j.foodres.2012.12.015.

WICZKOWSKI, Wieslaw; TOPOLSKA, Joanna; HONKE, Joanna. Anthocyanins profile and antioxidant capacity of red cabbages are influenced by genotype and vegetation period. **Journal of Functional Foods**, *[S. l.]*, v. 7, p. 201–211, 2014. DOI: 10.1016/j.jff.2014.02.011. Disponível em: http://www.sciencedirect.com/science/article/pii/S1756464614000619. Acesso em: 13 mar. 2017.

XIAO, Ran; LIU, Li; ZHANG, Dongjie; MA, Ying; NGADI, Michael O. Discrimination of organic and conventional rice by chemometric analysis of NIR spectra: a pilot study. **Journal of Food Measurement and Characterization**, *[S. l.]*, v. 13, n. 1, p. 238–249, 2019. DOI: 10.1007/s11694-018-9937-7. Disponível em: http://dx.doi.org/10.1007/s11694-018-9937-7.

ANEXOS

Gmail **Elem C. <elem.carames@gmail.com>**

Thank you for your order with RightsLink / Springer Nature

no-reply@copyright.com <no-reply@copyright.com> 12 de junho de 2020 10:09
Para: elem.carames@gmail.com

SPRINGER NATURE

Thank you for your order!

Dear Miss. Elem Caramês,

Thank you for placing your order through Copyright Clearance Center's RightsLink® service.

Order Summary

Licensee:	Miss Elem Caramês
Order Date:	Jun 12, 2020
Order Number:	4846500535626
Publication:	Food Analytical Methods
Title:	Bioactive Compounds and Antioxidant Capacity in Freeze-Dried Red Cabbage by FT-NIR and MIR Spectroscopy and Chemometric Tools
Type of Use:	Thesis/Dissertation
Order Ref:	FANM-D-19-00150
Order Total:	0.00 USD

View or print complete details of your order and the publisher's terms and conditions.

Sincerely,

Copyright Clearance Center

Tel: +1-855-239-3415 / +1-978-646-2777
customercare@copyright.com
https://myaccount.copyright.com

Copyright Clearance Center RightsLink®

Detection and identification of açai pulp adulteration by NIR and MIR as an alternative technique: Control charts and classification models

Author: E.T.S. Caramês,P.D. Alamar,J.A.L. Pallone

Publication: Food Research International

Publisher: Elsevier

Date: September 2019

Near infrared spectroscopy and smartphone-based imaging as fast alternatives for the evaluation of the bioactive potential of freeze-dried açai

Author:
Elem Tamirys dos Santos Caramês,Michel Rocha Baqueta,Deborah A. Conceição,Juliana Azevedo Lima Pallone

Publication: Food Research International

Publisher: Elsevier

Date: Available online 29 October 2020

Gmail **Elem C. <elem.carames@gmail.com>**

Food Analytical Methods - Submission Notification to co-author

1 mensagem

Food Analytical Methods <em@editorialmanager.com> 3 de julho de 2020 18:17
Responder a: Food Analytical Methods <jamaica.bihasa@springernature.com>
Para: Elem Tamirys dos Santos Caramês <elem.carames@gmail.com>

Re: "Multiple element analysis in freeze-dried açai pulp - a new method to adulteration detection"
Full author list: Elem Tamirys dos Santos Caramês; Letícia Schilling; Joyce Grazielle Siqueira Silva; José Luan da Paixão Teixeira; Juliana Pallone

Dear Msc Elem Tamirys dos Santos Caramês,

We have received the submission entitled: "Multiple element analysis in freeze-dried açai pulp - a new method to adulteration detection" for possible publication in Food Analytical Methods, and you are listed as one of the co-authors.

The manuscript has been submitted to the journal by Dr. Prof Juliana Pallone who will be able to track the status of the paper through his/her login.

If you have any objections, please contact the editorial office as soon as possible. If we do not hear back from you, we will assume you agree with your co-authorship.

Thank you very much.

With kind regards,

Springer Journals Editorial Office
Food Analytical Methods

As a result of the significant disruption that is being caused by the COVID-19 pandemic we are very aware that many researchers will have difficulty in meeting the timelines associated with our peer review process during normal times. Please do let us know if you need additional time. Our systems will continue to remind you of the original timelines but we intend to be highly flexible at this time.

This letter contains confidential information, is for your own use, and should not be forwarded to third parties.

Recipients of this email are registered users within the Editorial Manager database for this journal. We will keep your information on file to use in the process of submitting, evaluating and publishing a manuscript. For more information on how we use your personal details please see our privacy policy at https://www.springernature.com/production-privacy-policy. If you no longer wish to receive messages from this journal or you have questions regarding database management, please contact the Publication Office at the link below.

In compliance with data protection regulations, you may request that we remove your personal registration details at any time. (Use the following URL: https://www.editorialmanager.com/fanm/login.asp?a=r). Please contact the publication office if you have any questions.